Online ISSN: 1920-3853

Vol. 8, No. 2, June 2014

Print ISSN : 1715-9997

Canadian Journal of pure & applied sciences

an International Journal

SENRA
Academic Publishers
British Columbia

The Canadian Journal of Pure and Applied Sciences (CJPAS-ISSN 1715-9997) is a peer reviewed multi-disciplinary specialist journal aimed at promoting research worldwide in Agricultural Sciences, Biological Sciences, Chemical Sciences, Computer and Mathematical Sciences, Engineering, Environmental Sciences, Medicine and Physics (all subjects).

Every effort is made by the editors, board of editorial advisors and publishers to see that no inaccurate or misleading data, opinions, or statements appear in this journal, they wish to make clear that data and opinions appearing in the articles are the sole responsibility of the contributor concerned. The CJPAS accept no responsibility for the misleading data, opinion or statements.

CJPAS is Abstracted/Indexed in:
Thomson Reuters, EBSCO, Ulrich's Periodicals Directory, Scirus, CiteSeerX, Index Copernicus, Directory of Open Access Journals, Google Scholar, CABI, Chemical Abstracts, Zoological Records, Global Impact Factor Australia, J-Gate, HINARI, WorldCat, British Library, European Library, Biblioteca Central, The Intute Consortium, Genamics JournalSeek, bibliotek.dk, OAJSE, Zurich Open Repository and Archive Journal Database.

Global Impact Factor for 2012 = 2.657

Frequency:
3 times a year (Feb, June and Oct.)

Editorial Office
E-mail: editor@cjpas.ca
: editor@cjpas.net

SENRA Academic Publishers
5919 129 B Street Surrey
British Columbia V3X 0C5 Canada
www.cjpas.net
E-mail: senra@cjpas.ca

Print ISSN 1715-9997
Online ISSN 1920-3853

Volume 8, Number 2
June 2014

CANADIAN JOURNAL OF PURE AND APPLIED SCIENCES

Board of Editorial Advisors

Member
CANADIAN ASSOCIATION OF LEARNED JOURNALS

Canadian Journal of pure & applied sciences

Volume 8, Number 2
June 2014

CONTENTS

LIFE SCIENCES

AE Pillay, M Elkadi and S Stephen
Application of a Hyphenated Facility for Simultaneous Speciation Studies of Toxic Oxidation States [Cr^{3+}/Cr^{6+}] and [As^{3+}/As^{5+}] in Produced Water from Crude Oil 2807

Kishan Mahmud, MS Chowhdhury, Nadia Noor and SM Imamul Huq
Effects of Different Sources of Biochar Application on the Emission of a Number of Gases from Soil 2813

Amira Hassan Abdullah Al-Abdalall and Ebtisam Abdullah Al-Talib
Aflatoxin and Ochratoxin Production in Ground Coffee During Storage 2825

Mohagir AM, Syed S, Bup ND, Kamga, R and Kapseu C
Adsorption Isotherms of Decolourisation of Shea (*Vitellaria paradoxa* Gaertner F) Butter 2837

George Osei-Adjei, FC Mills-Robertson, SC K Tay, FB Apea-Bah and A Adu-Gyamfi
Microbial Characterization of Spoilage Microbes of Dry Herbal Medicinal Powders/Teas 2845

Kolawole OT and Akanji MA
Anti-Inflammatory and Antioxidant Activities of Ethanolic Extract of Leaves of *Newbouldia laevis* in Diabetic Rats 2851

Iman Bajalan, Masoumeh Zand and Shahram Rezaee
Allelopathic Effect of Various Organs of Walnut (*Juglans regia*) on Seed Germination of Wheat 2859

GS George, AA Uwakwe and ET Egoro
Evaluation of Reactive Glucose By-Products Dicarbonyls and Glycated Haemoglobin in Hyperglycemic Patients 2865

M Zaheer Khan, Tanveer Jabeen, S Ali Ghalib, Saima Siddiqui, M Safdar Alvi, Iqbal Saeed Khan, Ghazala Yasmeen, Afsheen Zehra, Fozia Tabbassum, Babar Hussain and Raheela Sharmeen
Effect of Right Bank Outfall Drain (RBOD) on Biodiversity of the Wetlands of Haleji Wetland Complex, Sindh 2871

Short Communication

Madhulika Singh, VS Jaiswal and Uma Jaiswal
Thidiazuron-Induced Anatomical Changes and Direct Shoot Morphogenesis in *Dendrocalamus strictus* Nees 2901

PHYSICAL SCIENCES

Om Parkash and Priyanka Kakkar
New Measures of Information and their Applications in Coding Theory 2905

Akpa Jackson Gunorubon and Raphael Nwokoma Raphael
Simulation of an Ammonia Synthesis Converter 2913

S Stephen, T Shah, AE Pillay and E Siores
A Study of Kinetics of Metal Leaching from Polypropylene Matrix using A Hyphenated Mass Spectrometric Technique 2925

KM Odunfa, RO Fagbenle, O O Oluwole and OS Ohunakin
Modeling of Thinliquid Fallingfilm in H_2O-LiBr and H_2O-LiCl Absorption Refrigeration Systems 2933

Godspower O Ekuobase and Ifeanyichukwu E Anyaorah
Tail Tolerance of Web Services Solution Built on Replication Oriented Architecture (ROA) 2943

Ashwani K Thukral and Om Parkash
A New Approach for the Logarithms of Real Negative Numbers 2955

Om Parkash and Mukesh
Portfolio Optimization using Measures of Cross Entropy 2963

Scientific Communication

Javad Mashayekhi Fard, Mohammad Ali Nekoui and Roya Amajdifard
Robust Multi-Objective Static Output Feedback Control Based on $H_2/H_\infty/\mu$ Combination 2969

Short Communication

Vinu PV, Sherimon PC and Reshmy Krishnan
Ontology Construction and Reasoning using Owl: A Case Study from Seafood Domain 2979

SENRA Academic Publishers, British Columbia
Vol. 8, No. 2, pp. 2807-2812, June 2014
Online ISSN: 1920-3853; Print ISSN: 1715-9997

Canadian Journal of pure & applied sciences

APPLICATION OF A HYPHENATED FACILITY FOR SIMULTANEOUS SPECIATION STUDIES OF TOXIC OXIDATION STATES [Cr^{3+}/Cr^{6+}] AND [As^{3+}/As^{5+}] IN PRODUCED WATER FROM CRUDE OIL

*AE Pillay, M Elkadi and S Stephen
Department of Chemistry, The Petroleum Institute, PO Box 2533, Abu Dhabi, UAE

ABSTRACT

Produced water is the aqueous component of crude oil and has not been previously characterized for noxious oxidation states: Cr^{3+}/Cr^{6+} and As^{3+} /As^{5+}. It is often returned to the environment where it could create an unwanted hazard. It remains unexplored in this context largely because standard HPLC techniques do not permit convenient simultaneous separation of Cr^{3+}/Cr^{6+} and As^{3+}/As^{5+} due to proximity of corresponding retention times. Our group has adapted a facile process for rapid elution and concurrent mass separation of all four species in an affiliated HPLC/ICP-MS system equipped with a dynamic reaction cell (DRC). Oxygen gas was circulated through the DRC to remove interferences and enhance detection of the eluted components, especially the arsenic constituents. The stationary phase consisted of a C8 deactivated silica based column (length 150 mm; internal diameter: 4.6 mm; particle size: 5 µm); and the mobile phase was composed of a mixture of TBAH/EDTA in 2% methanol/water, adjusted to a pH of 7.2. The rate of elution was 1 mL/min; and recorded retention times (min) were: As^{3+}: 1.81; As^{5+}: 5.50; Cr^{3+}: 1.83; and Cr^{6+}: 5.74. The oxygen flow rate in the DRC was 0.7 mL/min. The Cr^{3+}/ Cr^{6+} constituents were detected with m/z values of 52; the arsenic species coalesced with oxygen and were detected as adduct ions, AsO^{+}, m/z, 91. Standard reference materials were deployed to test the competency of the analytical system. Typical recorded levels in the samples were: Cr^{3+}: 0.5 – 20 mg/L; $Cr^{6+}/As^{3+}/As^{5+}$: 1-5 µg/L. Our results were evaluated in terms of the potential source of toxicity of produced water to the environment. The significance of the study to petroleum and environmental science is discussed.

Keywords: Cr^{3+}/Cr^{6+} and As^{3+} /As^{5+}, HPLC/ICP-MS, produced water, crude oil.

INTRODUCTION

The single most important advantage of a chemical speciation technique (Ball *et al*., 1998; Benramdane *et al*., 1999; Del Razo *et al*., 2001; Eary and Rai, 1987; Katz and Salem, 1993) is that it has the unique ability to accurately pinpoint constituent toxic agents in natural samples that pose an environmental threat (Korte and Fernando, 1991; Le *et al*., 2000; Burguera and Burguera, 1997; Le *et al*., 1996; Van Elteren *et al*., 2002). In this work a rapid procedure for toxic speciation of chromium and arsenic has been adapted (Nuebauer *et al*., 2004) for produced-water studies using a combined (hyphenated) high performance liquid chromatography DRC-ICP-MS system [dynamic reaction cell-inductively coupled plasma-mass spectrometry]. The affiliated DRC-ICP-MS arrangement is well known for its superior performance and high sensitivity. The facility was optimised with the express purpose of isolating these species in a single run, and is especially useful for low sample volumes (about 50 µL). When precious little sample is available, more than one isolation procedure may not be possible and complete separation in a single run is a great advantage. Other authors have used similar systems for individual speciation studies (Le *et al*., 1996; Van Elteren *et al*., 2002) but simultaneous speciation is conveniently accomplished with the HPLC-DRC-ICP-MS facility. Particularly low detection limits can be attained (ng/L); and the system is designed to produce results within minutes. A notable advantage of the technique is that there is no recourse to extensive sample pre-treatment or pre-concentration procedures.

Produced wastewater is the aqueous component separated from oil, and is usually returned to the environment. If such wastewater is disposed of in the environment, it could find its way into aquifers and pollute the water table. It could thus create an environmental hazard (Shearman, 1990; Robinson, 1993) especially if it contains noxious species such as Cr^{3+}/Cr^{6+} and As^{3+} /As^{5+}. According to the literature, produced water remains uncharacterised with regard to the species of interest, which are often present at levels beyond the reach of most modern techniques. Selected samples were subject to investigation to assay the species concerned and optimize the analytical performance of the system for routine studies of this nature. Our primary objective, therefore, was to conveniently adapt and optimize an HPLC-DRC-ICP-MS facility for rapid chromium and arsenic speciation studies in produced wastewater.

*Corresponding author email: apillay@pi.ac.ae

MATERIALS AND METHODS

HPLC

Samples of produced water were collected from different sites and processed for analysis. Isolation of the species of interest was achieved with a Perkin Elmer quaternary LC pump and solvent manager. The stationary and mobile phases were prepared according to Perkin Elmer specifications (Neubauer *et al*., 2004) and were considered optimum for peak shape and retention time. The mobile phase was composed of 1 mM tetrabutyl ammonium hydroxide (TBAH) + 0.5 mM EDTA (potassium salt) + 2% methanol in water. The mixture was adjusted to a pH of 7.2 with dilute HNO_3. The stationary phase consisted of a C8 column, packed with base deactivated silica; column length: 150 mm; internal diameter: 4.6 mm; particle size: 5.0 µm; pore size 140 Å. The column was conditioned with the mobile phase prior to analysis and rinsed thoroughly with a methanol/water mixture at the end of each analysis to maintain its stability. The rate of elution was 1 mL/min. Certified standards containing appropriate levels of the species of interest were obtained from VHG Labs, UK.

DRC-ICP-MS

A Perkin Elmer SCIEX DRC-e ICP-MS was commissioned for mass separation of the eluted species. The nebulizer gas flow in the instrument was 0.80 L/min. The eluted solutions were conveyed to the core of the ICP-MS (Fig. 1) which was equipped with a dynamic reaction cell (DRC) for the suppression and elimination of interferences. In the DRC oxygen was chosen as the reaction gas as it subdued ArC^+ interferences with Cr^+ at m/z 52; and combined with As^+ to form an adduct ion, AsO^+, m/z 91 (Neubauer *et al*., 2004). The formation of this adduct conveniently avoids interferences with other undesirable species: $ArCl^+$ and $CaCl^+$ at m/z 75 (Neubauer *et al*., 2004). The oxygen flow rate was 0.7 mL/min. The instrument itself was standardized with a certified multiple standard (Fluka 70007; 10.00 ppb per element) and is linear over several orders or magnitude for aqueous samples.

The composition of samples and standards was the same as that of the mobile phase. Prior to each run, the instrument underwent linear calibration and background correction. Marginal drift in instrumental measurements was compensated for by use of an internal standard. To test the analytical competency of the system, the repeatability of the instrument was examined for a range of elements in the multiple-standard. Based on the relative standard deviation (RSD) the results showed that in general values <5% were attained demonstrating that the precision of the system for aqueous samples was satisfactory (Table 1).

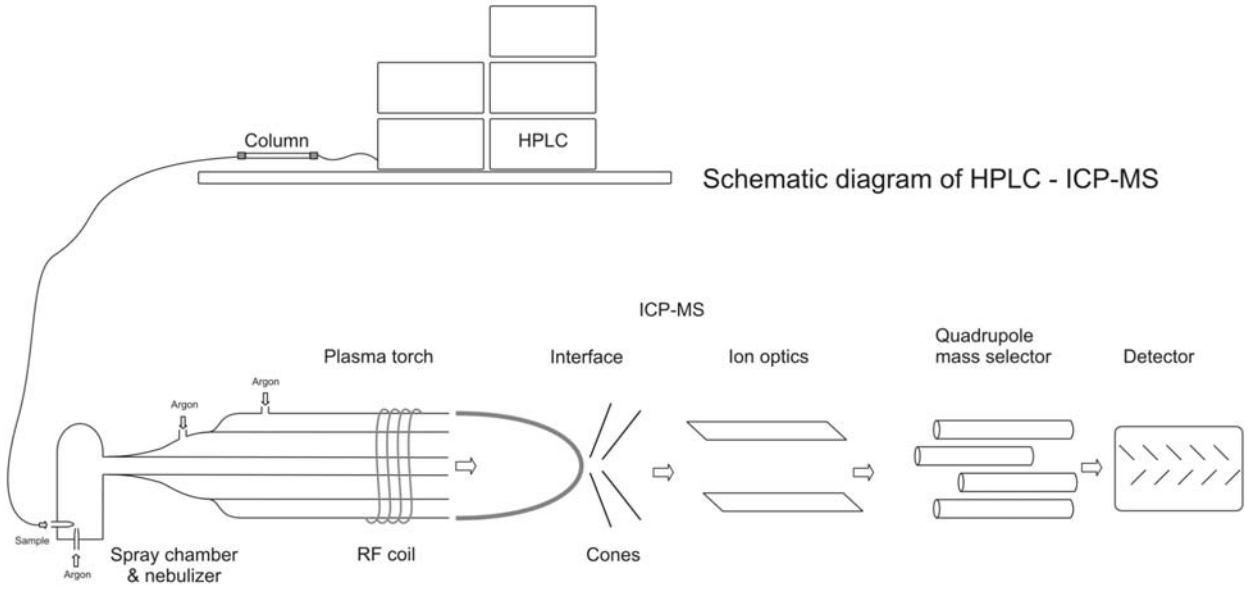

Fig. 1. Schematic of the HPLC/DRC-ICP-MS system.

RESULTS AND DISCUSSION

Speciation/Mass separation

Chemical speciation studies tend to be convoluted largely because of the complexities that accompany the isolation of the species. The primary difficulty encountered with standard HPLC techniques to isolate all four species (Cr^{3+}/Cr^{6+} and As^{3+}/As^{5+}) in a single run is the proximity of corresponding retention times. In this study the recorded retention times were: As^{3+}/As^{5+}: 1.81 and 5.50 min, respectively; and Cr^{3+}/ Cr^{6+}: 1.83 and 5.74 min, respectively. Clearly, in a conventional chromatographic separation overlap of these time intervals would hardly permit convenient collective separation of all four species – and would necessitate more than one isolation procedure. This is time consuming and presents difficulties, especially if sample sizes are limited to low volumes. The combination of chromatographic isolation followed by mass separation for all four oxidation states is unique and represents a marked attainment in instrumental analysis of this nature. Another noteworthy feature of the mass separation technique is its superior sensitivity.

The separation procedure itself was emulated from literature studies and adapted for our specific purpose (Neubauer *et al*., 2004). Baseline problems arose (Fig. 2) in cases where the use of oxygen in the DRC failed to completely eradicate the ArC^{+} interference associated with Cr^{+}. To resolve this situation the oxygen flow rate was carefully adjusted to optimize the signal to noise ratio.

Typical separation of the As^{3+} and As^{5+} species (standard) appears in figure 3. The peaks are distinct and clearly resolved, and the asymmetry factors (Dolan, 2003) relating to tailing are acceptable. The "hump" at about 7.8 min has not been identified, and it is not clear at this stage if this feature represents a constituent of the numerical analysis or is a minor perturbation due to slight aberrations in the solvent elution. However, it does not interfere with the overall analysis and could be an interesting subject of future investigation. The tailing factor is also satisfactory for the chromium species as delineated in the chromatogram in figure 4, which represents the Cr^{3+} component in produced water. The marginal shoulder on the peak (in Fig. 4) was attributed to

Table 1. Repeatability test of the ICP-MS for various elements (µg/L) in an aqueous standard.

Element	Run # 1	Run # 2	Run # 3	Run # 4	Mean	RSD %
V	9.51	9.74	9.90	9.51	9.67	1.97
Cr	9.82	9.61	9.39	9.82	9.66	2.13
Co	10.2	10.1	9.34	10.2	9.96	4.20
As	10.2	9.42	9.29	10.2	9.80	5.24
Mo	11.0	11.1	10.4	11.0	10.9	2.87
Cd	9.51	10.1	9.82	9.51	9.73	2.74
U	10.0	9.65	10.1	10.1	9.98	2.23

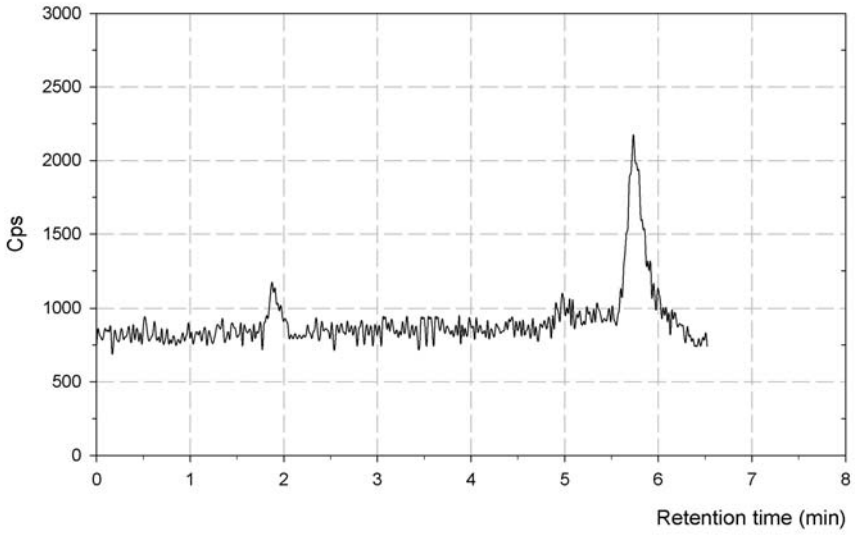

Fig. 2. Poor baseline in a typical chromatogram of chromium species due to interference from ArC^{+} .

Table 2. Levels of species of interest (µg/L) in produced water samples.

Species	Sample #1	Sample #2	Sample #3	Sample #4	Sample #5	Sample #6	Sample #7	Sample #8	Sample #9	Sample #10
Cr 3+	434± 9	1816± 9	2275± 8	867± 9	1965± 9	1725± 8	622± 18	1209± 33	1023± 30	624± 23
Cr 6+	4.51± 0.13	4.94± 0.14	4.97± 0.10	7.63± 0.29	7.21± 0.14	6.77± 0.16	7.23± 1.30	6.55± 0.17	6.44± 0.19	4.39± 0.11
As 3+	2.36± 0.04	4.16± 0.14	5.36± 0.12	15.5± 0.4	3.33± 0.07	3.74± 0.05	11.5± 0.2	10.3± 0.2	9.86± 0.20	6.97± 0.17
As 5+	0.79± 0.02	1.30± 0.04	1.58± 0.05	2.68± 0.10	0.85± 0.02	0.78± 0.02	1.04± 0.03	0.99± 0.03	2.05± 0.04	1.26± 0.04

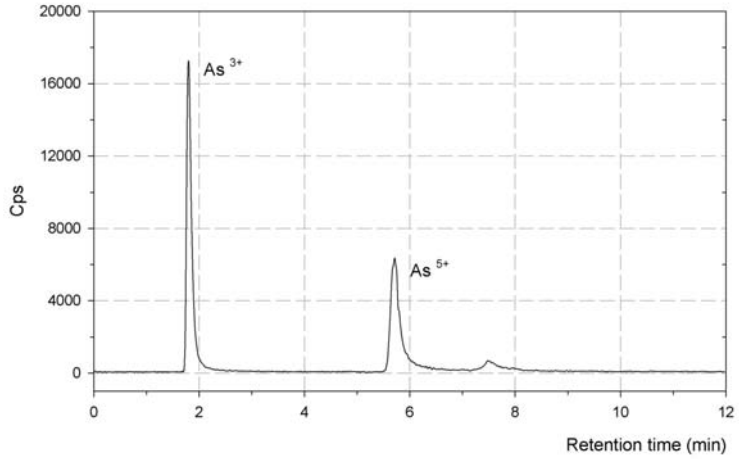

Fig. 3. Eluted arsenic species portraying distinct features of As^{3+} and As^{5+}

slight fluctuations in the elution rate. Table 2 presents typical concentrations of all species in produced water samples. The range of concentrations recorded in this study is as follows: Cr^{3+}: 0.5–20 mg/L; Cr^{6+}/As^{3+}/As^{5+}: 1-5 µg/L. To forecast produced water as a potential source of toxicity, it is necessary to consider acceptable levels in environmental/municipal waters (Neubauer *et al*., 2004): <1 µg/L for Cr^{3+}; <4 ug/L for Cr^{6+}; and <1 µg/L for As^{3+} /As^{5+}. From the perspective of a potential environmental threat to potable sources, the recorded values in table 2 show that Cr^{3+} levels are elevated, in some cases by a factor of more than 10. The levels of Cr^{6+}, As^{3+} and As^{5+} (in some samples) are also pronounced, indicating that produced water can be a significant source of toxicity. The toxic nature of these species to human health has been previously documented (Benramdane *et al*., 1999; Katz and Salem, 1993) and is discussed in more detail below.

Impact of the study

The primary significance of the study is that all four species can be conveniently eluted and detected in a single run (Fig. 5). Simultaneous separation of this nature is not conveniently achieved with other contemporary methods or with conventional HPLC systems because they are not as sensitive (Korte and Fernando, 1991). As aforementioned, a distinct advantage of accomplishing this isolation all at once is that if only small volumes of sample are available the determination is still practicable. The technology has implications for other studies such as biomedicine and immunology where only minimal volumes of body fluid are available for assay. The study also has environmental implications because it can be associated with sustainable development (Shearman, 1990; Robinson, 1993; Pillay *et al*., 2010). Produced waste water, if consigned to the environment, could affect subterranean sources. Many oil-bearing countries are arid regions, and depend on surface streams and underground supplies to feed livestock and for domestic purposes (Pillay *et al*., 2010). If such wastewater penetrates the water table, consequences could be serious. As a result, various components of the ecosystem could be affected leading to undesirable pollution. Wastewater extracted from oil, therefore, has the potential to become a significant source of ground water pollution, especially if it has elevated levels of chemical toxins (Benramdane *et al*., 1999; Korte and Fernando, 1991). The likely threat to sustainable development is therefore of material concern (Shearman, 1990; Robinson, 1993). The cytotoxic nature of chromium and arsenic species has grown in interest

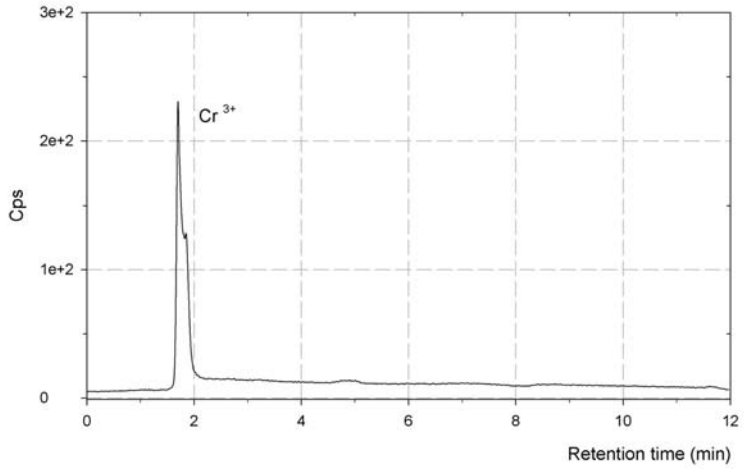

Fig. 4. Chromatogram of Cr^{3+} from produced water.

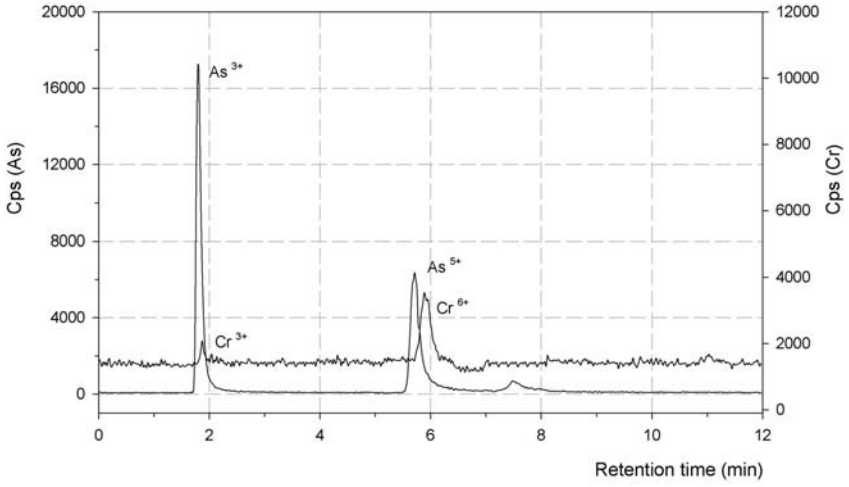

Fig. 5. All chromium and arsenic species in a single run.

(Benramdane *et al*., 1999; Katz and Salem, 1993). The hexavalent form of chromium (Cr^{6+}) is more toxic than its trivalent form, Cr^{3+} (Benramdane *et al*., 1999). However, elevated levels of Cr^{3+} in humans tend to inhibit iron uptake, which could lead to multiple disorders. On the other hand, trivalent arsenic (As^{3+}) is known to be more cytotoxic than the pentavalent species, As^{5+} (Katz and Salem, 1993). The presence of elevated levels of inorganic arsenic in humans leads to vascular diseases and cancer (Katz and Salem, 1993). Our results show Cr^{3+} concentrations represent a significant source of toxicity and could pose a hazard if produced water of this nature reaches potable water supplies. The $Cr^{6+}/As^{3+}/As^{5+}$ levels also appear menacing and remedial measures for removal of Cr and As species by chemical means would be apt prior to disposal of the produced water by-product. Another option would be either to immobilize the water by storing in vitreous slabs or in underground bunkers; or to convert it to a sludge using sand and aggregate, and subsequently constructing concrete blocks for storage in subterranean caverns (Pillay *et al*., 2010).

CONCLUSIONS

Our study provides significant speciation data (Cr^{3+}/Cr^{6+} and As^{3+} /As^{5+}) for produced water, which is of considerable practical interest to petroleum engineers and environmentalists. This essential information is not available in the documented literature and from this perspective our research breaks new ground. The fact that all four species can be isolated in a single run employing an HPLC/DRC-ICP-MS system implies the facility could be extended for rapid simultaneous assay of other toxic species including Se^{4+}/Se^{6+} and Hg^{2+}/Hg^{+}. The notable feature of this instrumental arrangement is that it caters for comparatively low sample volumes, which makes it useful for applications in other disciplines such as biomedicine and immunology. Our results were evaluated

in terms of the potential hazard to the environment that produced water could cause if it were a source of toxicity. The relevant levels recorded in our study were elevated suggesting they could pose a threat to potable water supplies if such wastewater is returned to the ecosystem. One suggested remedial measure is to immobilize the produced water in vitreous or concrete slabs for subterranean storage.

ACKNOWLEDGEMENTS

The authors wish to thank the Petroleum Institute for financial support.

REFERENCES

Ball, JW. and Nordstrom, DK. 1998. Critical evaluation and selection of standard state thermodynamic properties for chromium metal and its aqueous ions, hydrolysis species, oxides, and hydroxides. Journal of Chemical Engineering and Data. 43:895-918.

Benramdane, L., Bressolle, F. and Vallon, JJ. 1999. Arsenic speciation in humans and Food Products: a review. Journal of Chromatographic Science. 37:330-344.

Burguera, M. and Burguera, JL. 1997. Analytical methodology for speciation of arsenic in environmental and biological samples. Talanta. 44:1581-1604.

Del Razo, LM., Styblo, M., Cullen, WR. and Cullen, DJ. 2001. Determination of trivalent methylated arsenicals in biological matrices. Toxicology and Applied Pharmacology. 174:282-293.

Dolan, JW. 2003. Why Do Peaks Tail? LC troubleshooting. LC.GC Europe September. 1-4.

Eary, LE. and Rai, D. 1987. Kinetics of chromium (III) oxidation to chromium (VI) by reaction with manganese dioxide. Environmental Science and Technology. 21: 1187-1193.

Katz, SA. and Salem, H. 1993. The toxicology of chromium with respect to its chemical speciation: a review. Journal of Applied Toxicology. 13: 217-224.

Korte, NE. and Fernando, Q. 1991. A review of arsenic (III) in groundwater. Critical Reviews in Environmental Control. 21:1-40.

Le, XC., Ma, M. and Wong, NA. 1996. Speciation of Arsenic Compounds Using High-Performance Liquid Chromatography at Elevated Temperature and Selective Hydride Generation Atomic Fluorescence Detection. Anal. Chem. 68:4501-4506.

Le, XC., Yalcin, S. and Ma, M. 2000. Speciation of sub-microgram per liter levels of arsenic in water: on-site species separation integrated with sample collection. Environmental Science Technology. 34:2342-2347.

Neubauer, KR., Reuter, WM., Perrone, PA. and Grosser, ZA. 2004. Simultaneous arsenic and chromium speciation by HPLC/ICP-MS in environmental waters. Perkin Elmer Life and Analytical Sciences. Application Note. 1-4.

Pillay, AE., Salih, FM. and Maleek, MI. 2010. Radioactivity in Oily Sludge and Produced Waste Water from Oil: Environmental Concerns and Potential Remedial Measures. Sustainability. 2:890-901.

Robinson JG. 1993. The limits to caring: sustainable living and the loss to biodiversity. Conserv. Biol. 7:20-28.

Shearman, R. 1990. The meaning and ethics of sustainability. Environ. Manage.14:1-8.

Van, Elteren, JT., Stibilj, V. and Šlejkovec, Z. 2002. Speciation of inorganic arsenic in some bottled Slovene mineral waters using HPLC-HGAFS and selective co-precipitation combined with FI-HGAFS. Water Res. 36:2967-2974.

Received: Feb 10, 2014; Accepted: March 1, 2014

SENRA Academic Publishers, British Columbia
Vol. 8, No. 2, pp. 2813-2824, June 2014
Online ISSN: 1920-3853; Print ISSN: 1715-9997

Canadian Journal of pure & applied sciences

EFFECTS OF DIFFERENT SOURCES OF BIOCHAR APPLICATION ON THE EMISSION OF A NUMBER OF GASES FROM SOIL

Kishan Mahmud, MS Chowhdhury, Nadia Noor and *SM Imamul Huq
Bangladesh-Australia Centre for Environmental Research
Department of Soil, Water and Environment, University of Dhaka, Dhaka-1000, Bangladesh

ABSTRACT

Addition of biochar to soils has the potentials to reduce the emission of greenhouse gases from soil. The primary objectives of this study were to see the impacts of biochar and the corresponding biomass application on the emission of carbon dioxide (CO_2), carbon monoxide (CO), phosphine (PH_3) and volatile organic compounds (VOCs) from soil investigated in a closed container experiment. Three replications of seven different treatments were applied: i) soil only (control), soil incorporated with - ii) rice husk, iii) biochar produced from rice husk, iv) straw, v) biochar from straw, vi) saw dust and vii) biochar produced from saw dust. The study reveals that addition of biochar had significant effects ($P<0.05$) on reducing CO_2 and PH_3 emission while no statistically significant effects on VOCs emanation was evident. Application of biochar could not suppress the CO emissions. Our study indicates that, different types of biochars have different effects on the emission of different gases.

Keywords: Biochar, gas emission, soil health.

INTRODUCTION

Climate change is one of the most important challenges facing the modern world. Carbon dioxide (CO_2), methane (CH_4) and nitrogen oxides (NO_x) are important drivers of the anthropogenic greenhouse effect, which are released both through burning of fossil and biomass fuel as well as decomposition of above and below-ground organic matter. Over time, these emissions have contributed to the overall effects of global warming. Every year the world wide carbon dioxide (CO_2) emissions from energy needs increases, and by the year 2020 the world will produce 33.8 billion metric tons up from 29.7 billion metric tons in 2007 (US Energy Information Administration, 2010).

A growing body of evidence suggests that agricultural emissions contribute to environmental and human health problems. The Carbon dioxide emission from the soil to the atmosphere is the primary mechanism of carbon loss from the soil (Parkin and Kaspar, 2003) which in turn contribute to the global greenhouse gas emission. Forest ecosystems that are now net sinks for CO_2 might become net sources after about 2050, if the projected temperature rise becomes a reality (Cox *et al*., 2000). Agricultural intensification comes with a downside: a number of nitrogen-sulfur- and carbon-containing compounds, including ammonia, nitrogen oxides, nitrous oxide, hydrogen sulfide, methane, carbon dioxide and volatile organic compounds are emitted through agricultural operations (Aneja *et al.*, 2006). Some agricultural air pollutants (for example, ammonia, hydrogen sulfide, toxic organic compounds, pesticides, insecticides, and particulate matter) can affect human health as well as the comfort, health and production efficiency of animals (Donham *et al.*, 1982). According to some schools of thought, applying biochar into the soil to sequester carbon as well as to limit the emission of nitrogenous gases from soil is a realistic platform. The emergence of biochar, from the pyrolysis of biomass, as a carbon sink is not new and has been proposed before (Seifritz, 1993) but was not explicitly linked to an application to soil. The introduction of biochar (charcoal or carbon derived from biomass via pyrolysis) to the soil produces a long-term carbon sink in terrestrial ecosystems (Lehmann *et al*., 2006). Biochar slows down the decaying and mineralization of the biological carbon cycle to establish a carbon sink and a net carbon withdrawal from the atmosphere. Additionally calculations have shown that putting this biochar back into the soil can reduce emissions by 12-84 percent of current values; a positive form of sequestration that offers the chance to turn bio-energy into a carbon negative industry (Lehmann, 2007).

Albeit the promising prospect of biochar utilization, with some observations reporting negative consequences on soil and crop production along with the high initial energy consumption during the manufacturing of biochar, (Laird *et al*., 2008) however, the specific objectives of this study were to examine: (1) the comparative effectiveness of biochar and biomass application in suppressing the emission of carbon dioxide (CO_2), carbon monoxide (CO), phosphine (PH_3) and volatile organic compounds (VOCs) from soil and (2) the comparative effectiveness of the biochars of different provenances.

*Corresponding author email: imamhuq@hotmail.com

MATERIALS AND METHODS

Biochar production

Biochar was produced from the raw materials of disparate sources; rice husk, straw and saw dust, employing the process of slow pyrolysis. A large hollow earthen pot was filled with dry wooden chips (smeared with some diesel) and the opening end of the pot was covered with an iron net of considerable resilience to withstand high temperature. Four small earthen pots, filled with biomasses and made impregnable to air penetration, were placed upon the iron net. Wooden chips were kindled and the pyrolysis initiated. Forty five minutes later, the fire was put off and after considerable cooling period the small pots were inspected to confirm the biochar production. This system can be termed as open fire system.

The produced biochar were then subjected to further processing. The biochar particles were passed through a set of sieve of 2 to 0.2mm. Biochar samples were preserved in plastic containers. Labeling of the produced biochars was as follows:

1. Rice Husk-Biochar: BC-1,
2. Straw- Biochar: BC-2, and
3. Saw Dust- Biochar: BC-3

Biochar can be produced from different types of organic feedstock but for this study biomasses were collected from different corners of Bangladesh. For instance, rice husk was collected from a rice mill, straw from a rice field and saw dust from (mango wood) from a saw mill.

Biomasses were excised into small pieces only in case of straw and then were flailed in a grinder machine. Ground samples were screened through a 0.2mm stainless still sieve. The sieved samples were then mixed thoroughly for making a composite sample. Biomass samples were preserved in plastic containers. The labeling of the biomasses was as follows:

1. Rice Husk-Biomass: BM-1
2. Straw-Biomass: BM-2 and
3. Saw Dust-Biomass: BM-3

Soil sample collection

Soil samples were collected from a depth of 0-15cm by composite soil sampling method as suggested by Imamul Huq and Alam (2005) from Manikganj Sadar upazila, Manikganj, Bangladesh (51°.884 N and 90°06.219 E). The soils thus collected belong to the Young Brahmaputra Floodplain representing the Melandaha series (Fig. 1). The soil texture is silt loam (sand: 13.9%, silt: 74.1%,

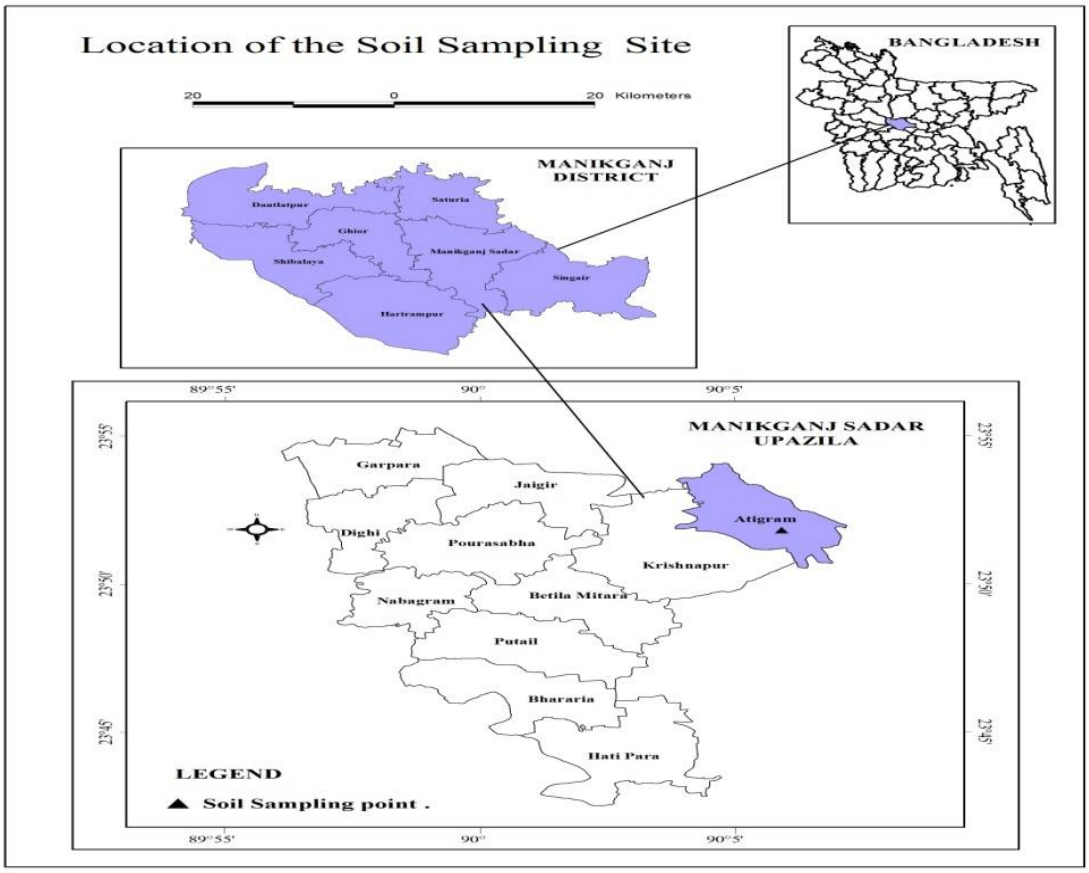

Fig. 1. The GPS-GIS based location map of the soil sampling site.

clay: 12.0%). The Melandaha series consists of intermittently or seasonally very shallowly flooded, imperfectly to poorly drained, very weakly developed medium textured soil. They have grey to olive grey, finely mottled, usually structure less, very fine sandy loam to silt loam below top soil. They are near neutral in reaction. The soil is Aeric Haplaquepts (Imamul Huq and Shoaib, 2013).

The collected soil samples were dried in air for 3 days (at ~40°C), freed from visible roots and debris. To expedite the drying process, the soil samples were exposed to sunlight and a consequent hammering (with a wooden hammer) to get rid of massive aggregates. Ground samples were screened through a 5mm stainless still sieve. The sieved samples were then mixed thoroughly for making a composite sample. Soil samples were preserved in plastic containers.

The experimental setup

For detecting and measuring the emissions of different gases, plastic containers of 5 liter capacities were procured from the local market. A total of 21 containers were used and each received a special modification treatment for capturing evolved gases. At first, the containers were washed properly with distilled water and dried in sunlight and stored. The containers were made completely air tight thus had no leaks in them. Two vents were made deliberately on each of the containers for two different purposes. The first one was made on the top of the lid in order to make a passage for inserting the probes which detected and measured evolved gases. The other one was made on the sides of each container to insert a canola for application of water during the incubation period. Plastic funnels were used to hold water and a 9 inches rubber tube acted as conduit between the funnel and the canola. A small piece of bamboo stick was tied to each container to hold the funnel on top of the whole system. Each funnel was wrapped with cotton and aluminum foil for proper concealment (Fig. 2). The foil and cotton were only removed when it was time to apply water to the system. A 2.5kg of the 5mm sieved soil was used for each pot. The sieved soil was mixed with biomass and biochar at the rate of 5ton/hectare (each pot with 2.5kg of soil received 5gm of biochar or biomass). All treatments were in triplicates. Volume inside each container after filling them with soil was 3.3liter. Surface area of the soil inside the container was calculated by the "πr^2" formula as the shape of the container was round. Impacts of the biochars as well as of the corresponding biomasses on the greenhouse gas emission from soil were observed over a period of 60 days. In the first month of incubation, observations were made on every alternate day. In the second month, observations were made every week for 4 consecutive weeks. The designs of the experiments are shown in table 1.

Table 1. Design of the container arrangement.

Treatment No.	Treatments	Symbols
1-3	Control soil (only soil)	C
4-6	Soil + Rice husk (Biomass)	BM-1
7-9	Soil + Rice straw(Biomass)	BM-2
10- 12	Soil + Saw dust (Biomass)	BM-3
13-15	Soil + Rice straw (Biochar)	BC-1
16-18	Soil + Rice husk (Biochar)	BC-2
19-21	Soil + Saw dust (Biochar)	BC-3

Detection and measurement of greenhouse gases

For the determination of CO_2 and CH_4 a portable CO_2 meter manufactured by Columbus Instruments was used. The results shown by this instrument is in percentage of the volume of air in the container. On the other hand, NO, PH_3, H_2S, VOCs, CO and NH_3 were detected and measured by an Indoor Air Quality monitor kit manufactured by Wolf stream which gave the data on parts per million basis.

The amount of gas emitted was converted to Kg/ha or gm/ha as follows:

For CO_2 (lit/ha) = (amount in ml × 10,000) / (surface area of the soil in the container ×1000)

As per law: $V_1/T_1 = V_2/T_2$

Here,
V_1 = Volume of the CO_2 in the container; T_1 = Temperature of the observation day; V_2 = Volume of gas at S.T.P. And T_2 = Standard temperature = 293 K

So volume of CO_2 in the container = $(V_2 \times T_2) / T_1$

Again, we know, $\rho = m \times v$

Where,
ρ = Density of CO_2 at standard temperature and pressure; v = Volume of CO_2 determined at standard temperature and pressure and m = Mass of CO_2

Now, $m = (\rho \times V_1)$ Kg/ha of CO_2.

For the gases other than CO_2, observed values in parts per million (ppm) were converted into percentage and then calculated as above.

Statistical analysis

All the data in the present experiment were statistically analyzed by using Microsoft Excel and/or MINITAB (version 16) Packages.

Fig. 2. Containers to capture evolved gases.

RESULTS AND DISCUSSION

Impact of Biochar and Biomass on the Evolution of Carbon Dioxide from Soil

The effects of biochar and biomass on the evolution of carbon dioxide (kg/ha) as affected by the various sources of biomasses and biochars were observed for over a period of 60 days. The gas evolved is expressed as kg ha^{-1} and the results are presented in the table 2 and the pattern of CO_2 evolution is graphically presented in the figures 3 (a, b, c).

The average emission of carbon dioxide from control soil (63.1kg/ha) is considerably lower compared to all the biomass treated soils (Table 2). Soils treated with biochars indicate higher average emission of carbon dioxide than the control soils, except for rice husk biochar treated soil (Table 2). While comparing the average carbon dioxide emission from biochar treated soils with their corresponding biomass counterparts, saw dust biochar application showed higher average values (87.6 kg/ha) while the remaining other two stated the opposite (Table 2).

Table 2 and the figures 3 (a, b, c) show the emission trends over 60 days of all the treatments and reveal somewhat resemblances in emission trends among each other except for saw dust treatment (both biomass and biochar). Throughout the entire experiment, the emission of carbon dioxide from BM-1 and BM-2 soils show increasing trends compared to BC-1 and BC-2 soils which exhibit a continuous declining trend (Fig. 3 a and b). The average carbon dioxide emissions from BM-1 and BM-2 soils were 98.2 kg/ha and 99.0 kg/ha, respectively, and are significantly higher compared to the average emissions from BC-1 and BC-2 soils (59.5 kg/ha and 71.1 kg/ha, respectively) (Table 2). The validation of these empirical data yielded significant results (P value 0.00) at

Table 2. Quantities of carbon dioxide (kg ha^{-1}) emitted from differently treated soils.

Day	Control	BM-1	BC-1	BM-2	BC-2	BM-3	BC-3
1	83.3	86.5	107.5	87.8	114.9	144.5	265.7
3	51.4	85.9	80.0	91	112.6	123.5	216.3
5	62.0	91.5	83.0	96.8	107.2	95.7	186.1
7	52.8	92.9	79.2	117.9	99.2	85.5	148.8
9	54.9	100.4	76.1	109.7	94	80.3	136.3
11	59.0	178	77.9	131	93.7	67.4	107.4
13	55.6	136.4	76.6	119.2	88.1	71.3	88.1
15	58.1	118.3	67.6	107.6	89.8	83.5	71.8
17	56.5	108.8	61.8	107.6	75.7	80.0	57.6
19	48.0	89.2	60.5	96.7	63.7	62.7	49.9
21	54.4	91.7	49.0	96.1	59.7	70.4	43.7
23	123.8	122.7	52.3	156.8	56.6	65.1	40.6
25	115.0	104.6	44.7	130.4	60.7	78.8	36.2
27	88.7	91.9	41.2	93.1	43.3	65.5	33.8
29	73.6	96.7	41.0	78.3	51.5	72.5	41.0
38	47.8	88.2	30.8	67.7	44.6	82.9	47.8
45	41.2	80.3	40.1	74.5	42.3	60.2	40.1
52	37.2	54.2	27.6	63.5	28.7	39.9	24.4
59	35.7	48.4	33.6	55.6	24.2	41.0	29.4
Average emission	63.1	98.2	59.5	99.0	71.1	77.4	87.6

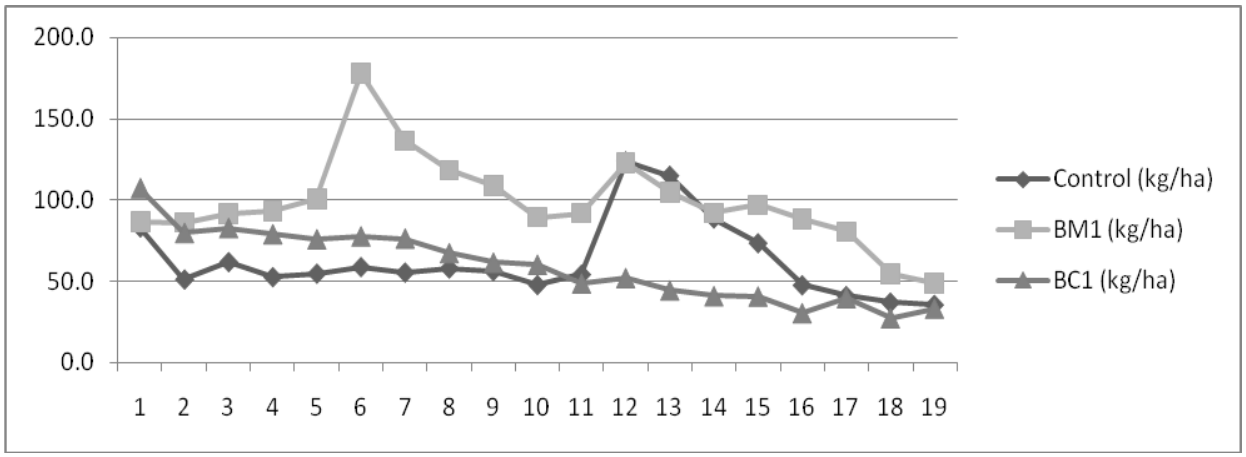

Fig. 3 (a). Emission trends of carbon dioxide from Control, BM-1 and BC-1 soils.

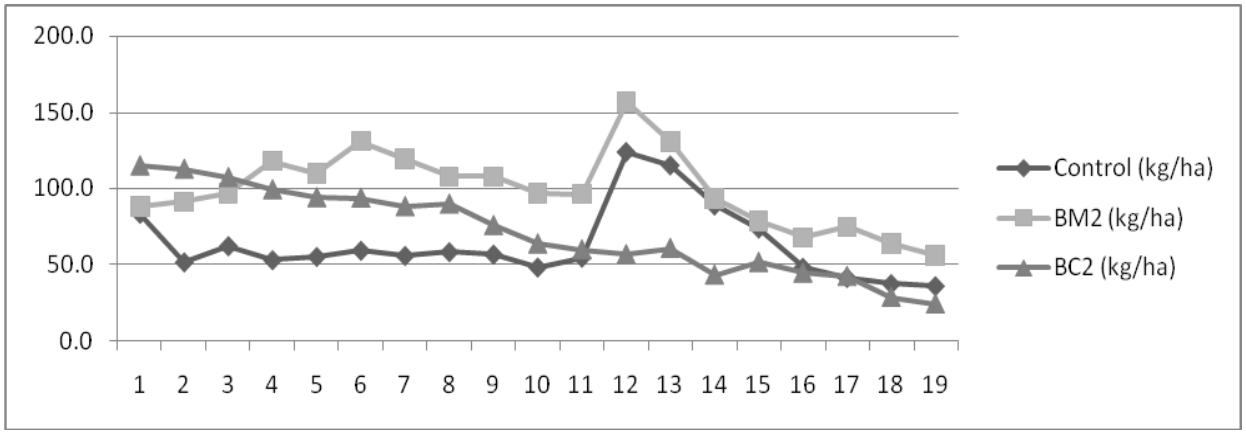

Fig. 3 (b). Emission trends of carbon dioxide from Control, BM-2 and BC-2 soils.

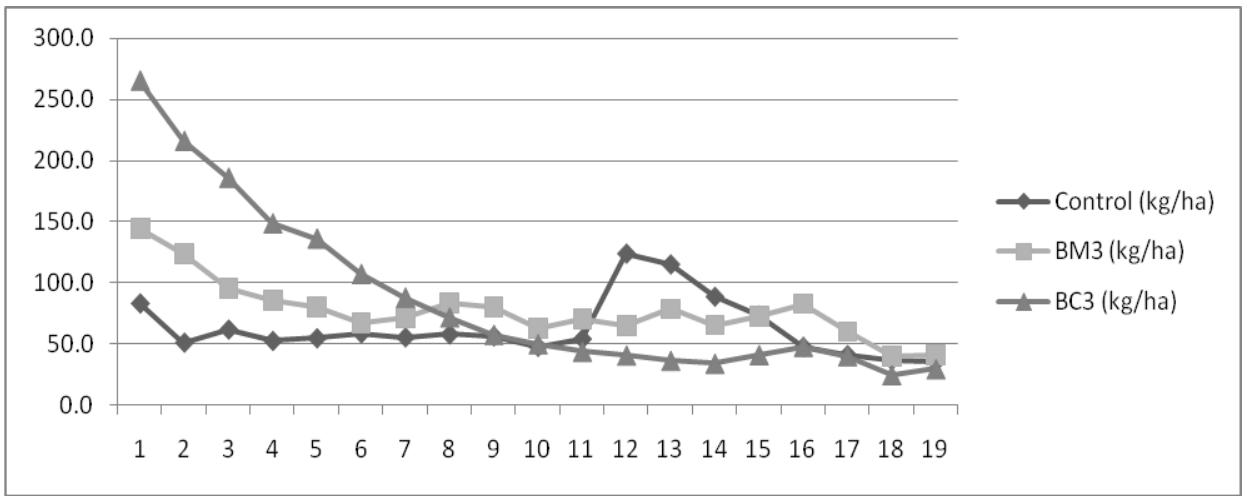

Fig. 3 (c). Emission trends of carbon dioxide from Control, BM-3 and BC-3 soils.

5% level. However, the observations indicated that biochar had a visible positive effect in reducing carbon dioxide emission from soil only after a certain period (16 days after the initiation of the experiment). It concurs with the findings of Yoo and Kang (2012) and Kammann *et al.* (2012) who stated that biochar created at higher pyrolysis temperatures caused a greater reduction in cumulative CO_2 release. Similar findings have also been mentioned by Qayyum *et al*. (2012) who measured cumulative CO_2 released from three soils amended with either nothing,

wheat straw (biomass), hydrochar (200°C), low-temperature biochar (sewage sludge pyrolyzed at 400°C), or charcoal (550°C). Cumulative CO_2 released generally followed the order: wheat straw (biomass) > hydrochar > low temperature biochar > charcoal = control. In our experiments, however, few erratic features were observed for carbon dioxide emission from BC-3 soil. In contrast to a high initial emission quantity (265.7kg/ha on day 1), the emission however gradually reduced eventually at the termination of the experiment. The soil incorporated with the corresponding biomass, BM-3, showed a low and steady pace throughout (Table 2 and Fig. 3c). The average emission of carbon dioxide from BC-3 soil and BM-3 soil were 87.6 kg/ha and 77.4 kg/ha, respectively (Table 2). Regardless of the treatments, Control, BM-1 and BM-2 soils showed a similar high emission peak at the fourth week of emission while the soils treated with the corresponding biochars did not show the peak, rather they exhibited a declining trend throughout (Figs. 3 a, b, c).

Impact of Biomass and Biochar on the Evolution of Carbon Monoxide from Soil

Results relating to the evolutions of carbon monoxide (kg/ha) are presented in the table 3 and the pattern of CO evolution is graphically presented in the figures 4 (a, b, c). In contrast to what has been observed for carbon dioxide emission, the soils treated with biochars, regardless of their disparate sources showed no significant effect in reducing carbon monoxide (P= 0.921 on day 30 and P=0.997 on day 60 at 5% level). The quantities emitted and the trend of emission from all the soils showed an anomalous pattern (Table 3 and Figs. 4 a, b and c). It was also observed that the average emission of carbon monoxide was the highest from the soil treated with biochar produced from saw dust (BC-3 soil) (3.64 kg/ha) over the other treatments in a 60 days period whereas the lowest average emission was observed from the control soil (3.54 kg/ha) (Table 3).

Carbon monoxide is apparently produced from the thermal decomposition of humic acids and other organic material (Conrad and Seiler, 1985). It appears that biochar has no significant effects on carbon monoxide emission. This is somewhat unexpected as due to biochar's inherent stability, it is hypothesized that application of biochar to soils results in greater soil carbon sequestration potential than would result from application of biomass of similar carbon content (Kwapinski *et al*., 2010). But as the soil surface is in contact with oxygen in the containers, majority of the carbon monoxide might have oxidized to carbon dioxide.

Impact of Biomass and Biochar on the Evolution of Phosphine from Soil

The effects of biochar and biomass on the evolution of phosphine (g/ha) from soil are presented in the table 4 and the pattern of phosphine evolution is graphically presented in the figures 5 (a, b, c).

Table 3. Quantities of carbon monoxide (kg/ha) emitted from differently treated soils.

Day	Control	BM-1	BC-1	BM-2	BC-2	BM-3	BC-3
3	3.31	3.31	3.28	3.31	3.26	3.31	3.26
5	3.28	3.34	3.46	3.34	3.46	3.43	3.49
7	3.41	3.43	3.47	3.43	3.51	3.47	3.52
9	3.49	3.49	3.49	3.49	3.52	3.48	3.54
11	3.56	3.62	3.54	3.55	3.55	3.54	3.54
13	3.59	3.59	3.65	3.59	3.63	3.61	3.59
15	3.53	3.51	3.58	3.51	3.57	3.54	3.57
17	3.41	3.64	3.69	3.64	3.70	3.69	3.72
19	3.72	3.73	3.73	3.73	3.74	3.72	3.75
21	3.54	3.59	3.67	3.59	3.69	3.64	3.71
23	3.78	3.87	3.92	3.87	3.93	3.92	3.96
25	3.75	3.76	3.79	3.76	3.79	3.79	3.79
29	3.83	3.82	3.77	3.82	3.79	3.77	3.81
38	3.28	3.25	3.32	3.25	3.31	3.27	3.31
45	3.13	3.17	3.30	3.17	3.34	3.27	3.38
52	3.74	3.84	3.96	3.84	3.98	3.95	3.99
59	3.90	3.94	3.94	3.94	3.95	3.92	3.93
Average emission	3.54	3.58	3.62	3.58	3.63	3.61	3.64

Table 4 and figure 5 (a, b and c) show that regardless of various applied treatments, all the soils have followed, though fluctuating, a resembling pattern. A steeper decreasing trend is particular in the biochar treated soils (Figs. 5 a, b and c). Soils treated with biochars exhibited lesser quantities of phosphine emission on an average compared to biomass treated soils as well as to the Control soil (Table 4). The average emission of phosphine from Control soil is the highest and soils receiving biochar treatments emitted the least (Table 4). The average emission from BM-1 soil (0.15gm/ha) is higher compared to BC-1 soil (0.13gm/ha) and this is true for the

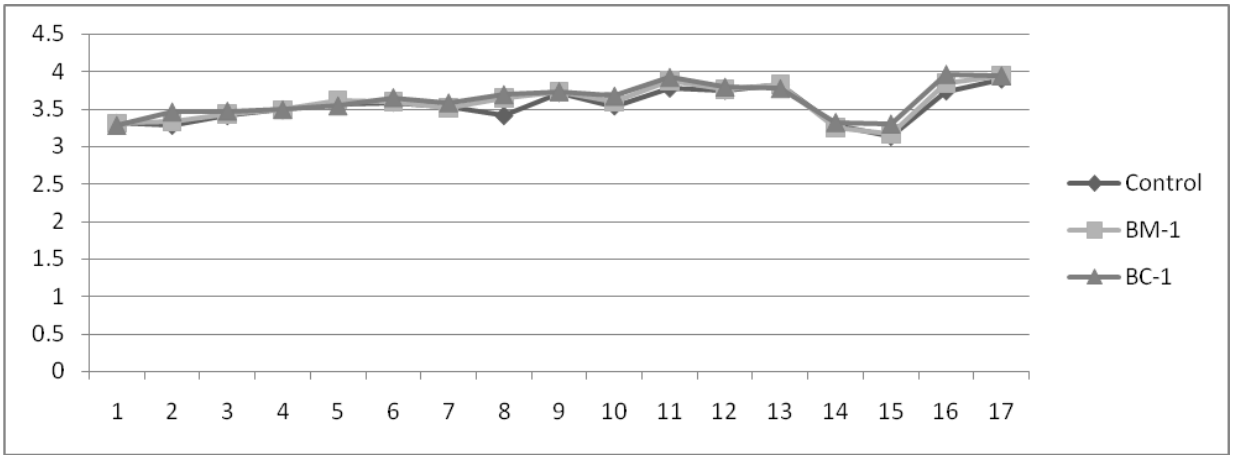

Fig. 4 (a). Emission trends of carbon monoxide from Control, BM-1 and BC-1 soils.

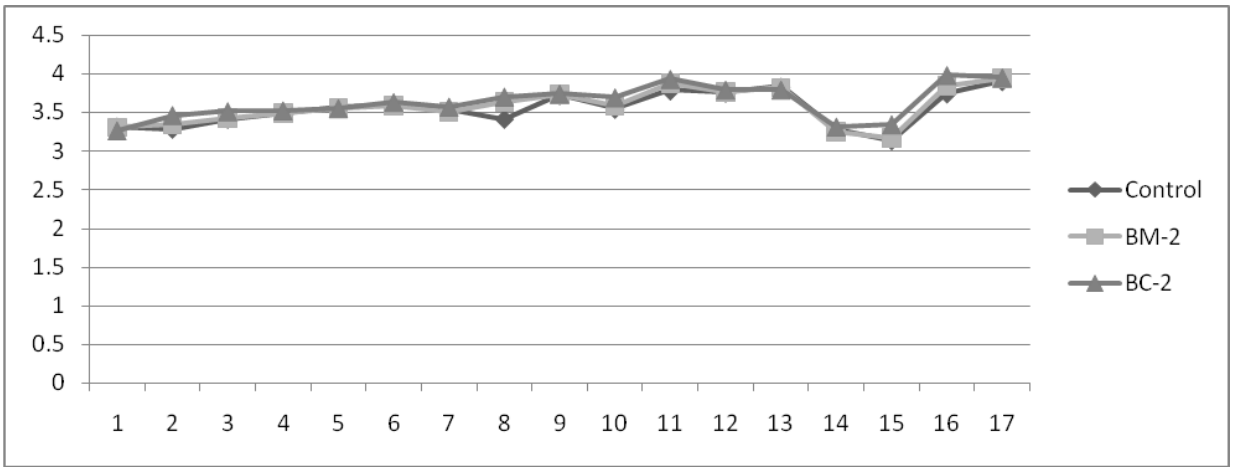

Fig. 4 (b). Emission trends of carbon monoxide from Control, BM-2 and BC-2 soils.

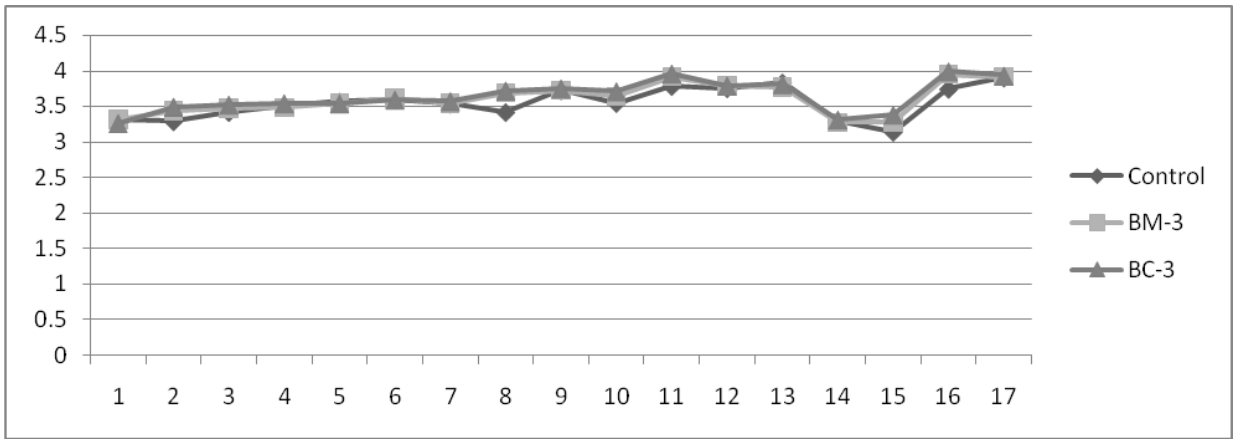

Fig. 4 (c). Emission trends of carbon monoxide from Control, BM-3 and BC-3 soils.

rest of the soils where phosphine emission from biomass (straw and saw dust) treated soils exceeded the average emission quantities compared to their corresponding biochar treatments (0.14 gm/ha from both biomass treated soils and 0.13gm/ha from both biochar treated soils) (Table 4).

Although, emission from saw dust treated soil was fairly high (0.13 gm/ha on day 7) from the inception compared to soil treated with corresponding biochar (0.09 gm/ha on day 7) yet, by the end of the experiment, BC-3 soil yielded far less (0.16 gm/ha on day 59) phosphine compared to BM-3 soil (0.19gm/ha on day 59) (Table 4). The initial emission from BM-1soil (0.13gm/ha on day 5) is lower compared to BC-1 soil (0.16gm/ha on day 5). In the mid-phase of the experiment phosphine emission from BC-1 is lower than the BM-1 soil on several occasions (Table 4) and finally by the terminal period of the experiment BC-1 yielded lower than BM-1 on an average (Table 4).

Gundale and DeLuca (2006) assessed that combustion or charring of organic materials can greatly enhance phosphorus availability from plant tissue by disproportionately volatilizing carbon and by cleaving organic phosphorus bonds, resulting in a residue of soluble phosphorus salts associated with the charred material which in turn will increase the phosphine emission from soil. The available phosphorus content in biochar treated soils have been found to have greatly increased compared to biomass treated soils after 60 days of incubation at field capacity (Personal communication, Khadiza Tahera Khan) and the conducted study complies with this finding as because decreased trends in emission of phosphine from biochar treated soils is observed. Moreover, several bacteria for instance, *Bacillus krulwichiae*, *Bacillus flexus*, *Bacillus sylvestris Aneurinibacillus aneurinilyticus*, *Paenibacillus apiaris*, *Bacillus siralis*, and *Bacillus badius* have been found in the differently treated soils after 30 days (Personal communication, Tazeen Fatima Khan) and perhaps these micro organisms are responsible for reinitiating the emission of phosphine gas after 30 days of incubation. The results are valid on a statistical ground indicating their significance (P value 0.00) at 5% level and indicate that biochar has a positive effect in reducing phosphine production from soil, however, this effect is visible only after a certain period (18 days after the initiation of the experiment)

Impact of Biomass and Biochar on the Evolution of Volatile Organic Compounds from Soil

The effects of biomass and biochar on the retention of volatile organic compounds (g/ha) from soils are presented in the table 5 and the patterns of VOCs are graphically presented in the figures 6 (a, b, c).

Table 5 and the figure 6 (a, b, c) express that regardless of

Table 4. Quantities of phosphine (gm/ha) emitted from differently treated soils.

Day	Control	BM-1	BC-1	BM-2	BC-2	BM-3	BC-3
3	0.12	0.12	0.12	0.12	0.15	0.12	0.12
5	0.16	0.13	0.16	0.13	0.16	0.16	0.13
7	0.13	0.13	0.09	0.09	0.09	0.13	0.09
9	0.13	0.13	0.13	0.16	0.13	0.16	0.13
11	0.16	0.16	0.13	0.16	0.16	0.13	0.16
13	0.16	0.16	0.16	0.13	0.13	0.16	0.13
15	0.13	0.13	0.10	0.13	0.13	0.13	0.13
17	0.19	0.19	0.19	0.19	0.19	0.19	0.19
19	0.19	0.22	0.16	0.19	0.16	0.16	0.16
21	0.16	0.16	0.19	0.19	0.16	0.19	0.16
23	0.22	0.19	0.16	0.19	0.16	0.16	0.16
25	0.19	0.13	0.10	0.13	0.10	0.13	0.10
29	0.09	0.09	0.06	0.13	0.06	0.09	0.06
38	0.10	0.06	0.03	0.03	0.03	0.06	0.03
45	0.10	0.10	0.10	0.10	0.10	0.10	0.10
52	0.22	0.19	0.19	0.19	0.16	0.19	0.16
59	0.19	0.19	0.19	0.19	0.19	0.19	0.16
Average emission	0.15	0.15	0.13	0.14	0.13	0.14	0.13

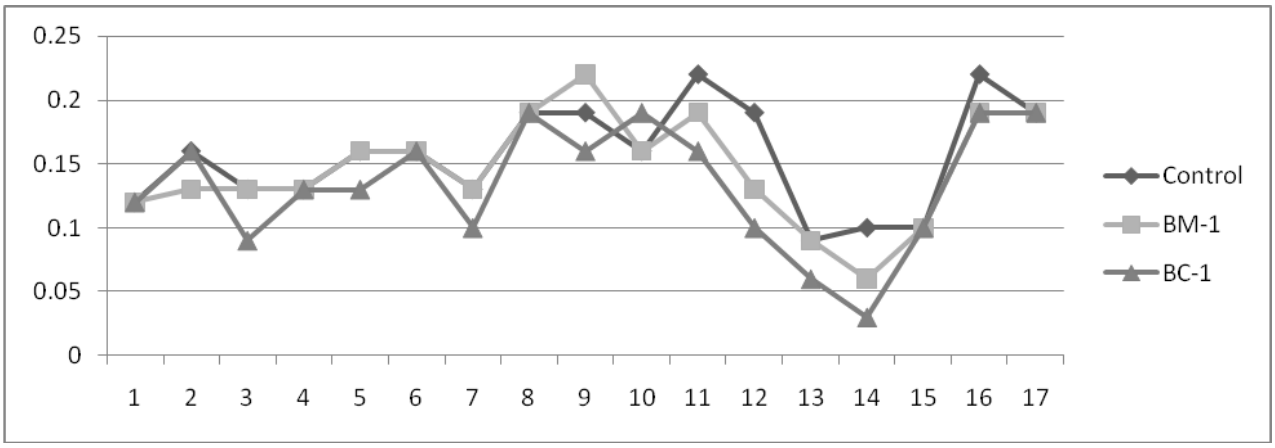

Fig. 5 (a). Emission trends of phosphine from Control, BM-1 and BC-1 soils.

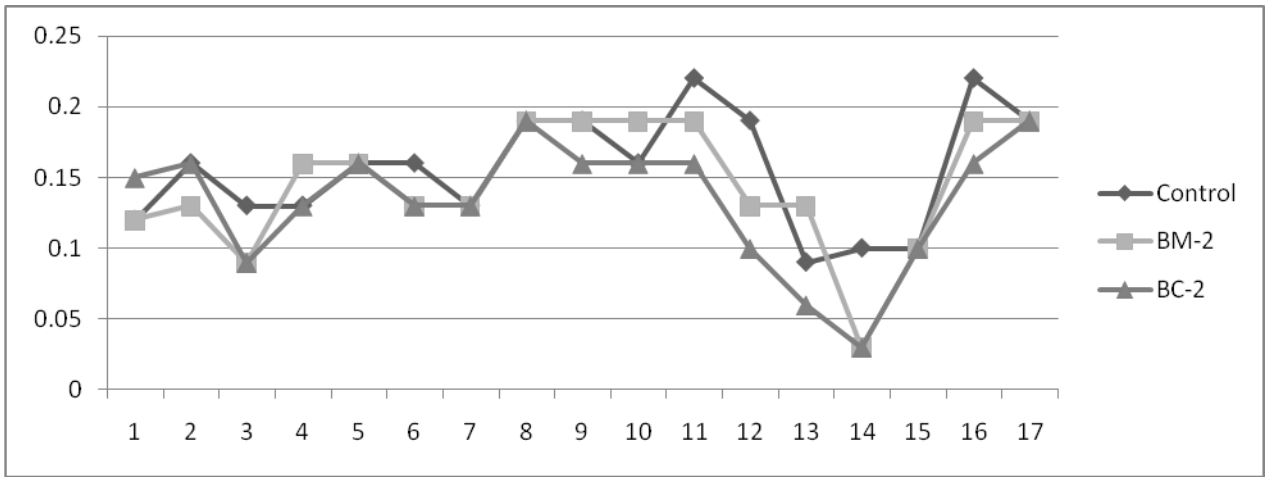

Fig. 5 (b). Emission trends of phosphine from Control, BM-2 and BC-2 soils.

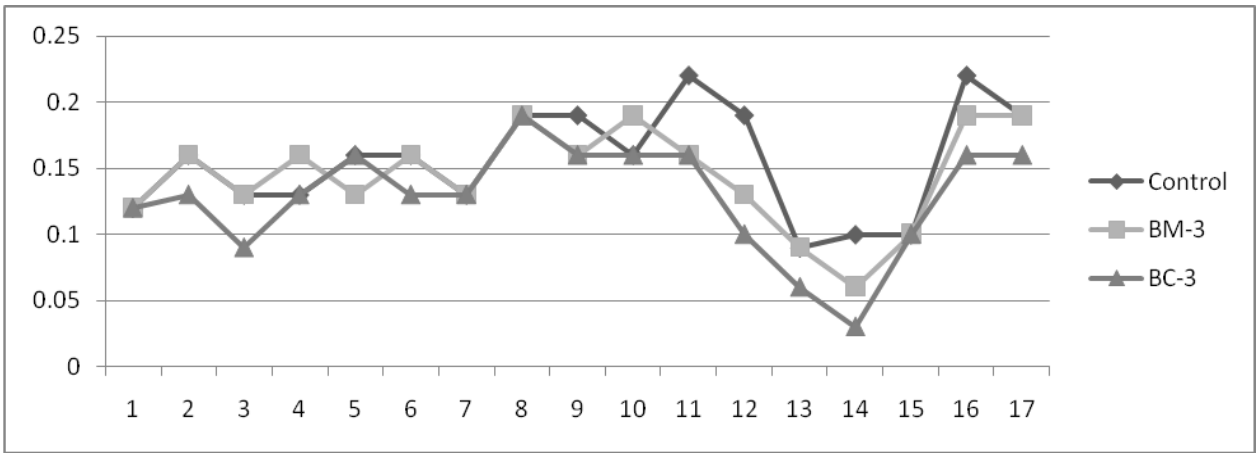

Fig. 5 (c). Emission trends of phosphine from Control, BM-3 and BC-3 soils.

various applied treatments, the production of volatile organic compounds followed a definite pattern in all cases. The Control soil showed the least amount of volatile organic compound production. On an average, emission was the least from the Control soil (9.5gm/ha) whereas soil receiving biochar treatments of saw dust, BC-3 soil, yielded the highest amount (10.4gm/ha) which was almost identical compared to the emission from its corresponding biomass (10.3gm/ha) (Table 5). The average emission from soils treated with biomass rice

husk was (10.08gm/ha) higher than their corresponding biochar (9.37gm/ha) treatments, whereas emission from the soils having biomass straw also expelled higher (10.3gm/ha) amount compared to the soil treated with the corresponding biochar (9.6 gm/ha) (Table 5). Among the biochar treated soils, average emission of volatile organic compounds from BC-1 (9.37gm/ha) was the least indicating the fact that rice husk biochar is better in suppressing volatile organic compounds loss (Table 5).

To surmise, except for BC-3 soil, the retention of volatile organic compounds was more prominent in the case of soil treated with biochar produced from rice husk (BC-1 soil) than all the biomass treated soils. Statistical analysis, based on the empirical data, revealed significant results (P value 0.426) at 5% level and this phenomenon was only visible after 5 days of the experiment.

A very interesting feature of volatile organic compounds emanation from soil was observed in the mid- phase of the experiment. During the fourth and fifth week, discharge of VOCs from all the soils, regardless of their applied treatment, reduced down to nearly nil and on day 29, emission from the soils treated with biochars literally seized to exist (0.00gm/ha) (Table 5 and Figs. 6 a, b and c). This might have ensued from the fact that after 30 days, soils were exhausted of carbonaceous compounds; the microbes could not attack biochar and biochar adhered particles due to the recalcitrant factor. After sixth week, emission restarted and gained an increase. This might be due to the microbial metabolism upon the debris (dead cells of microbes) existing within the soil or the activities of some resilient bacteria. Several bacteria for instance, *Bacillus krulwichiae*, *Bacillus siralis*, and *Bacillus badius* have been found in the similarly treated soils after 30 days (Personal communication, Tazeen Fatima Khan) and these might be the reason for the reinitiating of volatile organic compounds emission after 30 days of incubation.

It is well documented that a wide range of highly oxygenated volatile organic compounds (e.g. levoglucosan, hydroxylacetaldehyde, furfurals, methoxyphenols and carboxylic compounds) are retained on the pores of the surface of biochar and some of these compounds have the potentiality to react with nitrous oxide in order to fix it within the soil (Milne *et al.*, 1998) and this is in agreement with the present observations.

CONCLUSION

The Global temperature rise and its consequences have long been debated over the last century. Despite of all the debates, numerous studies explained that the earth is gradually warming up due to the greenhouse effect. New and substantial measures are needed to be employed in order to combat this crisis and mitigating the greenhouse gases should be the focal concern. Along with anthropogenic activities, soil itself emits greenhouse

Table 5. Quantities of volatile organic compounds (gm/ha) emitted from differently treated soils.

Day	Control	BM-1	BC-1	BM-2	BC-2	BM-3	BC-3
3	9.5	10.08	11.26	10.4	12.2	10.7	11.0
5	12.0	11.98	10.09	11.7	12.3	11.4	12.3
7	11.4	11.08	10.77	11.1	10.4	11.4	10.1
9	12.4	12.36	13.31	13.3	13.6	13.3	13.0
11	14.9	15.17	14.85	15.5	14.9	15.8	15.2
13	14.2	14.16	12.59	14.2	12.6	14.5	13.2
15	9.8	10.78	12.04	11.4	12.7	12.0	12.4
17	13.4	14.39	14.71	14.7	16.6	15.0	16.3
19	15.9	16.57	15.61	16.2	14.7	15.6	14.7
21	10.2	10.56	10.56	9.6	9.9	10.6	10.6
23	8.3	12.49	11.85	12.5	11.5	11.8	11.2
25	0.2	0.29	8.31	0.2	10.2	0.2	7.0
29	0.3	2.84	0.0	4.7	0.0	2.2	0.0
38	8.0	7.65	5.74	7.7	4.8	7.7	5.1
45	6.3	6.66	3.80	6.3	3.2	6.7	7.0
52	7.3	7.33	3.50	8.6	2.9	8.3	8.0
59	6.9	6.94	0.32	7.6	1.6	7.6	9.1
Average emission	9.5	10.08	9.37	10.3	9.6	10.3	10.4

gases through natural means as well as through human induced actions like intensive agriculture. There are significant scopes for greenhouse gas mitigation in agriculture, but for the potential to be completely realized numerous barriers need to be overcome. To minimize the emission of these greenhouse gases and some other harmful gases to the environment a relatively new but revised approach is the utilization of biochar. The application of biochar as a significant means of mitigating carbon dioxide, carbon monoxide and other harmful gases

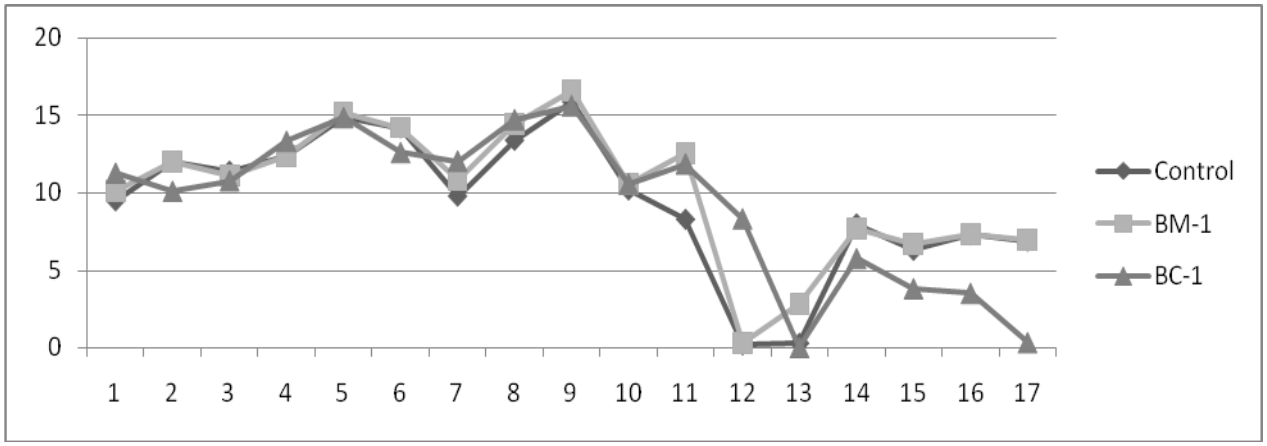

Fig. 6 (a). Emission trends of volatile organic compounds from Control, BM-1 and BC-1 soils.

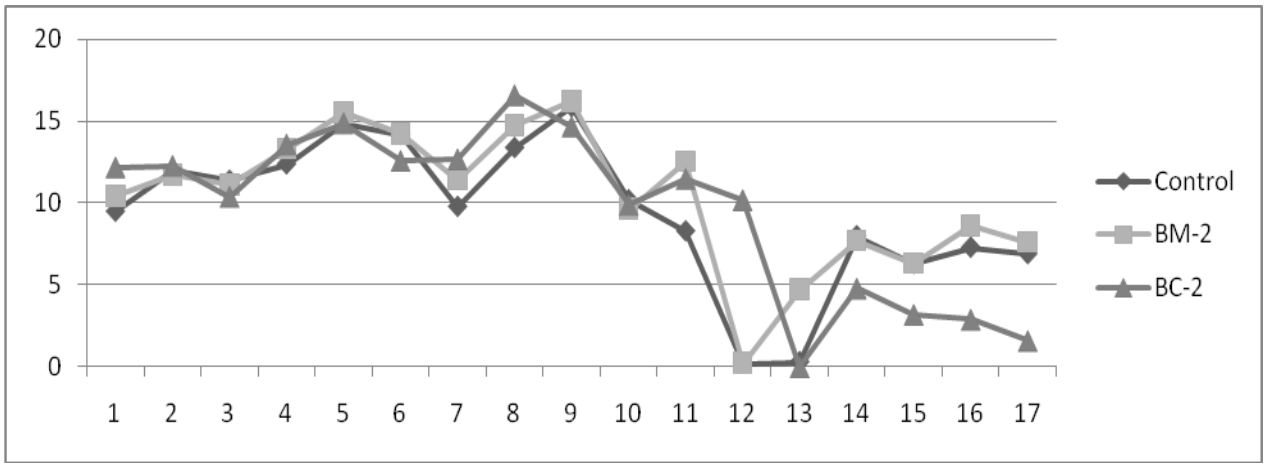

Fig. 6 (b). Emission trends of volatile organic compounds from Control, BM-2 and BC-2 soils.

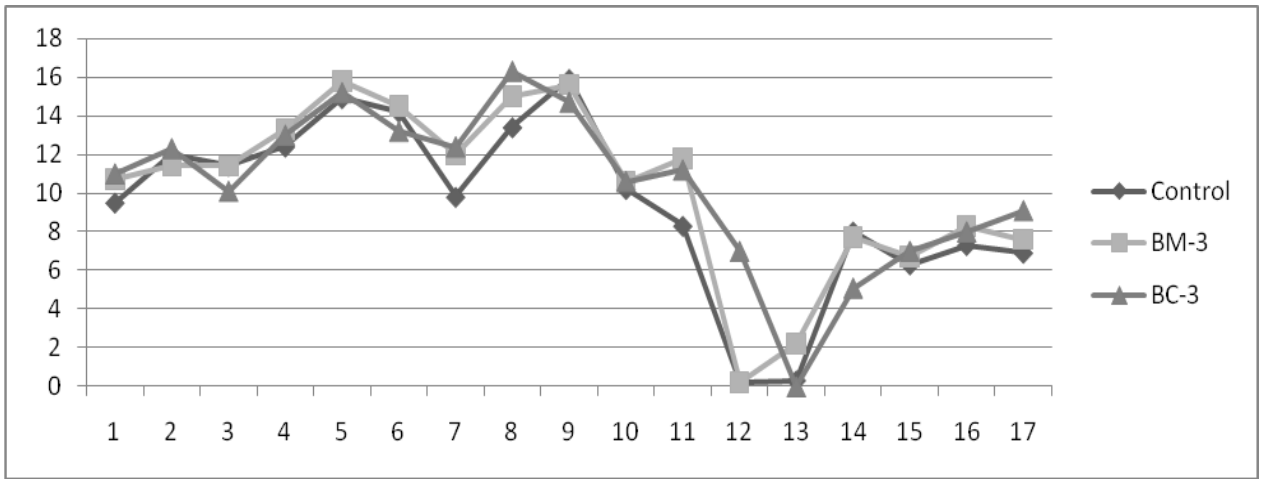

Fig. 6 (c). Emission trends of volatile organic compounds from Control, BM-3 and BC-3 soils.

like phosphine and retaining volatile organics in soil could be highly beneficial to Bangladesh and the rest of the world. This is a simplistic low cost means of adding nutrients to soil and helping agriculture flourish. It can, therefore be useful in the developing countries. With carbon capturing, there is very little impact on people or other organisms and the effects of global warming could be reduced. Environmental protection and human health will be the leading benefactors in large scale biochar production.

ACKNOWLEDGEMENT

Technical helps rendered by Dr. A. H. Khan and Mr. A. T. M. Kamal during the calibration of the instruments are greatly acknowledged.

REFERENCES

Aneja, VP., Viney, P., Aneja, BJ., Roelle, PA., Schlesinger, WH., Knighton, R., Niyogi, D., Gilliam, W., Jennings, G. and Duke, CS. 2006. Proceedings, Workshop on Agricultural Air Quality: State of the Science, held at North Carolina State University, Raleigh, North Carolina. http://ncsu.edu/airworkshop/.

Conrad, R. and Seiler, W. 1985. Characteristics of Abiological CO Formation from Soil Organic Matter, Humic Acids, and Phenolic Compounds. Environ. Sci. Technol. 19:1165-1169.

Cox, PM., Betts, RA., Jones, CD., Spall, SA. and Totterdell, IJ. 2000. Acceleration of Global Warming Due to Carbon-Cycle Feedbacks in a Coupled Climate Model. Nature, London. 408:184-187.

Donham, KJ., Knapp, LW., Monson, R. and Gustafson, M. 1982. Acute Toxic Exposure to Gases from Liquid Manure. J. Occup. Med. 24:142-145.

Gundale, MJ. and Deluca,TH. 2006. Temperature and Substrate Influence the Chemical Properties of Charcoal in the Ponderosa Pine/Douglas-Fir Ecosystem. Forest Ecol.Manage. 31: 86-93.

Imamul Huq, SM. and Alam, MD. 2005. A Handbook on Analyses of Soil, Plant and Water. BACER-DU, University of Dhaka, Bangladesh. pp 32.

Imamul Huq, SM. and Shoaib, JU. 2013. The Soils of Bangladesh, (e-Book). Springer Dordrecht Heidelberg New York London. pp165.

Kammann, C., Ratering, S., Eckhard, C. and Muller, C. 2012. Biochar and Hydrochar Effects on Greenhouse Gas (Carbon Dioxide, Nitrous Oxide, Methane) Fluxes from Soils. J. Environ. Qual. 41:1052-1066.

Kwapinski, W., Byrne, CMP., Kryachko, E., Wolfram, P., Adley, C., Leahy, JJ., Novotny, EH. and Hayes, MHB. 2010. Biochar from Biomass and Waste. Waste Biomass Valor. 1:177-89.

Laird, DA. 2008. The Charcoal Vision: A Win-Win Scenario for Simultaneously Producing Bio-Energy, Permanently Sequestering Carbon, While Improving Soil and Water Quality. Agron. J. 100:178-181.

Lehmann, J., Gaunt, J. and Rondon, M. 2006. Bio-Char Sequestration in Terrestrial Ecosystems – A Review. Mitigation and Adaptation Strategies for Global Change.11:403-427.

Lehmann, J. 2007. Bio-Energy in the Black. Front. Ecol. Environ. 5(7):381-387.

Milne, TA., Evans, RJ. and Abatzoglou, N. 1998. Biomass Gasifier ‘Tars`: Their Nature, Formation, and Conversion, Report no. NREL/TP-570-25357, National Renewable Energy Laboratory, Colorado. www.nrel.gov/docs/fy99osti/25357.

Parkin, TB. and Kaspar, TC. 2003. Temperature Controls on Diurnal Carbon Dioxide Flux: Implications for Estimating Soil Carbon Loss. Soil Sci. Soc. Am. J. 67:1763-1772.

Qayyum, MF., Steffens, D., Reisenauer, HP. and Schubert, S. 2012. Kinetics of Carbon Mineralization of Biochars Compared with Wheat Straw in Three Soils. J. Environ. Qual. 41:1210-1220.

Seifritz, W. 1993. Should We Store Carbon in Charcoal? Int. J. Hydrogen Energy. 18:405-407.

US Energy Information Administration. 2010. International Energy Outlook, US Department of Energy, Washington, DC, USA.

Yoo, G. and Kang, H. 2012. Effects of Biochar Addition on Greenhouse Gas Emissions and Microbial Responses in a Short-Term Laboratory Experiment. J. Environ. Qual. 41:1193-1202.

Received: Dec 11, 2013; Accepted: Jan 23, 2014

SENRA Academic Publishers, British Columbia
Vol. 8, No. 2, pp. 2825-2836, June 2014
Online ISSN: 1920-3853; Print ISSN: 1715-9997

Canadian Journal of pure&applied sciences

AFLATOXIN AND OCHRATOXIN PRODUCTION IN GROUND COFFEE DURING STORAGE

*Amira Hassan Abdullah Al-Abdalall and Ebtisam Abdullah Al-Talib
Department of Biology, Faculty of Science, Dammam University, El-Dammam, Kingdom of Saudi Arabia

ABSTRACT

Coffee beans can be affected by storage microorganisms, the most notable of those are the fungi that cause severe deterioration of the infected beans. The objective of this study was to investigate the existence of fungi in the samples of Arabica and Robusta ground coffee, as it was observed that they were contaminated with fungi, based on the degree of roasting, humidity and storage duration. The results show the capability of the fungi to produce aflatoxin and ochratoxin A in ground coffee of harari and barri as well as Robusta coffee stored in various temperatures and moisture conditions. Aflatoxin and ochratoxin A were produced in most samples in various amounts. Furthermore, there was not any correlation between the number of existing fungi and the concentration and types of these toxins. For the samples stored in 10% humidity, the total of aflatoxin in barri and dark roasted coffee was 4.387 µg/g, but cappuccino was free of aflatoxin. For the samples under relative humidity of 25%, the french coffee was the most contaminated with toxins with Aflatoxin concentration of 10.436 µg/g, whereas Barri mild roasted coffee was the least contaminated with total Aflatoxin concentration of 0.547 µg/g. In the samples of the relative humidity of 45% stored for 30 days at room temperature, the Barri white roasted coffee was the most contaminated samples, as the total toxins 4.604 µg/g, whereas there wasn't Aflatoxin in Nescafe samples. Regarding Ochratoxins, it has been observed that in twelve samples out of thirty three samples, the fungi couldn't produce ochratoxins. That means that 63.64% of the total samples have produced such toxin, and Cappuccino samples stored for 30 days in 10% humidity have been contaminated with the highest rate of Ochratoxin with 1.40µg/g.

Keywords: Ochratoxin A, Aflatoxin, ground coffee, storage, *Aspergillus*

INTRODUCTION

Ochratoxin A (OTA) can be found in various food products, including the green coffee beans, roasted coffee and instant coffee. It has been found that such toxins are genotoxic, carcinogenic, teratogenic, and immune suppressive, thus causing harm to animals including human beings as stated by Schlatter *et al.* (1996) and Holzhauser *et al*. (2003). Many studies have confirmed the ability of stored fungi to produce toxins, mainly Ochratoxins in the green coffee beans (Nakajima *et al.*, 1997; Romani *et al.*, 2000; Otteneder and Majerus, 2001; Pittet and Royer, 2002; Batista *et al.*, 2002). Surveys conducted on green coffee beans stored from different origins established that African coffee samples contained the highest concentration of Ochratoxins compared to samples of American and Asian origin (Pardo *et al.*, 2004). Filamentous fungi can affect the quality and safety of the final product due to production of mycotoxins during preparation and storage (Batista *et al.*, 2002; Taniwaki *et al.*, 2003; Quiroz *et al.*, 2005; Taniwaki, 2006). Ochratoxin A (OTA) is a mycotoxin produced by secondary metabolism of many filamentous species belonging to the genera *Aspergillus* and *Penicillium* (Keeper-Goodman and Scott, 1989; Miller and Trenholm, 1994; Bredenkamp *et al*., 1989; Budavari, 1989).

Little information is available on the existence of toxins of Ochratoxin A in coffee beans during hydration and mechanical treatment and the impact of these operations on the existence and production of Ochratoxin A. The data published so far indicates that the process of removing pulp reduces the risk of contamination by these toxins through fermentation during drying and there is a need to study the microbiological processes (Frank, 2001), and to protect coffee from contamination by Ochratoxin A, there is a need to know what fungi are capable of producing these toxins and their relationship with drying of coffee grains and process of removing pulp, It was found that there are low concentrations of these toxins in the coffee produced by many countries (Buchcli *et al*., 1998; Pardo *et al*., 2004). Humans are inevitably exposed to a certain levels of these toxins. The pollution with this toxin can happen during the process of drying (Urbano *et al*., 2001), where they noticed the presence of these toxins in the beans prior to storage and pointed out the possibility that the harvest and post-harvest stage may cause the pollution. The frequent occurrence of pollution was confirmed by Le-Bars and Le-Bars (2000) in crops all over the world, which is the

Corresponding author email: dr2000amira@hotmail.com

main fungal poison tainting coffee beans. It has been suggested that *A. niger* and closely related species such as *A.carbonarius* can produce Ochratoxin A in the coffee beans (Bucheli *et al*., 1998), while the *Aspergillus ochraceus* Fungus is the most significant producer of Ochratoxin A in coffee beans (Pitt, 2000).

Heenan *et al*. (1998) and Taniwaki *et al*. (2003) stated that 2-3% of *A. niger* separated from coffee beans was able to produce ochratoxin whereas 13% of *A. niger* taken from Thailand coffee was able to produce OTA and OTB. But these contaminations are few compared with *A. carbonarius* which is considered as the most contaminating source for the Thailand coffee.

The existence of ochratoxin A in the coffee is not desirable because it could hamper the coffee trade and affect the economics of coffee-producing countries. The European Commission did not specify minimum levels of ochratoxin A in coffee. There is only one recommendation, in which there is a reference to the level of 3 mg/kg, which was a proposal of a member in the European Union (Romani *et al*., 2000). Another study, Silva *et al*. (2000) reported that contamination of Arabic coffee beans (*Coffea arabica* L.) with ochratoxin A as a result of fungal contamination with *Aspergillus* species including: *A. suphureus, A. ochraceus, A. melleus, A. dimorphicus, A. Sclerotiorum, A. auricomus, A. ochraceus, A. sulphureus, A. sclerotiorum* were producing ochratoxin, as well as *A. niger. A. foetidus* taken from 128 samples, (44.29%) of them is capable of producing ochratoxin A while (30.80%) is not able to produce this toxin.

In a previous study carried out by Joosten *et al*. (2001) on more than 14 samples of green coffee from Southern Thailand, it was found to be contaminated by black molds, and it was observed that half of them were related to *A. carbonarius*. Based on this, we assume that the black fungus, especially fungus *A. carbonarius* plays an important role in the contamination of coffee beans with OTA in Southern Thailand.

Through the studies carried out by Taniwaki *et al*. (2003) on the arabic coffee, the results indicate that *A. niger* is the major fungus exists in the coffee, where it produced ochratoxin with the rate of 63% of the total ochratoxin produced, while the *A. ochraceus* was 31% of the total isolates and produced 3% of the total ochratoxin, and he also stated that 75% of fungi isolated were able to produce ochratoxin. Also *A. carbonarius* was isolated from 6% of the samples taken from the warmer areas during storage, and 77% of the isolates of fungus was capable of producing the toxins.

The increase in the production of ochratoxin in coffee stored at different moisture levels for a period of 20-30 days of storage was observed. There was also a notable difference in the variation and physiological characters of fungi, and usually the poor storage and high humidity caused the production of ochratoxin within ten days (Ahmed and Magan 2006), while Betancourt and Frank (1983) stated that it is necessary that the humidity content in the coffee beans should be less than 14.5% to prevent the mold during storage.

Premila and Sanchez (2006) studied the effects of temperature and various farm environments on the growth of *A. flavus* and the production of Aflatoxins contaminated peanuts in Georgia. The results have shown that the fungus could grow at a temperature of 10^{o}C and produced aflatoxin, as well as the temperature of 37^{o}C. They got the highest production of fungal growth and toxin at a temperature of 27, 30^{o}C in three different farm environments which are potato Dextrose agar (PDA) and nutrient agar (NA) and corn maltose agar (CMA).

Bokhari (2007) reported that the beans of coffee were highly polluted with toxins fungi, especially those producing ochratoxin A. The incidence of this pollution and production of mycotoxins starts from the harvest, where production is affected by the moisture content of the beans and grow during transport and during storage and marketing.

In a study performed by Ilic *et al*. (2007) on Vietnamese robusta coffee beans, it was found that *A. nige*r is the only type which produces OTA. Leong *et al*. (2007) tested the ability of 13 isolates of the fungus *A. carbonarius* isolated from Arabic coffee samples and robusta coffee arbica on toxin OTA production and found that 11 of them were able to produce these toxins.

Moslem *et al*. (2010) were able to isolate a group of fungi associated with the beans of coffee where *A. flavus* achieved highest frequency rate of 50%, followed by the *A. carbonarius*. They found that 80% of the isolates of the *A. flavus* were able to produce OTA toxins. Alborch *et al*. (2011) studied the ability of *A. niger and A. carbonarius* isolated from corn beans to produce OTA toxins where they noted that the optimum temperature to produce the highest rate of toxins of the two fungi was 15^{o}C.

Iqbal *et al*. (2011) found that contamination of samples of chilli with Aflatoxin increased to 61% of samples stored at a temperature of 25, 30^{O}C from those stored at 20^{O}C and number of fungi increased directly proportional to increasing the storage period.

Aflatoxin contaminated coffee is considered a global problem. Taniwaki (2006) mentioned that a lot of green coffee beans samples were contaminated with these toxins in varying degrees ranging from 2.0 - 360 µg/kg. This study aimed at studying the effect of storage period, temperature, humidity and degree of roasting on fungal

pollution and producing aflatoxins and ochratoxin in ground coffee.

MATERIALS AND METHODS

Storage studies on ground coffee

The Fungal invasion and ability of *Aspergillus* and *Penicillium* to produce aflatoxins and ochratoxins were studied, where plastic boxes were equipped with 100 grams of ground coffee for tested varieties and then placed in the center of each packet Cup small glass by concentration calculated from sulfuric acid so that each can has the required concentration (10, 25, 45%) of the relative humidity (Solomen, 1951). Then all boxes were stored at room temperature (25 ± 2) and for different periods of time (30, 20, 10 days). The results were counted of numbers of fungal colonies per 1gram of ground coffee (Alvnindia and Acda, 2010).

Mycotoxins analysis

Apparatus of High Performance Liquid Chromatography (HPLC) system

The High Performance Liquid Chromatography (HPLC) system consisted of Waters Binary pump Model 1525, a Model Waters 1500 Rheodyne manual injector, a Waters 2475 Multi-Wavelength Fluorescence Detector, and a data workstation with software Breeze 2. A phenomenex C_{18} (250x 4.6mm i.d), 5um from Waters corporation (USA) for aflatoxins**.** A HyperClone 5µ ODS column (C_{18}) 120A° , DIM: 250 x 4.60mm (Phenomenex).

Extraction of Aflatoxins by VICAM method (2000)

Sample Extraction

Weigh 25g sample with 5g salt sodium chloride and place in blender jar. Add to jar 125ml methanol: water (70:30). Cover blender jar and blend at high speed for 1 minute. Remove cover from the jar and pour the extract into fluted filter paper. Collect filtrate in a clean vessel.

Extract Dilution

Pippet or pour 15ml filtered extract into a clean vessel. Dilute extract with 30mL of purified water, mix well. Filter diluted extract through the glass microfiber filter into a glass syringe barrel using markings on barrel to measure 4ml.

Immunoaffinity Chromatography

Pass 15 ml filtered diluted extract (15ml = 1g sample equivalent) completely through AflaTest ®-P affinity column at a rate of about 1-2 drops/second until the air comes through column. Pass 5ml of purified water through the column at a rate of about 2 drops/second. Elute affinity column by passing 1.0ml HPLC grade methanol through the column at a rate of 1-2 drops/second and collecting all of the sample eluate (1ml) in a glass vial. Evaporated to dryness under a stream of nitrogen and was determined of HPLC.

Detection and determination of Aflatoxins by HPLC

Derivatization

The derivatives of samples and standard were done as follow:100µl of trifluoracetic acid (TFA) were added to samples and mixed well for 30 s and the mixture stand for 15min. 900µl of water: acetonitrile (9:1 v/v) were added and mixed well by vortex for 30 s and the mixture was used for HPLC analysis.

HPLC conditions

The mobile phase consists of Acetonitile/Water/ methanol (1:6:3). The separation was performed at ambient temperature at a flow rate of 1.0 ml/min. The injection volume was 20µl for both standard solutions and sample extracts. The fluorescence detector was operated at an excitation wavelength of 365nm and an emission wavelength of 450nm. AFB_1 concentration in the samples was determined from the standard curve, using peak area for quantification.

Ochratoxin analysis

HPLC Equipment

The HPLC system consisted of Waters Binary pump Model 1525, a Model Waters 1500 Rheodyne manual injector, a Watres 2475 Multi-Wavelength Fluorescence Detector, and a data workstation with software Breeze 2.

Chemicals and Reagents

OTA standard, Chartist, microfiber filter 1.5µm, and filter papers were purchased from VICAM. Milford, MA USA. Acetonitrile, glacial acetic acid HPLC grade were obtained from BDH, England. Sodium chlorid, sodium biocarbonate, sodium hydrogen phosphate, potassium dihydrogen phosphate and potassium chloride were purchased from (BDH, Merck chemicals). And tween -20 obtained from Sigma (St. Louis, MO, USA).

HPLC condition

A Symmetry C_{18} (5 µm particle size, 150 mm X 4.6 mm i.d.) from the Waters Corporation (USA), were used along with a mobile phase of Acetonitile/Water/ acetic acid (55:43:2). The separation was performed at ambient temperature at a flow rate of 1.0 ml/min. The injection volume was 50µL for both standard solutions and sample extracts. The fluorescence detector was operated at an excitation wavelength of 330nm and an emission wavelength of 470nm. OTA concentrations in coffee extracts were determined from the standard curve, using peak area for quantitation.

Instant coffee

The instant coffee extraction carried out according to the method of Pittet *et al*. (1996). Briefly: Five gram of soluble coffee was weighed accurately into plastic centrifuge bottles and mixed with respectively 100ml of methanol-3% aqueous sodium hydrogen carbonate

(50:50). The suspension was blended for 3min at medium speed using a blander. Then homogenized sample was filtered through 11cm Whatman GF/B glass microfiber filter under reduced pressure. Then 4 ml of filtrate was transferred to a graduated cylinder and diluted to 100 ml with PBS pH 7.4. The whole diluted extract was applied to an immunoaffinity column, at a slow, steady flow rate of 2-3 m/min. After washing the column with 10 ml of distilled water, OTA was eluted with 1.5ml of methanol. To ensure complete removal of the bound toxin, the methanol was left in contact with the column for at least 3 min. This was achieved by reversing the flow of methanol (back flushing) two or three times. The elute was then evaporated to dryness under a stream of nitrogen at 40°C, and the residue was redissolved in 3 ml of HPLC mobile phase.

Statistical Analysis

The results obtained in this research were analyzed statistically using the sixteenth version of SPSS16 program where transaction averages were compared at the abstract level (0.05) using the least significant difference test (LSD) designed by Norusis (1999).

RESULTS

1. Effect of storage period and the percentage of moisture and the degree of roasting on the fungi presence in ground coffee for Arabic coffee types

Results in table 1, show the storage of ground coffee for 10days on the humidity rates of 10, 25, 45% and at room temperature indicate the presence of many fungi in ground coffee as varied in their distribution to the different classes and gave the following percentages 61, 41, 25.19, 9.44, 1.57, 0.78, 0.78% for each of *A. alliaceus, A. niger, A. flavus, A. melleus, A. fumigates, F. solani, Penicillium* sp., respectively.

Table 2 related to the storage of ground coffee according to the previous conditions for a period of 20days indicates the occurrence of fluctuation in the fungi existence, and the isolated fungi were in descending order as follows: *A. niger* (76,03%), followed by *A. tubingensis* (13,22%), *A. flavus* (7,43%), *A. melleus* (1,65%), *A. alliaceus* (0,82%) and *Aspergillus* sp. (0.82%).

The results of table 3 related to the storage of the ground coffee for the period of 30days at different humidity ratios a diversity of fungal isolates in terms of the number and types and in descending order were as follows:

70.87, 12.62, 5.82, 4.85, 2.91, 1.94, 0.97% for the *A. niger, A. alliaceus, A. flavus, A. melleus, Aspergillus* sp., *Penicillium* sp., *F. solani* respectively.

Table 1. Effect of storage (10 days), relative humidity, and the degree of roasting on the fungal diversity of coffee samples of Arabica ground coffee for harari and barri varieties.

Isolates		Harari dark			Harari mild			Harari white			Barri dark			Barri mild			Barri white			Total isolates	% Frequency
		Humidity %																			
		10	25	45	10	25	45	10	25	45	10	25	45	10	25	45	10	25	45		
A. niger		5	3	8	4	2	2	3	4	-	-	-	-	1	-	-	-	-	-	32	25.19
A. flavus		-	-	-	1	1	-	1	1	1	-	2	-	2	-	1	1	-	1	12	9.44
A.fumigatus		-	-	-	1	-	-	-	-	-	-	-	-	-	-	-	-	-	-	1	0.78
A. melleus		-	2	-	-	-	-	-	-	-	-	-	-	-	-	-	-	-	-	2	1.57
A. alliaceus		-	2	6	1	6	10	-	1	3	9	11	5	5	4	5	4	4	2	78	61.41
F. solani		-	-	-	-	-	-	1	-	-	-	-	-	-	-	-	-	-	-	1	0.78
Penicillium sp.		-	-	-	-	-	-	1	-	-	-	-	-	-	-	-	-	-	-	1	0.78
Total isolates	Total	5	7	14	7	9	12	6	6	4	9	13	5	8	4	6	5	4	3		
	Each of roasted degree	26			28			16			27			18			12			127	
	Each variety	70									57										

Table 2. Effect of storage (20 days), relative humidity, and the degree of roasting on the fungal diversity of coffee samples of Arabica ground coffee for harari and barri varieties.

Isolates		Harari dark			Harari mild			Harari white			Barri dark			Barri mild			Barri white			Total isolates	% Frequency
		Humidity %																			
		10	25	45	10	25	45	10	25	45	10	25	45	10	25	45	10	25	45		
A. niger		7	8	5	4	4	7	3	2	-	7	7	12	2	3	14	1	3	3	92	76.03
A. flavus		-	1	1	1	1	1	1	-	-	-	-	-	-	2	-	1	-	-	9	7.43
A. melleus		-	-	-	1	-	-	1	-	-	-	-	-	-	-	-	-	-	-	2	1.65
A. alliaceus		-	-	-	-	-	-	1	-	-	-	-	-	-	-	-	-	-	-	1	0.82
A. tubingensis		-	-	4	7	-	1	2	-	-	-	1	-	1	-	-	-	-	-	16	13.22
Aspergillus sp.		-	-	-	-	-	-	-	-	-	-	-	-	-	1	-	-	-	-	1	0.82
Total isolates	Total	7	9	10	31	5	9	8	2	-	7	8	12	3	6	14	2	3	3		
	Each of roasted degree	26			27			10			27			23			8			121	
	Each variety	63									58										

Table 3. Effect of storage (30 days), relative humidity, and the degree of roasting on the fungal diversity of coffee samples of Arabica ground coffee for harari and barri varieties.

Isolates		Harari dark			Harari mild			Harari white			Barri dark			Barri mild			Barri white			Total isolates	% Frequency
		Humidity %																			
		10	25	45	10	25	45	10	25	45	10	25	45	10	25	45	10	25	45		
A. niger		3	6	10	3	3	6	3	2	2	10	8	2	-	4	1	6	2	2	73	70.87
A. flavus		-	-	1	-	-	-	-	-	-	2	-	1	-	1	-	-	-	1	6	5.82
A. melleus		1	-	-	1	-	1	-	-	-	-	-	-	1	1	-	-	-	-	5	4.85
A. alliaceus		-	-	-	-	-	-	-	-	1	-	-	9	1	2	-	-	-	-	13	12.62
F. solani		-	-	-	-	-	-	-	-	-	-	-	-	-	-	-	-	1	-	1	0.97
Penicillium sp.		-	-	-	-	-	-	-	-	-	1	-	-	-	-	-	-	-	1	2	1.94
Aspergillus sp		1	1	-	-	-	-	-	-	-	1	-	-	-	-	-	-	-	-	3	2.91
Total isolates	Total	5	7	11	4	3	7	4	2	3	13	8	12	1	8	2	6	3	4		
	Each of roasted degree	23			14			9			33			11			13			103	
	Each variety	46									57										

Table 4 related to averages general activity of fungi at tested humidity levels and periods of storage and the degree of roasting varieties of ground Arabic coffee indicates that the storage period has an effect, where there was a decrease in the rate of fungal pollution with increased storage up to 30 days, where the rate was 36.18, 34.47, 29.34% after storage for 10, 20, 30 days.

With regard to the items, the results show that was more polluted with fungi where the rate of fungi was 50.99% compared Barri varieties in which the percentage of fungal contamination is up to 49.01%.

2. Effect of the storage period and the percentage of moisture on the fungal presence in the types of ground coffee of Robusta Coffee

Results shown in table 5 related to robusta ground coffee stored for 10days indicate the existence of fungi isolated from tested samples and a group of fungi were isolated in descending order by repetition of isolation as follows: 23.40, 27.21, 21.27, 12.76, 10.63, 4.25, 2.12, 2.12, 2.12% for each of *A. melleus, A. flavus, A. alliaceus, A. niger, Alternaria* sp., *Paecilomyces variotii, A. fumigates, F. solani, Penicillium* sp., respectively.

The results shown in table 6 related to the storage of coffee for 20days indicate a diversity of fungi isolated from tested samples and were, in descending order as follows: 22.44, 20.40, 18.36, 16,32, 14.28, 8, 16%) for each *of E. nidulans, A. flavus, A. tubingensis, A. melleus, A. niger, F. solani*, respectively.

Whereas results in table 7 related to the storage for the period of 30days indicate noted decrease in fungi, and ordered dissentingly as follow: *A.niger* (40,74%), followed by *A. melleus* (33,33%), *A. flavus* (7,40%), *A. alliaceus* (7,40%), *E. nidulans* (7.40%) and finally *Aspergillus* sp. (3.70%).

Also the storage period may affect the incidence averages as the general averages show a rise in the number of fungi with the increase in the storage period up to 20days and then decreased again after 30days of storage where it was 38.21, 39.84, 21.95% after 10, 20, 30days, respectively.

With regard to the percentage of humidity, the results in table 8 indicated that there is a difference in the numbers of fungi where a decrease generally observed in the number of fungi with the increased humidity ratio to 35.77, 33.33, 30.09%, when humidity rates are 10, 25, 45%, respectively.

As for the different varieties of coffee it has been observed that there is a remarkable variation in the degree of fungal contamination where pollution averages show the pollution of Turkish coffee at 83.26%, followed by cappuccino with the rate of 58.23% and french coffee with the rate of 33.20% and finally Nescafe without caffeine in 38, 11%.

Table 4. Average general activity of fungi at tested humidity levels and periods of storage and the degree of roasting varieties for ground arabic coffee.

Impact factor			Harari dark	Harari mild	Harari white	Barri dark	Barri mild	Barri white	Total isolates
Total isolates	Each humidity levels	10%	17	24	18	29	12	13	113 (32.19%)
		25%	23	17	10	29	18	10	107 (30.48%)
		45%	35	28	7	29	22	10	131 (37.32%)
	Each periods of storage	10 days	26	28	16	27	18	12	127 (36.18%)
		20 days	26	27	10	27	23	8	121 (34.47%)
		30 days	23	14	9	33	11	13	103 (29.34%)
	Each periods of storage		75 (21.37%)	69 (19.66%)	35 (9.97%)	87 (24.78%)	52 (14.81%)	33 (9.40%)	
	Each variety		179(50.99%)			172(49.01%)			

Table 5. Effect of storage for 10 days and relative humidity on the fungal diversity of coffee samples of Robusta ground coffee.

Isolates		Nescaffee			Cappuccino			Turkish coffee			French coffee			Nescaffee with out			Total isolates	% Frequency
		Humidity %																
		10	25	45	10	25	45	10	25	45	10	25	45	10	25	45		
A. niger		-	1	-	-	-	-	-	2	-	1	-	1	-	-	1	6	12.76
A. flavus		-	-	-	-	5	-	-	1	1	-	2	-	1	-	-	10	21.27
A. fumigatus		1	-	-	-	-	-	-	-	-	-	-	-	-	-	-	1	2.12
A. melleus		1	-	-	2	4	-	-	4	-	-	-	-	-	-	-	11	23.40
A. alliaceus		-	-	-	-	-	-	6	-	-	-	-	3	-	-	1	10	21.27
F. solani		1	-	-	-	-	-	-	-	-	-	-	-	-	-	-	1	2.12
Alternaria		-	-	-	5	-	-	-	-	-	-	-	-	-	-	-	5	10.63
P. variotii		-	-	-	-	-	-	-	-	-	-	-	2	-	-	-	2	4.25
Penicillium		-	-	-	-	-	-	-	-	-	-	1	-	-	-	-	1	2.12
Total isolates	Total	2	1	1	7	9	-	7	7	-	1	3	6	1	-	2	47	
	Each variety	4			16			14			10			3				

Table 6. Effect of storage for 10 days and relative humidity on the fungal diversity of coffee samples of Robusta ground coffee.

Isolates		Nescaffee			Cappuccino			Turkish coffee			French coffee			Nescaffee with out			Total isolates	% Frequency
		Humidity %																
		10	25	45	10	25	45	10	25	45	10	25	45	10	25	45		
A. niger		-	-	-	-	-	-	-	-	1	1	-	3	-	1	1	7	14.28
A. flavus		-	-	-	1	1	1	-	1	-	1	3	-	-	-	2	10	20.40
A. melleus		-	-	-	-	-	2	3	-	-	1	1	1	-	-	-	8	16.32
A. tubingensis		1	-	-	-	-	-	5	-	-	1	-	-	1	-	1	9	18.36
E. nidulans		11	-	-	-	-	-	-	-	-	-	-	-	-	-	-	11	22.44
F. solani		2	-	-	-	-	-	-	-	-	-	-	-	-	-	2	4	8.16
Total isolates	Total	14	-	-	1	1	3	8	1	1	4	4	4	1	1	6	49	
	Each variaty	14			5			10			12			8				

Table 7. Effect of storage for 10 days and relative humidity on the fungal diversity of coffee samples of Robusta ground coffe.

Isolates		Nescaffee			Cappuccino			Turkish coffee			French coffee			Nescaffee with out			Total isolates	% Frequency
		Humidity %																
		10	25	45	10	25	45	10	25	45	10	25	45	10	25	45		
A. niger		-	1	-	-	2	2	-	3	-	1	1	-	-	-	1	11	40.74
A. flavus		-	-	-	-	1	-	3	-	1	-	-	-	-	-	-	2	7.40
A. melleus		-	-	1	1	-	1	1	3	-	-	-	1	-	1	-	9	33.33
A. alliaceus		-	1	-	-	-	1	-	-	-	-	-	-	-	-	-	2	7.40
E. nidulans		1	-	-	-	-	-	-	-	-	-	-	-	1	-	-	2	7.40
Aspergillus sp.		-	-	-	-	-	-	-	1	-	-	-	-	-	-	-	1	3.70
Total isolates	Total	1	2	1	1	3	4	1	7	1	1	1	1	1	1	1	27	
	Each variaty	4			8			9			3			3				

Table 8. Averages general activity of fungi at tested humidity levels and periods of storage in ground Robusta coffee

Impact factor			Nescaffee	Cappuccino	Turkish coffee	French coffee	Nescaffee with out	Total
Total isolates	Humidity %	10%	17	9	9	6	3	44(35.77%)
		25%	3	13	15	8	2	41(33.33%)
		45%	2	7	9	11	9	38(30.09%)
	Each periods of storage	10 days	4	16	14	10	3	47(38.21%)
		20 days	14	5	10	12	8	49(39.84%)
		30 days	4	8	9	3	3	27(21.95%)
	Each variaty		22 (17.89%)	29 (23.58%)	33 (26.83%)	25 (20.33%)	14 (11.38%)	123

3. Qualitative and quantitative assessment of aflatoxins and ochratoxin in ground coffee of arabica and robusta coffee

Results shown in table 9 regarding the qualitative and quantitative assessment of mycotoxins of aflatoxin and ochratoxin in crushed of harari and barri coffee, and also the types of robust stored at room temperature for 30days at the different humidity ratios indicated that these toxins were produced in all samples with varying degrees and it wasn't observed that there is a correlation between the number of fungi and the concentrations and types of these toxins. It was also found that the concentration of toxins was not associated with a fixed relationship with humidity, and in general it has been observed that in the samples stored at 10% samples of Barri coffee samples which is black roasted, the Aflatoxin toxins were 4.382µg/g while cappuccino samples were not having any concentration of Aflatoxins.

Regarding the samples with a relative humidity of 25%, the most polluted samples were French coffee, where Aflatoxin concentration reached 463.10µg/g, while the coffee samples of Barri type which are mild roasted are the least polluted with toxins where total aflatoxins were 547.0µg/g of the coffee.

Table 9. Qualitative and quantitative assessment of aflatoxins and ochratoxin in ground coffee of arabica and robusta coffee after stored for 30 days at 25 ± 2°C and different degree of humidity.

Varieties	Humidity 45 %						Humidity 25 %						Humidity 10 %					
	B1	B2	G1	G2	Total	OTA	B1	B2	G1	G2	Total	OTA	B1	B2	G1	G1	Total	OTA
Harari dark	1.184	0.5	0.586	0.806	3.076	ND	1.422	0.5	1.006	0.604	3.532	ND	2.322	0.468	0.008	0.756	3.554	ND
Harari mild	1.138	0.028	ND	ND	1.166	0.61	1.184	0.032	ND	ND	1.216	0.31	2.748	ND	ND	1.362	4.11	ND
Harari white	0.616	0.188	0.05	0.04	0.894	0.39	0.710	0.182	ND	0.202	1.094	0.62	0.616	ND	ND	0.202	0.818	0.39
Barri dark	1.422	0.344	1.002	0.554	3.322	0.23	1.468	0.406	0.920	0.604	3.398	0.20	2.086	0.468	1.172	0.656	4.382	0.30
Barri mild	1.896	0.656	1.172	0.604	4.328	0.15	0.355	0.091	ND	0.101	0.547	0.35	1.848	0.406	1.006	0.6.4	3.864	25
Barri white	2.086	0.624	1.088	0.806	4.604	0.30	1.80	0.648	0.920	0.656	4.024	0.76	1.848	0.656	1.170	0.604	4.278	0.30
Nescaffee	ND	ND	ND	ND	-	0.6	6.634	0.156	ND	ND	6.79	ND	1.326	0.188	0.334	0.302	2.152	0.17
Cappu-ccino	0.094	0.124	ND	ND	0.218	0.6	2.086	0.592	1.006	0.908	4.592	0.18	ND	ND	ND	ND	-	1.40
Turkish coffee	0.468	0.188	0.334	0.352	2.342	ND	1.942	0.250	1.256	0.454	3.902	ND	1.322	ND	ND	ND	1.322	ND
French coffee	0.355	ND	ND	ND	0.355	ND	5.687	ND	3.264	1.512	10.463	0.18	1.421	ND	ND	ND	1.421	0.22
Nescaffee with out	1.468	0.406	1.172	0.554	3.6	ND	0.758	ND	0.026	ND	0.784	ND	0.710	ND	0.05	ND	0.760	ND
Average	1.066	0.278	0.491	0.338	2.173	0.262	2.186	0.259	0.764	0.458	3.668	0.236	1.477	0.199	0.340	0.408	2.424	2.526
L.S.D. at 0.05%	5.01	3.79	3.11	3.31	4.21	3.39	3.54	3.60	2.59	3.23	4.11	3.03	6.06	2.62	2.21	3.11	4.89	1.12

The samples with relative humidity of 45% and stored also for 30days at room temperature were sampled product of Barri variety of light roasting, which were more samples in terms of Aflatoxins totaling 604.4µg/g while there is no producing of aflatoxins in samples of Nescafe.

With regard to the production of fungi to ochratoxin in ground coffee, it was observed that twelve samples of the total of thirty-three samples, the fungus were unable to produce of ochratoxin, that is 64.63% of the samples produced fungi with this toxin, where cappuccino samples stored for thirty days with 10% humidity were contaminated with Ochratoxin by 40.1µg/g, while the highest production of this poison in moisture of 25% were in the samples of light barri where it was 76.0µg/g. Also, the pollution of harari variety was noted in the relative humidity of 45% with the highest percentage of ochratoxin which was 61.0µg/g.

DISCUSSION

The results of qualitative and quantitative assessment of aflatoxin and ochratoxin in ground coffee of arabica and robusta stored at room temperature for 30days at different humidity ratios indicated that these toxins were produced in all samples with varying degrees and there wasn't any correlation between the number of fungi and the concentrations and types of these toxins. And it was also found that the concentration of toxins was not associated with a stable relationship with the humidity.

With regard to the production of ochratoxin in ground coffee, it was observed that in twelve of the total samples of thirty-three fungi cannot produce of Ochratoxin, that is in 64.63% of the samples the fungus produced this toxin. This high rate corresponds with the results of many researchers such as (Nehad *et al.*, 2007; Moslem *et al*., 2010; Iqbal *et al.*, 2011). Another study, Taniwakin *et al*. (2003) and Logrieco *et al*. (2003) stated that *A. ochraceus* can be the primarily responsible for the pollution of coffee with ochratoxin. While, Taniwaki *et al*. (2003) considered that *A. carbonarius, A. niger, A. ochraceus* are the main producing for OTA toxins in Brazilian coffee beans, which found that 77% of the isolates fungus were able to produce toxins of OTA.

RECOMMENDATIONS

The current research proved that there is serious damage happens to the coffee during storage and this damage is in contamination with fungi of store which is harmful, especially *Aspergillus, Penicillium, Fusarium* which are resulted in the produce of several mycotoxins. The matter increases this damage is the high temperature of storage and humidity. Therefore, this study recommends the following as an attempt to avoid the fungal attack and minimize the damage as much as possible, where toxins of ochratoxin and aflatoxin were found in tested coffee as well as the ability of all fungal isolates to produce mycotoxins which requires us not to stand idly by, so we recommend the need for periodic inspection of samples of coffee in stores and eliminate what may be contaminated with these mycotoxins. We also advise more stringent laws to prevent the entry of any shipments of coffee products contaminated with either fungi or its toxins.

REFERENCES

Ahmed, R. and Magan, N. 2006. Monsooned coffee: impact of environmental factors on fungal community structure, enzyme production profiles and ochratoxin. Aspects of Appl. Biol. (Abstract).

Alborch, L., Bragulat, MR., Abarca, ML. and Cabañe, FJ. 2011. Effect of water activity, temperature and incubation time on growth and ochratoxin A production by *Aspergillus niger* and *Aspergillus carbonarius* on maize kernels. International J. of Food Microbiol. 147(1):53-57.

Alvindia, DG. and Acda, MA. 2010. Mycoflora of coffee beans in the Philippines. J. ISSAAS. 16:116-125.

Batista, LR., Chalffoun, SM., Prado. G., Schwan, RF. and Wheals, AE. 2002. Toxigenic fungi associated with processed (green) coffee beans (*Coffea arabica L.).* Int. J. Food Microbiol. 62:1-8.

Betancourt, LE. and Frank, HK. 1983. Behavior of ochratoxin A during green coffee roasting and soluble coffee manufacture. J. Agric. Food Chem. 46:673-675.

Bokhari, FM. 2007. Mycotoxins and toxigenic fungi in Arabic coffee beans in Saudi Arabia. Adv. Biol. Res. 1:56-66.

Bucheli, P., Meyer, I., Pittet, A., Vuataz, G. and Viani, R. 1998. Industrial storage of green robusta under tropical conditions and its impact on raw material quality and Ochratoxin A content. J. Agric. Food Chem. 46:4507-4511.

Bredenkamp, MW., Dillen, JLM., Van Rooyen, PH. and Steyn, PS.1989. Crystal structures and conformational analysis of ochratoxin A and B: Probing the chemical structure causing toxicity. J. Chem. Soc. 2:1835-1839.

Budavari, S. (editor). 1989. In: The Merck Index. An Encyclopedia of Chemicals, Drugs and Biologicals. 11th Edition, Merck & Co., Rahway, NJ, USA.

Frank, JM. 2001. On the activity of fungi in coffee in relation to ochratoxin A production. 19th ASIC Coffee Conference, Trieste, Italy.

Heenan, CN., Shaw, KJ. and Pitt, JI. 1998. Ochratoxin A production by *Aspergillus carbonarius* and *A. niger*

isolates and detecting using coconut cream agar. J. Food Mycol.1:67-72.

Holzhauser, D., Delatour, T., Marin-Kuan, M., Junod, S., Guignard, G., Pigue, D., Richoz, J., Bezencon, C., Schilter, B. and Cavin, C. 2003. Ochratoxin A: toxicity and carcinogenicity. Toxicol. Letters. 144:65.

Ilic, Z., Bui, T., Tran-Dinh, N., Dang, MHV., Kennedy, I. and Carter, D. 2007. Survey of Vietnamese coffee beans for the presence of ochratoxigenic Aspergilli. Mycopathol. 163:177-182.

Iqbal, CZ., Paterson, RM., Bhatti, IA., Asi, MR., Sheikh, MA. and Bhatti, HN. 2011. Aflatoxin B1 in chilies from the Punjab region, Pakistan. Mycotox Res. 26:205-209.

Joosten, H., Goetz, J., Pittet, A., Schellenberg, M. and Bucheli, P. 2001. Production of ochratoxin A by *Aspergillus carbonarius* on coffee cherries. International J. of Food Microbiol. 65:39-44.

Keeper-Goodman, T. and Scott, PM. 1989. Risk assessment of the mycotoxin ochratoxin. Biomed. Environ. Sci. 2:179-248.

Le-Bars, J. and Le-Bars, P. 2000. Mycotoxigenesis in grains application to mycotoxic prevention in coffee. Coffee Biotechnol. and Quality. Sera, Netherlands: Kluwer Academic Publishers. 355-368.

Leong, SL., Hien, LT., An, TV., Trang, NT., Hocking, AD. and Scott, ES. 2007. Ochratoxin A-producing aspergilli in Vietnamese green coffee beans. Letters in Appl. Microbiol. 45:301-306.

Logrieco, A., Bottalico, A., Mulé, G. and Moretti, A. 2003. Epidemiology of toxigenic fungi and their associated mycotoxins for some Mediterranean crops. Eur. J. Plant Pathol. 109:645-667.

Miller, JD. and Trenholm, HL. 1994. Mycotoxins in Grain: Compounds other than Aflatoxin. Eagan Press; St. Paul, MN, USA.

Moslem, MA., Mashraqi, A., Abd-Elsalam, KA., Bahkali, AH. and Elnagaer, MA. 2010. Molecular detection of ochratoxigenic *Aspergillus* species isolated from coffee beans in Saudi Arabia. Genet. Mol. Res. 9(4):2292-2299 .

Nakajima, M., Tsubouchi, H., Miyabe, M. and Ueno, Y. 1997. Survey of aflatoxin B1 and ochratoxin A in commercial green coffee beans by high-performance liquid chromatography linked with immunoaffinity chromatography. Food Agric. Immunol. 9:77-83.

Nehad, EA., Farag, MM., Kawther, MS., Abdel-Samad, AKM. and Naguib, K. 2007. An Exposure and in take Assessment of Ochratoxin A from Imported Coffee Beans in Egypt. World J. of Agricultural Sciences. 3(3):285-294.

Norusis, MJ. 1999. SPSS/PC + Statistics 6.0 for the IBM PC/XT/AT and PS/2. Library of Congress, USA.

Otteneder, H. and Majerus, P. 2001. Ochratoxin A (OTA) in coffee: nation-wide evaluation of data collected by German Food Control 1995-1999. Food Addit. Contam. 18:431-435.

Pardo, E., Marin, S., Ramos, AJ. and Sanchis, V. 2004. Occurrence of ochratoxigenic fungi and ochratoxin A in green coffee from different origins. Food Sci. Technol. Inter. 10:45-49.

Pitt, JI. 2000. A laboratory guide to common *Penicillium* species (3rd edi.). CSIRO. pp197.

Pittet, A. and Royer, D. 2002. Rapid, low cost thin-layer chromatographic screening method for the detection of ochratoxin A in green coffee at a control level of 10µg/kg. J. Agric. Food Chem. 50:243-247.

Pittet, A., Tornare, D., Huggett, A. and Viani, R. 1996. Liquid chromatographic determination of ochratoxin A in pure and adultered soluble coffee using an immunoaffinity column clean up procedure. Journal of Agricultural and Food Chemistry. 44:3564-3569.

Premila, A. and Sanchez, A. 2006. Effects of substrate and temperature on growth of *Aspergillus flavus* in peanuts from Georgia. Georgia Journal of Science.

Quiroz, SML., Rios, GO, Barel, M., Guyot, B., Galindo-Schorr, S. and Guiraud, JP. 2005. Influence of coffee processing, water activity, temperature and pH on mould growth and ochratoxin A production in coffee.: HWS-Mycotoxin Research. ASIC 2004. 20th International Conference on Coffee Science, Bangalore, India.

Romani, S., Sacchett,i G., Lopez, CC., Pinnavia, GG. and Rosa, MD. 2000. Screening on the occurrence of ochratoxin A in green coffee beans of different origins and types. J. Agric. Food Chem. 48:3616-3619.

Studer, RJ. and Rasonyi, T. 1996. Carcinogenicity and kinetic aspects of ochratoxin A. Food Additives and Contaminants. 13:43-44.

Silva, CF., Batista, LR., Chalfoun, S. and Schwan, RF. 2000. Ochratoxin A and Fungi Toxigenic in Brazilian Coffee Beans (*Coffea arabica* L.) Universidade Federal de Lavras, Lavras, MG, Brazil. pp12.

Solomen, ME. 1951. Control of humidity with potassiumhydroxide, sulphuric acid and other solutions. Bull. Ent. Res. 42:543-554.

Taniwaki, M. 2006. An update on ochratoxigenic fungi and ochratoxin A in coffee. In: Advances in Food Mycology. Eds. Hocking, AD., Pitt, JI., Samson, RA. and Thrane, U. Springer, New York. 189-202.

Taniwaki, MH., Pitt, JI., Teixeira, AA. and Iamanaka, BT. 2003. The Source of ochratoxin A in Brazilian coffee and its formation in relation to processing methods. Int. J. Food Microbiol. 82:173-179.

Urbano, GR., Taniwaki, MH., Leitao, MF. and Vicentini, MC. 2001. Occurrence of ochratoxin Aproducing fungi in raw Brazilian coffee. J. Food Prot. 64:1226-1230.

Vicam. 2000. The leading mycotoxin testing solutions. Available source: http://vicam.com/home.

Received: Dec 26, 2013; Revised: Jan 16, 2014; Accepted: Jan 21, 2014

SENRA Academic Publishers, British Columbia
Vol. 8, No. 2, pp. 2837-2844, June 2014
Online ISSN: 1920-3853; Print ISSN: 1715-9997

Canadian Journal of pure&applied sciences

ADSORPTION ISOTHERMS OF DECOLOURISATION OF SHEA (*VITELLARIA PARADOXA* GAERTNER F) BUTTER

*Mohagir AM[1], Syed S[2], Bup N D[3], Kamga, R[4] and Kapseu C[4]
[1]Faculty of Science and Technologies, University of Sarh, PO Box 105, Chad
[2]Chemical Engineering Department, King Saud University, PO Box 800, Riyadh-11421, Saudi Arabia
[3] Higher Institute of the Sahel, University of Maroua, Cameroon
[4]National Advanced School of Agro-Process Industries,University of Ngaoundere, Cameroon

ABSTRACT

The objective of this paper was to study the adsorption isotherms of decolourisation of shea butter. The adsorption of pigments from aqueous extracted shea butter using tonsil fuller earth was carried out. The absorbance of crude and decolourised black and yellow shea butter using 1, 2, 3, 4 and 5 mass % of the adsorbent at different temperatures (55, 65, 65, 75, 85 and 95°C) were measured. The experimental data obtained were analysed and fitted to Freundlich and Langmuir equations. Langmuir adsorption isotherm model fitted well the decolourisation of yellow shea butter at 95°C, while Freundlich model significantly fitted the decolourisation of black shea butter at 65°C. Gibbs free energy, enthalpy and entropy of adsorption were generated from the experimental data. The absolute value of enthalpy of adsorption showed that the decolourisation process of shea butter is a physical phenomenon, whereas the negative values of Gibbs free energy suggested that, the adsorption is spontaneous process.

Keywords: Shea butter, decolourisation, tonsil fuller earth, adsorption isotherm, Freundlich, Langmuir.

INTRODUCTION

Shea tree *(Vitellaria paradoxa* Gaertn), produces kernels which have an oil content of about 35-60% called shea butter (Kamga *et al*., 1999). Shea butter is used as cooking oil for some population of African Sahel region. It is used also in traditional medicines and as raw material for many industries such as soap, cosmetics, Pharmaceutics, chocolate, and confectionary (Booth and Wickens, 1988). The aqueous extraction of shea butter, though very tediousness, is still very predominant in the central African region and is the main source of supply of local markets with shea butter. The traditionally extracted butter has shown to be of an inferior quality, producers supply poor quality shea butter (yellow, brown and dark colored, poor hygienic conditions and with high acid and peroxide values). Refining is a step that may be included in the processing chain to improve the quality. Unfortunately only very few papers are found in the literature for the refining of shea butter (Bike Mbah *et al*., 2005). There are two types of shea butter in Chad, namely cosmetic (yellow) and edible (black). Their methods of preparation were described previously (Mohagir, 2003). To produce edible shea butter, shea kernels are roasted in red heated sand in a steel pot and then crushed with wooden mortar and finally grounds. The difference between the two methods is that the production of yellow shea butter not includes the roasting step. Bleaching of vegetable oils is performed for the removal of colour materials, phospholipids, soaps and oxidative products such as peroxides (Norris, 1982). Pigments have the state of a stable colloid in the oil. Their separation needs sufficient means to break the stability of the colloids and this is the essential role of adsorbent (Brimberg, 1982). Adsorption of pigments from vegetable oils with various types of adsorbents has been extremely reviewed (Norris, 1982; Brimberg, 1982; Achife and Ibemesi, 1989; Boki *et al*., 1992; Topallar, 1998). Isotherm plots represent the partition of pigments and other colouring materials between solid phase (adsorbent) and liquid phase (oil). It is a measure of the position of equilibrium in the adsorption process. The purpose of this study is to examine the applicability of Freundlich and Langmuir equations to the adsorption isotherms for the decolourisation of aqueous extracted shea butter using tonsil fuller earth.

MATERIALS AND METHODS

Materials

Aqueous black and yellow extracted shea butters were purchased from local Koumra market, Chad. Adsorbent used is tonsil fuller earth (240 FE, Olifants, Republic of South Africa). The absorbance of oil samples was measured using double beam UV-Visible Spectrophotometer model (SECOMAM, ISO 9001, France).

*Corresponding author email: amohagir2003@yahoo.fr

Methods

Decolourisation procedure

The decolourisation apparatus was composed of 250 ml conical flask equipped with a mechanical agitator of model (Heidolph, RZR1, Germany). The flask was immersed in a thermostated water bath. In each experiment, 30 g of crude shea butter was heated and maintained at the desired temperature for 15 min before adding the adsorbent. After the addition of adsorbent mass%, the mixture was continuously heated and stirred. The agitation rate used was that just enough to keep the clay dispersed (150rpm). After decolourisation (30min), the agitation was stopped and the mixture was filtered immediately by using Joseph filter paper (celite 545) and vacuum filtration pump (960101, Osi-DVD-Bolong, Italy).

Modelling of Isotherms

In this study, the adsorption data were analysed according to Freundlich and Langmuir isotherms (equation 1, 2) which are the most widely utilised models in this domain. Moreover, the correlation coefficient (R^2) was used to judge the applicability of the isotherms

$$\text{Freundlich model}: X/m = KX_e^{1/n} \quad (1)$$

$$\text{Langmuir model}: X_e/(X/m) = \frac{1}{X_{max} * b} + \frac{X_e}{X_{max}} \quad (2)$$

Where X is the relative amount of pigments adsorbed (mg/g), m is the mass of adsorbent (g), K and n are Freundlich constants; K is related to bonding energy, it can be defined as an adsorption or distribution coefficient which describes the amount of pigments adsorbed onto adsorbent agent for the unit equilibrium concentration. The Freundlich constant n is a measure of the adsorption intensity that ranges between 1 and 10 (Tsai *et al*., 2004). X_e is the residual relative amount of pigments at equilibrium (mg/g); X_{max} is the quantity of pigment adsorbed at monolayer or the maximum coverage (mg/g), b is Langmuir adsorption equilibrium constant (g/mg) that is related to direct measurement of the intensity of adsorption process.

The values of X and X_e were obtained from the absorbance of pigment at a wavelength in which the overall absorbance's curve in the selected zone shows maximum peak (Brimberg, 1982). These quantities were calculated using the relation (3)

$$X = \frac{A_0 - A_t}{A_0}, X_e = \frac{A_t}{A_0} \text{ or } = 1 - X \quad (3)$$

Where A_0 and A_t are the absorbance of crude and decolourised oil at equilibrium time t respectively.

Before measuring the absorbance, the black and yellow shea butter was diluted with petroleum ether (1:3 and 1:1) respectively and the absorbance of diluted samples was measured at the pre determined wave length (440 nm).

Freundlich isotherms were generated by plotting log (X/m) versus log (X_e) from the logarithm form of equation 1 and then K and n were determined from the intercept (log K) and slope (1/n). From equation 2, a plot of (X_e/(X/m)) against X_e represents Langmuir isotherms. Langmuir constants X_{max} and b were calculated from slope ($1/X_{max}$) and intercept ($1/ (X_{max}*b)$).

Determination of enthalpy, entropy and Gibbs free energy of adsorption

One of the more important applications of adsorption isotherms data is their utilisation is the determination of some thermodynamic properties such as enthalpy of adsorption ($\Delta H^o_{ad,}$) and the change in standard entropy ($\Delta S^o_{ad.}$). These parameters can be used to evaluate the mechanism of adsorption of pigments onto any adsorbent (Sabah and Celik, 2005; Sabah, 2007). The parameters were determined using Van't Hoff equation (4).

Where, R is the universal gas constant (8.314 $Jmol^{-1}K^{-1}$) and T is the temperature in Kelvin. The plot of Ln (X_e) versus (1/T) yields straight line with intercept ($\Delta S^o_{ad}/R$) and slope ($\Delta H^o_{ad}/R$).

$$Ln(X_e) = \frac{\Delta S^0 ad}{R} - \frac{\Delta H^0 ad}{RT} \quad (4)$$

Gibbs free energy of adsorption ΔG^o_{ad} was calculated from equation 5 as recommended by some authors (Sabah, 2007).

$$\Delta G^0_{ad} = -RTLn(X_e) \quad (5)$$

RESULTS AND DISCUSSION

The absorbance of crude black and yellow shea butter (A_0) was recorded as 1.72 and 2.10 (% light transmission) respectively. On the other hand, the absorbance of the two decolourised samples (A_t) using 1, 2, 3, 4 and 5 mass % of tonsil fuller earth at different temperatures (55, 65, 65, 75, 85 and 95°C) are presented in table 1 and 2.

The decrease in absorbance with increase in adsorbent mass % at constant temperature (Table 1and 2) could be attributed to the greater availability of exchangeable sites of adsorbent.

It is observed that at constant adsorbent mass % (Table 1), the absorbance increased as temperature increased. This means that either the relative amount of pigment adsorbed

Table 1. The absorbance of decolourised black shea butter (A_t) at different adsorbent dose and temperatures.

Adsorbent dose (mass %)					
Temperature (°C)	1	2	3	4	5
55	$0.597^{I}e \pm 0.01$	$0.568^{I}d \pm 0.02$	$0.526^{I}c \pm 0.01$	$0.512^{I}b \pm 0.04$	$0.430^{I}a \pm 0.02$
65	$0.627^{II}e \pm 0.02$	$0.584^{II}d \pm 0.02$	$0.534^{II}c \pm 0.02$	$0.523^{II}b \pm 0.03$	$0.460^{II}a \pm 0.01$
75	$0.703^{III}e \pm 0.04$	$0.658^{III}d \pm 0.01$	$0.538^{III}c \pm 0.03$	$0.529^{III}b \pm 0.01$	$0.468^{III}a \pm 0.04$
85	$0.817^{IV}e \pm 0.01$	$0,672^{IV}d \pm 0.04$	$0.556^{IV}c \pm 0.01$	$0.548^{IV}b \pm 0.02$	$0.491^{IV}a \pm 0.02$
95	$0.890^{V}e \pm 0.02$	$0.730^{V}d \pm 0.01$	$0.602^{V}c \pm 0.03$	$0.572^{V}b \pm 0.03$	$0.548^{V}a \pm 0.02$

Absorbances in the same row with different letters are significantly different ($P < 0.05$)
Absorbances in the same column with different superscripts are significantly different ($P < 0.05$)

Table 2. The absorbance of decolourised yellow shea butter (A_t) at different adsorbent dose and temperatures.

Adsorbent dose (mass %)					
Temperature (°C)	1	2	3	4	5
55	$0.582^{I}e \pm 0.03$	$0.477^{I}d \pm 0.01$	$0.456^{I}c \pm 0.02$	$0.445^{I}b \pm 0.03$	$0.377^{I}a \pm 0.01$
65	$0.535^{II}e \pm 0.01$	$0.460^{II}d \pm 0.02$	$0.446^{II}c \pm 0.01$	$0.418^{II}b \pm 0.01$	$0.363^{II}a \pm 0.03$
75	$0.458^{III}e \pm 0.04$	$0.442^{III}d \pm 0.03$	$0.427^{III}c \pm 0.04$	$0.395^{III}b \pm 0.01$	$0.355^{III}a \pm 0.02$
85	$0.453^{IV}e \pm 0.01$	$0.437^{IV}d \pm 0.02$	$0.413^{IV}c \pm 0.02$	$0.388^{IV}b \pm 0.04$	$0.338^{IV}a \pm 0.04$
95	$0.447^{V}e \pm 0.02$	$0.415^{V}d \pm 0.04$	$0.405^{V}c \pm 0.01$	$0.358^{V}b \pm 0.02$	$0.332^{V}a \pm 0.02$

Absorbances in the same row with different letters are significantly different ($P < 0.05$)
Absorbances in the same column with different superscripts are significantly different ($P < 0.05$)

Table 3. Model constants and coefficients of determination for decolourisation of black shea butter at different temperatures.

	Freundlich constants			Langmuir constants		
Temperature (°C)	n	K	R^2	X_{max}	b	R^2
55	4.09	34.44	0.76	0.13	2.41	0.75
65	4.67	57.02	0.97	0.14	2.41	0.90
75	3.11	7.76	0.90	0.12	1.93	0.85
85	2.52	3.38	0.91	0.12	1.58	0.86
95	2.42	2.38	0.90	0.11	1.42	0.83

Table 4. Model constants and coefficients of determination for decolourisation of yellow shea butter at different temperatures.

	Freundlich constants			Langmuir constants		
Temperature (°C)	n	K	R^2	X_{max}	b	R^2
55	3.62	70.80	0.91	0.10	3.10	0.90
65	4.05	166.73	0.91	0.11	3.38	0.96
75	4.54	180.02	0.79	0.10	4.04	0.93
85	4.67	683.91	0.78	0.10	4.00	0.91
95	4.74	916.22	0.86	0.11	4.13	0.97

X decreased and the residual relative amount of pigments at equilibrium X_e increased during the decolourisation of black shea butter or colour development might be occurring due to oxidation enhancement caused by the increase in temperature. Sabah and Çelik reported that peroxides act by reducing absorbance of chlorophyll and other pigments through their oxidation, and therefore decrease the bleaching performance of adsorbent (Sabah and Celik, 2005). On the other hand, during the decolourisation of yellow shea butter at constant adsorbent mass % as shown in table 2, it is observed that as temperature increased the absorbance decreased, which is the opposite of what was observed for the decolourisation of black shea butter. In this case, the amounts of pigment adsorbed X increased and the residual relative amount X_e in the liquid phase decreased.

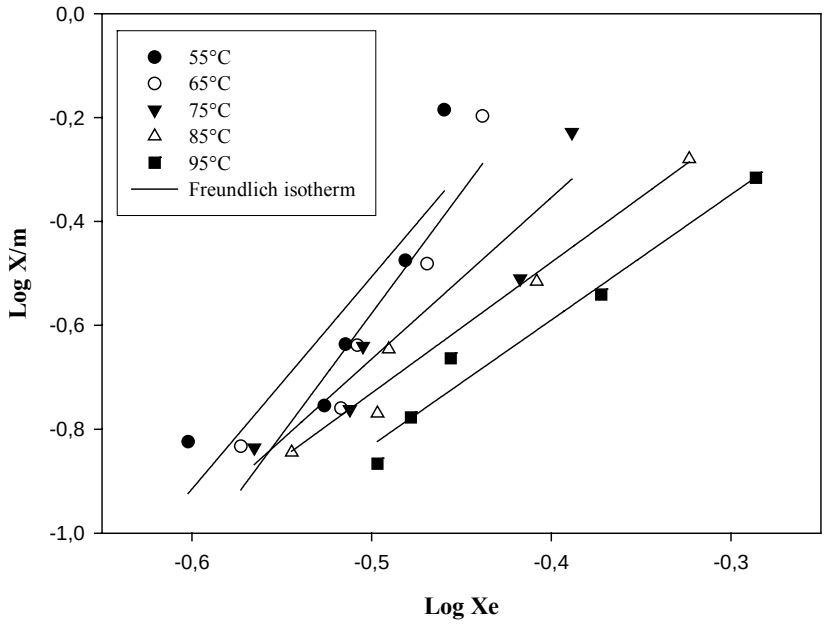

Fig. 1. Freundlich adsorption isotherms of black shea butter (stirred at 150 rpm, heated for 30min). X the relative amount of pigments adsorbed at adsorbent mass m; X_e the residual relative amount of pigments at equilibrium.

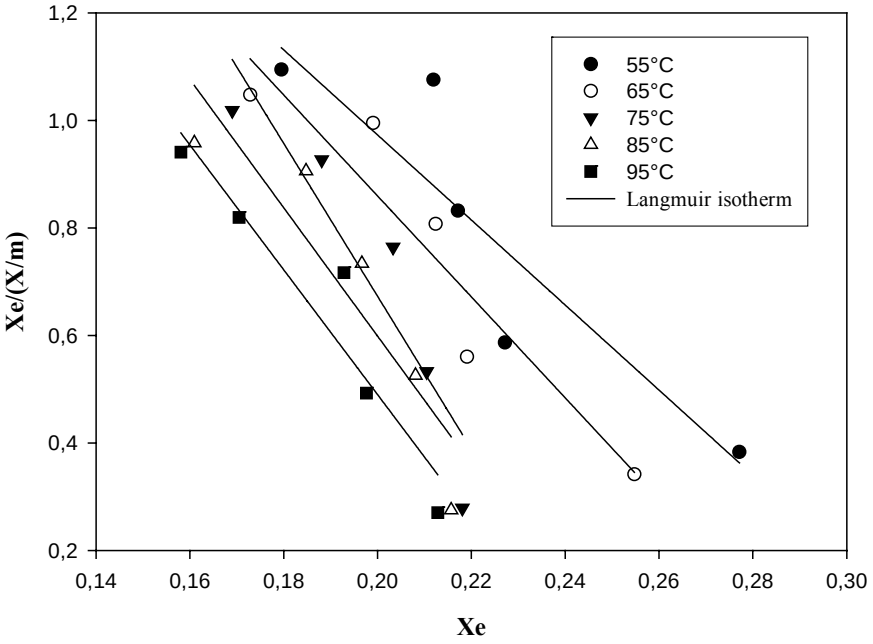

Fig. 2. Langmuir adsorption isotherms of black shea butter (stirred at 150rpm, heated for 30min). X the relative amount of pigments adsorbed at adsorbent mass m; X_e the residual relative amount of pigments at equilibrium.

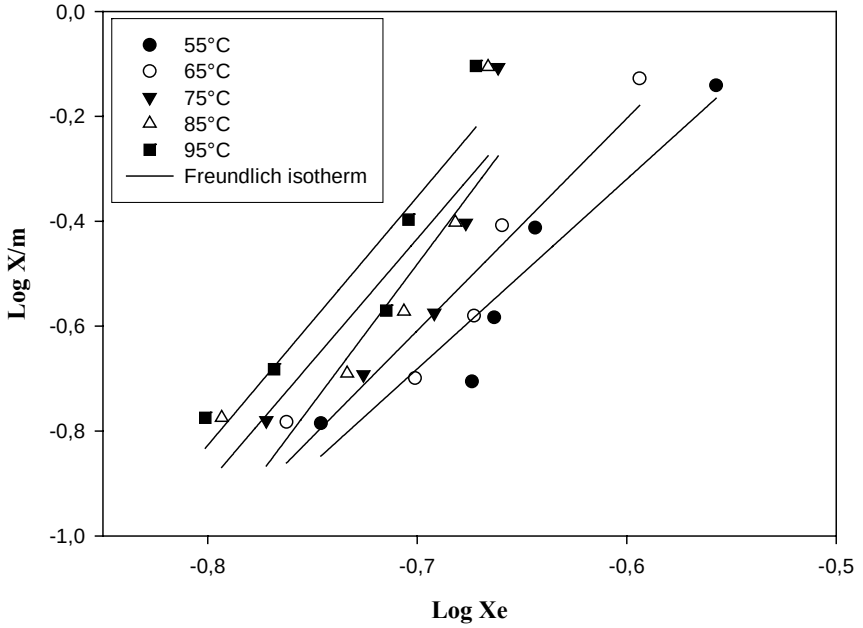

Fig. 3. Freundlich adsorption isotherms of yellow shea butter (stirred at 150 rpm, heated for 30min). X the relative amount of pigments adsorbed at adsorbent mass m; X_e the residual relative amount of pigments at equilibrium.

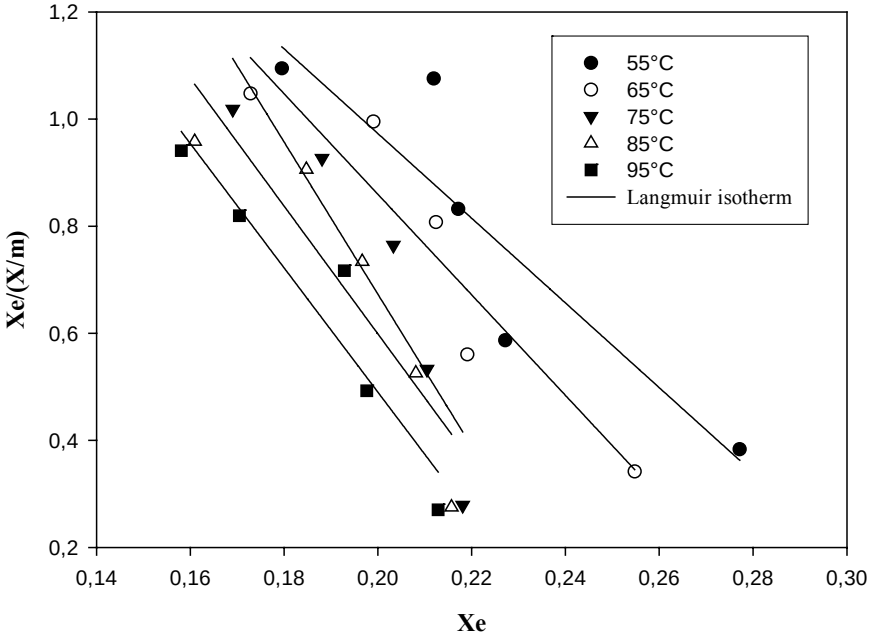

Fig. 4. Langmuir adsorption isotherms of yellow shea butter (stirred at 150 rpm, heated for 30min). X the relative amount of pigments adsorbed at adsorbent mass m; X_e the residual relative amount of pigments at equilibrium

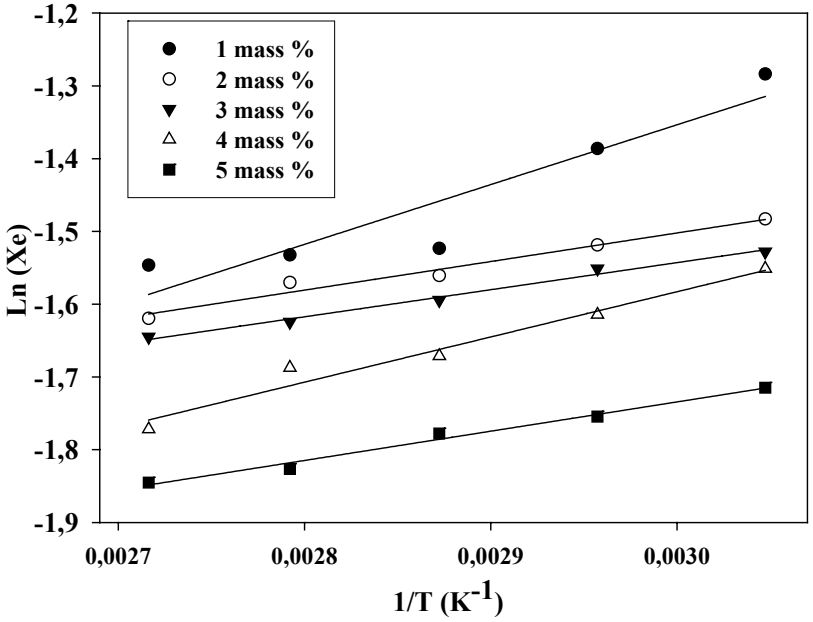

Fig. 5. Temperature dependence of the equilibrium at 1, 2, 3, 4 and 5 adsorbent mass %. Xe the residual relative amount of pigments at equilibrium; T temperature in Kelvin

These observations seem to support the assertion that higher temperatures create more adsorption sites in the adsorbent (Sabah *et al*., 2007).

Adsorption isotherms of black shea butter

The Freundlich and Langmuir adsorption isotherms of the decolourisation of black shea butter with tonsil fuller earth at various temperatures are presented in figure 1 and 2. The values of Freundlich and Langmuir constants in addition to the correlation coefficients are presented in table 3. Data presented in table 3, it is noticed that the adsorption intensity (n, b) reached a maximum at 65°C and then decreased along the range of temperature 65-95°C. Sabah (2007) reported that bleaching of some vegetable oils at high temperature (80-100ºC) and at even high dosages of adsorbent is ineffective in provoking pigment adsorption, because high temperatures encourage oxidation that produces peroxides. The peroxides act to oxidise the pigments and therefore decrease the bleaching performance of the adsorbent. From these results, it could be stated that for decolourisation of black shea butter using tonsil fuller earth, a better decolourising power attained at a temperature of 65°C (K= 57.02, n = 4.67) as indicated by the Freundlich model (R^2 = 97%). The values of n (2.42 - 4.67) appear to be in agreement with the usual range of 1 - 10 obtained for favourable adsorption. A similar trend was observed in the Langmuir model, i.e. highest value of adsorption capacity (X_{max}= 0.1) and intensity of adsorption (b = 2.41) attained at the same temperature (65°C) with R^2 = 90%. It was reported that a bleaching process where b from Langmuir equation is high implies that a small quantity of adsorbent would be consumed (Sabah, 2007). In other words, bleaching earth adsorbs much pigment during colour removal. From these results it might be reported that the adsorption of pigments in black shea butter using tonsil fuller earth obeys the Freundlich model at temperature of 65°C. Hence black shea butter should be decolourised at 65°C.

Adsorption isotherms of yellow shea butter

Figure 3 and 4 show Freundlich and Langmuir adsorption isotherms of the decolourisation of yellow shea butter using tonsil fuller earth at different temperatures. It is noticed that the application of the two models in decolourisation of yellow shea butter vary according to the data in table 4.

These data show that, for the decolourisation of yellow shea butter using tonsil fuller earth, the intensity of adsorption n of Freundlich model and b of Langmuir model increased with an increase in temperature (Table 4). Highest values were achieved at 95 °C for both cases. On the other hand, though the capacity of adsorption (X_{max}) of Langmuir model not followed a clear pattern, the capacity of adsorption K of Freundlich model increased with an increase of temperature and the highest value (916.22) attained at 95°C. Furthermore, the values of the coefficient of determination of the Freundlich and Langmuir isotherms at 95°C indicate that the Freundlich model explained only 86% of the adsorption process,

while Langmuir model explained 97%. Therefore, the Langmuir model better fitted the adsorption isotherm data of decolourisation of yellow shea butter.

Determination of the enthalpy of adsorption, change in entropy and Gibbs free energy

Temperature dependence of the residual relative amount of pigments at equilibrium (Xe) (Fig. 5) at 1, 2, 3, 4, and 5 adsorbent mass % provides the calculation of the heat of adsorption (ΔH^o_{ad}) and the change in standard entropy (ΔS^0_{ad}). From the data in table 5, it is observed that decolourisation of yellow shea butter using tonsil fuller earth is a physical phenomenon, since all the values of enthalpy of adsorption (ΔH^o_{ad}) were less than 20 kJ/mol (Sabah, 2007). The values of coefficients of determination (Table 5) suggested that the adsorption isotherm data were well fitted (R^2 = 0.97-0.99). The negative values of ΔH^0_{ad} (-3.03 -7.05) for the decolourisation of yellow shea butter indicated that the decolourisation is an exothermic process, while the negative values of ΔS^0_{ad} (-0.022 - 0.032 $kJmol^{-1}$) referred to a high binding strength between the colour material and the adsorbent (Liu *et al*., 2004). The negative values of ΔG^o_{ad} in table 6 suggesting that, the adsorption process is spontaneous and that the overall process is thermodynamically favourable. It is also shown that the magnitude of ΔG° generally increased as temperature increased, indicating a greater driving force to sorption, and subsequently leading to higher adsorption capacity at higher temperatures i.e. higher temperatures favour the removal of pigments.

CONCLUSION

Langmuir adsorption isotherm model fitted well the decolourisation of yellow shea butter at 95°C, while Freundlich model fitted well the decolourisation of black shea butter at 65°C. Moreover, the absolute value of enthalpy of adsorption showed that the decolourisation process of shea butter is a physical phenomenon, whereas the negative values of Gibbs free energy suggested that, the adsorption is spontaneous process. Also, the negative values of entropy referred to a high binding strength between the pigments and the adsorbent.

ACKNOWLEDGEMENTS

The authors express their gratitude to the French Government through EGIDE program (Centre Français pour l'Accueil et les Echanges Internationaux) for the financial support.

Symbols used

A_0 Absorbance of crude shea butter
A_t Absorbance of decolourised shea butter at equilibrium time t
b Langmuir adsorption equilibrium constant (g/mg)
m Mass of adsorbent (g)
n, K Freundlich constants
R Universal gas constant (8.31414 $Jmol^{-1}K^{-1}$)
R^2 Correlation coefficient
T Temperature (Kelvin)
X Relative amount of pigments adsorbed (mg/g)
X_e Residual relative amount of pigments at equilibrium (mg/g)
X_{max} Quantity of pigment adsorbed at monolayer (mg)
ΔG^o_{ad} Gibbs free energy of adsorption ($kJmol^{-1}$)
ΔH_{ad} Enthalpy (heat) of adsorption ($kJmol^{-1}$)
ΔS^o_{ad} Change in standard entropy ($kJmol^{-1}$)

REFERENCES

Achife, EC. and Ibemesi, JA, 1989. Applicability of Freundlich and Langmuir adsorption isotherms in the bleaching of rubber and melon seed oils. J. Am. Oil Chem. Soc. 66:247-252.

Bike, Mbah, JB., Kamga, R., Nguetnkam JP. and Fanni, J. 2005. Adsorption of pigments and free fatty acids from shea butter on activated Cameroonian clays. Eur. J. Lipid Sci. Technol. 107: 387-394.

Boki, K., Kubo, M., Wada, T. and Tamura, T. 1992. Bleaching of alkali- refined vegetable oils with clay minerals. Ibid. 69:233-236.

Booth, SFM. and Wickens, GE. 1988. Non-timber uses of selected arid zone trees and shrubs in Africa. FAO. Conservation guide. Rome, Italy. 19:34-45

Brimberg, U. 1982. Kinetics of bleaching of vegetable oils. J. Am. Oil. Chem. Soc. 59:74-78.

Kamga, R., Tchiegang, C. and Kapseu, C. 1999. Comparative study of refining of shea butter and palm oil. Annals of Faculty of Sciences, University of Yaoundé 1. Math, Computer, Phys. Chem. 2:117-124.

Lui Fu-qiang, Chen Jin-long, Lon Chao, Li Ai-min, Gao Guan-dao. and Zhang, Quan-xing. 2004. Adsorption of 1, 2, 4-acid by weakly basic resin: Isotherm, thermodynamics and kinetics. Chinese Journal of Polymer Science. 22 (3):219-224.

Mohagir, AM. 2003. Aqueous extraction of butter from kernels of shea tree (*Butyrospermum parkii* G.Don Kotschy). M. Sc. Eng. Thesis in ENSAI (National School of Agro- Industrial Sciences), University of Ngaoundéré, Ngaoundéré, Cameroon. pp87.

Norris, FA. 1982. Refining and Bleaching in: Bailey's Industrial Oil and Fat Products. (Vol. 2, edi. 4). Ed. Swern, D. John Wiley and Sons. 253-765.

Sabah, E. 2007. Decolourisation of vegetable oils: Chlorophyll-a adsorption by acid activated sepiolite. J. Colloid Interface Sci. Doi: 10. 1016/j.jcis.2007.01.044

Sabah, E. and Çelik, MS. 2005. Sepiolite: An effective bleaching adsorbent for the physical refining of degummed rapeseed oil. J. Am. Oil. Chem. Soc. 82:911-916.

Sabah, E., Çinar M. and Çelik, MS. 2007. Decolorization of vegetable oils: Adsorption mechanism of β-carotene on acid activated sepiolite. Food Chemistry. 100:1661-1668.

Topallar, H. 1998. The adsorption isotherms of bleaching of sunflower-seed oil. Tr. J. of chemistry. 22: 143-148.

Tsai, WT., Change CY., Ing CH. and Change, CF. 2004. Adsorption of acid dyes from aqueous solution on activated bleaching earth. Journal of Colloid and Interface Science. 275:72-78.

Received: Nov , 2013; Accepted: Jan 22,2014

SENRA Academic Publishers, British Columbia
Vol. 8, No. 2, pp. 2845-2849, June 2014
Online ISSN: 1920-3853; Print ISSN: 1715-9997

Canadian Journal of pure&applied sciences

MICROBIAL CHARACTERIZATION OF SPOILAGE MICROBES OF DRY HERBAL MEDICINAL POWDERS/TEAS

*George Osei-Adjei[1], FC Mills-Robertson[2], SC K Tay[3], FB Apea-Bah[4] and A Adu-Gyamfi[4]
[1]Accra Polytechnic, Science Laboratory Technology Department, PO Box 561, Accra
[2]Biochemistry Department, Kwame Nkrumah University of Science and Technology, Ghana
[3]Department of Clinical Microbiology, School of Medical Sciences
Kwame Nkrumah University of Science and Technology
[4]Biotechnology and Nuclear Agriculture Research Institute, Ghana Atomic Energy Commission
Box LG 80, Legon, Accra, Ghana

ABSTRACT

The study investigated and characterized the microbes that contaminate and cause spoilage of most dry herbal medicinal powders/teas sold on the Ghanaian Market. Also investigated was the microbial load of these herbal powders/teas using pour plate and/or spread plate methods. Ten herbal medicinal powders were analyzed. The powdered herbal medicinal powders were taken through irradiation processes at the Ghana Atomic Energy Commission. The results showed that all the dry powders were contaminated. The microbial load count of the samples indicated thirty percent (3 out of 10) of the dry powders achieved the specifications for both aerobic bacteria and fungal growth whilst one hundred percent (10 out of 10) of the dry powders irradiated were free from microbial contamination. The characterization of the isolated microbes confirmed the dominance of members of the genus *Bacillus*, *Rhizopus, Aspergillus* and *Candida* in the dry powders included. In conclusion, the study confirmed that most herbal medicinal products on the Ghanaian market are contaminated with pathogenic bacteria, yeasts and moulds. Therefore, there is the need for constant monitoring and control of the standards of herbal medicines.

Keywords: Herbal powders, microbial load, contaminants, spoilage, irradiation.

INTRODUCTION

Herbal medicine/phytomedicine/botanical medicine refers to the use of seeds, berries, roots, leaves, stem bark, or flowers of plants for medicinal purposes. According to WHO (2006), about 70 to 80% of the populations of most countries of the developing world rely on herbal or indigenous forms of medicine. Herbal medicines are often easy to prepare, affordable and accessible to the vast rural populace (Abbiw, 1990). It can therefore serve as a forerunner in the primary medical care of the population. Calixto (2000) proposed that phytomedicines, if combined with the preventive model of medical practices, could be among the most cost-effective, practical ways to shift the focus of modern health care from disease treatment to prevention. Due to the relatively high cost of the conventional pharmaceutical dosage forms, the increased resistance of bacteria to most antibiotics and the reduced side effects, the search for natural remedies has become necessary (Okeke *et al*., 1999; Hack, 2005). However, medicinal plant materials normally carry a large number of microbes originating from the soil (Adeleye *et al*., 2005). Additionally, contaminants may be introduced during harvesting, handling, and production of various herbal remedies (Adeleye *et al*., 2005; WHO, 1998; Sofowora, 1982). Herbal and natural products can be safer than synthetic medicines by imposing regulatory standards to improve shelf life of products and reduce risk on consumers` life. This study was designed to investigate the microbial contaminants that cause spoilage of dry herbal medicinal powders/teas produced by herbal manufacturing outlets in Ghana.

MATERIALS AND METHODS

Materials

The microbial quality of 10 dry herbal medicinal powders/teas sold by the manufacturers were examined for their microbial profiles.

Method

1g of the dry powders/teas were aseptically transferred separately and mixed in 9ml of sterile peptone water in Stomacher bags using the Stomacher machine for 10s.
Ten-fold serial dilutions were made and viability assessed using the pour plate and/or spread plate method in triplicates and plates incubated at 30°C for 3 days in the case of bacteria and at 25°C for 3-5 days for yeasts and moulds.

Microbial load count

Bacteria were enumerated on Plate Count Agar, Violet

*Corresponding author email: geoadjei@hotmail.com

Red Bile Agar, deMann-Rogosa-Sharpe Agar and Glucose Yeast extract Calcium Carbonate Agar. Yeasts and moulds were enumerated on Malt Extract Agar containing specific antibiotics. The viable aerobic bacterial count were assessed using well established methods

Microbial identification

The pure isolates were examined by their colonial and cell morphology, Gram reaction and other biochemical tests. Identification of species was carried out by assaying cultures in the Analytical Profile Index (API) galleries (Biomerieux, France).

RESULTS AND DISCUSSION

The results of the mean microbial load counts of the control and irradiated powders. The values for 6 of the powders were within the acceptable range for APC whilst on the malt extract agar only 4 were within the acceptable range (EP, 2007). In combination counts 3 out of the 10 herbal powders did not exceed the limits for microbial load. All the 10 powders were irradiated at different doses of 5.0 kGy, 7.5 kGy, 10.0 kGy and 24.0 kGy. The results from table 1 confirmed total elimination/inhibition of microbes in all the 10 products analyzed after irradiation.

Microbial isolates

Table 2 shows the microbial content of the dry powders analyzed. A total of six bacterial and six fungal species were isolated from the dry powders. *Bacillus subtilis* (47.1%) were the most prevalent bacteria isolated from the dry powders. Of the fungal isolates, the most common were the moulds, *Rhizopus stolonifer*, *Aspergillus niger* and a yeast called *Candida silvicola*, representing 35.7, 28.6 and 14.3% of the total fungal population respectively.

Ghana today has an increased public awareness and usage of herbal medicinal products in the treatment and/or prevention of diseases (Abbiw, 1990). The relatively high cost of the conventional pharmaceutical dosage forms and inaccessibility of the orthodox medical services to most people particularly in the rural areas are contributing factors (Krogsgaard *et al*., 1984; Abbiw, 1990). Since there have been increased usage, health authorities and health professionals are concerned about the safety, efficacy and quality of these medicines (WHO, 2004). The methods used in harvesting, handling, processing, storage and distribution of herbal medicines subject them to contamination by various microorganisms, some of which may be responsible for spoilage (WHO, 2004).

The results of this study showed that the samples analyzed were contaminated to various extents with

Table 1. Mean microbial load count of control and irradiated powders.

Product/Media		Mean Microbial Load of Irradiated Powders (cfu/g)				
		Control (0.0kGy)	5.0kGy	7.5kGy	10.0kGy	24.0kGy
	PCA	$8.0 \times 10^3 \pm 1.00$	No growth	No growth	No growth	No growth
XLV	MEA	$2.0 \times 10^3 \pm 1.00$	"	"	"	"
	PCA	$2.3 \times 10^3 \pm 2.00$	"	"	"	"
FEF	MEA	$4.0 \times 10^2 \pm 1.00$	"	"	"	"
	PCA	$8.8 \times 10^2 \pm 2.08$	"	"	"	"
KPN	MEA	No growth	"	"	"	"
	PCA	$1.6 \times 10^3 \pm 2.00$	"	"	"	"
BLG	MEA	$5.0 \times 10^2 \pm 2.00$	"	"	"	"
	PCA	$3.2 \times 10^5 \pm 2.65$	"	"	"	"
LPT	MEA	TNTC	"	"	"	"
	PCA	TNTC	"	"	"	"
APS	MEA	$3.1 \times 10^5 \pm 2.65$	"	"	"	"
	PCA	$4.2 \times 10^4 \pm 2.65$	"	"	"	"
TAA	MEA	$2.1 \times 10^3 \pm 2.00$	"	"	"	"
	PCA	$3.4 \times 10^5 \pm 4.00$	"	"	"	"
CHD	MEA	$3.0 \times 10^2 \pm 3.61$	"	"	"	"
	PCA	$2.6 \times 10^4 \pm 3.04$	"	"	"	"
SPP	MEA	$5.3 \times 10^3 \pm 4.20$	"	"	"	"
	PCA	$1.35 \times 10^5 \pm 3.61$	"	"	"	"
CND	MEA	$1.9 \times 10^4 \pm 2.00$	"	"	"	"

Key: kGy - kiloGray

Table 2. Microbial content of dry powders.

Product	Microbial isolate	
	Bacteria	Fungi
XLV	*Staphylococcus aureus* *Bacillus subtilis*	*Aspergillus niger*
FEF	*Bacillus licheniformis* *Escherichia vulneris*	*Aspergillus niger* *Penicillium digitatum*
KPN	*Bacillus subtilis*	-
BLG	*Bacillus subtilis*	*Rhizopus stolonifer* *Aspergillus niger*
LPT	*Bacillus subtilis* *Serratia ficaria*	*Rhizopus stolonifer*
APS	*Bacillus megaterium* *Bacillus subtilis* *Enterobacter aerogenes* *Klebsiella oxytoca*	*Rhizopus stolonifer* *Candida silvicola,* *Geotrichum spp*
TAA	*Bacillus subtilis* *Serratia ficaria*	*Rhizopus stolonifer*
CHD	*Bacillus circulans*	*Aspergillus niger*
SPP	*Bacillus subtilis*	*Aspergillus flavus*
CND	*Bacillus subtilis*	*Rhizopus stolonifer* *Candida silvicola*

bacteria and fungi. The limits of microbial contamination for raw materials are: total aerobic bacteria, maximum 10^7 cfu/g, moulds and yeast, maximum 10^5 cfu/g, *Escherichia coli*, maximum 10^4 cfu/g, Enterobacteria and other Gram negative bacteria, maximum 10^4 cfu/g. *Shigella* and *Salmonella* must be absent per gram according to the World Health Organization (WHO, 2004). The microbial load count of the isolated and characterized microbes from the raw materials indicated the presence of the following bacteria species: *Escherichia coli, Proteus vulgaris, Serratia ficaria, Bacillus cereus, Staphylococcus aureus, Bacillus subtilis and Bacillus licheniformis*. The isolation of pathogenic strains, including *B. cereus, S. aureus* and *E. coli* is very important, because of health concern. They are known to cause human illness (Dohmai *et al*., 2008). Fungal isolates encountered included *Aspergillus niger, Aspergillus flavus, Aspergillus sulphureus, Penicillium digitatum, Fusarium oxysporum, Mycelia sterilia* and *Cladosporon herbarum* whilst the yeasts strains isolated were *Trichosporon mucoides, Candida membranifasciens* and *Candida krusei*. Research work by Efuntoye (1996), revealed the presence of *A. parasiticus, A. flavus and A. ochraceus* on dried medicinal herbs from the Nigerian market, whilst Czech *et al.* (2001) reported bacterial and fungal contamination of medicinal herbs in Austria. Martins *et al*. (2001a) isolated several *Aspergillus* species including *A. niger* from orange tree leaves. The isolation of various aspergilli, especially *A. flavus* is of highest concern because it is known to produce aflatoxins. *A. niger, A. versicolor* and *Penicillium* spp. also have the potential for toxigenesis (El-Kady *et al*., 1994; Perone *et al*., 2006). Their presence in the raw materials should be kept as low as possible and the moisture content of the product maintained at levels that do not allow fungal growth (Lugauskas *et al*., 2006).

The results of the microbial load count of the dry powders (Table 2) was one hundred percent (10 out of 10) contaminated by aerobic bacteria and ninety percent (9 out of 10) contaminated by fungi. However, forty percent (4 out of 10) of the powders were found to have exceeded the acceptable limit for APC whilst sixty percent (6 out of 10) of the powders were found to have exceeded the acceptable limit for moulds and yeasts count (EP, 2007). KPN was found to be free from fungal contamination. A total of nine bacterial and six fungal species (Table 2) were isolated from the powders with *Bacillus* species found to be contaminating all the ten powders. The presence of *Bacillus* species in the powders may be as a result of inadequate heat processing, improper handling of products and contaminated processing equipment (Frazier and Westhoff, 2003) although these stages of processing were not investigated but are known to be predisposing factors. The isolation of *Staphylococcus aureus* from XLV makes it a health risk since this organism is capable of causing human infection such as boils, skin sepsis, toxic shock syndrome, scalded skin syndrome, pneumonia, osteomyelitis and food poisoning (Jawetz *et al*., 2004). The dominating fungal contaminants were *Rhizopus stolonifer* (35.7%), *Aspergillus niger* (28.6%) and the yeast, *Candida silvicola* (14.3%). Apart from *R. stolonifer*,

A. niger and *C. silvicola*, *A. flavus*, *P. digitatum* and *Geotrichum* species were confirmed to contaminate the powders. Romagnoli *et al*. (2007) reported that dried material from plant origin such as spices are commonly heavily contaminated with xerophilic storage moulds and bacteria. The level of mould contamination in powders depends largely on the environmental conditions during cultivation, harvesting, storage and processing (Romagnoli *et al*., 2007). Moulds normally proliferate and spoil the product and possibly produce mycotoxins if the moisture of the product increases during storage (Romagnoli *et al*., 2007). This might have been responsible for the organisms isolated from the medicinal powders of plant origin investigated in the present study.

The results of the irradiated powders (Table 2) confirmed that the ionizing radiation destroyed/inhibited all the spoilage and pathogenic bacteria and fungi present in the powders at all the doses used. The destruction/inhibition of microbial contaminants can prolong the shelf-life of products in cases where microbial spoilage is the limiting factor (Satin, 1996). As a result, irradiation is used for purposes such as reducing or eliminating food borne pathogens, disinfecting food, and extending product shelf-life. The result of the irradiated medicinal powders of plant origin is not different from this practice in USA by application (Marsden, 1994).

The volume of irradiated spices and dried vegetable seasonings globally has increased significantly from about 5,000 tonnes in 1990 to over 60,000 tonnes in 1997 (WHO, 1997). Irradiation will therefore be useful in preventing contamination of herbal medicinal products.

CONCLUSION

The study demonstrated the presence of microbial contaminants in the products at levels most times exceeding the acceptable limits of microbial load count. The presence of *Aspergillus* species isolated from the products has the potential for toxin production in the products. This study also confirmed that exposure of the powders to ionizing radiations resulted in the elimination/inhibition of spoilage and pathogenic bacteria and fungi. Irradiation can therefore be the best and effective method for reducing and eliminating product pathogens and thereby extending product shelf-life.

REFERENCES

Abbiw, DK. 1990. Useful plants of Ghana. Intermediate Technology Publications and the Royal Botanic Gardens, UK. 118-205.

Adeleye, IA., Okogi, G. and Ojo, EO. 2005. Microbial contamination of herbal preparations In Lagos, Nigeria. J. of Health, Nutrition and population. 23 (3):296-297.

Calixto, JB. 2000. Efficacy, safety, quality control, marketing and regulatory guidelines for herbal medicines (Phytotherapeutic agents). Braz. J. Microbiology. 33:179-189.

Czech E., Kneifel W. and Kopp, B. 2001. Microbiological status of commercially available medicinal herbal drugs – a screening study. Planta Med. 67:263-9.

Dohmae, S., Okubo, T., Higuchi, W., Takano, T., Isobe, H., Baranovich, T., Kobayashi, S., Uchiyama, M., Tanabe, Y., Itoh, M. and Yamamoto, T. 2008. Bacillus cereus nosocomial Infection from reused towels in Japan. J. Hosp. Infection. 69 (4): 361-7.

Efuntoye, MO. 1996. Fungi associated with herbal drug plants during storage. Mycopathologia. 136:115-8.

El-Kady, I., El-Maraghy, S. and Zohri, AN. 1994. Mycotoxin producing potential of some isolates of Aspergillus flavus and Eurotium groups from meat products. Microbiol. Res. 149(3): 297-307.

European Pharmacopoeia. 2007. Directorate for the Quality of Medicines of the Council of Europe (5th edi.). Strasbourg, France.

Frazier, WC. and Westhoff, DC. 2003. Food Microbiology (4th edi.). McGraw-Hill Publishing Company Limited. 66-67.

Hack, SK. 2005. Do not put too much value on conventional medicine. J. Ethnopharmacol. 100:37-39.

Jawetz, E., Melnick, JL., Adelberg, EA. 2004. Medical Microbiology (24th edi.). McGraw Hill Publishers. 223-229.

Krogsgaard-Larsen, P., Cristensen, SB. and Kofod, H. 1984. Natural products and drug development, Munksgaard, Copenhagan. pp110.

Lugauskas, A., Raila, A., Railiene, M. and Raudoniene, V. 2006. Toxic micromycetes in grain raw material during its processing. Ann. Agric. Environ. Med. 13(1):147-61.

Marsden, JL. 1994. Irradiation and food safety. American Meat Institute Issues Briefing. 1- 4.

Martins, HM., Martins, ML., Dias, MI. and Bernado, F. 2001[a]. Evaluation of microbiological quality of medicinal plants used in natural infusions. Int. J. Food Microbiol. 68:149-53.

Okeke, IN., Lamikanra, A. and Elderman. 1999. Socioeconomic and behavioural factors leading to acquired bacterial resistance to antibiotics in developing countries. Emerging Infectious Diseases. 5:18-27.

Perrone, G., Mulè, G., Susca, A., Battilani, P., Pietri, A. and Logrieco, A. 2006. Ochratoxin A production and amplified fragment length polymorphism analysis of Aspergillus carbonarius, Aspergillus tubingensis, and

Aspergillus niger strains isolated from grapes in Italy. Appl. Environ. Microbiol. 72(1): 680-685.

Romagnoli, B., Menna, V., Gruppioni, N. and Bergamini, C. 2007. Aflatoxins in spices, aromatic herbs, herbs-teas and medicinal plants marketed in Italy. Food Control 18:697-701.

Satin, M. 1996. Food Irradiation: A Guidebook (2nd edi.). CRC Press.

Sofowora, A. 1982. Medicinal plants and traditional medicine in Africa. Chichester. Wiley. pp256.

World Health Organization (WHO). 1997. Food Irradiation: Sky is the Limit. WHO Press Release WHO/68, 19 September, 1997. WHO Press Office, Geneva.

World Health Organization (WHO). 1998. Regulatory situation of herbal medicine: A world wide review. World Health Organization, Geneva.

World Health Organization (WHO). 2004. Revised Draft WHO guidelines for assessing safety and quality of herbal medicines with reference to contaminants and residues.

World Health Organization (WHO). 2006. Traditional Medicine.

Received: Oct 9, 2013; Accepted: Jan 15, 2014

SENRA Academic Publishers, British Columbia
Vol. 8, No. 2, pp. 2851-2857, June 2014
Online ISSN: 1920-3853; Print ISSN: 1715-9997

Canadian Journal of pure & applied sciences

ANTI-INFLAMMATORY AND ANTIOXIDANT ACTIVITIES OF ETHANOLIC EXTRACT OF LEAVES OF *NEWBOULDIA LAEVIS* IN DIABETIC RATS

*Kolawole OT[1] and Akanji MA[2]
[1]Department of Pharmacology and Therapeutics, Ladoke Akintola University of Technology, Ogbomoso
[2]Department of Biochemistry, University of Ilorin, Ilorin, Nigeria

ABSTRACT

This study was designed to evaluate anti-inflammatory and antioxidant potentials of ethanolic extract of leaves of *Newbouldia laevis* in diabetic rats. Diabetes was induced in rats by intravenous injection of freshly prepared solution of streptozotocin (60 mg/kg body weight). Diabetic rats were then treated with extract of the leaves of *N. laevis* (500 mg/kg body weight) for 28 days after which serum levels of tumor necrosis factor alpha (TNF-α) and interleukin -1 beta (IL-1β) were estimated using ELISA kit while serum concentration of nitric oxide (NO) was determined by Griess assay. The activities of catalase (CAT), reduced glutathione (GSH), glutathione peroxidase (GPx) and superoxide dismutase (SOD) were also estimated. Free radical scavenging activity of the extract was measured by decrease in the absorbance of methanol solution of 1,1-diphenyl-2-picrylhydrazyl (DPPH). The extract significantly reduced ($P < 0.05$) serum levels of nitric oxide, IL-1β as well as TNF-α in diabetic rats. The activities of CAT, GSH, GPx and SOD were significantly increased ($P < 0.05$) in treated diabetic rats compared to diabetic control. The extract also possesses free radical scavenging activity against DPPH with IC_{50} of 7.2 µg/ml. The study showed that ethanolic extract of *N. laevis* leaves possesses anti-inflammatory and antioxidant properties in streptozotocin-induced diabetic rats.

Keywords: *Newbouldia laevis*, inflammation, antioxidant, diabetes, cytokines.

INTRODUCTION

Under normal physiologic condition, inflammation is a protective response elicited by tissue injury. It is the mechanism through which the body destroys or neutralizes invading harmful agents and also restores homeostasis after stress (Lumeng and Saltiel, 2011). During inflammatory process, cytokines such as tumor necrosis factor alpha (TNF-α), interferon gamma (IFN-γ) and Interleukin 1β (IL-1β) are released when monocytes and macrophages are activated. However, activation of macrophages must be tightly regulated in order to avoid unrestrained inflammatory process through inappropriate release of cytokines (Sakic *et al*., 2011). When there is distortion in the normal regulatory control of the inflammatory process, the innate and acute phase responses are sustained and disease progression ensues. The connection between inflammation and free radical generation has also been established (Yeh *et al*., 2005). Overproduction of radicals such as superoxide anions, hydroxyl radical, hydrogen peroxide and nitric oxide (NO) results in oxidative stress and chronic inflammation. The reaction products of these radicals trigger lipid peroxidation, oxidation of enzymes and proteins and modifications of nucleic acids (Barrera, 2012). This is the fundamental mechanism underlying many pathological conditions.

Reports from several clinical and experimental studies have linked increased oxidative stress and low grade chronic inflammation with the development of insulin-dependent diabetes as well as noninsulin-dependent diabetes (Ferreira *et al*., 2010; Parveen *et al*., 2012). In diabetes, chronic hyperglycemia leads to increased generation of superoxide by the mitochondrial electron transport chain (Tushuizen *et al*., 2005). An imbalance in the generation and scavenging of reactive oxygen species (ROS) and reactive nitrogen species (RNS) results in oxidative stress. This eventually leads to altered function of intracellular proteins, DNA damage, and activation of NF- kB which triggers abnormal changes in gene expression as well as increased generation of pro-inflammatory cytokines and inducible nitric oxide (Mohora *et al*., 2007). As ROS and RNS accumulate, more and more beta cells of the pancreas get destroyed and this contributes to the progression and complications of diabetes. Therefore, agents with antioxidant and anti-inflammatory activities are expected to be effective in the treatment of diabetes and its complications.

In spite of the health benefits of the current antidiabetic drugs, each drug has its own range of side effects which may compromise the disease status or even worsen the condition in some cases. Some of the side effects of antidiabetic drugs which may offset their benefits include weight gain, hyperinsulinemia, hypoglycemia, edema and

*Corresponding author email: tymkol@yahoo.co.uk

volume expansion (Modi, 2007). Thus, the prevalence of the disease continues to rise worldwide and there is little that could be done to prevent its complications. Therefore, there is the need to search for better antidiabetic remedies with good antioxidant and anti-inflammatory properties.

Medicinal plants have contributed greatly to the development of modern drugs, including those used in the management of diabetes mellitus. It is estimated that more than 400 plant species are used as anti-diabetic remedy, but only a limited number of them have been studied and validated for their antidiabetic properties using laboratory diabetic animal models and in clinical studies using human subjects (Sharma *et al*., 2011). *Galega officinalis*, *Momordica charantia*, *Gymnema sylvestre*, and *Opuntia streptacantha* are among plants that have been reported to be effective in the management of diabetes by virtue of their anti-inflammatory and antioxidant properties (Bnouham *et al*., 2006; Gupta and Sharma, 2006).

Newbouldia laevis (P. Beauv) is one of the plants employed in the management of diabetes in Nigeria, which have not been subjected to proper scientific investigations. Its common names are 'African border tree' and 'fertility tree'. The leaves of the plant are soaked in ethanol and the filtrate is taken orally to treat diabetes. The extract of the leaves has been reported to lower blood glucose level in diabetic rats (Owolabi *et al*., 2011). The anti-inflammatory, analgesic and antipyretic properties of the stem bark and flowers of the plant have been studied (Olajide *et al*., 1997). In this study, the leaf extract of *N. laevis* was evaluated for antioxidant and anti-inflammatory activities in diabetic rats.

MATERIALS AND METHODS

Collection of plant material

Leaves of *Newbouldia laevis* were collected from the premises of College of Health Sciences, Ladoke Akintola University of Technology, Mercyland, Osogbo Campus, Nigeria. The plant sample was identified and authenticated by a taxonomist in Forestry Research Institute of Nigeria (FRIN), Ibadan, Nigeria. A voucher specimen was deposited in the herbarium of the institute (voucher specimen no: FHI 107753).

Preparation of plant extract

The leaves were thoroughly washed with distilled water to remove soil and other debris that may contaminate the plant sample. The washed sample was then air-dried under shade in the laboratory for 5 days and the dry plant sample was pulverized using an electric grinding machine. The resultant powder sample weighing 500g was then extracted with 80% ethanol at 70^0C by continuous hot percolation using a Soxhlet apparatus. The extraction was carried out for 24h and the resulting ethanolic extract was concentrated at 40^oC in a rotary evaporator. The solid sample obtained weighed 47.5g (yield = 9.5%). The crude ethanolic extract (NLet) was kept in air-tight container and stored in a refrigerator at 4^0C until the time of use.

Experimental animals

Male Wistar rats weighing 180-200g were obtained from the Animal Holding Unit of the Department of Pharmacology and Therapeutics, Ladoke Akintola University of Technology (LAUTECH), Nigeria. The animals were housed in polypropylene cages inside a well-ventilated room. The animals were maintained under standard laboratory conditions of temperature (22 ± 2° C), relative humidity (55-65%) and 12 hour light/dark cycle. They were allowed to acclimatize for 2 weeks before the experiment. During the experimental period, animals were fed with a standard balanced commercial pellet diet (Ladokun Feeds Ltd. Ibadan, Nigeria) and potable tap water *ad libitum*.

Ethical consideration

All experimental procedures were conducted in accordance with the National Institute of Health Guide for the Care and Use of Laboratory Animals (National Institute of Health, 1985) as well as Ethical Guidelines for the Use of Laboratory Animals in LAUTECH, Nigeria.

Induction of Diabetes mellitus

Experimental diabetes was induced in rats, which had fasted for 12hr by a single intravenous injection through the tail vein of a freshly prepared solution of streptozotocin (STZ) (60mg/kg b.wt) dissolved in 0.1M cold citrate buffer, pH 4.5 (Chen *et al*., 2005). The rats were allowed to drink 5% glucose solution overnight to overcome drug-induced hypoglycemia. Estimation of fasting blood glucose (FBG) was done 72hours after injection of STZ to confirm induction of diabetes and then on the 7th day to investigate the stability of diabetic condition. Fasting blood glucose was estimated by One Touch® glucometer (Lifescan, Inc. 1995 Milpas, California, USA). Blood sample for the FBG determination was obtained from the tail vein of the rats and those with blood glucose value ≥ 200 mg/dl were selected for the study.

Biochemical assays

After treating diabetic rats with NLet (500mg/kg body weight) for 28 days, serum levels of TNF- α and IL-1β were estimated using Rat TNF-α and Rat IL-1β ELISA kits (RayBiotech Inc, USA). Measurement of NO was carried out as described by Zahedi *et al*. (2008) using Griess Reagent System procured from Sigma-Aldrich (St Louis, MO, USA). The activities of enzymatic antioxidants in rat liver were estimated. Catalase (CAT) activity was assayed as described by Sinha (1972). The activity of glutathione peroxidase (GPx) was determined as described by Rotruck *et al*. (1973). The level of

reduced glutathione (GSH) was estimated using the method of Jollow *et al*. (1974). Superoxide dismutase (SOD) activity was assayed by the method of Kakkar *et al*. (1984). Glibenclamide (5mg/kg body weight) was used as reference drug. Free radical scavenging activity of the extract was measured by decrease in the absorbance of methanol solution of 1,1-diphenyl-2-picrylhydrazyl (DPPH) (Hantano *et al*., 1989) and ascorbic acid was used as reference drugs.

Statistical analysis

Data obtained from the experiments are expressed as mean ± standard error of mean (SEM). Data were subjected to one-way analysis of variance (ANOVA) followed by Student's t- test. A level of $P < 0.05$ was taken as significant. GraphPad Prism version 5.0 for windows was used for these statistical analyses (GraphPad software, San Diego California, USA).

RESULTS AND DISCUSSION

The results indicate that *N. leavis* extract has free radical scavenging activity against DPPH. The concentration of NLet that caused 50% inhibition (IC_{50}) was 7.2µg/ml while that of the standard drug, ascorbic acid was 4.4µg/ml. The result is presented in figure 1.

The extract stimulated the activity of enzymatic antioxidants in diabetic rats. In the rat liver, the cellular levels of reduced glutathione (GSH), superoxide dismutase (SOD), catalase (CAT) and glutathione peroxidase (GPx) decreased significantly ($P < 0.05$) in the diabetic control group relative to the non-diabetic control. Compared with the diabetic control group, there was a significant increase ($P < 0.05$) in the levels of the antioxidants in the groups treated with glibenclamide and NLet. NLet increased the level of GSH (53.1%), CAT (21.5%), GPx (20.2%) and SOD (33%) relative to diabetic control. There was no significant difference ($P > 0.05$) between NLet-treated group and the glibenclamide-treated group. The results are presented in figure 2.

As shown in figure 3, serum level of NO was significantly increased ($P < 0.05$) in diabetic control group compared to non-diabetic control group. NLet reduced serum level of NO in diabetic rats and the reduction was significantly different ($P < 0.05$) compared to diabetic control. Likewise, serum level of tumor necrosis factor alpha (TNF-α) and interleukin -1β (IL-1β) increased significantly in diabetic control when compared with non-diabetic control. This was reversed by NLet and the serum levels of both TNF-α (Fig. 4) and IL-1β (Fig. 5) in the NLet-treated group was significantly different from those of the diabetic controls.

Diabetes mellitus is usually accompanied by increased levels of free radicals and decreased concentration or activity of antioxidants. Excess production of free radicals triggers the process of oxidative stress that can seriously alter the cell membranes and other structures such as proteins, lipids and deoxyribonucleic acid (DNA). Oxidative stress sets in when cells cannot adequately mop up the excess free radicals formed. In other words, oxidative stress results when there is an imbalance between the formation and neutralization of free radicals (Genestra, 2007). Numerous studies have shown that enzymatic antioxidant defense system is compromised in diabetes (Martin *et al*., 2003; Atef and Ezz, 2012).

Superoxide dismutase, catalase, glutathione peroxidase and reduced glutathione play significant role in protecting against tissue damage by free radicals. The functions of these antioxidants are interconnected and a decrease in their concentration leads to the accumulation of lipid peroxides and increased oxidative stress (Kaleem *et al*., 2006). In diabetes, hyperglycemia promotes glucose oxidation and this further leads to free radical accumulation. This is followed by protein glycation and oxidative degeneration. In this situation, the concentration and activity of the enzymatic antioxidants are significantly reduced. In uncontrolled or poorly controlled diabetes, advanced glycation endproducts (AGEs) are irreversibly formed. These are involved in the pathogenesis of many of the irreversible complications of diabetes, including hypertrophy, hyperplasia, expanded extracellular matrix and vascular complications (Martin *et al*., 2003).

In the present study, the ethanolic extract of the leaves of *Newbouldia laevis* was demonstrated to have free radical scavenging activity against DPPH with IC_{50} of 7.2µg/ml. The results also showed that the extract stimulated the activity of SOD, CAT, GPx and GSH in the liver of diabetic rats and there was no significant difference ($P > 0.05$) between the group treated with NLet and the glibenclamide-treated group. This indicates that NLet contains antioxidant principles that can protect the enzymatic antioxidant system against damage by excessive oxidative stress.

Inflammatory cytokines are important mediators of β-cell destruction in animal models of diabetes as well as in human islets. A combination of interleukin-1(IL-1), γ-interferon (INF-γ) and tumor necrosis factor (TNF) stimulates inducible nitric oxide synthase (iNOS) expression in the islet and this leads to increased production of nitric oxide (NO) that causes the destruction of the islet cells (Thomas *et al*., 2002).

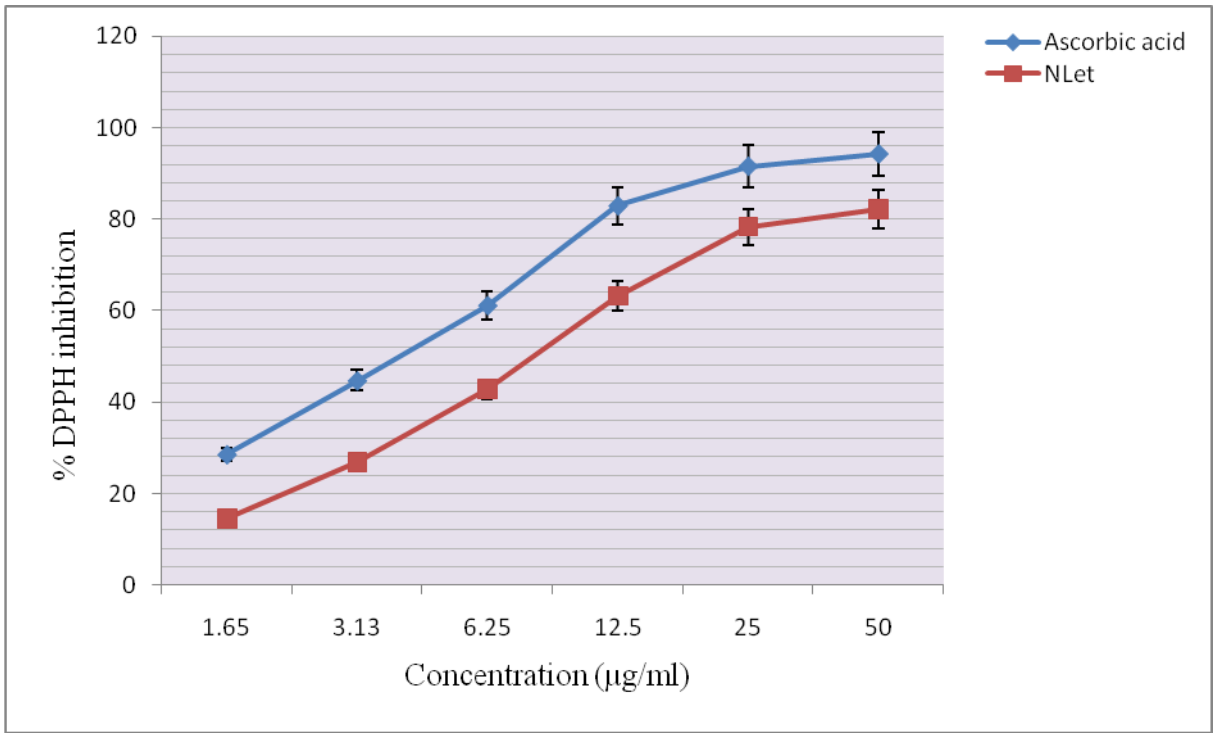

Fig. 1. DPPH free radical scavenging activity of *N. laevis* extract.
Values are means ± SEM of three replicates.

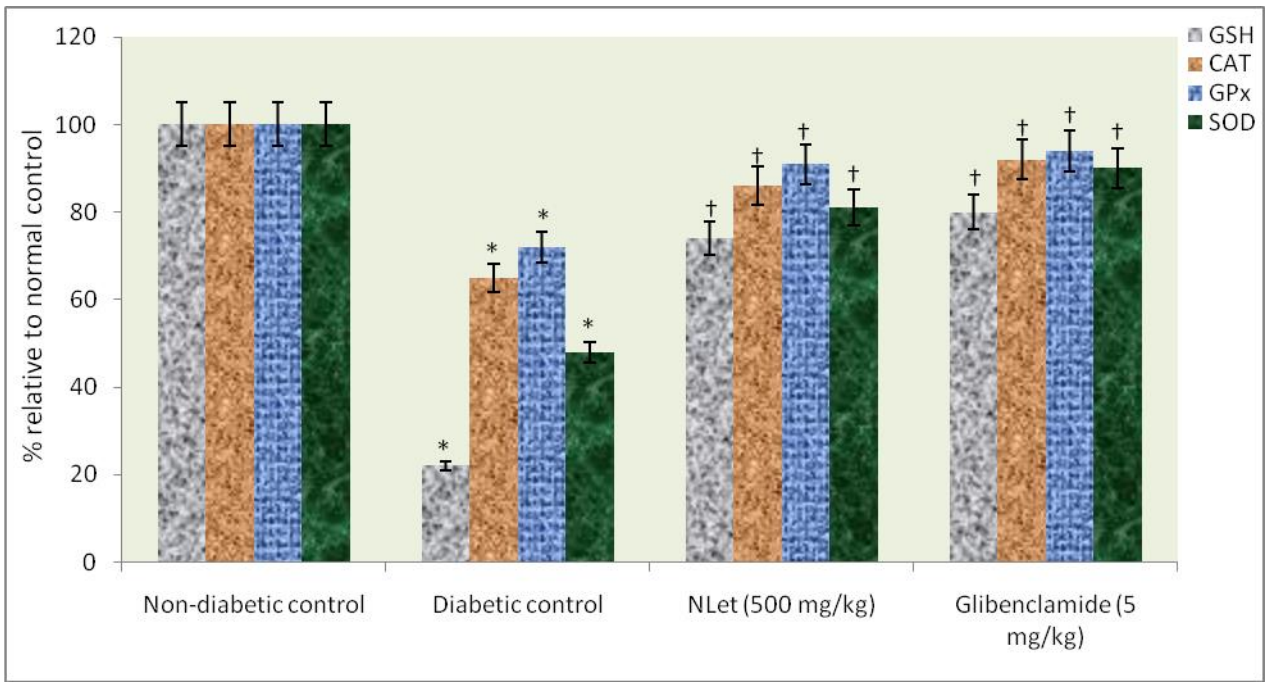

Fig. 2. Effect of *N. laevis* leaf extract on the activity of enzymatic antioxidants in the liver of diabetic rats. Values represent mean ± SEM (n = 6). $^{*}P < 0.05$ compared with normal control; $^{\dagger}P < 0.05$ compared with diabetic control.

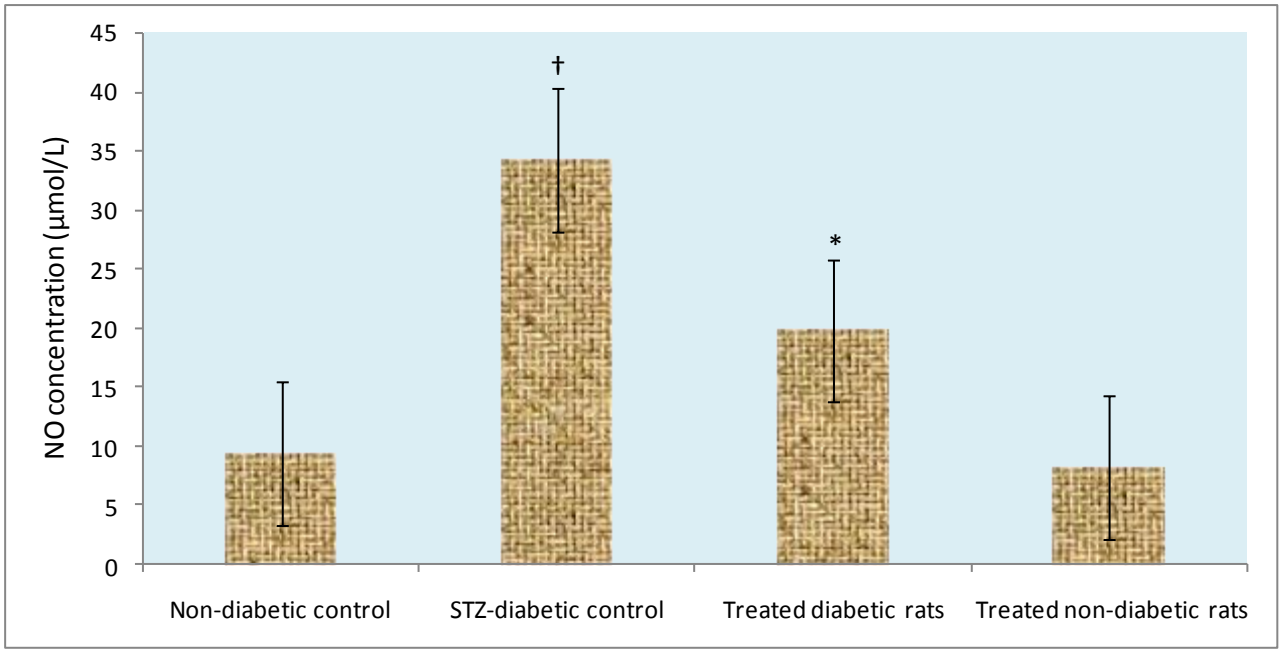

Fig. 3. Effects of *N. laevis* leaf extract on serum level of nitric oxide in diabetic rats. †P < 0.05 compared with the non-diabetic control; *P < 0.05 compared with diabetic control. Values represent mean ± SEM (n = 6).

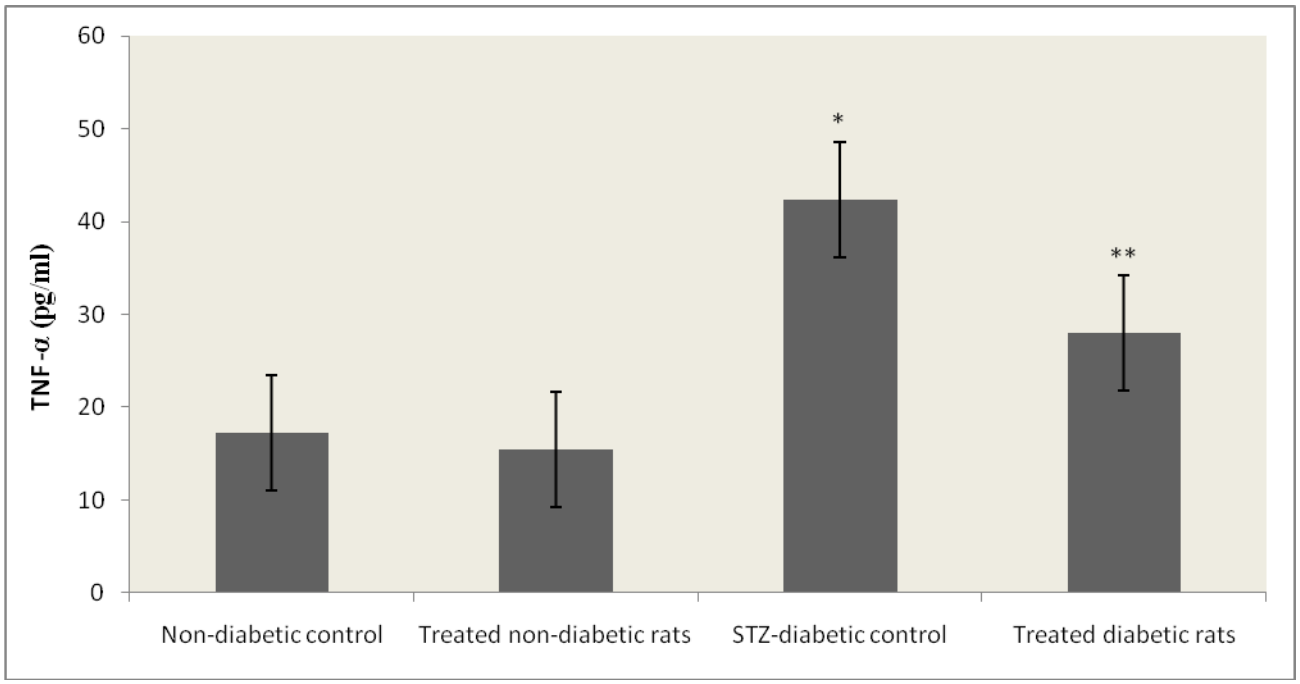

Fig. 4. Effect of *N. laevis* extract on the serum level of TNF -α in diabetic and non-diabetic rats. Values represent mean ± SEM (n = 3). *P < 0.05 compared with non-diabetic control; **P < 0.05 compared with STZ-diabetic group.

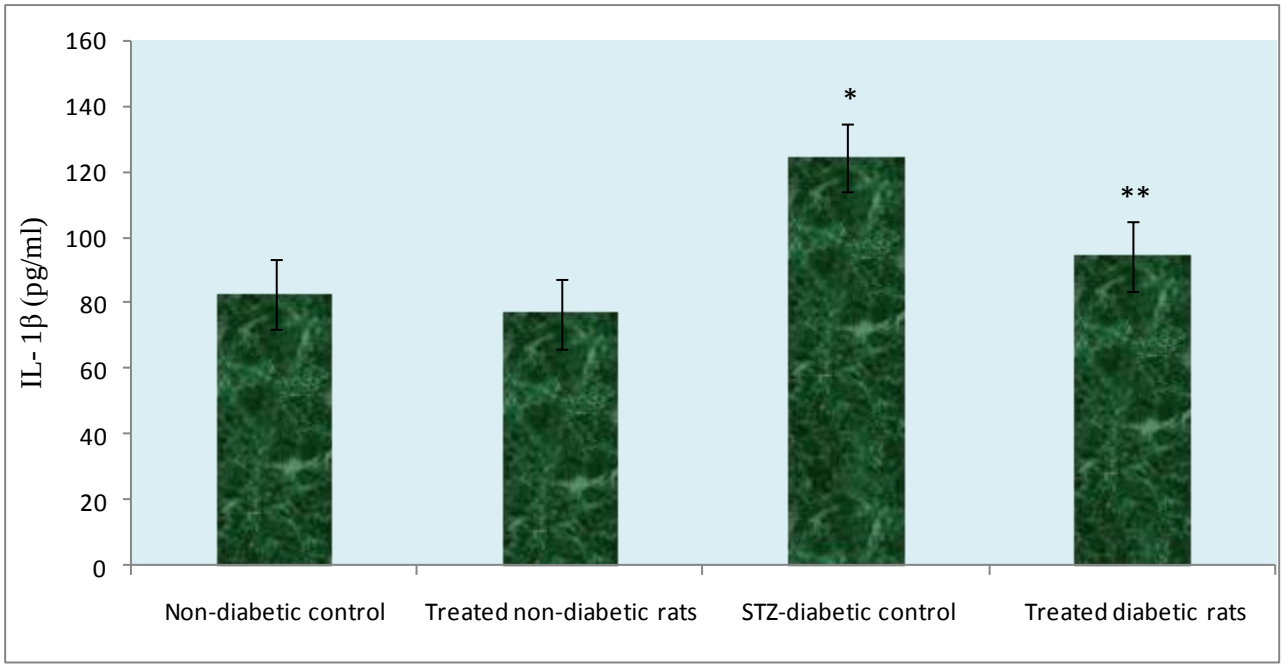

Fig. 5. Effect of *N. laevis* extract on the serum level of IL- 1β in diabetic and non-diabetic rats.
Values represent mean ± SEM (n = 3). *P < 0.05 compared with non-diabetic control; **P < 0.05 compared with STZ-diabetic control.

A number of studies have also shown that NO produced by macrophage and /or endothelial cells can mediate β-cell damage independent of local cytokine release. Thus, macrophage-generated NO, cytokine-induced NO and other radicals contribute to β-cell destruction. In this study, serum levels of NO, interleukin -1β (IL-1β), and tumor necrosis factor –alpha (TNF-α) were significantly increased in diabetic control rats. This is an indication of excess production of NO and cytokines in the diabetic rats. Treatment with NLet significantly reduced the levels of these parameters.

CONCLUSION

The results of this study suggest that ethanolic extract of the leaves of *N. laevis* possesses anti-inflammatory and antioxidant activities that could enhance amelioration of β-cell destruction and other oxidative stress-induced complications in diabetes mellitus.

REFERENCES

Atef, AA. and Ezz, MK. 2012. Evaluation of the antioxidant effects of resveratrol against hyperglycemia - induced oxidative stress in type 2 diabetic rat model. J Appl Sci Res. 8(3):1576-1584

Barrera, G. 2012. Oxidative stress and lipid peroxidation products in cancer progression and therapy. ISRN Oncology. DOI:10.5402/2012/137289.

Bnouham, M., Ziyyat, A., Mekhfi, H., Tahri, A. and Legssyer, A. 2006. Medicinal plants with potential antidiabetic activity - A review of ten years of herbal medicine research (1990-2000). Int J. Diabetes and Metab. 14:1-25.

Chen, H., Brahmbhatt, S., Gupta, A. and Sharma, AC. 2005. Duration of streptozotocin-induced diabetes differentially affects p38-mitogen- activated protein kinase (MAPK) phosphorylation in renal and vascular dysfunction. Cardiovascular Diabetology. 4:3

Ferreira, L., Teixeira-de-Lemos, E., Pinto, F., Parada, B., Mega, C., Helena Vala, H., Pinto, R., Garrido, P., Sereno, J., Fernandes, R., Santos, P., Velada, I., Melo, A., Nunes, S., Teixeira, F. and Reis, F. 2010. Effects of sitagliptin treatment on dysmetabolism, inflammation, and oxidative stress in an animal model of type 2 diabetes (ZDF Rat). Mediators of Inflammation. DOI:10.1155/2010/592760.

Genestra, M. 2007. Oxyl radicals, redox-sensitive signalling cascades and antioxidants -Review. Cellular Signalling. 19:1807-1819.

Gupta, VK. and Sharma, SK. 2006. Plants as natural antioxidants. Natural Product Radiance 5(4):326-334.

Hantano, T., Edamatsu, R., Yoshida, T. and Okuda, T. 1989. Phenolic constituents of licorice II. Structures of licopyranocoumarin, licoarylcoumarin and glisoflavone, and inhibitory effects of licorice phenolics on xanthine oxidase. Chem Pharm Bull. 37:3005-3009.

Jollow, D., Mitchell, L., Zampaglione, N. and Gillete, J. 1974. Bromobenzene induced liver necrosis: protective role of glutathione and evidence for 3, 4-bromobenzenoxide as the hepatotoxic intermediate. Pharmacology. 11:151-169.

Kakkar, P., Das, B. and Viswanathan, PN. 1984. A modified spectrophotometric assay of superoxide dismutase. Ind J. Biochem Biophys. 21:130-132.

Kaleem, M., Asif, M., Ahmed, OU. and Bano, B. 2006. Antidiabetic and antioxidant activity of *Annona squamosa* extract in streptozotocin-induced diabetic rats. Singapore Med J. 47(8):670-675.

Lumeng, CN. and Saltiel, AR. 2011. Inflammatory links between obesity and metabolic disease. J. Clin Invest. 121(6):3111-2117.

Martin, AC., Sanders, RA. and Watkins, JB III. 2003. Diabetes, oxidative stress and antioxidants: A review. J. Biochem Mol Toxicol. 17:24-38.

Modi, P. 2007. Diabetes beyond insulin: Review of new drugs for treatment of diabetes mellitus. Curr Drug Discov Technol. 4(1):39-47.

Mohora, M., Virgolici, B., Coman, A., Muscurel, C., Gaman, L., Gruia, V. and Greabu, M. 2007. Diabetic foot patients with and without retinopathy and plasma oxidative stress. Rom J. Intern Med. 1:45-51.

National Institute of Health. 1985. Guide for the use of laboratory animals. DHHS, PHS, NIH Publication No. 85- 23 (1985 Revised).

Olajide, OA., Awe, SO. and Makinde, JM. 1997. Pharmacological studies on *Newbouldia laevis* stem bark. Fitoterapia. 68:439-443.

Owolabi, OJ., Amaechina, FC. and Okoro, M. 2011. Effect of ethanol leaf extract of *Newbouldia laevis* of blood glucose levels in diabetic rats. Tropical J Pharm Res. 10(3):249-254.

Parveen, K., Ishrat, T., Malik, S., Kausar, MA. and Siddiqui, WA. 2012. Modulatory effects of Pycnogenol® in a rat model of insulin dependent diabetes mellitus: biochemical, histological, and immunohistochemical evidences. Protoplasma. DOI 10.1007/s00709-012-0418-2.

Rotruck, JT., Pope, AL., Ganther, HE., Swanson, AB., Hafeman, DG. and Hoekstra, WG. 1973. Selenium: Biochemical role as a component of glutathione peroxidase. Science. 179:588-590.

Sakic, K., Zura, M., Sakic, L., Malenica, B., Bagatin, D. and Sturm, D. 2011. Anaesthetic technique and cytokine response. Periodicum Biologorum. 113(2):151-156.

Sharma, M., Siddique, MW., Shamim, AM., Gyanesh, S. and Pillai, KK. 2011. Evaluation of antidiabetic and antioxidant effects of seabuckthorn (*Hippophae rhamnoides* L.) in streptozotocin-nicotinamide induced diabetic rats. The Open Conference Proceedings Journal. 2:53-58.

Sinha, AK. 1972. Colorimetric assay of catalase. Anal Biochem. 47:389- 394.

Thomas, HE., Darwiche, R., Corbett, JA. and Kay, TWH. 2002. Interleukin-1 plus γ-interferon-induced pancreatic β-cell dysfunction is mediated by β-cell nitric oxide production. Diabetes. 51:311-315.

Tushuizen, ME., Diamant, M. and Heine, RJ. 2005. Postprandial dysmetabolism and cardiovascular disease in type 2 diabetes. Postgrad. Med. J. 81:1-6.

Yeh, C., Hou, M., Tsai, S., Lin, S., Hsiao, J., Huang, J., Wang, L., Wu, S., Hou, LA., Ma, H. and Tsai, L. 2005. Superoxide anion radical, lipid peroxides and antioxidant status in the blood of patients with breast cancer. Clin. Chim. Acta. 361:104-111.

Zahedi, AS., Ghasemi, A. and Azizi, F. 2008. Serum nitric oxide metabolites in subjects with metabolic syndrome. Clin Biochem. 41:1342-1347.

Received: Oct 16, 2013; Accepted: Jan 25, 2014

SENRA Academic Publishers, British Columbia
Vol. 8, No. 2, pp. 2859-2863, June 2014
Online ISSN: 1920-3853; Print ISSN: 1715-9997

Canadian Journal of pure&applied sciences

ALLELOPATHIC EFFECT OF VARIOUS ORGANS OF WALNUT (*JUGLANS REGIA*) ON SEED GERMINATION OF WHEAT

*Iman Bajalan[1,2], Masoumeh Zand[2] and Shahram Rezaee[2]
[1]Young Researchers and Elite Club, Borujerd Branch, Islamic Azad University, Borujerd, Iran
[2]Department of Agriculture, College of Agriculture, Borujerd Branch, Islamic Azad University, Borujerd, Iran

ABSTRACT

This study is an attempt to analyze the allelopathic effect of various organs of walnut on germination of wheat experimentally and in a quiet accidentally frame of 10 treatments and 4 replications for it. The treatments of the experiment included an aqueous extract of the root, leaf, and fruit's green skin (each of them in concentrations of 25, 50, and 100% percent) and distilled water (control). The Results showed that the strong allelopathic effect of the extract of various organs of walnut on germination of wheat seeds in such a way that the statistical comparison indicates the reduction of germination percentage of seeds in treating the aqueous extracts in comparison with control in the level of one percent. Moreover, the results indicated that the extract of the fruit's green skin has a stronger allelopathic effect comparable with the leaf and root.

Keywords: Aqueous extract, allelopathy, germination, walnut's various organs.

INTRODUCTION

Regarding the widespread and indiscriminate use of chemical poisons, especially herbicides in the last decade taking use of allelopathic plants and also their remainders in the soil in order to control the plants and provide the suitable condition of growth has been considered (Inderjit and Keating, 1999). Broad and extensive researches have been done on this issue. The researches show significant reduction of the parameters which are relevant to germination of various numbers of wheat in reaction to the allelopathic activity of aqueous extract of some weeds (Kiarostami, 2004). In other experiments the extract of aerial organ and saffron chromium (Eghbali *et al*., 2008) and walnut leaf (Roohi *et al*., 2009) were tried on wheat plant and all of them indicated the reduction of germinating speed of wheat. In another research the allelopathic effects of wheat on weeds have been proved (Lehman and Blum, 1997; Alsaadawi *et al*., 1998).

Walnut is an important tree with multi-purpose uses so that it can be used in gardening for the fruit, in the forest for its valuable wood and in pharmacy as an herb (Ebrahimi *et al*., 2009). This research was done in order to compare and analyze the allelopathic effect of various organs of the walnut tree in different concentrations on the germination characteristics of wheat.

MATERIALS AND METHODS

In order to study the allelopathic effect of the extract of various organs of walnut trees on germination of wheat, an experiment was conducted in a completely accidental plan with 10 treatments and 4 replications in the Laboratory of Department of Agriculture and Resources of I.A.U of Broujerd. The experimental treatments contained 25, 50, and 100% of the extract of organs like the root, leaf and the green skin of walnut fruit. The root organ was taken from a three year old tree and it was drained with the purpose of abstaining extract from the mentioned organs. The action of draining was done in the shadow and it continued until reaching to the stable weight. Out of each organ ten percent strong weight extract – a mass (50g with 500ml water) was prepared by putting it on the shaker machine for 24 hours. Four layers of cotton fabric have been used to separate the plant's tissues and solid organs from the extract (Ghorbani *et al*., 2008). Then it was centrifuged with the speed of 2000rpm for 15 minutes. In the next step, by adding distilled water to these strong extracts, aqueous extracts with the concentrations of zero (control) 25, 50, and 100% were made. Thirty wheat seeds were placed in every Petri dish containing filter paper and for each treatment four replications were repeated. According to the plan, 7ml from the prepared aqueous extract from every organ with various concentrations was added to the Petri dishes containing seeds. The Petri dishes were placed inside the garments and in temperature of 20 ^{0}C. The first count of germinated seeds was done 48 hours later. The seeds which were germinated for 2ml were considered as grown seeds.

At the end of the experiment of germination rate, the percentage of germination, the length of the root, the shoot and fresh and dry weight of the seedling were measured. In this experiment, the total weight of the

*Corresponding author email: bajalan_iman@yahoo.com

seedling has been considered as the seedling weight. To measure the dry weight, 7 days after the beginning of the experiment, the samples were kept in the oven for 24 hours at the temperature of 70^0C. The following parameters, previously reported by others, such as Jefferson and Pennacchio (2003).

Rate of germination (RG) = $\sum_i^d = 1 \frac{ni}{di}$

Where,
N is a daily increase in seedling number
D is the number of days from seed placement

The data analysis was done by a piece of software called SPSS 15. Moreover, the average of the data was compared by use of Duncan and with the probability level of 1%.

RESULTS AND DISCUSSION

The results indicate that the studied wheat seeds reacted differently toward the extract received from various levels of organs of walnut tree. Results depicted that various organs of walnut tree by having an allelopathic effect on the total number of germinated seeds reduced the germinated seeds in each day. The percentage and the rate of germination decreased significantly by increasing the concentration of extracts when compared with control. Previous studies also revealed that allelopathic materials of the walnut leaf reduced wheat germination (Rohi *et al*., 2009). Scott and Sullivan (2007) in their experiment proved that Juglone and the extract of walnut leaf have a deterrent effect on photosynthesis, respiration, growth speed of the root and the stem in corn and soya plants which are cultivated in hydroponic environments (Jose and Gillespie, 1998). The results indicated that the extract of walnut's organs prevents germination moreover it prevents the stem's growth so that in the concentration of 100 percent, a reduction of 73/64 to 97/04 was observed.

Percentage and Rate of Germination

The results indicated that the percentage of the germination of wheat seed significantly reduces under the influence of the extract of walnut's organs. 100% concentration of root's extract reduced the percentage of germination of 26/7% and the 100% concentration of the fruit reduced the germination to 84/17% compared with Control. Among the used treatments, the least reduction of germination after Control treatment belongs to 25-percent- treatment of root extract (Fig. 1).

The results show that different concentrations of the extracts of walnut tree's organs have a significant effect on germination rate of wheat seed (Fig. 2). The achieved results from comparing the means of germination rates of wheat seeds indicate that by increasing the concentration of the extract, germination rate decreases, this amount was respectively, for concentrations of 25, 50 and 100 percent for the root of 13/5, 16/2 and 27/83, for the leaf of 4/1, 9/65 and 25/4 and for the extract of fruit's green skin 1/35, 7/05 and 23/55. The increasing of growth rate in low concentrations decreased remarkably because of the delay in germination and its notable reduction in high concentrations was because of not germinating (Fig. 2).

Length of Shoot and Root: Results show the length of the shoot and root, notably decrease under the influence of the extract of walnut tree's organs. Results gained from comparing the means indicate that the tallest length of the root (5/896cm) is related to control treatment and the shortest length of the shoot is related to 100-percent-treatment of the extract of walnut fruit's green skin (/04 cm) (Fig. 3).

The results achieved by comparing the means show the longest length of the stem (4/535 cm) belongs to control treatment and the shortest one belongs to 100% treatment of fruit's green skin (039 cm) (Fig. 4).

Seedling's Fresh and Dry Weights: The extracts of various organs in 25% concentration had the least influence on seedling's weight, this amount is respective for the concentration of 25% of root, leaf and fruit's green skin 34/14, 36/61 and 44/87% (Fig. 5).

Moreover, seedling's dry weight remarkably reduced under the influence of different extracts of walnut's organs (Fig. 6). This amount for concentrations of 100% of root, leaf and the fruit's green leaf is 73/34, 93/75 and 97/09%, respectively. The smallest percentage of reduction of seedling's dry weight belongs to the treatment of 25% of the root 22/67% (Fig. 6).

The result of this research indicates the allelopathic effects not only lead to the reduction of germination rate but they also cause delay in germination, decrease of the length of the root and stem and reduction of seedling's weight. Delay in germination can have a negative effect in comparison with other plants which in turn can exacerbate the allelopathic effects and plant's being weaker. A plant which owns weaker roots will fail in terms of environmental stresses such as low soil moisture or nutritional stresses with other plants. Moreover, allelopathic compounds can be effective on hairy roots and other roots of the plant and this phenomenon is a reason of reduction of water uptake in the plant (Chon *et al*., 2005).

Walnut leaks juglone to its environment during its lifelong time (Scott and Sullivan, 2007). Juglone has been isolated from many plants in the walnut family (Juglandaceae) including *Juglans nigra*, *Juglans regia* and others (Prataviera *et al*., 1983). Juglone is phytotoxic,

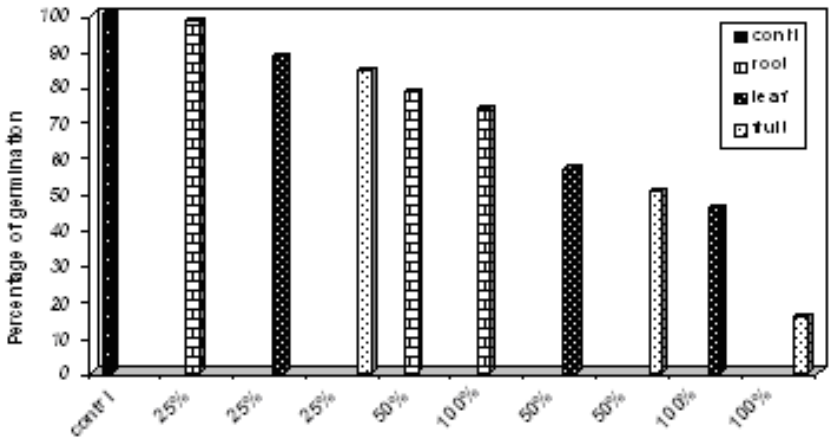

Fig. 1. The percentage of germination of wheat in various concentrations of walnut's organs.

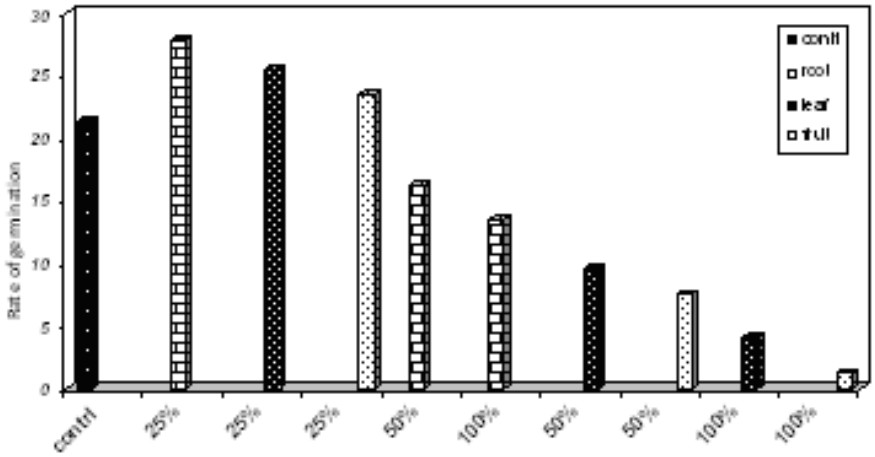

Fig. 2. The rate of germination of wheat in various concentrations of walnut's organs.

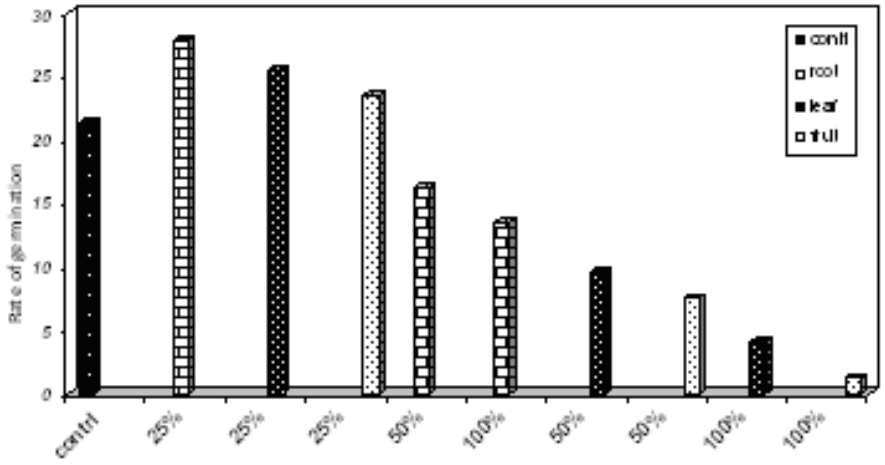

Fig. 3. The average of the fresh weight of wheat in various concentrations of walnut's organs.

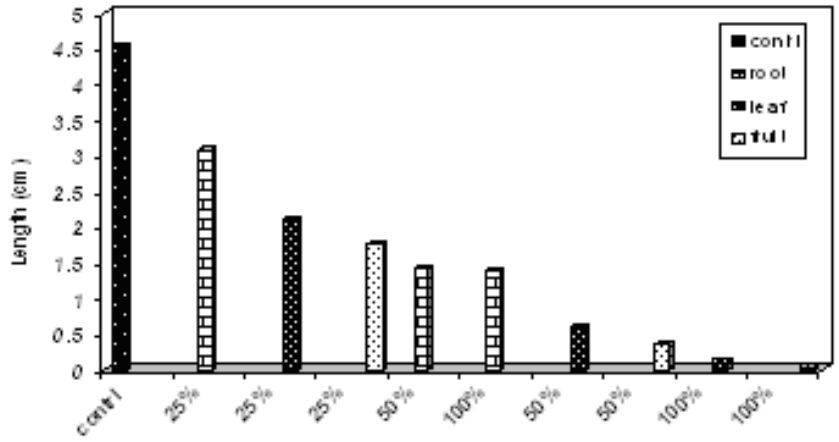

Fig. 4. The percentage of the length of the stem of wheat in various concentrations of walnut's organs.

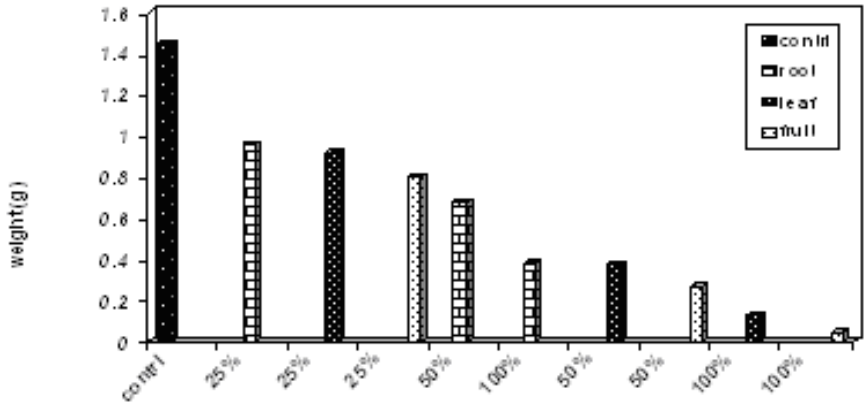

Fig. 5. The average of the fresh weight of wheat in various concentrations of walnut's organs.

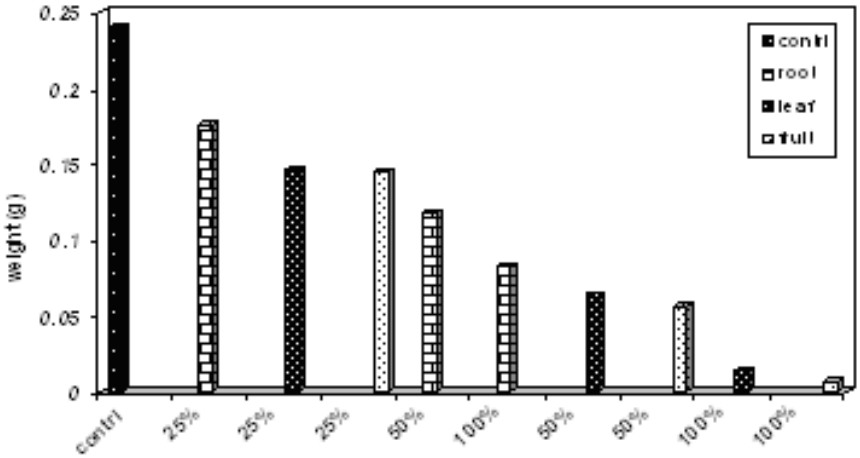

Fig. 6. The average of dry weight of wheat in various concentrations of walnut's organs.

but the mechanisms of growth inhibition have not been fully explained (Hejl and Koster, 2004). Juglone (5-hydroxy-1,4-napthoquinone) is a chemical compound in walnut's allelophathy (Terzi and Kocacaliskan, 2009). Juglone exists in the leaves, stem, tree's skin, fruit's skin and roots which are oxidized to 5-hydroxy-1,4-napthoquinone when exposed to soil or air (Rietveld, 1983). So far, the effect of juglone has been studied in a lot of studies. In an experiment, it is mentioned that juglone and the extract of walnut leaf leads to quality and quantity yield reduction of strawberries.

The results gained by this study show that wheat plant reacts differently toward the extracts of various organs of the walnut and these reactions increases by increasing the percentage of the used extract and this is because of the difference in the amount of Juglone in various organs during the growth season. With more researches on this issue, it is possible that by using juglone in preparing poisons and herbicides to take use of this compound as a suitable substitute for pest control, diseases and weeds. Also, by studying the various organs of wheat and analyzing their sensitivity degree to this compound we can begin to produce resistant varieties to it. More information on this issue is in need of more researches.

REFERENCES

Alsaadawi, IS., KHY. Zwain and HA, Shahata. 1998. Allelopathic inhibition of growth of rice by wheat residues. Allelopathy Journal. 5:163-169.

Chon, SU., HG. Jang, DK. Kim, YM. Kim, HO., Boo. and Kim, YJ. 2005. Allelopathic potential in lettuce *(Lactuca sativa* L.*)* plants. Scientia horticulture, 106: 309-317.

Ebrahimi, A., MR. Fatahi, ZA. Zamani. and Vahdati, K. 2009. An investigation on genetic diversity of 608 Persian walnut accessions for screening of some genotypes of superior traits. Iranian Journal of Horticultural Sciences. 40(4):83-94.

Eghbali, SH., Rashed, M., Mohasel, A. Nursery, M. and Kazerooni, M. 2008. Allelopathic effects of saffron on the Chromium residue and shoot growth of wheat, rye, vetch and beans. Iranian Journal of Field Crops Research. 6 (2):227-234.

Ghorbani, ML., Bakhshi Khaniki, GR. and Shojaei, A. 2008. Examination of the effects of Allelopathy of *Artemisia sieberi* Besser subsp. Siberia on seed germination and *Avena lodoviciana* and *Amaranthus retroflexus* seedling growth**.** Pajouhesh-va-sazandegi. 21:129-134.

Hejl, AM. and Koster, KL. 2004. Disrupts root plasma membrane H+-ATPase activity and impairs water uptake, root respiration, and growth in soybean *(Glycine max)* and corn *(Zea mays).* Journal of Chemical Ecology. 30:453-471.

Inderjit, K. and Keating, L. 1999. Allelopathy: Principal and Practice. John Promises for Biological Control in: Advance in Agronomy. Ed. Sparks, Dl. Academic Press. 67:141-231.

Jefferson, LV. and Pennacchio, M. 2003. Allelopathic effects of foliage extracts from four Chenopodiaceae species on seed germination. Journal of Arid Environments. 55 (2):275-285.

Jose, S. and Gillespie, AR. 1998. Allelopathy in black walnut *(Juglans nigra* L.*)* Alley cropping. II. Effects of juglan on hydroponically grown corn *(Zea mays* L.*)* and soybean *(Glycine max* L. Mar.*)* Growth and physiology. Plant and Soil. 203 (2):199-206.

Kiarostami, K. 2004. Allelopathic effect of weeds on germination and seedling growth of different cultivars of wheat. Pajouhesh-va-sazandegi, 16:66-73.

Lehman, ME. And Blum, U. 1997. Cover crop debris effects on weed emergence as modified by environmental factors. Allelopathy Journal. 4:69-88.

Prataviera, AG., Kuniyuki, AH. and Ryugo, K. 1983. Growth inhibitors in xylem exudates of persian walnuts *(Juglans regia* L.*)* and their possible role in graft failure. J. Am. Soc. Hort. Sci. 108:1043-1045.

Rietveld, WJ. 1983. Allelopathic effects of juglone on germination and growth of several herbaceous and woody species. Journal of Chemical Ecology. 9:295-308.

Roohi , A., Saeedi, M. and Nikazad, P. 2009. Allelopathic effects of aqueous extract of walnut *(Juglans regia*) on germination and seedling growth characteristics of wheat *(Triticum astivum),* onion *(Allium cepa)* and lettuce *(Lactuca sativa).* Journal of Field Crops Research. 7 (2):457-464.

Scott, R. and Sullivan, WC. 2007. A review of suitable companion crops for black walnut. Agroforestry Systems. 71(3):185-193.

Terzi, I. and Kocacaliskan, I. 2009. Alleviation of juglone stress by plant growth regulators in germination of cress seeds. Scientific Research and Essay. 4 (5):436-439.

Received: Dec 4, 2013; Accepted: Jan 14, 2014

SENRA Academic Publishers, British Columbia
Vol. 8, No. 2, pp. 2865-2870, June 2014
Online ISSN: 1920-3853; Print ISSN: 1715-9997

Canadian Journal of pure&applied sciences

EVALUATION OF REACTIVE GLUCOSE BY-PRODUCTS DICARBONYLS AND GLYCATED HAEMOGLOBIN IN HYPERGLYCEMIC PATIENTS

*GS George[1], AA Uwakwe[2] and ET Egoro[3]
[1]Department of Medical Laboratory Science, Niger Delta University, Wilberforce Island Bayelsa State
[2]Department of Biochemistry, University of Port Harcourt
[3]Department of Medical Laboratory Science, Niger Delta University, Wilberforce Island Bayelsa State, Nigeria

ABSTRACT

To examine the effect of hyperglycemia on production of glucose by-products, we determined the concentration of glyoxal, methylglyoxal along with glucose, insulin and glycated haemoglobin (HbA1c). Using radioimmunoassay, chromatographic and spectophotometric techniques, the interactions of these compounds have been used to elucidate a possible cause of clinical significance in the diabetic state. Our study has shown that the selected analytes interacts in uncommon ways to exercerbate glycemic stress. We observed a positive linear relationship between glucose concentration and glycated haemoglobin and identified glucose excess as being a responsible factor controlling the creation of glucose by-products. Concomitant with the knowledge of the fact that both compounds are detoxified by the activity of their respective glyoxylase, we observed glyoxal concentration 3-4 folds higher than methylglyoxal in patients investigated. Further analysis of data with a scatter plot of subjects according to their blood glucose and HbA1c, glyoxal and methyloxal shows a positive linear correlation and the linear regression had a coefficient of r=0.820 significant at $P > 0.05$. The biochemical evidence suggests that production of carbonyls increases glucose toxicity and imposes the need to provide substances that will inhibit their formation. This is expected to enhance diabetes mellitus management.

Keywords: Reactive Glucose, dicarbonyls, glycated haemoglobin, hyperglycemic.

INTRODUCTION

Diabetes mellitus is a heterogeneous metabolic disorder characterized by chronic hyperglycemia due to dynamic interactions between varying defects of insulin secretion and action. The role of glucose in the pathogenesis of diabetic complications has attracted scientific scrutiny raising questions as to whether glucose is a reactant or an inert molecule in the pathogenesis of diabetic complications.

The study of glucose by-products notably glyoxal, methyglyloxal, dimethylglyoxal and 3-deoxyglucosone has attracted tremendous attention in recent years on account of their clinical significance in chronic and age related diseases as shown by Thornally *et al.* (1999). Oxidative stress is now known to be a feature of these diseases notably diabetes mellitus in which intracellular hyperglycemia in insulin dependent cells, such as nerves, kidney, lens and erythrocytes modulates the genesis of microvascular complications due to the production of advanced glycation end products (AGEs) (Dalle-Donnea *et al*. (2003) and Brownlee (2005). Further examination of periodicals by Maritin *et al*. (2003) and Brownlee (2001) has shown that these processes occur via non-enzymatic glycosylation of both intracellular and extracellular matrix proteins like collagens and extraceullular matrix proteins which inhibits nitric oxide production. The result of these stress induced metabolic activities is the modification of lipids, proteins and carbohydrates which are expressed in the generation of reactive carbonyls compounds such as glyoxal, methylglyoxal, dimethylglyoxal and 3-deoxyglucosone.

Previous scientific studies have shown that reactive carbonyl compounds are glycolytic mediators of reactive carbonyl stress which have been implicated in diabetes (Saka, 2011). It has earlier been shown that the Milliard reaction (Advanced glycated end product) exacerbate protein glycation, raises synthesis of reactive oxygen species (ROS) and metal ions which have been involved as participants in complications of diabetes. Oxygen is now known to be a fixative of irreversible damage via this advanced glycated end product reaction.

Our understanding of recent studies have elucidated the fact that advanced glycated end products of the Milliard reaction can be inhibited as reflected in Brownlee *et al*. (1986) and Payrox and Sternberg (2006). The vitamin B_6 pyridoxamine is considered an Amadorin or post Amadori inhibitor, which is known to trap products from Amadori compound fructoselysine, the first stable glucose aduct protein. The other significant roles played by pyridoxine includes blocking oxidation, trapping reactive carbonyl and dicarbonyl compounds, chelation of metal ion catalyst and scavenging of reactive oxygen species as shown by

*Corresponding author email: ozunugborie@gmail.com

Khalifa *et al*. (1999), Reddy and Beyaz (2006) and Jomova *et al.* (2010). Some authors have shown other carbonyl trapping agents with reactive nucleophilic functional groups invitro as expressed in rodent models of diabetes. These compounds include 2,3-diaminophenazone, penicillamine and several derivatives of aminoguanidine.

In this work we have studied some of the metabolites which are very important in diabetic complications.

MATERIALS AND METHODS

At the Federal Medical Centre, Yenagoa, Bayelsa State, Nigeria, blood and urine samples were collected from hyperglycemic patients (n=80) with Fasting blood glucose value ≥20.0mmol/l and urine glucosuria. Control subjects (n=60) with Fasting blood glucose level ranging between 3.5-6.7 mmol/l without glucosuria were included.

Analytical Methods

The Fasting Blood Glucose was determined by the glucose oxidase method using Randox Kits and values measured with spectrophotometer set at 540nm wavelength. Urine samples were evaluated for the presence of glucose with the aid of N-multistix manufactured by Macherry-Nagel (Germany). Glycated Haemoglobin was determined by ion-exchange high performance liquid chromatography, HPLC-Esi/ms approach with UV detection. Radioimmunoassay was used for the determination of insulin with the aid of Cx 9 Automated Machine (Beckman) with Beckman assay kits.

Glyoxal and methylglyoxal were measured by the analytical method developed by Merc making use of stillbenediamine (SD) as derivating reagent at a separation time of 5 minutes and SDS as micellular medium at pH 8 and sodium tetraborate (0.1m) as buffer.

RESULTS AND DISCUSSION

Assay of the biochemical parameters determined are shown in tables 1 and 2. The results of the study gave consistent proof of the fact that the degree of hyperglycemia positively strongly correlates with the concentration of HbA1c, glucose, glyoxal and methylglyoxal and a negative correlation with insulin level. We have shown in figure 1 graphically the interrelationship of glycated haemoglobin in intact and lysed cells. Figures 2, 3 and 4 are scatter plots of some parameters determined.

Evidence of the fact that the development of complications in diabetics is strongly connected with the invivo surrounding factors such as genetics and excess production of oxygen free radicals have been proven. The determination of concentration of Fasting blood glucose, glycated Haemoglobin, insulin and the carbonyl compounds were deployed in this study to further demonstrate the influence of these parameters in diabetes mellitus. It is known that diabetes is associated with chronic complications such as macrovascular (cerebrovascular and coronary artery disease) and microvascular (nephropathy, neuropathy and eye disease). This work confirms the fact that a greater percentage of diabetic patients have one form of complications or the other at the time of diagnosis.

Table 1. Comparative values of measured profiles.

Parameters	Control (n=60)	Hyperglycemic (n=80)	P-value (≥ 0.050)
FBG (mmol/l)	4.8 ± 1.2	25.49 ± 0.48	
Insulin (iu/mol)	5.3 ± 0.2	0.18 ± 0.003	
HbA1c (mmol/mol)	42 ± 5	150 ± 6.7	
GO (ng/ml)	0.18 ± 0.12	0.54 ± 0.03	
MGO (ng/ml)	0.03 ± 0.4	0.19 ± 0.009	

Values are mean ± SD

Table 2. Determination of levels of glycated haemoglobin intact and disrupted cells.

Intact cells		Disrupted cells	
HbA1c (mmol/mol)	Glucose (mmol/l)	HbA1c (mmol/mol)	Glucose (mmol/l)
35.0	5.0	48.0	4.7
35.0	5.0	42.0	4.0
35.0	5.0	53.0	8.0
39.0	6.0	75.0	10.0
40.0	7.0	85.0	15.0
40.0	7.0	88.0	20.0
42.0	8.0	92.0	25.0
47.0	10.0	96.0	30.0

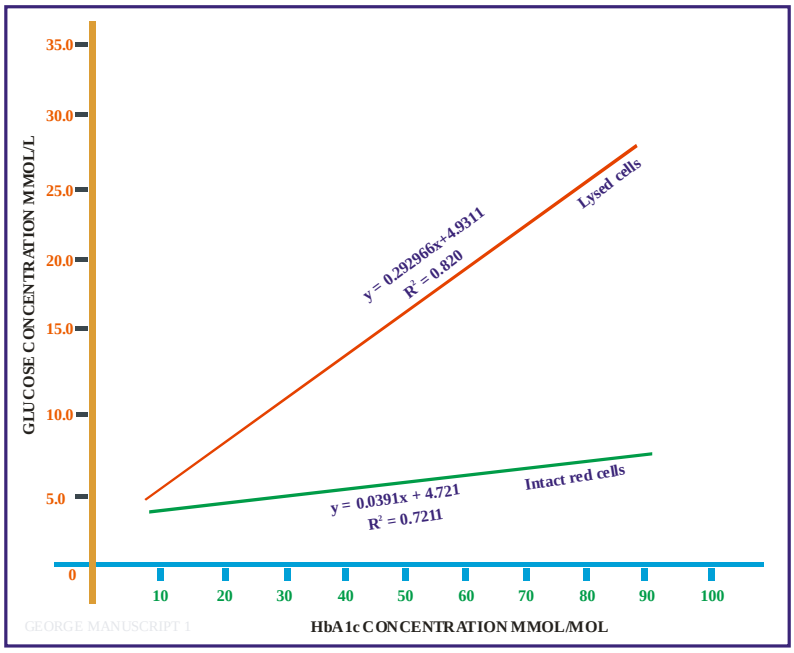

Fig 1. Graph of FBG against HbA1c (lysed and intact).

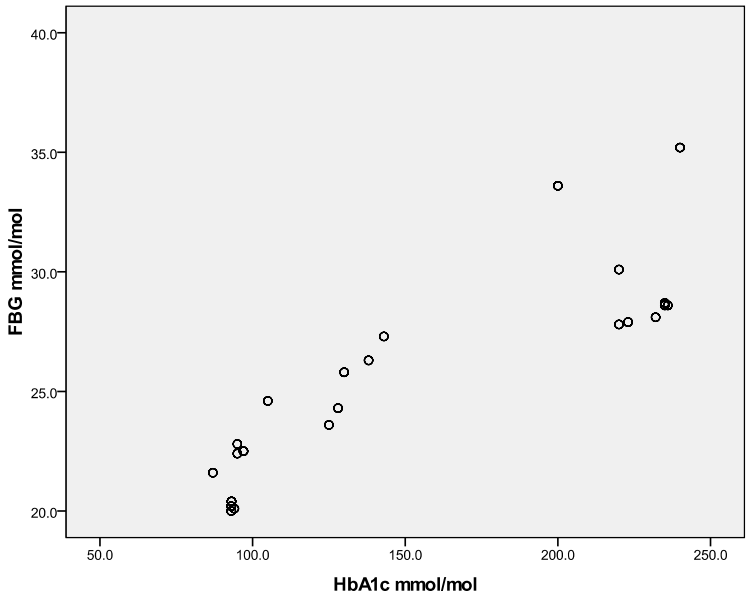

Fig. 2. Scatter plot of FBG against HbA1c.

Earlier reports showing that strong electrophilic carbonyl compounds notably glyoxal, methylglyoxal and 3-deaoxyglycosone produced in hyperglycemics are responsible for the observed glycemic stress in diabetes mellitus has been demonstrated by Odeti *et al*. (1999). Carbonyl groups result from protein oxidation and their level in tissues and plasma is a relatively stable marker of oxidative damage. Although the synthesis and eventual release of these compounds may be insidious, their sustained generation progressively causes glycation of protein which are known to contain both acidic and basic groups. A major consequence of glycation is the alteration of functional properties of proteins as elucidated by Giaco and Brownlee (2010). The elevated levels of glucose, glycated haemoglobin and the carbonyls, glyoxal and methylglyoxal observed in this study correlates with earlier findings suggesting that a major cause of lipid peroxidation is carbonyl stress. It is known that oxidative stress modulates lipids, protein and carbohydrate in ways that enhances the production of carbonyl compounds.

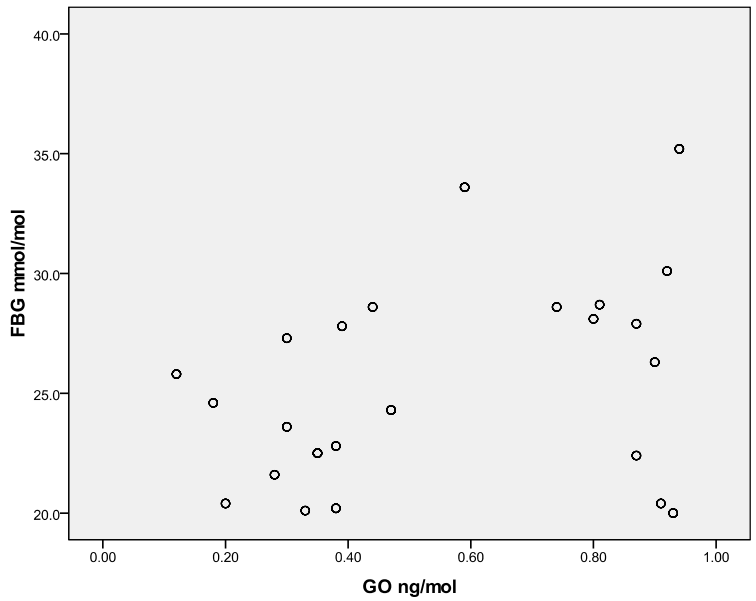

Fig. 3. Scatter plot of FBG against GO.

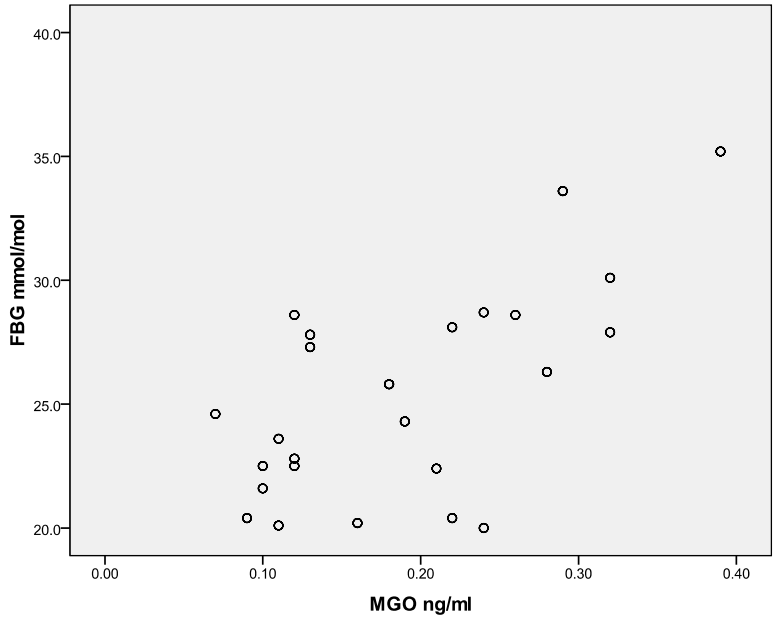

Fig. 4. Scatter plot of FBG against MGO.

Other pathways through which carbonyl could be formed are available by mechanisms which modify proteins leading to development of activated glycated end product like pentosidine and carboxymethyllysine which are known to crosslink protein (Baynes,1991; Thornally, 2004; Goh and Cooper, 2008). Recent periodicals of Riboulet-Charvey *et al*. (2006) and Pennathir *et al*. (2005) have elucidated the fact that methylglyoxal can cause inhibition of insulin stimulated phosphorylation of kinase, a factor known to have a negative effect in the insulin-stimulated phosporylaton of protein kinase with direct inhibitory role of insulin in the induced phosphorylation of substrates. The hormone insulin is a major vehicle for intracellular control and overrides the normal cellular controls. The complex nature of carbonyls compounds which are formed as a result of complications of diabetes could further act to synergise the non-enzymatic reaction that precipitates glycated end products. This may lead to receptor binding of the peptide and further exacerbate hyperglycemic condition. This view seem to lend

credence to earlier works of Zythen *et al*. (2008), Thornally (2008) and Whiting *et al*. (2008).

To further buttress the influence of glycation, we measured the glycation of haemoglobin in lysate and intact red blood cells and confirmed higher values in the lysate. A correlation coefficient determined for this gave a value of $y=0.292966x + 4.9311$ $R^2=0.820$ for the lysate and $y=0.0391x + 4.721$, $R^2=0.7211$ for the intact cells.

We observed a close relationship of the carbonyl concentration and the level of hyperglycemia which established the fact that they can be used as stable markers of oxidative damage. HbA1c, a marker of glycemic control was also related to the level of carbonyl. These results strongly suggest that impairment of glycemic control has link with oxidation. This is further buttressed by the fact that glycation cascade also releases free radicals becoming responsible for further oxidative attack which supports earlier studies of Pinaki *et al.* (2010), Tomic *et al.* (2013) and Konukoglu *et al*. (2002). The fact established here is that increased oxidative stress if any in the diabetic group is undoubtedly induced by hyperglycemia.

CONCLUSION

This work has identified some factors implicated in the production of toxic glucose by products and underscores the need for effective glycemic control which is required to prevent complications. The need to develop drug therapy which would act as inhibitors of signaling compounds for activated glycated end product formation may eventually prevent production of carbonyls and reduce the associated toxicity while providing glycemic stress reducing antioxidants.

ACKNOWLEDGEMENT

We hereby profoundly acknowledge the support of the Ethical Research Committee of Federal Medical Centre, Yenagoa, Bayelsa State, Nigeria and the management of Geotech Medical Laboratory for the use of their equipment and other facilities.

REFERENCES

Baynes, JW. 1991. Role of oxidative stress in development of complications in diabetes. Diabetes. 40:405-415.

Brownlee, M. 2005. The Pathophysiology of diabetic complication: a unifying mechanism. Diabetes. 54:1615-1625.

Brownlee, M. 2001. Biochemistry and Molecular Biology of diabetic complications. Nature. 414:813-20

Brownlee, M., Vlassara, H., Kooney, A., Ulrich, P. and Cerami, A. 1986. Aminoguanidine prevents diabetes-induced arterial wall protein cross-linking. Science. 232:1629-1632.

Dalle-Donnea., Ranieri, R., Daniela, G., Aldo, M., R. and Colombo, I. 2003. Review-Protein carbonyl groups as Biomarkers of oxidative stress. Clinica Chimica Acta. 329:23-38.

Giacco, F. and Brownlee, M. 2010. Oxidative stress and diabetic complications. Circ Res. 103:1058-1070.

Goh, SY. and Cooper, ME. 2008. Clinical Review. The role of advanced glycation end products in progression and complications of diabetes. J clin Endocrinol Metab. 93:1143-52.

Jomova, K., Vondrakova, D., Lawson, M. and Valko, M. 2010. Metals, Oxidative stress and neurodegenerative disorders. Mol cell Biochem. 345:91-104.

Khalifa, RG., Baynes, JW. and Hudson, BG. 1999. Amadorins: Novel post-Amadori inhibitors of advanced glycation reactions. Biochem Biophys Res. 257:251-258.

Konukoglu, D., Kemerli, GD., Sabuncu, T. and Hatemi, HH. 2002. Protein carbonyl content in erythrocyte membrane in type 2 diabetic patients. Horm Metab Res. 34(7):367-70.

Maritim, AC., Sanders, RA. and Watkins, JB. 2003. Diabetes, Oxidative stress and antioxidants: A Review J Biochem Mol Toxicol. 17:24-38.

Odeti, P., Garibaldi, S., Noberasco, G., Aragnol S, Valentini S, Traverso, N. and Marinari, UM .1999. Levels of carbonyl groups in plasma proteins of type 2 diabetes mellitus subject. Acta Diabetologica 36 (4):179-183.

Payroux, J. and Sternberg, M. 2006. Advanced Glycation end products (AGEs): Pharmacological inhibition in diabetes. Pathol Biol (Paris). 54:405-419.

Pennathir, S., Ido, Y., Heller, JI., Danda, R., Pergola, P., Williamson, JR. and Heinecke, JW. 2005. Reactive carbonyls and polysaturated fatty acids produce a hydroxyl radical-like species: a potential pathway for oxidative damage of retinal proteins in diabetes. J Biochem. 280(24):22706-14.

Pinaki, S., Raushik, K., Moham, C., Modal, I., Chakraborty. and Manoj, Kar. 2010. Elevated level of carbonyl compounds correlates with insulin resistance in type 2 diabetes. Annal Acad Med Singapore. 39:909-12.

Reddy, VP. and Beyaz, A. 2006. Inhibitors of the Maillard reaction and AGE breakers as therapeutics for multiple diseases. Drug Disco Today. 11:646-654.

Riboulet-Charvey A., Pierron, A., Durand, L., Murdaca, J., Guidicelli, J. and Van Obherghen, E. 2006. Methylglyoxal impairs the insulin signaling pathways

independent of the formation of intracellular reactive oxygen species. Diabetes 55:1289-99.

Saka, P. 2011. Endocrinology Medical article: Elevated level of carbonyl compound correlates with insulin resistance in type 2 diabetes. Annals, Academy of Medicine, Singapore.

Thornalley, PJ., Langborg, A. and Minhas, HS. 1999. Formation of glyoxal, methylglyoxal and 3-deoxyglucosone in the glycation of proteins by glucose. Biochem J. 344:109-16.

Thornalley, PJ. 2004. Glycation, Receptor-mediator cell activation and vascular complications of diabetes. Diab Vasc Dis Res. 1:21-2.

Thornalley, PJ. 2008. Proteins and Nucleotide damage by glyoxal and methylglyoxal and disease. Drug metab drug interact. 23:125-50.

Tomic, M, L Jubic, S. and Katstelan, S. 2013. The role of inflammation and endothelia dysfunction in the pathogenesis of diabetic retinopathy. Coil Antropol. 37 (Suppl.).1:51-7.

Whiting, PH., Kalansoriya, A., Holbrook, I., Hadad, F. and Jennings, PE. 2008. The relationship between chronic glycemic control and oxidative stress in type 2 diabetes mellitus. Br J Biomed Sci. 65(2):71-4.

Zyhen, Y., Lix, K., Wang, Y. and Cai, L. 2008. The role of zinc, copper and iron in the pathogenesis of diabetes and diabetic complications: therapeutic effects by chelators. Hemoglobin. 32:135-145.

Received: Dec 19, 2013; Revised: Jan 25, 2014; Accepted: Jan 27, 2014

SENRA Academic Publishers, British Columbia
Vol. 8, No. 2, pp. 2871-2900, June 2014
Online ISSN: 1920-3853; Print ISSN: 1715-9997

Canadian Journal of pure & applied sciences

EFFECT OF RIGHT BANK OUTFALL DRAIN (RBOD) ON BIODIVERSITY OF THE WETLANDS OF HALEJI WETLAND COMPLEX, SINDH

M Zaheer Khan, *Tanveer Jabeen, S Ali Ghalib, Saima Siddiqui, M Safdar Alvi, Iqbal Saeed Khan, Ghazala Yasmeen, Afsheen Zehra, Fozia Tabbassum, Babar Hussain, and Raheela Sharmeen
Wildlife Section, Department of Zoology, University of Karachi, Karachi-75270

ABSTRACT

In the present study, the effects of Right Bank Outfall Drain (RBOD) on the fauna of the wetlands were studied and inventories of the fauna and the flora were prepared. During the study period from 2007 – 2012, water samples taken from three sampling sites from the study areas viz., RBOD at Gharo, near Haleji Lake and near Keenjhar Lake were analyzed for physico-chemical parameters, pesticides and heavy metals. The mean salinity value of all sampling sites was recorded. RBOD at Gharo and RBOD near Keenjhar Lake showed high salinity value as per limit of World Health Organization standard. Water samples taken from RBOD near Keenjhar Lake showed pesticide OC compounds below the Maximum Acceptable Concentration (MAC). However, no serious adverse effects of environmental pollution were detected on the aquatic biodiversity except for some minor toxic effects due to the presence of heavy metals in water. Regarding biodiversity, two species of protozoans, 104 species of arthropods, 23 species of zooplanktons, 13 species of molluscs, 228 species of birds, 28 species of mammals, 31 species of reptiles, 2 species of amphibians and 59 species of fishes were recorded from the study areas. The biodiversity of RBOD is in decline mainly due to hunting, capturing, habitat destruction, cutting of trees, commercial fishing, anthropogenic activities and growing human population around the RBOD area.

Keywords: Right bank outfall drain, biodiversity of Sindh, environmental effects, threatened species.

INTRODUCTION

The province of Sindh forms the lower Indus basin and lies between 23^0 35' and 28^0 30' northern latitude and 66^0 42' and 71^0 10' east longitude (Khan *et al*., 2014). The different ecosystems of Sindh include wetlands, deserts, river, mangrove forests, agricultural and coastal areas. The River Indus act as a key source of water in Pakistan and majority of the population of Sindh depends on this River. There are many canals and barrages coming out of this River and giving lives to wetland birds all over the Sindh (Yahya, 2007). Sindh estuarine and coastal wetlands serve as nursery grounds for the lobsters, shrimps and fish. Each year during the migration season, over one million of water birds belonging to 108 species, visit Sindh wetlands (Khan, 2006). Thatta is an important district of Sindh Province due to its wetlands, Wildlife Protected Areas and Cultural Heritage Sites. Right Bank Outfall Drain at Gharo Creek, near Haleji Lake and near Keenjhar Lake all in Thatta district were selected for the present study (Figs. 1 and 2). In Sindh, after the Left Bank Outfall Drain project, the Right Bank Outfall Drain is the second biggest project.

Right Bank Outfall Drain

Presently, Pakistan is facing two big problems which are salinity and water logging and to resolve these issues many measures have been taken in Sindh. Right Bank Outfall Drain is a major measure which was carried out on the right bank of the Indus. Right Bank Outfall Drain is a long term project to drain out sewerage and water from towns and agricultural lands on the right bank of the River Indus. It carries effluents from the upper Sindh and adjacent areas of Balochistan and these are ultimately drained into the Arabian Sea. The RBOD is planned to take care of saline water and to dispose off directly into the Sea. But at present, since there is no outlet, the saline effluents flowing through main Nara Valley Drain are discharged as per force into Manchar Lake and Hammal Lake. This saline water contains agricultural waste like fertilizers, pesticides and domestic sewage, and these effluents have degraded and spoiled both the lakes. Currently, the Government has designed to outfall the poisonous effluent directly into the Sea through Gharo Creek.

The disposal of saline effluents into river near Sehwan causing risk for the peoples of Karachi, Hyderabad and small towns who draw their drinking water requirements direct from River Indus and Canal system of Keenjhar Lake. Presently, the effluent from the RBOD is disposed into Manchhar Lake. The principal features of the wetlands to be affected by the RBOD passing nearby, have been underlined below:

*Corresponding author email: tanveer_jabeen@live.com

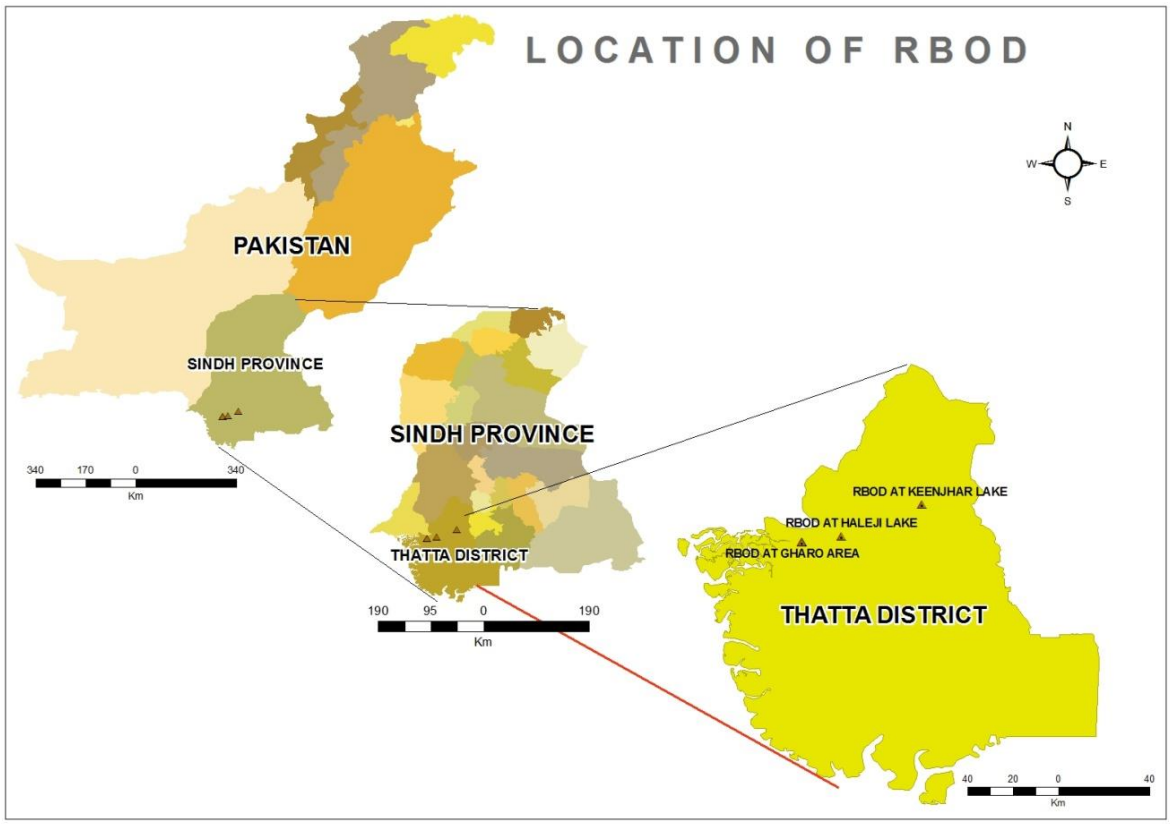

Fig. 1. Map showing study areas of RBOD.

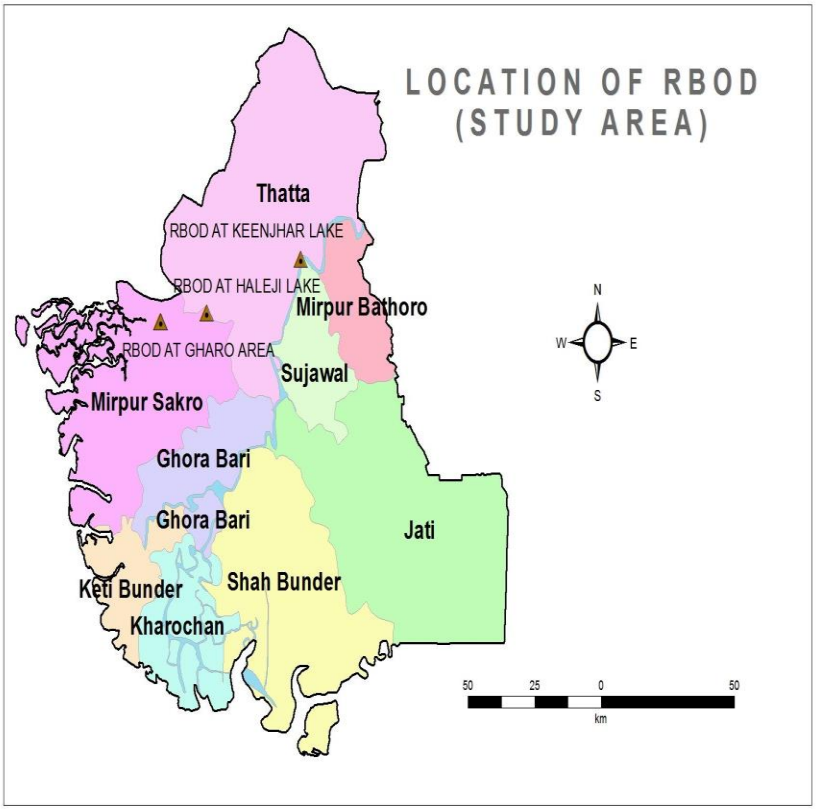

Fig. 2. Map of District Thatta showing the study areas.

1. Gharo Creek

Gharo Creek is located at 67° 11' E and 24° 47' N. It is about 5.5km long, 500m wide with a minimum depth of 7.5 meters and maximum depth of 17 meters. The total surface area of Gharo Creek is about 64,370ha (Fig. 3). It is placed towards the south east of Karachi. On the southern part of Gharo Creek are mangroves, as the western part is mostly reclaimed area for Port Qasim facility. The total length of Gharo Creek is about 30km and the total wastewater generation is about 30,000-35,000 gallons/day, which is discharged into the Sea without any treatment. In addition the bank of the creek is also used as a solid waste dumping site. Several pathogens, nutrients and chemicals that come along with the waste matter of Gharo city are not only detrimental to aquatic life, but also result in reduced biodiversity (Ahmed, 1995). The area near the city is also used for agricultural purpose. The agriculture runoff contains large amount of pesticides that ultimately find their way to the creek (Khan *et al*., 2004). Gharo Creek is a mangrove area, which provides nutrient requirements for species of shrimp and fish, and provides protection from storms and also provides excellent opportunities for research and development work.

2. Keenjhar Lake (Ramsar Site)

Keenjhar Lake is located on 68° 03' E, 24° 56' N, about 19 km North–East of Thatta town and 100 km away from

Fig. 3. View of RBOD at Gharo area.

Fig. 4. RBOD area near Keenjhar Lake.

Fig. 5. RBOD area near Haleji Lake.

Karachi. The Lake has an area of 13,468ha and the largest sweet water reservoir in Sindh and supplies water to the villages around the lake, and to Karachi city, Keti Bunder and Thatta. The maximum depth of the lake is 8m, it is also a Wildlife Sanctuary. The lake is associated with adjacent brackish seepage lagoons and marshes which are in a stony desert and made up of alternating layers of sandstone and limestone (Khan *et al*., 2012b).

RBOD near Keenjhar Lake

The RBOD flows approximately 3.5 kilometers away from the southern tip of Keenjhar Lake. After crossing Nai-Baran, the Drain is going through riverine area, keeping it on East of Keenjhar Lake between K.B. Feeder Link Canal and Indus River (Fig. 4). Keenjhar Lake is also a significant fish providing point.

3. Haleji Lake (Ramsar Site)

Haleji Lake (Wildlife Sanctuary) is located at 67°46' E and 24°47' N about 21km from Thatta and 88 km from Karachi. The lake is spread upto an area of 1,704ha with the level of water about 1-1.5m and maximum depth is 5-6m. Haleji Lake is a perennial fresh water lake associated with marshes and adjacent brackish seepage lagoons, set in a stony desert of limestone and sandstone bedrock (Khan *et al*., 2012b). In the late thirties, it used to be a shallow depression, which was converted into a freshwater reservoir by draining of saline water, building of embankments around the lake and filling its tip by Jam Branch Canal carrying water from Keenjhar Lake, which has remained the principal source of water. Haleji is well known for its Pelican and Cormorant Islands. It is also a breeding area of Herons and Egrets and many other birds. Presently it is infested with aquatic weeds and major portion is covered with aquatic grass.

RBOD near Haleji Lake

Presently, the RBOD flows along the edge of Haleji Lake with a discharge of 330 cusecs and a depth of 13 to 15 ft of water just 3 to 4 ft below ground level (Fig. 5). The RBOD drain has a common ground and flows very close to Haleji Lake the distance between RBOD and Haleji Lake hardly 50 to 100ft. The water level is 20-30 ft below the level of the lake area. Due to very short distance from RBOD, Haleji Lake may be affected by the seepage of its water to the drain. So as the ongoing construction work of RBOD may cause degradation in the area of Haleji Lake (Khan *et al*., 2012b).

4. Hadero Lake

Hadero Lake is located at 67° 52' E and 24° 49' N, about 10km northwest of Thatta town and 85 km away from Karachi, and having an area of 1,321ha. The lake is not deeper than 1.7m. The Lake is situated between the Haleji and Keenjhar Lakes. The substratum is made up of alternating layers of sandstone and limestone with rocky and sandy western and northern shores, bounded by stony desert. The lake is fed by the SLM drain, which links up through the Jam branch canal, and by a number of seasonal streams entering on the north shore. Its main source of water is the runoff from the surrounding catchment, there is no outlet. Hadero Lake is important for Ducks, Coots, Pelicans, Flamingoes and birds of prey. However, it has drastically dropped due to pollution and hunting. The RBOD stretching from Sehwan to Gharo Creek in the Arabian Sea is passing nearby in this lake for a distance of 2.3 canal miles. Presently the supply of drain water to Hadero Lake has been out off and the drain water now into the RBOD channel passing nearby with the result that the water level in the Hadero has gone down and the fauna has been affected (Gabol *et al.*, 2005). The

fishery is the main source of income of the residents who are living near the Lake.

MATERIALS AND METHODS

Study Areas

The following 20 important areas were selected for the present study (Table 1).

Table 1. Wildlife Habitats in RBOD study areas.

S. No.	Name of study area	Co-ordinates
1.	RBOD at Gharo	24 44 26.6 N 67 35 35.1 E 24 44 25.8 N 67 35 31.4 E 24 44.438 N 67 35.523 E 24 44.419 N 67 35.490 E 24 44.461 N 67 35.546 E
2.	RBOD near Haleji Lake	24 45 43.12 N 67 44 48.87E
3.	Haleji Lake Turning Point	24 44 22.38 N 67 44 40.65 E
4.	Main Haleji Lake	24 47 14.39 N 67 45 24.93 E 24 47.243 N 67 45.421 E
5.	Near Haleji Information Centre	24 47 12.2 N 67 47 24.0 E
6.	Near Haleji Rest House	24 49. 161 N 67 46. 171 E 24 47. 446 N 67 44. 940 E
7.	Haleji Seepage Lagoon/Villages	24 49 19.3 N 67 45 36.7 E
8.	Near Haleji Regulator	24 49 19.3 N 67 47 58.0 E
9.	10km from Makli towards Keenjhar Lake	24 44.600 N 67 47.728 E
10.	RBOD near Keenjhar Lake	24 53 25.50 N 68 03 54.86 E
11.	Keenjhar Information Centre	24 53 45.74 N 68 03 10.39 E 24 53 46.20 N 68 03 11.12 E
12.	Keenjhar Main Lake Area	24 54 990 N 68 04 387 E 24 58.378 N 68 05.566 E 24 54.657 N 68 06.501 E 25 06.628 N 68 07.636 E
13.	Keenjhar Reservoir Area	24 54.40 N 68 04.21 E
14.	Chiliya	24 50 190 N 68 00 081 E
15.	Jhimpir	25 02.163 N 68 05.740 E
16.	Moldi	24 58.06 N 68 01.38 E
17.	Chakro	24 01 69.6 N 68 02 06.0 E
18.	Sonehri	25 01.067 N 68 07.877 E
19.	Adam Bhambhro	24 51.102 N 67 59.761 E
20.	K.B. Feeder Canal	25 02 21.7 N 68 07 55.2 E

Methodology of Physico-Chemical Samples Collection and Analysis

During the study from 2007-2012, conductivity meter was used for the estimation of Conductivity, Total Dissolved Solids, Turbidity, Salinity, and pH was recorded by pH meter. Alkalinity, Carbon dioxide and Phosphates were examined by the process of Acid Base Titration (Titrimetric methods), Total Hardness, Calcium, Magnesium and Chloride were analyzed by using EDTA (Complexometric Titration), Basic Oxygen Demand was examined by Incubation Method-Redox Titration, while Sulphate was analyzed by Gravimetric method, Nitrate was analyzed by Brucine Colorimetric Method and Cadmium, Chromium, Lead and Nickle were analyzed by atomic absorption spectro-photometric method (WHO, 1982, 1993).

Methodology for Vertebrates

Mammals

The mammals were identified by Roberts (1997, 2005a, b).

Roadside Counts

In this method motor vehicles have been used along the road trails while the sighted number of individuals of the species being estimated is tallied and related to the number of kilometers travelled (Brower *et al*., 1990). Roadside counts methods have some advantaged, such as: traveling on a vehicle does not disturb the animals and there is a chance to observe the animals along the road / track from a few meters distance. Other advantages of this method are large areas can be covered in passage of short time and easily using only two persons and a vehicle (Khan *et al*., 2012b, c).

Tracks Counts

Track counts have been used for locating and recording the presence of animals.

Pellet Counts

This technique involves removing all pellet groups from plots and then estimating from subsequent observations on those plots the number of groups per hectare to compare animal use of the area between sampling periods.

Small Mammals

One effective way to survey small mammals is active searching. This method is equally applicable to both nocturnal and diurnal species in potential and suitable micro habitats along the canal banks, open plains, particularly in bushy areas and agriculture fields. Active searching is very effective for inventory of *Gerbillus, Meriones, Hystrix,* and *Hemiechinus* spp.

A mixture of different food grains mixed with fragrant seeds may be used as bait for the attraction of the small mammals. Wheat and rice are used as food grain while peanut butter, coriander, oats and onion are used for fragrance. This bait is found to be highly successful in the study area probably due to the overall food shortage and fragrance.

Traps and trapping procedure

Sherman traps are used to collect the live specimens. Fifty traps are set in a specific area on a line approximately 500 m long and approximately 10m apart. Each trap was marked by a colorful ribbon to locate the traps easily. The traps are set in the afternoon and checked early in the morning. The specimens are transferred into polythene bags and were identified in the field and released.

To investigate nocturnal species, night surveys are conducted in exposed areas of potential habitats on the ground. This methodology involves the use of a powerful torch light, sticks, long boots and gloves etc.

Birds

For field identification of birds, field guides such as Grewal *et al*. (2002), Grimmett *et al*. (1998) and Kazmierczak (2000) was used. Secondary data on the overall status of the birds recorded from RBOD were taken from Grimmett *et al*. (1998) and Roberts (1992). Each major habitat type in the study area was identified and surveys were made to record the species of birds found in each discreet habitat such as lakes, canals, ponds, marshes, forest, agriculture fields, vicinity of human habitation and fallow lands. The number of birds observed in each habitat type was also recorded with particular emphasis on the key species and relate the data to other components of the study area such as vegetation, water and soil, etc. The most commonly used field methods in birds surveying is the "Line Transects" method. It is based on recording birds continually along a predefined route within a predefined survey unit. It can be used in terrestrial, freshwater and marine systems to survey individual species, or group of species. It is to examine birds - habitat relationships and to derive relative and absolute measures of bird abundance.

Line Transects are suitable for extensive, open and uniform habitats and for large and conspicuous species. Double counting of birds becomes a minor issue as the observer is continually on the move. Line Transects are suited to situations where access is good and these are very useful for bird-habitat studies (Khan *et al*., 2010; Khan *et al*., 2012b,c).

In the present studies, each sample area was transversed examined by 2 observers separately; birds were searched on each side of the strip for 150m so that each study strip was 300m wide. To evaluate the numbers of water birds utilizing a site, whether from a stationary point or by moving through the area, we used binoculars or a telescope.

Reptiles and Amphibians

Various survey techniques have been employed for the observation of reptiles and amphibians (Khan *et al*., 2010; Khan *et al*., 2012a,b,c).

A. Direct Counting

One-hour Plot Searching

This consists of searching approximately 20ha (with a 250 meter radius of sampling points) for one hour exactly and recording the number of individuals of each species seen. Similarly, night survey was done with the help of search lights and torches.

Pitfall Traps

Reptiles and amphibians were also detected using a line or pitfall traps. Each pitfall line consists of 30meters of low, flexible nylon fencing pinned to the ground to divert the movements of small ground dwelling animals, mainly reptiles with six 3-liter meter bucket buried in the ground with its lips at ground level along and below the fence, so that the fence straddled each bucket. The use of pitfall lines are restricted to sites where the ground surface is soft enough to dig or sandy areas. Pitfall lines are set for one night only. Team members reach early in the morning before sunrise and record the total number of reptiles of each species found in the bucket.

Turning of Stones, Rocks and Rotten Trees Process

Nocturnal reptiles and amphibians take shelter or rest hiding themselves under the space of stones or rocks. Therefore, in the day time survey, stones or rocks or rotten fallen trees are turned to locate and record the presence of species (Auffenburg and Rahman, 1991).

Study of Basking Behavior

This method of sighting or locating Crocodiles is the most suitable, but it is applied mostly in the winter season. In winter, the temperature of the water of the water bodies becomes very low. Crocodiles come outside the lake for enjoying sunshine to keep themselves warm. Thus, the counting of crocodiles becomes very easy at a particular area during this season.

B. Indirect Counting

Presence of signs like fecal pellets, tracks, den or tunnels (egg laying excavation)

Evidences from the impression of a finger or foot prints, or tail, the presence of fecal pellets, tracks and existence of tunnels (egg laying excavation) help a lot for finding the existence and range of reptilian fauna.

Fish Collection Technique

The methods used for obtaining the representative sample of fish fauna are the gill netting and cast netting. A standard length of a 200m covering maximum of representative habitats, was used to obtain a representative sample (Khan *et al*., 2012b,c).

Gill Netting

Three nets were used for gill netting, each measuring 15m length with mesh size 2.5x2.5cm and 1.5x1.5cm. Usually the gill nets were used in the morning.

Cast Netting

Cast nets with identified circumference were casted in a stretch of 200m. Five cast nets were used on a line at different stations along the bank of the reservoir. Fish fauna were collected and identified and released after identification. The data collected through the two methods was pooled and called as the representative sampling of the study site.

Methodology for Surveys of Invertebrates

Protozoans

Sterilized screw capped glass bottles were used for the collection of samples from the selected study areas. Samples were quickly transferred and readily brought to the laboratory for analysis. The samples were kept at room temperature.

The protozoans were identified through shape, body structure, external features, locomotion and behavior (Edmondson, 1966; APHA 1992; Curds, 1982; Curds *et al.*, 1983).

Survey of Terrestrial Macroinvertebrates

Collection protocols, and standardizing procedures

Specimens belonging to diverse groups of Invertebrates were collected from the various localities of the selected study areas using a variety of collection protocols and techniques.

Sampling Methods for Flighted Terrestrial Macroinvertebrates

Traditional insect hand net

Insects were found upon the bushes, in grasses and on the bark of trees. With the help of traditional insect hand net the insects were collected.

Light trap

This method is used for nocturnal flying insects. The essential light trap comprised an electric bulb, a white sheet as a reflective surface and a funnel to collect insects; insects were collected close to the light source.

Sticky traps

This method is used for flying insects. Range of substrates (e.g. plates, dishes) coated in long-lasting glue. The efficacy of the traps was increased by the use of different colors, mostly depending on target species. Insects were removed from trap using solvents.

Yellow pan traps

This method is used for an extensive variety of insects. Simple method based on a yellow pan (mostly yellow color attracts insects) with vertical baffles the pan was then placed on the ground and added one or two drops of detergent to reduce water tension. Insects were attracted to container and just go down in the water. After the collecting period sieve the catch to remove the liquid and then transferred the contents to a long-term storage preservative such as ethanol.

Sampling Methods for ground dwelling Macro-invertebrates

Hand picking and use of forceps

Hand picking, through bare hands or with the help of long forceps, which has been adopted for the present studies, is by far the very productive method for capturing different groups of terrestrial invertebrates especially arachnids (spiders, solifugids) and myriopods etc.

Pitfall traps

This method is used for ground-dwelling invertebrates (e.g. ants, beetles, spiders). The ground-dwelling invertebrates were collected using pitfall traps. This is the most commonly employed sampling technique in biodiversity inventories. It is used for collecting invertebrates that move along the ground.

Shaking and beating

This method is used for leaf beetles, weevils and Lepidoptera larvae. This is the most widely used method for collecting invertebrates associated with plants. It was used to sample any part of the plant, including branches, leaves, flower heads and even dead wood. A sheet or beating tray is laid out under the plant which is then shaken and beaten and the dislodged invertebrates are collected quickly before they escaped.

Sweep nets

It is an inexpensive and usually used means of sampling invertebrates from vegetation. The net was swang a set number of times through ground vegetation (grass and shrubs), as pacing. To prevent invertebrates escaping the

mouth of the net was closed as soon as sweeping was completed.

Sampling Methods for Aquatic invertebrate fauna

For aquatic invertebrates, several sampling methods have been used which are as follows:

Plankton net and drag nets/dip nets

The target group is zooplankton and other aquatic invertebrates. The dip netting is the better way to discover macro-invertebrates like stoneflies, dragon flies, damsel flies, mayflies, water mites, water beetles, water striders, water boatman and water pennies, which are abundant in the water.

Random sampling

Zooplanktons are unequally distributed over wide space and time scales in the water bodies. As it was not possible to sample all of the zooplankton from the lakes and other reservoirs using a single collection method, random sampling was used as the probable procedure in which each and every species has the equal chance and probability to be caught during sampling. Every individual is chosen entirely by chance and the likelihood of a biased data collection is thus reduced.

Precautions in field

Sample labels were accurately completed, including sample ID, date, reservoir name, collecting location, sampler's name and placed into the sample container. All nets, pans and trays were rinsed properly after sampling at a given site, picked and examined free of organisms or debris. Remaining organisms were placed in the sample containers.

Preservation and storage of the specimens

All invertebrate specimens, including the zooplankton were preserved by the addition of grades of 70% ethyl alcohol and formaldehyde. These fluids suffice to preserve the samples indefinitely and in addition have the effect of sending all the plankton to the bottom of the jar. All zooplankton are delicate and simply get damaged,

Table 2. Water quality analysis of RBOD study areas during 2007- 2012.

Parameters	Average Pre-monsoon					Average Post-monsoon				
	2007	2008	2009	2011	2012	2007	2008	2009	2011	2012
Colour	A	A	A	A	A	A	A	A	A	A
Odour	O	O	O	O	O	O	O	O	O	O
Water Temperature (°C)	28	29	30	29	30	17.66	17.33	17	18	19
Air Temperature (°C)	31.33	32.33	33.33	32.33	33	20.66	20.33	20	21.33	22.66
Conductivity (µs/cm)	1940.66	1792	1755.33	1024.66	1934	3428.33	3005.66	3146.33	3457.66	3159
TDS (mg/l)	1086	1075.33	1009.33	995	1035	2057	2030.33	2010.33	1990.33	1990.33
pH	7.786	7.782	7.77	7.77	7.115	7.803	7.801	7.79	7.785	7.799
Turbidity (NTU)	1.58	1.61	1.21	0.82	1.03	2.95	2.71	2.54	2.09	1.38
Alkalinity (mg/l)	202.33	197.66	196.33	195	201.33	117.66	114.66	113	117.66	116.66
Total Hardness (mg/l)	589	566	543.66	537.66	577	555.66	533.33	510.66	493.33	557.66
Salinity (mg/l)	6.13	6.06	5.83	5.66	5.66	5.2	5.03	4.73	4.53	4.83
BOD (mg/l)	4.65	4.58	4.06	3.99	3.44	5.40	5.33	5.22	5.16	4.07
Carbon dioxide (mg/l)	1.33	1.33	1.33	1.66	1.33	1.33	1.66	1.66	1.33	1.33
Calcium (mg/l)	104.04	102.7	101.69	100.01	100.01	75.35	74.01	73.00	71.33	71.33
Magnesium (mg/l)	541.45	504.03	500.40	494.76	501.42	525.99	519.26	513.94	508.69	486.33
Sulphates (mg/l)	135.33	125	114.66	101	98.33	185.33	174	226.66	213	142.66
Chloride (mg/l)	692.66	683	671	661.66	656.66	666	656	640.66	632.66	642.66
Nitrates (mg/l)	0.210	0.205	0.202	0.198	0.170	0.192	0.189	0.185	0.179	0.150
Phosphates (mg/l)	0.87	0.90	0.85	0.80	0.87	0.61	0.56	0.54	0.506	0.57
Cadmium (mg/l)	0.007	0.006	0.005	0.003	0.002	0.009	0.007	0.008	0.006	0.010
Chromium (mg/l)	0.044	0.041	0.043	0.041	0.022	0.054	0.052	0.053	0.052	0.054
Lead (mg/l)	0.82	0.79	0.85	0.84	0.96	0.83	0.77	0.80	0.68	0.82
Nickel (mg/l)	0.72	0.55	0.51	0.59	0.89	0.79	0.69	0.66	0.69	0.84

therefore sample handling was gentle. It is advisable not to concentrate the sample too much. Zooplanktons were sub-sampled by adding water to bring the samples to a known volume (500 or 1000ml). The concentrated samples were then stored in appropriate bottles and plastic screw tapped jars. The place of origin, date, mesh-size of the net, length and depth of the haul were written permanent ink on quality paper and placed in the jar as the labels outer surface usually peel off after some time.

Counting and studying the zooplankton

The volume of the zooplankton was determined by the displacement method. First, the total volume of the concentrated sample in addition the preserving fluid was measured. Then the plankton was filtered off, by a filter paper in a funnel, and the volume of the filtrate is measured. The volume of the plankton was then obtained by the difference between the two volumes. A measure of the total catch was also prepared by weighing the filtered plankton. One ml of the concentrated sample may include so many organisms that it would be not easy to count them. Diluted 1ml sample to 100ml and then from it 1 ml was in use. Identification and counting the samples was completed under a dissecting microscope with dark-field illumination. Staining was not essential, although a drop of glycerin was put on each individual specimen isolated from the jar in order to avoid any damage to the samples.

RESULTS

Physico-chemical Parameters of RBOD

During 2007-2012, several standard physico-chemical parameters were analyzed to determine water quality, pollution, Temperature, Conductivity, Total Dissolved Solids, pH, Turbidity, Alkalinity, Total Hardness, Salinity, Basic Oxygen Demand, Carbondioxide, Calcium, Magnesium, Sulphate, Chloride, Nitrate, Phosphate, Cadmium, Chromium, Lead and Nickel were selected for the analysis of water quality. Parameters were analyzed seasonally. The water temperature in pre-monsoon was observed from 27 to 32°C, while in post monsoon, it varied from 16 to 20°C (Table 2).

Bioecological Studies

There are 2 protozoans species (Table 3), 104 species of arthropods (Table 4), 23 species of zooplanktons (Table 5), 13 species of molluscs (Table 6), 28 species of mammals (Table 7), 228 species of birds (Table 8), 31 species of reptiles (Table 9), 2 species of amphibians (Table 10), 59 species of fishes (Table 11) were recorded.

Species Status

Mammals

In the RBOD study area Palm Squirrel (*Funambulus pennantii*), Indian Desert Jird (*Meriones hurrianae*), Indian Gerbil (*Tatera indica*), Balochistan Gerbil (*Gerbillus nanus*), House Mouse (*Mus musculus*) and Roof Rat (*Rattus rattus*) were recorded as common species. While, Small Indian Civet (*Viverricula indica*) (Fig. 6), Desert Fox (*Vulpes vulpes*) (Fig. 7) were observed as rare species. The threatened species of mammals in the area include Fishing Cat (*Prionailurus viverrina*), and Smooth-coated Indian Otter (*Lutrogale perspicillata*).

Fig. 6. Small Indian Civet (*Viverricula indica*).

Fig. 7. Desert Fox (*Vulpes vulpes*).

Birds

Among birds, 262 species in all have been recorded. During the present study, 228 species of birds have been recorded (Table 8). The threatened bird species of the area are Pallas's Fishing Eagle (*Haliaeetus leucoryphus*) (Fig. 8), Ferruginous Duck (*Aythya nyroca*) (Fig. 9), Imperial Eagle (*Aquila heliaca*) (Fig. 10), Lesser White-fronted Goose (*Anser erythropus*) (Fig. 11), Egyptian Vulture (*Neophron percnopterus*) (Fig. 12), White-backed Vulture (*Gyps bengalensis*) (Fig. 13), Cotton Teal (*Nettapus coromandelianus*) (Fig. 14), White Stork (*Ciconia ciconia*) (Fig. 15), Marbled Teal (*Marmaronetta angustirostris*) (Fig. 16), White Ibis (*Threskiornis melanocephala*) (Fig. 17), Dalmatian Pelican (*Pelecanus crispus*) (Fig. 18), and Black-bellied Tern (*Sterna acuticauda*) (Fig. 19).

Fig. 8. Pallas's Fishing Eagle (*Haliaeetus leucoryphus*).

Fig. 9. Ferruginous Duck (*Aythya nyroca*).

Fig. 10. Imperial Eagle (*Aquila heliaca*).

Fig. 11. Lesser White-fronted Goose (*Anser erythropus*).

Fig. 12. Egyptian Vulture (*Neophron perenopterus*).

13. White-backed Vulture (*Gyps bengalensis*).

Fig. 14. Cotton Teal (*Nettapus coromandelianus*).

Fig. 15. White Stork (*Ciconia ciconia*).

Fig. 16. Marbled Teal (*Marmaronetta angustirostris*).

Fig. 17. White Ibis (*Threskiornis melanocephala*).

Fig. 18. Dalmatian Pelican (*Pelecanus crispus*).

Fig. 19. Black-bellied Tern (*Sterna acuticauda*).

Table 3. List of Protozoans recorded from RBOD study areas.

S. No.	Order	Family	Scientific Name
1.	Euglenoidina	Euglenaceae	*Euglena* sp.
2.	Volvocales	Volvocaceae	*Volvox* sp.

Table 4. List of Arthropods recorded from RBOD study areas.

S. No.	Order	Family	Scientific Name
1.	Hemiptera	Alcyrodidae	*Aleurolobus barodensis*
2.	Hemiptera	Alcyrodidae	*Neomaskellia* sp.
3.	Hemiptera	Pyrrhocoridae	*Dysdercus cingulatus*
4.	Hemiptera	Pentatomidae	*Bagrada picta*
5.	Hemiptera	Pentatomidae	*Scotinophara limosa*
6.	Hemiptera	Alydidae	*Leptocorisa acuta*
7.	Hemiptera	Aphididae	*Microsiphum granarium*
8.	Hemiptera	Aphididae	*Myzus persicae*
9.	Hemiptera	Diaspididae	*Aspidiotus* sp.
10.	Hemiptera	Pseudococcidae	*Pseudococcus saccharicola*
11.	Hemiptera	Pseudococcidae	*Icerya* sp.
12.	Hemiptera	Pseudococcidae	*Ripersia sacchari*
13.	Hemiptera	Diaspididae	*Aspidiotus* sp.
14.	Hemiptera	Lophopidae	*Pyrilla perpusilla*
15.	Hemiptera	Cicadellidae	*Nephotettix* sp.
16.	Hemiptera	Jassidae	*Idiocerus atkinsoni*
17.	Hemiptera	Lygaeidae	*Cavelarius excavatus*
18.	Hemiptera	Cicadellidae	*Nephotettix virescens*
19.	Hemiptera	Cicadellidae	*Amrasca devastans*
20.	Hemiptera	Cicadellidae	*Jacobiasca signata*
21.	Hemiptera	Cicadellidae	*Jacobiasca* sp.
22.	Hemiptera	Delphacidae	*Sogata distincta*
23.	Hemiptera	Delphacidae	*Sogatella furcifera*
24.	Hemiptera	Delphacidae	*Nilaparvata lugens*
25.	Hemiptera	Tingidae	*Urintius sentis*
26.	Hemiptera	Nepidae	*Nepa* sp.
27.	Hymenoptera	Apidae	*Apis* sp.
28.	Hymenoptera	Tenthridinidae	*Athalia proxima*
29.	Isoptera	Termitidae	*Odontotermes assmuthi*
30.	Isoptera	Termitidae	*Microtermes obesi*
31.	Thysanoptera	Thripidae	*Thrips oryzae*
32.	Thysanoptera	Thripidae	*Thrips tabaci*
33.	Thysanoptera	Thripidae	*Scirtothrips dorsalis*
34.	Lepidoptera	Arctiidae	*Amsacta lactinea*
35.	Lepidoptera	Noctuidae	*Sesamia inferens*
36.	Lepidoptera	Noctuidae	*Thysanoplusia orichalcea*
37.	Lepidoptera	Noctuidae	*Mythimna loreyi*
38.	Lepidoptera	Noctuidae	*Mythimna separata*
39.	Lepidoptera	Noctuidae	*Spodoptera exigua*
40.	Lepidoptera	Noctuidae	*Spodoptera litura*
41.	Lepidoptera	Noctuidae	*Agrotis ipsilon*
42.	Lepidoptera	Noctuidae	*Plusia* sp.
43.	Lepidoptera	Noctuidae	*Agrotis spinifera*
44.	Lepidoptera	Noctuidae	*Ochropleura berculea*

continued…

Table 4 continue

S. No.	Order	Family	Scientific Name
45.	Lepidoptera	Noctuidae	*Autogropha nigrisigna*
46.	Lepidoptera	Pyranstidae	*Leucinodes orbonalis*
47.	Lepidoptera	Plutellidae	*Plutella xylostella*
48.	Lepidoptera	Papilionidae	*Papilio demoleus*
49.	Lepidoptera	Pieridae	*Pieris brassicae*
50.	Lepidoptera	Pieridae	*Pieris rapae*
51.	Lepidoptera	Pyralidae	*Bissetia steniella*
52.	Lepidoptera	Pyralidae	*Chilo suppressalis*
53.	Lepidoptera	Pyralidae	*Chilo infuscatellus*
54.	Lepidoptera	Pyralidae	*Chilo partellus*
55.	Lepidoptera	Pyralidae	*Emmalocera depressella*
56.	Lepidoptera	Pyralidae	*Scirpophaga incertulas*
57.	Lepidoptera	Pyralidae	*Scirpophaga nivella*
58.	Lepidoptera	Pyralidae	*Scirpophaga innotata*
59.	Lepidoptera	Pyralidae	*Scirpophaga* sp.
60.	Orthoptera	Acrididae	*Oxya* sp.
61.	Orthoptera	Acrididae	*Acridella nasuta*
62.	Orthoptera	Acrididae	*Acrotylus insubricus*
63.	Orthoptera	Acrididae	*Hieroglyphus* sp.
64.	Orthoptera	Acrididae	*Chrotogonus* sp.
65.	Orthoptera	Acrididae	*Chrotogonus concavus*
66.	Orthoptera	Gryllidae	*Acheta domestica*
67.	Orthoptera	Gryllidae	*Gryllotalpa* sp.
68.	Orthoptera	Mantidae	*Mantis* sp.
69.	Coleoptera	Chrysomelidae	*Dicladispa armigera*
70.	Coleoptera	Chrysomelidae	*Raphidopalpa foveicollis*
71.	Coleoptera	Curculionidae	*Myllocerus* sp.
72.	Coleoptera	Curculionidae	*Cosmopolites sordidus*
73.	Coleoptera	Coccinellidae	*Epilachna dodecastigma*
74.	Coleoptera	Hispidae	*Hispa armigera*
75.	Coleoptera	Dynastidae	*Oryctes rhinoceros*
76.	Odonata	Gomphidae	*Gomphus* sp.
77.	Diptera	Anthomyiidae	*Atherigona indica*
78.	Diptera	Muscidae	*Musca domestica*
79.	Diptera	Culicidae	*Aedes aegypti*
80.	Diptera	Culicidae	*Culex fatigans*
81.	Diptera	Culicidae	*Culex pipiense*
82.	Diptera	Culicidae	*Culex tarsalis*
83.	Diptera	Culicidae	*Culex quinquefasciatus*
84.	Diptera	Culicidae	*Anopheles barbirostris*
85.	Diptera	Culicidae	*Anopheles barianensis*
86.	Diptera	Culicidae	*Anopheles claviger*
87.	Diptera	Culicidae	*Anopheles gigas simlensis*
88.	Diptera	Culicidae	*Anopheles nigerrimus*
89.	Diptera	Culicidae	*Anopheles culicifacies*
90.	Diptera	Culicidae	*Anopheles peditaeniatus*
91.	Diptera	Culicidae	*Anopheles maculatus*
92.	Diptera	Culicidae	*Anopheles moghulensis*
93.	Diptera	Culicidae	*Anopheles pallidus*

continued…

Table 4 continue

S. No.	Order	Family	Scientific Name
94.	Diptera	Culicidae	*Anopheles pulcherrimus*
95.	Diptera	Culicidae	*Anopheles willmori*
96.	Diptera	Culicidae	*Anopheles sergenti*
97.	Diptera	Culicidae	*Anopheles splendidus*
98.	Diptera	Culicidae	*Anopheles stephensi*
99.	Diptera	Trypetidae	*Bactocera cucurbitae*
100.	Diptera	Trypetidae	*Bactocera zonata*
101.	Araneae	Thomisidae	*Thomisus* sp.
102.	Araneae	Araneidae	*Cyclosa* sp.
103.	Decapoda	Penaeidae	*Penaeus merguiensis*
104.	Decapoda	Penaeidae	*Penaeus japonicus*

Table 5. List of Zooplankton recorded from RBOD study areas.

S. No.	**Rotifera**
1.	*Brachionus quadridentatus*
2.	*Brachionus falcatus*
3.	*Brachionus buda pestinensis*
4.	*Brachionus rubens*
5.	*Euchlanis* sp.
6.	*Keratella tropica*
7.	*Keratella volga*
8.	*Lecane* sp.
9.	*Mytilina* sp.
10.	*Platyias quadricornus*
Cladocera	
11.	*Alona rectangula*
12.	*Bosmina longirostris*
13.	*Bosminopsis deitersi*
14.	*Ceriodaphnia reticulata*
15.	*Chydorus parvuus*
16.	*Chydorus ovalis*
17.	*Daphnia* sp.
18.	*Macrocthrix rosea*
19.	*Moina* sp.
S. No.	
20.	*Sida* sp.
21.	*Simocephalus vetulus*
Copepoda	
22.	*Cyclopoid* sp.
23.	*Calonoid* sp.

Table 6. List of Molluscs recorded from RBOD study areas.

S. No.	**Class**	**Species**
1.	Gastropoda	*Bellamya naticoides*
2.		*Bellamya dissimilis*
3.		*Bellamya bengalensis*
4.	Gastropoda	*Thiara tuberculata*
5.		*Gyraulus euphraticus*
6.		*Lymnaea acuminata*
7.		*Indoplanorbis exusta*
8.		*Physa acuta*
9.	Bivalvia	*Lamellidense marginalis*
10.		*Lamellidense corrianus*
11.		*Parreysia caerula*
12.		*Parreysia pachysoma*
13.		*Parreysia wynegungaensis*

Reptiles

In the present study, 31 species of reptiles were recorded (Table 9).

Amphibians

Among amphibians, Skittering Frog (*Euphlyctis cyanophlyctis*) and Indus Toad (*Duttaphrynus stomaticus*) are common (Table 10).

Fishes

There are 59 fish species were recorded. *Catla catla, Aorichthys aor, Bagarius bagarius, Gudusia chapra, Wallago attu, Channa marulia, Xenentodon cancila, Labeo rohita, Heteropneustes fossilis, Cirrhinus mrigala, Notopterus notopterus, Hypophthalmichthys molitrix, Aristchthys nobilis* and *Ctenpharyngodon idella* are some important fishes of the study area (Table 11).

Flora

As regards the flora, 262 species of plants were recorded. *Typha angustata*, *Phragmites karka* and *Hydrilla verticillata* were found common aquatic floral species in the area. *Salvinia molesta* and *Eichhornia crasspes* were recorded as exotic species, whereas *Tamarix* spp. was found abundant.

Table 7. List of Mammals recorded from RBOD study areas.

S. No.	Order	Family	Scientific Name	Common Name	Status	Previously recorded	Presently Recorded
1.	Rodentia	Hystricidae	*Hystrix indica*	Indian Crested Porcupine	LC	+	+
2.	Rodentia	Sciuridae	*Funambulus pennantii*	Palm Squirrel	C	+	+
3.	Rodentia	Muridae	*Mus saxicola*	Grey Spiny Mouse	LC	+	+
4.	Rodentia	Muridae	*Rattus rattus*	Roof Rat / House Rat	C	+	+
5.	Rodentia	Muridae	*Mus musculus*	House Mouse	C	+	+
6.	Rodentia	Muridae	*Mus booduga*	Little Indian Field Mouse	LC	+	+
7.	Rodentia	Muridae	*Nesokia indica*	Short-tailed Mole Rat	LC	+	+
8.	Rodentia	Muridae	*Meriones hurrianae*	Indian Desert Jird	C	+	+
9.	Rodentia	Muridae	*Tatera indica*	Indian Gerbil	C	+	+
10.	Rodentia	Muridae	*Gerbillus nanus*	Balochistan Gerbil	C	+	+
11.	Insectivora	Erinaceidae	*Paraechinus micropus*	Indian Hedgehog	LC	+	+
12.	Insectivora	Erinaceidae	*Hemiechinus collaris*	Long-eared Desert Hedgehog	LC	+	+
13.	Insectivora	Soricidae	*Suncus murinus*	House Shrew	LC	+	+
14.	Chiroptera	Vespertilionidae	*Pipistrellus kuhlii*	Kuhl's Bat	S	+	+
15.	Chiroptera	Megadermatidae	*Hipposideros fulvus*	Leaf-nosed Bat	LC	+	+
16.	Chiroptera	Rhinopomatidae	*Rhinopoma microphyllum*	Large Mouse-tailed Bat	LC	+	+
17.	Chiroptera	Pteropidae	*Rousettus aegypticus*	Egyptian Bat	LC	--	+
18.	Lagomorpha	Leporidae	*Lepus nigricollis*	Desert Hare / Indian Hare	LC	+	+
19.	Artiodactyla	Suidae	*Sus scrofa*	Indian Wild Boar	LC	+	--
20.	Pholidota	Manidae	*Manis crassicaudata*	Indian Pangolin	Rr	+	--
21.	Carnivora	Mustelidae	*Lutrogale perspicillata*	Smooth-coated Otter	Rr	+	+
22.	Carnivora	Canidae	*Vulpes vulpes*	Desert Fox/Red Fox	Rr	+	+
23.	Carnivora	Canidae	*Canis aureus*	Asiatic Jackal	LC	+	+
24.	Carnivora	Canidae	*Vulpes bengalensis*	Indian Fox	S	+	+
25.	Carnivora	Herpestidae	*Herpestes javanicus*	Small Mongoose	LC	+	+
26.	Carnivora	Herpestidae	*Herpestes edwardsi*	Grey Mongoose	LC	+	+
27.	Carnivora	Felidae	*Felis sylvestris*	Indian Desert Cat	S	+	+
28.	Carnivora	Felidae	*Felis chaus*	Jungle Cat	S	+	+
29.	Carnivora	Felidae	*Prionailurus viverrina*	Fishing Cat	Rr	+	+
30.	Carnivora	Viverridae	*Viverricula indica*	Small Indian Civet	Rr	+	+

Legends: C = Common; LC = Less Common; S = Scarce; Rr = Rare; + = Present; -- = Absent

Table 8. List of Birds recorded from RBOD study areas.

S. No.	Order	Family	Scientific Name	Common Name	Occurrence	Status	
						Previous	Present
1.	Podicipediformes	Podicipedidae	*Podiceps cristatus*	Great Crested Grebe	WV	+	--
2.	Podicipediformes	Podicipedidae	*Tachybaptes ruficollis*	Little Grebe	R	+	+
3.	Pelecaniformes	Phalacrocoracidae	*Phalacrocorax carbo*	Large Cormorant	R	+	+
4.	Pelecaniformes	Phalacrocoracidae	*Phalacrocorax fuscicollis*	Indian Shag	R	+	--
5.	Pelecaniformes	Phalacrocoracidae	*Phalacrocorax niger*	Little Cormorant	R	+	+
6.	Pelecaniformes	Phalacrocoracidae	*Anhinga melanogaster*	Darter	O	+	--
7.	Pelecaniformes	Pelecanidae	*Pelecanus crispus*	Dalmatian Pelican	WV	+	+
8.	Pelecaniformes	Pelecanidae	*Pelecanus onocrotalus*	White Pelican	WV	+	+
9.	Ciconiformes	Ardeidae	*Ardea cinerea*	Grey Heron	R	+	+
10.	Ciconiformes	Ardeidae	*Ardea purpurea*	Purple Heron	R	+	+
11.	Ciconiformes	Ardeidae	*Buturoides striatus*	Little Green Heron	R	--	+
12.	Ciconiformes	Ardeidae	*Ardeola grayii*	Indian Pond Heron	R	+	+
13.	Ciconiformes	Ardeidae	*Egretta alba*	Large Egret	R	+	+
14.	Ciconiformes	Ardeidae	*Bubulcus ibis*	Cattle Egret	R	+	+
15.	Ciconiformes	Ardeidae	*Egretta intermedia*	Intermediate Egret	R	+	+
16.	Ciconiformes	Ardeidae	*Egretta garzetta*	Little Egret	R	+	+
17.	Ciconiformes	Ardeidae	*Egretta gularis*	Indian Reef Heron	O	+	+
18.	Ciconiformes	Ardeidae	*Nycticorax nycticorax*	Night Heron	R	+	+
19.	Ciconiformes	Ardeidae	*Ixobrychus cinnamomeus*	Chestnut Bittern	SV	+	+
20.	Ciconiformes	Ardeidae	*Ixobrychus sinensis*	Yellow Bittern	SV	+	+
21.	Ciconiformes	Ardeidae	*Dupetor flavicollis*	Black Bittern	SV	+	+
22.	Ciconiformes	Ciconiidae	*Anastomus oscitans*	Openbill Stork	O	+	--
23.	Ciconiformes	Ciconiidae	*Ciconia ciconia*	White Stork	O	+	--
24.	Ciconiformes	Threskiornithidae	*Threskiornis melanocephala*	White Ibis	R	+	+
25.	Ciconiformes	Threskiornithidae	*Plegadis falcinellus*	Glossy Ibis	R	+	+
26.	Ciconiformes	Threskiornithidae	*Platalea leucorodia*	Spoonbill	WV	+	+
27.	Ciconiformes	Phoenicopteridae	*Phoenicopterus roseus*	Greater Flamingo	O	+	+
28.	Anseriformes	Anatidae	*Anser albifrons*	White-fronted Goose	WV	--	--

continued..

Table 8 continue…

S. No.	Order	Family	Scientific Name	Common Name	Occurrence	Status	
						Previous	Present
29.	Anseriformes	Anatidae	*Dendrocygna javanica*	Lesser Whistling Teal	SV	+	--
30.	Anseriformes	Anatidae	*Dendrocygna bicolor*	Large Whistling Teal	O	+	--
31.	Anseriformes	Anatidae	*Cygnus columbianus*	Bewick's Swan	O	--	--
32.	Anseriformes	Anatidae	*Tadorna ferruginea*	Ruddy Shelduck	WV	+	+
33.	Anseriformes	Anatidae	*Tadorna tadorna*	Common Shelduck	O	+	+
34.	Anseriformes	Anatidae	*Anser erythropus*	LesserWhite-fronted Goose	WV	+	--
35.	Anseriformes	Anatidae	*Marmaronetta angustirostris*	Marbled Teal	WV	+	+
36.	Anseriformes	Anatidae	*Anas acuta*	Pintail	WV	+	+
37.	Anseriformes	Anatidae	*Anas creca*	Common Teal	WV	+	+
38.	Anseriformes	Anatidae	*Anas querquedula*	Garganey	PM	+	+
39.	Anseriformes	Anatidae	*Anas poecilorhyncha*	Spotbill Duck	R	+	--
40.	Anseriformes	Anatidae	*Anas platyrhynchos*	Mallard	WV	+	+
41.	Anseriformes	Anatidae	*Anas strepera*	Gadwall	WV	+	+
42.	Anseriformes	Anatidae	*Anas penelope*	Wigeon	WV	+	+
43.	Anseriformes	Anatidae	*Anas clypeata*	Shoveller	WV	+	+
44.	Anseriformes	Anatidae	*Aythya ferina*	Common Pochard	WV	+	+
45.	Anseriformes	Anatidae	*Aythya nyroca*	Ferruginous Duck	WV	+	+
46.	Anseriformes	Anatidae	*Aythya marila*	Scaup Duck	O	+	--
47.	Anseriformes	Anatidae	*Aythya fuligula*	Tufted Duck	WV	+	+
48.	Anseriformes	Anatidae	*Netta rufina*	Red-crested Pochard	O	+	--
49.	Anseriformes	Anatidae	*Nettapus coromandelianus*	Cotton Teal	R	+	--
50.	Falconiformes	Accipitridae	*Elanus caeruleus*	Black-winged Kite	R	+	+
51.	Falconiformes	Accipitridae	*Milvus migruns*	Black Kite	R	+	+
52.	Falconiformes	Accipitridae	*Haliastur indus*	Brahminy Kite	O	+	+
53.	Falconiformes	Accipitridae	*Haliaeetus albicilla*	White-tailed Sea Eagle	O	+	--
54.	Falconiformes	Accipitridae	*Neophron percnopterus*	Egyptian Vulture	R	--	+
55.	Falconiformes	Accipitridae	*Haliaeetus leucoryphus*	Pallas's Fishing Eagle	R	+	+
56.	Falconiformes	Accipitridae	*Gyps bengalensis*	White-backed Vulture	R	+	--
57.	Falconiformes	Accipitridae	*Gyps fulvus*	Griffon Vulture	WV	+	+
58.	Falconiformes	Accipitridae	*Aegypius monachus*	Cinereous Vulture	WV	+	+
59.	Falconiformes	Accipitridae	*Circaetus gallicus*	Short-toed Eagle	O	+	+

continued..

Table 8 continue…

S. No.	Order	Family	Scientific Name	Common Name	Occurrence	Status	
						Previous	Present
60.	Falconiformes	Accipitridae	*Circus aeruginosus*	Marsh Harrier	WV	+	+
61.	Falconiformes	Accipitridae	*Circus macrourus*	Pallid Harrier	WV	+	+
62.	Falconiformes	Accipitridae	*Accipitier badius*	Shikra	R	+	+
63.	Falconiformes	Accipitridae	*Butastur teesa*	White-eyed Buzzard	R	+	+
64.	Falconiformes	Accipitridae	*Buteo vulpinus*	Desert Buzzard	WV	+	+
65.	Falconiformes	Accipitridae	*Buteo rufinus*	Long-legged Buzzard	WV	+	+
66.	Falconiformes	Accipitridae	*Aquila clanga*	Greater Spotted Eagle	WV	+	+
67.	Falconiformes	Accipitridae	*Aquila rapax*	Tawny Eagle	R	+	+
68.	Falconiformes	Accipitridae	*Aquila heliaca*	Imperial Eagle	WV	+	+
69.	Falconiformes	Accipitridae	*Aquila nipalensis*	Steppe Eagle	WV	+	+
70.	Falconiformes	Accipitridae	*Hieraaetus pennatus*	Booted Eagle	WV	+	--
71.	Falconiformes	Accipitridae	*Hieraaetus fasciatus*	Bonelli's Eagle	R	+	--
72.	Falconiformes	Pandionidae	*Pandion haliaetus*	Osprey	WV	+	+
73.	Falconiformes	Falconidae	*Falco tinnunculus*	Kestrel	R	+	+
74.	Falconiformes	Falconidae	*Falco chiquera*	Red-headed Merlin	R	+	+
75.	Falconiformes	Falconidae	*Falco columbarius*	Merlin	WV	--	+
76.	Galliformes	Phasianidae	*Francolinus francolinus*	Black Partridge	R	+	+
77.	Galliformes	Phasianidae	*Francolinus pondicerianus*	Grey Partridge	R	+	+
78.	Galliformes	Phasianidae	*Conturnix coturnix*	Common Quail	PM	+	+
79.	Gruiformes	Rallidae	*Rallus aquaticus*	Water Rail	WV	+	+
80.	Gruiformes	Rallidae	*Porzana porzana*	Spotted Crake	WV	+	+
81.	Gruiformes	Rallidae	*Amaurornis phoenicurus*	White-breasted Water Hen	R	+	+
82.	Gruiformes	Rallidae	*Gallinula chloropus*	Indian Moorhen	R	+	+
83.	Gruiformes	Rallidae	*Porphyrio porphyrio*	Purple Moorhen	R	+	+
84.	Gruiformes	Rallidae	*Fulica atra*	Coot	WV	+	+
85.	Gruiformes	Rallidae	*Gallicrex cinerea*	Watercock	WV	+	+
86.	Gruiformes	Gruidae	*Grus grus*	Common Crane	PM	+	--
87.	Gruiformes	Gruidae	*Anthropoides virgo*	Demoiselle Crane	PM	+	--
88.	Charadriiformes	Jacanidae	*Hydrophasianus chirurgus*	Pheasant-tailed Jacana	R	+	+
89.	Charadriiformes	Jacanidae	*Metopidius indicus*	Bronze-winged Jacana	O	+	--
90.	Charadriiformes	Haematopodidae	*Haematopus ostralegus*	Oystercatcher	WV	--	+

continued..

Table 8 continue…

S. No.	Order	Family	Scientific Name	Common Name	Occurrence	Status	
						Previous	Present
91.	Charadriiformes	Charadriidae	*Vanellus leucurus*	White-tailed Lapwing	WV	+	+
92.	Charadriiformes	Charadriidae	*Vanellus indicus*	Red-wattled Lapwing	R	+	+
93.	Charadriiformes	Charadriidae	*Vanellus vanellus*	Green Plover	O	+	+
94.	Charadriiformes	Charadriidae	*Vanellus malabaricus*	Yellow-wattled Lapwing	SV	+	+
95.	Charadriiformes	Charadriidae	*Pluvialis squatarola*	Black-bellied Plover	WV	+	--
96.	Charadriiformes	Charadriidae	*Pluvialis dominica*	Eastern Golden Plover	WV	+	--
97.	Charadriiformes	Charadriidae	*Charadrius dubius*	Little Ringed Plover	WV	+	+
98.	Charadriiformes	Charadriidae	*Charadrius alexandrines*	Kentish Plover	WV	+	+
99.	Charadriiformes	Recurvirostridae	*Himantopus himantopus*	Black-winged Stilt	R	+	+
100.	Charadriiformes	Recurvirostridae	*Recurvirostra avosetta*	Avocet	O	+	+
101.	Charadriiformes	Burhinidae	*Glareola pratincola*	Collared Pratincole	SV	+	+
102.	Charadriiformes	Burhinidae	*Glareola lacteal*	Small Indian Pratincole	SV	+	+
103.	Charadriiformes	Scolopacidae	*Numenius phaeopus*	Whimbrel	PM	+	+
104.	Charadriiformes	Scolopacidae	*Numenius arquata*	Curlew	PM	+	+
105.	Charadriiformes	Scolopacidae	*Limosa limosa*	Black-tailed Godwit	WV	+	+
106.	Charadriiformes	Scolopacidae	*Limosa lapponica*	Bartailed Godwit	WV	--	+
107.	Charadriiformes	Scolopacidae	*Tringa erythropus*	Spotted Red Shank	WV	+	+
108.	Charadriiformes	Scolopacidae	*Tringa totanus*	Common Red Shank	WV	+	+
109.	Charadriiformes	Scolopacidae	*Tringa stagnatilis*	Marsh Sandpiper	WV	+	+
110.	Charadriiformes	Scolopacidae	*Tringa nebularia*	Green Shank	WV	+	+
111.	Charadriiformes	Scolopacidae	*Tringa ochropus*	Green Sandpiper	WV	+	+
112.	Charadriiformes	Scolopacidae	*Tringa glareola*	Wood Sandpiper	WV	+	+
113.	Charadriiformes	Scolopacidae	*Tringa terek*	Terek Sandpiper	WV	+	+
114.	Charadriiformes	Scolopacidae	*Tringa hypoleucos*	Common Sandpiper	WV	+	+
115.	Charadriiformes	Scolopacidae	*Capella gallinago*	Common Snipe	WV	+	+
116.	Charadriiformes	Scolopacidae	*Calidris minutus*	Little Stint	WV	+	+
117.	Charadriiformes	Scolopacidae	*Calidris temminckii*	Temminck's Stint	WV	+	+
118.	Charadriiformes	Scolopacidae	*Calidris alpinus*	Dunlin	WV	+	+
119.	Charadriiformes	Scolopacidae	*Philomachus pugnax*	Ruff	PM	+	+
120.	Charadriiformes	Glareolidae	*Cursorius coromandelicus*	Indian Courser	R	--	+
121.	Charadriiformes	Laridae	*Larus argentatus*	Herring Gull	WV	+	+

continued..

Table 8 continue…

S. No.	Order	Family	Scientific Name	Common Name	Occurrence	Status	
						Previous	Present
122.	Charadriiformes	Laridae	*Larus fuscus*	LesserBlack-backed Gull	WV	--	+
123.	Charadriiformes	Laridae	*Larus ichthyaetus*	GreatBlack-headed Gull	WV	+	+
124.	Charadriiformes	Laridae	*Larus brunnicephalus*	Brown-headed Gull	WV	+	+
125.	Charadriiformes	Laridae	*Larus ridibundus*	Black-headed Gull	WV	+	+
126.	Charadriiformes	Laridae	*Larus genei*	Slender-billed Gull	WV	+	+
127.	Charadriiformes	Laridae	*Larus canus*	Mew Gull	O	+	--
128.	Charadriiformes	Sternidae	*Chlidonias hybrida*	Whiskered Tern	R	+	+
129.	Charadriiformes	Sternidae	*Chlidonias leucopterus*	White-winged Black Tern	PM	+	+
130.	Charadriiformes	Sternidae	*Gelochelidon nilotica*	Gull-billed Tern	R	+	+
131.	Charadriiformes	Sternidae	*Hydroprogne caspia*	Caspian Tern	R	+	+
132.	Charadriiformes	Sternidae	*Sterna aurantia*	River Tern	WV	+	+
133.	Charadriiformes	Sternidae	*Sterna hirundo*	Common Tern	SV	--	+
134.	Charadriiformes	Sternidae	*Sterna repressa*	White Cheecked Tern	SV	--	+
135.	Charadriiformes	Sternidae	*Sterna acuticauda*	Black-bellied Tern	R	+	+
136.	Charadriiformes	Sternidae	*Sterna albifrons*	Little Tern	PM	+	+
137.	Charadriiformes	Sternidae	*Sterna bergii*	Large Crested Tern	O	+	--
138.	Charadriiformes	Sternidae	*Sterna sandvicensis*	Sandwich Tern	M	--	+
139.	Charadriiformes	Rhynchopidae	*Rynchops albicollis*	Indian Skimmer	PM	+	--
140.	Columbiformes	Pteroclididae	*Pterocles exustus*	Chestnut-bellied Sandgrouse	O	+	+
141.	Columbiformes	Pteroclididae	*Pterocles senegallus*	Spotted Sandgrouse	WV	--	+
142.	Columbiformes	Pteroclididae	*Pterocles orientalis*	Black-bellied Sandgrouse	WV	--	+
143.	Columbiformes	Pteroclididae	*Pterocles alehata*	Pintailed Sandgrouse	R	--	+
144.	Columbiformes	Columbidae	*Treron phoenicoptera*	Yellow Footed Green Pigeon	WV	+	+
145.	Columbiformes	Columbidae	*Columba livia*	Blue Rock Pigeon	R	+	+
146.	Columbiformes	Columbidae	*Columba eversmanni*	Yellow-eyed or Eastern Rock Pigeon	O	+	+
147.	Columbiformes	Columbidae	*Treron bicincta*	Orange-breasted Green Pigeon	O	--	+
148.	Columbiformes	Columbidae	*Streptopelia decaocto*	Ring Dove	R	+	+
149.	Columbiformes	Columbidae	*Streptopelia tranquebarica*	Red Turtle Dove	SV	+	+

continued..

Table 8 continue…

S. No.	Order	Family	Scientific Name	Common Name	Occurrence	Status	
						Previous	Present
150.	Columbiformes	Columbidae	*Streptopelia senegalensis*	Little Brown Dove	R	+	+
151.	Psittaciformes	Psittacidae	*Psittacula krameri*	Rose Ringed Parakeet	R	+	+
152.	Cuculiformes	Cuculidae	*Clamator jacobinus*	Pied-crested Cuckoo	SV	+	+
153.	Cuculiformes	Cuculidae	*Eudynamys scolopacea*	Koel	R	+	+
154.	Cuculiformes	Cuculidae	*Centropus sinensis*	Greater Coucal	R	+	+
155.	Strigiformes	Tytonidae	*Tyto alba*	Indian Barn Owl	R	--	+
156.	Strigiformes	Strigidae	*Otus brucei*	Striated Scops Owl	WV	--	+
157.	Strigiformes	Strigidae	*Otus scops*	Eastern Scops Owl	WV	--	+
158.	Strigiformes	Strigidae	*Otus bakkamoena*	Collared Scops Owl	O	+	+
159.	Strigiformes	Strigidae	*Bubo bubo*	Eagle Owl	O	+	+
160.	Strigiformes	Strigidae	*Athene brama*	Spotted Owlet	R	+	+
161.	Strigiformes	Strigidae	*Asio otus*	Long-eared Owl	WV	--	+
162.	Strigiformes	Strigidae	*Asio flammeus*	Short-eared Owl	WV	--	+
163.	Caprimulgiformes	Caprimulgidae	*Caprimulgus asiaticus*	Indian Little Nightjar	R	+	+
164.	Caprimulgiformes	Caprimulgidae	*Caprimulgus europaeus*	European Nightjar	SV	+	+
165.	Caprimulgiformes	Caprimulgidae	*Caprimulgus mahrattensis*	Syke's Nightjar	R	+	+
166.	Apodiformes	Apodidae	*Apus affinis*	House Swift	R	+	+
167.	Coraciformes	Alcedinidae	*Ceryle rudis*	Pied Kingfisher	R	+	+
168.	Coraciformes	Alcedinidae	*Alcedo atthis*	Common Kingfisher	R	+	+
169.	Coraciformes	Alcedinidae	*Halcyon smyrnensis*	White-breasted Kingfisher	R	+	+
170.	Coraciformes	Meropidae	*Merops superciliosus*	Blue-cheeked Bee-eater	SBV	+	+
171.	Coraciformes	Meropidae	*Merops orientalis*	Green Bee-eater	R	+	+
172.	Coraciformes	Meropidae	*Merops apiaster*	European Bee-eater	R	--	+
173.	Coraciformes	Coraciidae	*Coracias garrulus*	European Roller	R	+	--
174.	Coraciformes	Coraciidae	*Coracias bengalensis*	Indian Roller	R	+	+
175.	Coraciformes	Upupidae	*Upupa epops*	Hoopoe	WV	+	+
176.	Piciformes	Picidae	*Dinopium bengalensis*	Lesser Golden-backed Woodpecker	R	+	+
177.	Piciformes	Picidae	*Picoides mahrattensis*	Yellow-fronted Pied Woodpecker	R	+	+
178.	Piciformes	Picidae	*Jynx torquilla*	Wryneck	PM	+	+
179.	Passeriformes	Alaudidae	*Mirafra erythroptera*	Indian/Red-winged Bush Lark	O	+	+

continued..

Table 8 continue…

S. No.	Order	Family	Scientific Name	Common Name	Occurrence	Status	
						Previous	Present
180.	Passeriformes	Alaudidae	*Eremopterix grisea*	Ashy-crowned Finch Lark	R	+	+
181.	Passeriformes	Alaudidae	*Eremopterix nigriceps*	Black-crowned Finch Lark	R	+	+
182.	Passeriformes	Alaudidae	*Ammomanes deserti*	Desert Finch Lark	R	+	+
183.	Passeriformes	Alaudidae	*Calandrella rufescens*	Lesser Short-toed Lark	WV	--	+
184.	Passeriformes	Alaudidae	*Calandrella raytal*	Indus Sand Lark	R	--	+
185.	Passeriformes	Alaudidae	*Galerida cristata*	Crested Lark	R	+	+
186.	Passeriformes	Alaudidae	*Alauda gulgula*	Oriental Sky Lark	R	+	+
187.	Passeriformes	Hirundinidae	*Riparia riparia*	Collared Sand Martin	WV	--	+
188.	Passeriformes	Hirundinidae	*Riparia paludicola*	Grey-throated Sand Martin	WV	+	+
189.	Passeriformes	Hirundinidae	*Hirundo smithi*	Wire-tailed Swallow	SV	+	+
190.	Passeriformes	Hirundinidae	*Hirundo rustica*	Barn Swallow	WV	+	+
191.	Passeriformes	Hirundinidae	*Hirundo daurica*	Red-rumped Swallow	WV	+	+
192.	Passeriformes	Motacillidae	*Anthus novaeseelandiae*	Paddyfield Pipit	R	+	+
193.	Passeriformes	Motacillidae	*Anthus campestris*	Tawny Pipit	WV	+	--
194.	Passeriformes	Motacillidae	*Anthus trivialis*	Tree Pipit	PM	+	+
195.	Passeriformes	Motacillidae	*Anthus spinoletta*	Water Pipit	WV	--	+
196.	Passeriformes	Motacillidae	*Motacilla flava*	Yellow Wagtail	PM	+	+
197.	Passeriformes	Motacillidae	*Motacilla citreola*	Yellow-headed Wagtail	WV	+	+
198.	Passeriformes	Motacillidae	*Motacilla alba*	Pied Wagtail	WV	+	+
199.	Passeriformes	Motacillidae	*Motacilla maderaspatensis*	White-browed Pied Wagtail	R	+	+
200.	Passeriformes	Laniidae	*Lanius isabellinus*	Isabelline Shrike	WV	+	+
201.	Passeriformes	Laniidae	*Lanius excubitor*	Grey Shrike	R/SBV	+	+
202.	Passeriformes	Laniidae	*Lanius vittatus*	Bay-backed Shrike	R	+	+
203.	Passeriformes	Laniidae	*Lanius schach*	Rufous-backed Shrike	R	+	+
204.	Passeriformes	Dicruridae	*Dicrurus adsimilis*	Black Drongo/ King Crow	R	+	+
205.	Passeriformes	Sturnidae	*Sturnus roseus*	Rosy Pastor	PM	+	+
206.	Passeriformes	Sturnidae	*Acridotheres ginginianus*	Bank Myna	R	+	+
207.	Passeriformes	Sturnidae	*Sturnus vulgaris*	Common Starling	O	+	+
208.	Passeriformes	Sturnidae	*Acridotheres tristis*	Indian Myna	R	+	+
209.	Passeriformes	Corvidae	*Dendrocitta vagabunda*	Tree Pie	R	+	+

continued..

Table 8 continue…

S. No.	Order	Family	Scientific Name	Common Name	Occurrence	Status	
						Previous	Present
210.	Passeriformes	Corvidae	*Corvus splendens*	House Crow	R	+	+
211.	Passeriformes	Corvidae	*Corvus corax*	Common Raven	R/WV	+	+
212.	Passeriformes	Campephagidae	*Tephrodornis pondicerianus*	Common Wood Shrike	R	+	+
213.	Passeriformes	Campephagidae	*Pericrocotus cinnamomeus*	Wandering Minivet	O	+	--
214.	Passeriformes	Pyconotidae	*Pycnonotus leucogenys*	White-cheeked Bulbul	R	+	+
215.	Passeriformes	Pyconotidae	*Pycnonotus cafer*	Red-vented Bulbul	R	+	+
216.	Passeriformes	Timaliidae	*Turdoides caudatus*	Common Babbler	R	+	+
217.	Passeriformes	Timaliidae	*Turdoides earlei*	Striated Babbler	R	+	+
218.	Passeriformes	Timaliidae	*Turdoides striatus*	Jungle Babbler	R	+	+
219.	Passeriformes	Nectariniidae	*Nectarinia asiatica*	Purple Sunbird	R	+	+
220.	Passeriformes	Muscicapidae	*Muscicapa striata*	Spotted Flycatcher	PM	+	+
221.	Passeriformes	Muscicapidae	*Ficedula parva*	Red-throated Flycatcher	PM	+	+
222.	Passeriformes	Monarchidae	*Hypothymus azurea*	Black-naped Flycatcher	WV	+	--
223.	Passeriformes	Sylviidae	*Orthotomus sutorius*	Tailor Bird	R	+	+
224.	Passeriformes	Sylviidae	*Acrocephalus agricola*	Paddy-field Warbler	WV	+	+
225.	Passeriformes	Sylviidae	*Acrocephalus stentoreus*	Clamorous Great Reed Warbler	WV	+	+
226.	Passeriformes	Sylviidae	*Cettia cetti*	Cetti's Warbler	WV	+	+
227.	Passeriformes	Sylviidae	*Acrocephalus dumetorum*	Blyth's Reed Warbler	PM	+	+
228.	Passeriformes	Sylviidae	*Prinia inornata*	Plain Prinia	R	+	+
229.	Passeriformes	Sylviidae	*Prinia buchanani*	Rufous-fronted Long-tailed Warbler	R	+	+
230.	Passeriformes	Sylviidae	*Prinia gracilis*	Streaked Wren Warbler	R	+	+
231.	Passeriformes	Sylviidae	*Prinia flaviventris*	Yellow Bellied Long-tailed Warbler	R	+	+
232.	Passeriformes	Sylviidae	*Prinia burnesii*	Long-tailed Grass Warbler	R	+	+
233.	Passeriformes	Sylviidae	*Hippolais caligata*	Syke's Tree Warbler	WV	+	+
234.	Passeriformes	Sylviidae	*Sylvia hortensis*	Orphean Warbler	WV	+	+
235.	Passeriformes	Sylviidae	*Sylvia curruca*	LesserWhite-throat	WV	+	+
236.	Passeriformes	Sylviidae	*Sylvia communis*	CommonWhite-throat	PM	+	+

continued..

Table 8 continue…

S. No.	Order	Family	Scientific Name	Common Name	Occurrence	Status	
						Previous	Present
237.	Passeriformes	Sylviidae	*Sylvia nana*	Desert Warbler	WV	+	+
238.	Passeriformes	Sylviidae	*Phylloscopus collybita*	Brown Leaf Warbler	WV	+	+
239.	Passeriformes	Sylviidae	*Phylloscopus sindianus*	Sind Chiffchaff	WV	--	+
240.	Passeriformes	Sylviidae	*Phylloscopus neglectus*	Plain Leaf Warbler	WV	+	+
241.	Passeriformes	Sylviidae	*Phylloscopus nitidus*	Bright Green Leaf Warbler	WV	+	+
242.	Passeriformes	Turdidae	*Erythropygia galacototes*	Rufous chat/ Rufous-tailed Scrub Robin	PM	+	+
243.	Passeriformes	Turdidae	*Luscinia svecicus*	Bluethroat	WV	+	+
244.	Passeriformes	Turdidae	*Phoenicurus ochruros*	Black Redstart	WV	+	+
245.	Passeriformes	Turdidae	*Saxicola caprata*	Pied Bush Chat	R	+	+
246.	Passeriformes	Turdidae	*Oenanthe deserti*	Desert Wheatear	WV	+	+
247.	Passeriformes	Turdidae	*Oenanthe picata*	Pied Chat	WV	+	+
248.	Passeriformes	Turdidae	*Oenanthe alboniger*	Hume's Wheatear	R	+	+
249.	Passeriformes	Turdidae	*Saxicoloides fulicata*	Indian Robin	R	+	+
250.	Passeriformes	Rhipiduridae	*Rhipidura aureola*	White-browed Fantail Flycatcher	R	+	+
251.	Passeriformes	Passeridae	*Passer domesticus*	House Sparrow	R	+	+
252.	Passeriformes	Passeridae	*Passer hispaniolensis*	Spanish Sparrow	PM	+	+
253.	Passeriformes	Passeridae	*Passer pyrrhonotus*	Sindh Jungle Sparrow	R	+	+
254.	Passeriformes	Passeridae	*Pectronia xanthocollis*	Yellow-throated Sparrow	SV	+	+
255.	Passeriformes	Ploceidae	*Ploceus philippinus*	Baya	R	+	+
256.	Passeriformes	Ploceidae	*Ploceus manyar*	Streaked Weaver	SV	+	+
257.	Passeriformes	Estrildidae	*Lonchura malabarica*	White-throated Munia/Indian Silver Bill	R	+	+
258.	Passeriformes	Fringillidae	*Fringilla montifringilla*	Brambling	O	+	--
259.	Passeriformes	Fringillidae	*Bucanetes githaginea*	Trumpeter Finch	R	+	--
260.	Passeriformes	Emberizidae	*Emberiza buchanani*	Grey-necked Bunting	PM	+	--
261.	Passeriformes	Emberizidae	*Emberiza melanocephala*	Black-headed Bunting	WV	+	+
262.	Passeriformes	Emberizidae	*Emberiza striolata*	Striped Bunting	R	+	--

Legends: R = Resident; WV = Winter Visitor; SV = Summer Visitor; SBV = Summer Breeding Visitors; YRV = Year Round Visitors; O = Vagrant; PM = Passage Migrant; S = Scarce; + - Present; -- - Absent.

Table 9. List of Reptiles recorded from RBOD study areas.

S. No.	Order	Family	Scientific Name	Common Name	Status
1.	Squamata	Elapidae	*Bungarus caeruleus*	Indian Krait	LC
2.	Squamata	Elapidae	*Naja naja*	Indian Cobra / Spectacled Cobra	LC
3.	Squamata	Colubridae	*Oligodon taeniolatus*	Streaked Kukri Snake	LC
4.	Squamata	Colubridae	*Platyceps rhodorachis*	Cliff Racer	LC
5.	Squamata	Colubridae	*Platyceps ventromaculatus*	Glossy-bellied Racer / Plain's Racer	C
6.	Squamata	Colubridae	*Psammophis condanarus*	Indian Sand Snake / Oriental Sand Snake	LC
7.	Squamata	Colubridae	*Psammophis leithii*	Ribbon Snake	LC
8.	Squamata	Colubridae	*Ptyas mucosus*	Dhaman / Rope Snake	C
9.	Squamata	Colubridae	*Spalerosophis diadema*	Royal Snake	LC
10.	Squamata	Colubridae	*Xenochrophis piscator*	Checkered-keel Back	LC
11.	Squamata	Viperidae	*Echis carinatus*	Saw-scaled Viper	LC
12.	Squamata	Viperidae	*Daboia russelii*	Russel's Viper	LC
13.	Squamata	Boidae	*Eryx johnii*	Common Sand Boa	LC
14.	Squamata	Boidae	*Eryx conicus*	Sand Boa	LC
15.	Squamata	Lacertidae	*Acanthodactylus cantoris*	Indian Fringe-toed Lizard	C
16.	Squamata	Varanidae	*Varanus griseus*	Desert Monitor Lizard	LC
17.	Squamata	Varanidae	*Varanus bengalensis*	Indian Monitor Lizard	LC
18.	Squamata	Uromastycidae	*Saara hardwickii*	Indian Spiny-tailed Lizard	LC
19.	Squamata	Agamidae	*Trapelus megalonyx*	Afghan Ground Agama	LC
20.	Squamata	Agamidae	*Trapelus agilis*	Brilliant Agama / Agile Agama	LC
21.	Squamata	Agamidae	*Calotes versicolor*	Indian Garden Lizard/Common Tree Lizard	C
22.	Squamata	Eublepharidae	*Eublepharis macularius*	Fat-tailed Gecko / Pakistani Leopard Gecko	LC
23.	Squamata	Geckonidae	*Cyrtopodion kachhensis*	Warty Rock Gecko / Kutch Gecko	LC
24.	Squamata	Geckonidae	*Cyrtopodion scaber*	Keeled Rock Gecko	LC
25.	Squamata	Geckonidae	*Crossobamon orientalis*	Sindh Sand Gecko	LC
26.	Squamata	Geckonidae	*Hemidactylus flavivirdis*	Yellow-bellied House Gecko	LC
27.	Squamata	Geckonidae	*Hemidactylus brookii*	Spotted Indian House Gecko/Brook's Gecko	LC
28.	Squamata	Geckonidae	*Hemidactylus leschenaultii*	Bark Gecko / Marbled Tree Gecko	LC
29.	Chelonia	Trionychidae	*Lissemys punctata*	Indian Flap-shell Turtle	C
30.	Testudines	Emydidae	*Geoclemys hamiltonii*	Spotted Pond Turtle	C
31.	Crocodilia	Crocodylidae	*Crocodylus palustris*	Marsh Crocodile	LC

Legends: C= Common; LC= Less Common

Table 10. List of Amphibians recorded from RBOD study areas.

S. No.	Order	Family	Scientific Name	Common Name	Status
1.	Anura	Ranidae	*Euphlyctis cyanophlyctis*	Skittering Frog	Common
2.	Anura	Bufonidae	*Duttaphrynus stomaticus*	Indus Toad	Common

Table 11. List of Fish fauna recorded from RBOD study areas.

S. No.	Order	Family	Scientific Name
1.	Cypriniformes	Cyprinidae	*Salmostoma bacaila*
2.	Cypriniformes	Cyprinidae	*Securicula gora*
3.	Cypriniformes	Cyprinidae	*Barilius vagra*
4.	Cypriniformes	Cyprinidae	*Amblypharyngodon mola*
5.	Cypriniformes	Cyprinidae	*Chela cachius*
6.	Cypriniformes	Cyprinidae	*Aspidoparia morar*
7.	Cypriniformes	Cyprinidae	*Esomus danricus*
8.	Cypriniformes	Cyprinidae	*Barbodes sarana*
9.	Cypriniformes	Cyprinidae	*Rasbora daniconius*
10.	Cypriniformes	Cyprinidae	*Catla catla*
11.	Cypriniformes	Cyprinidae	*Cirrhinus reba*

continued..

Table 11 continue…

S. No.	Order	Family	Scientific Name
12.	Cypriniformes	Cyprinidae	*Cirrhinus mrigala*
13.	Cypriniformes	Cyprinidae	*Labeo dero*
14.	Cypriniformes	Cyprinidae	*Labeo calbasu*
15.	Cypriniformes	Cyprinidae	*Labeo fimbriatus*
16.	Cypriniformes	Cyprinidae	*Labeo gonius*
17.	Cypriniformes	Cyprinidae	*Labeo dyocheilus*
18.	Cypriniformes	Cyprinidae	*Labeo rohita*
19.	Cypriniformes	Cyprinidae	*Osteobrama cotio*
20.	Cypriniformes	Cyprinidae	*Puntius ticto*
21.	Cypriniformes	Cyprinidae	*Puntius chola*
22.	Cypriniformes	Cyprinidae	*Puntius sophore*
23.	Cypriniformes	Cyprinidae	*Ctenpharyngodon idella*
24.	Cypriniformes	Cyprinidae	*Cyprinus carpio*
25.	Cypriniformes	Cyprinidae	*Hypophthalmichthys molitrix*
26.	Cypriniformes	Cyprinidae	*Aristchthys nobilis*
27.	Clupeiformes	Clupeidae	*Gudusia chapra*
28.	Osteoglossiformes	Notopteridae	*Notopterus notopterus*
29.	Osteoglossiformes	Notopteridae	*Notopterus chitala*
30.	Siluriformes	Bagridae	*Aorichthys aor*
31.	Siluriformes	Bagridae	*Rita rita*
32.	Siluriformes	Bagridae	*Mystus gulio*
33.	Siluriformes	Bagridae	*Mystus vittatus*
34.	Siluriformes	Bagridae	*Mystus bleekeri*
35.	Siluriformes	Bagridae	*Mystus cavasius*
36.	Siluriformes	Sisoridae	*Bagarius bagarius*
37.	Siluriformes	Sisoridae	*Gagata cenia*
38.	Siluriformes	Sisoridae	*Nangra nangra*
39.	Siluriformes	Siluridae	*Ompok bimaculatus*
40.	Siluriformes	Siluridae	*Wallago attu*
41.	Siluriformes	Heteropneustidae	*Heteropneustes fossilis*
42.	Siluriformes	Schilbeidae	*Ailia coila*
43.	Siluriformes	Schilbeidae	*Clupisoma garua*
44.	Siluriformes	Schilbeidae	*Clupisoma naziri*
45.	Siluriformes	Schilbeidae	*Eutropiichthys vacha*
46.	Beloniformes	Belonidae	*Xenentodon cancila*
47.	Channiformes	Channidae	*Channa marulia*
48.	Channiformes	Channidae	*Channa punctata*
49.	Channiformes	Channidae	*Channa striata*
50.	Perciformes	Chandidae	*Chanda nama*
51.	Perciformes	Chandidae	*Parambassis baculis*
52.	Perciformes	Chandidae	*Parambassis ranga*
53.	Perciformes	Badidae	*Badis badis*
54.	Perciformes	Mugilidae	*Sicamugil cascasia*
55.	Perciformes	Gobidae	*Glossogobium giuris*
56.	Perciformes	Belontidae	*Colisa fasciata*
57.	Perciformes	Belontidae	*Colisa lalia*
58.	Perciformes	Cichlidae	*Oreochromis mossambicus*
59.	Synbranchiformes	Mastcembelidae	*Mastacembelus armatus*

DISCUSSION

The water samples of the year 2010 were uncollectable due to flooding in the area as water become diluted. The present study reveals that RBOD is continuously receiving the discharges containing polluted water through three sources viz., municipal wastewater, industrial wastewater and agricultural runoff. The continuous accumulation causes a potential threat to aquatic life. The poisonous metals such as Mercury, Lead, Zinc, Copper, Cadmium and Chromium etc. in the industrial wastes and storm water drainage in the urban areas prove fatal for most living organisms. These toxic materials through water currents in the under surface

water have reached and have polluted most freshwater resources (Abbas, 2011).

In the present work, water samples taken from the RBOD near Keenjhar Lake showed pesticide OC compounds below the Maximum Acceptable Concentration (MAC). The data show 0.001mg/l DDT of OC groups analyzed presently in the ground water of RBOD near Keenjhar Lake. The concentration of these compounds and their continuous accumulation in the benthic deposit and their entry in food chain need to be addressed immediately.

The environmental impacts of OC group DDT pesticide residues and their effect on human health is an important matter of concern. The effect of DDT on estrogen behavior in human suggested the implication of these compounds in breast cancer (Carvalhado *et al*., 1998). Pesticides that are soluble in both water and fats are generally taken up more quickly by animals and man as the traces of these pesticides with their metabolites and breakdown products are universally present in abiotic and biotic environment (Tiel, 1972). In addition, the proportion of pesticides that is absorbed by the gut depends on the movement of the gut and the rate of way of food stuff through it.

In another study, pesticide residues of deltamethrin, aldrin, dieldrin, DDT and DDE in muscles, fat and liver of three Labeo species of fishes were found in Keenjhar and Haleji Lakes (Saqib *et al*., 2005).

The increased use of pesticides in a franzy to increase production of crops is also complicating the problem. The increased usage of even the most persistent and toxic chemicals like DDT is also continued (Nasir *et al*., 1987). The quantity of OC compounds and their metabolites were found in a higher amount in Sindh lakes as reported by Siddiqui (1998). He also noted dieldrin and other OC compounds from muscles and fat bodies of waterbirds on different lakes of Sindh. Detection of pesticide residues deltamethrin, aldrin, dieldrin, DDT, cypermethrin, DDE and melathion of the water samples of Gharo Creek showed no considerable concentration of pesticides (Khan, 2004).

The quantity of OC and OP compounds were estimated above the Maximum Acceptable Concentration in Haleji Lake and below the MAC in Keenjhar Lake as reported by Abbas (2011). During our study, no adverse effects of environmental pollution were found on the aquatic biodiversity except for some minor toxic effects due to the presence of heavy metals in water. All the physico-chemical parameter values were observed as per limit of World Health Organization standard. The depletion of Dissolved Oxygen indicated organic pollution harmful for aquatic biodiversity (Khan *et al*., 2012).

The salinity values near Gharo and near Keenjhar were observed high as per limit of World Health Organization standard, but having no adverse effect on aquatic biodiversity. Higher value of salinity presented during summer may be due to evaporation and comparatively low value was recorded during winter and rainy season. The rain water, however, causes dilution, aeration and additional biological activity as the BOD and COD pressure is decreased and solubility level of air in water is increased (Abbas, 2011). The desalination of the RBOD drainage water through treatment plants is not costly because of post-purification benefits for agriculture and adjacent affected wetlands.

It is also marked from these studies that dissolved oxygen content, salinity and pH do not affect the growth of copepods. The population of copepods shows growth pattern which only corresponds with the variation of temperature.

In January and December, beside the other factors, deficiency of nutrient salts due to accumulation is responsible for the decline of population of plankton (Welch, 1952). In summer temperature, increase in predation and downward migration are the factors responsible for the low population. The adults die out soon after breeding, and summer period is the peak of breeding. All these factors probably acting simultaneously are responsible for the extremely low population during May and June (Baqai and Rehana, 1973). During all the study period in pre-monsoon and post- monsoon the populations of copepods have a maximum.

Environmental Problems in RBOD

The RBOD is presently passing across the southern tip of Hadero Lake. For the present alignment there is a risk of pollution of Hadero Lake. The RBOD drain flows very close to Haleji Lake, the distance between RBOD and Haleji Lake is hardly 50 to 100ft. The water level is 20-30ft below the level of the lake area. Since the water level in Haleji Lake would be higher, (average depth 17ft) than that of the Drain. There is a possibility of the lake water spilling over the embankment and flowing into the drain in wet years of excessive rainfall. Due to very short distance from RBOD, Haleji Lake may be affected by the seepage of its water to the drain. Necessary measures have to be adopted to ensure environmental sustainability, safety of Haleji Lake from saline water intrusion and safety of RBOD from spilling of lake waters into RBOD and consequent flooding.

A very undesirable situation is prevailing for the last many years of discharging about 20 to 25 cusecs of untreated industrial wastewater from Kotri and Nooriabad Industrial Area into K.B Feeder, a channel which provides drinking water to Karachi. The logic in favour is the higher dilution rate and those 20 to 25 cusecs after all, is

an insignificant volume compared to K.B. Feeder discharge of 10,000 cusecs. Environmentally, this is an unacceptable practice. With the completion of RBOD, the industrial wastewater will be discharged into the drain whose alignment lies between the K.B Feeder and Kotri Industrial Area. This is very significant positive environmental impact as far as saving of K.B Feeder is concerned.

The largest part of the marginal area of the drain is presently surrounded with water lilies like Lotus, Phragmites and Typha along with Mesquites elsewhere. The open water area is dominated by submerged aquatic vegetation filling the whole water profile from bottom to surface. As a result the open area is reducing which is the habitat of many waterbirds. Some agriculture lands close to the marginal area which may in the long run affect the water quality of the water body. Runoff from agricultural fields containing chemical fertilizers triggers pollution. There are some social impacts such as washing of clothes and grazing of cattle. These social impacts may affect and contaminate the water but not to a great extent. Water is available in deep or shallow pools in the drain beds. The drain beds have risen due to sedimentation. At the RBOD area near Keenjhar Lake water is found in stagnant condition and it has resulted in the deterioration of water quality. In the study area, about 20% residents of towns and big villages are having water supply system, whereas remaining residents getting water from hand pumps, canal and river for drinking and domestic use. The villages which are near to the river are having fresh ground water, whereas the water logged area of Thatta ground water is brackish. In Thatta area from Chillya to Gharo residents living near to proposed drain are getting water from K.G. Canal and distributaries and also children and adults doing fishing practice and take bath from this drain water. This polluted water is not suitable for health and may cause diseases. The main health issue that relates to stagnant water (drainage near Keenjhar Lake) is Malaria. Due to using this polluted water, the general health of the majority of respondents was extremely poor. In every village, at least such diseases were described as common. These are Malaria, Common Fever, Diarrhea, Gynecological problems, Eye infection, Typhoid, Skin diseases and Cough.

All the stakeholders and residents are having negative remarks about the RBOD project, because of lack of information and awareness. They are under the impression that the drain will carry the industrial effluent, which will destroy agriculture land, crop and livestock and also would harm human health. The drain will divide their land in two parts. Approach roads from main Highway to RBOD passing through their land/village will destroy the crop lands during the construction phase. A large number of families at least 5,000 will be affected from the construction phase of RBOD. Any big project like RBOD is required for proper planning and compensation requirements for the people to whom it affected. If acceptable compensation and alternative source of property is provided, then it will be become very easy to make this project successful as well as acceptable for the concerned families.

Currently, all the polluted and contaminated water from MNVD is partly flowing into the Manchar Lake and partly being used for irrigation by the local cultivators. The quality of water is marginally suitable for irrigation with potential hazard for the soil, which is harmful to the environment and ecology of the lake, but after the flow of RBOD, it will directly dispose off into the Sea via Gharo and it will be very much beneficial for the environment. It is hoped that the construction of RBOD will save Manchar Lake and surrounding areas and carry the saline drainage water to the Arabian Sea. The discharge of K.G drain into Gharo Creek for the last three decades did not have any significant negative impact on the ecology of Gharo Creek as compared with the discharge of untreated sewage flowing through Malir River into Ghizri Creek and Lyari into Keamari which has significantly impacted the ecology and marine life of these two outfall areas.

Therefore, the construction of RBOD from Sehwan to Sea via Gharo Creek carrying the saline water from northern area drainage units will go a long way off in saving River Indus from permanent damage and is by far one of the very important mitigation measures to protect Manchar Lake and River Indus. River Indus is the life line of Pakistan and Sindh and no cost will be too great to save it from permanent damage and pollution.

Further studies are needed to collect more data for preparing a conservation plan for the management of Right Bank Outfall Drain. There is a need to increase public awareness regarding the importance and implement a monitoring program to provide protection of biodiversity and to enhance public co-operation in the conservation and management of the Drain and the threatened species.

CONCLUSION

On the basis of the present study, it is concluded that the environmentally RBOD project is a step in the right direction to save Manchar Lake and River Indus downstream of Sehwan from salinization and also take care of saline water and channel it into the Sea. The environmental issues likely to cause negative impacts, during construction and post construction era, can be handled with proper mitigation measures. The present study being the first study of its kind, will serve as a

baseline data for the future researchers on the biodiversity and environment of the area.

ACKNOWLEDGMENTS

The authors are deeply thankful to Free Software Foundation for using of some bird photos and also thank Mr. Abdur Razzaq Khan for his field surveys support.

REFERENCES

Abbas, D. 2011. Effects of environmental pollution on aquatic vertebrates and inventories of Haleji and Keenjhar Lakes: Ramsar Sites. Ph.D. Thesis. Department of Zoology, University of Karachi.

Ahmed, M. 1995. Elements of training course in coastal oceanography and pollution for coastal zone managers in Pakistan. In: Resorce Volume for Tertiary Level Education and Training in Coastal Zone Management. Eds. May, JE., Ponniah, W. and Pnadanm, M. NETLAP Publication No. 13. UNEP. Bangkok, Thailand. 15-29.

A.P.H.A. 1992. Standard Methods for the Examination of Water and Wastewater. (18th edi.). APHA, Washington, DC, USA.

Auffenberg, W. and Rahman, H. 1991. Studies on Pakistan Reptiles. Pt. I. The genus *Echis* (Viperidae). Bull. Florida Mus. Nat. Hist. 35(5):263-314.

Baqai, IU. and Rehana, I. 1973. Seasonal fluctuation of Fresh-water Copepods of Keenjhar Lake, Sind, and its correlation with physioco-chemical factors. Pakistan J. Zool. 5(2):165-168.

Brower, J., Zar, J. and Ende, C. 1990. Field and Laboratory Methods for General Ecology. Wm. C. Brown Publishers. 2460 Kerper Boulevard, Dubuque, A 52001.

Carvalhado, FP., Nhan, DD., Zhong, C., Tavares, T. and Klaine, S. 1998. Tracking Pesticides in the Tropics. IAEA Bulletin. 40:3.

Curds, CR. 1982. The Ecology and Role of Protozoa in Aerobic Sewage Treatment Processes. Ann. Rev. Microbiol. 36:27-46.

Curds, CR., Gates, MA. and Roberts, DMCL. 1983. British and other Freshwater Ciliated Protozoa, Part II. Cambridge University Press, London.

Edmondson, WT. 1966. Fresh Water Biology, John Wiley and Sons, USA.

Gabol, K., Khan, MZ. and Ghalib, SA. 2005. Some Observation on the Birds and Physio-chemical Parameters of Hadero Lake Sindh. J. Nat. Hist. Wildl. 4(1):121-125.

Grewal, B., Pfister, O. and Harvey, B. 2002. A Photographic Guide to the Birds of India and the Indian Subcontinent including Pakistan, Nepal, Bhutan, Sri Lanka and the Maldives, Singapore: Periplus.

Grimmett, R., Inskipp, C. and Inskipp, T. 1998. Birds of the Indian sub-continent. Oxford University Press, Delhi. pp890.

Kazmierczak, K. 2000. A Field Guide to the Birds of India, Sri Lanka, Pakistan, Nepal, Bhutan, Bangladesh and the Maldives. New Delhi, India.

Khan, MZ. 2004. Effect of Pesticides on Amphibians and Reptiles. Exper. J. Zool. India. 7(1):39-47.

Khan, MA., Hany, O., Hashmi, I., Kazmi, QB. and Khan, MA. 2004. Pesticide Pollution of Gharo Creek: A Preliminary Studies. Pakistan Journal of Marine Sciences. 13(1&2):11-14.

Khan, MZ. 2006. Current Status and Biodiversity of Indus Dolphin Reserve and Indus Delta Wetlands (Ramsar Sites). Refereed Proceeding 9th International Riversymposium, Brisbane, Australia. 1-17.

Khan, MZ., Ghalib, SA. and Hussain, B. 2010. Status and New Nesting Sites of Sea Turtles in Pakistan. Chelonian Conservation and Biology. 9(1):119-123.

Khan, MZ., Ghalib, SA., Siddiqui, S., Siddiqui, TF., Farooqi, RY., Yasmeen, G., Abbas, D. and Zehra, A. 2012[a]. Current Status and Distribution of Reptiles of Sind. Journal of Basic and Applied Sciences. 8:26-34.

Khan, MZ., Abbas, D., Ghalib, SA., Yasmeen, R., Siddiqui, S., Nazia, M., Zehra, A., Begum, A., Jabeen, T., Yasmeen, G. and Latif, TA. 2012[b]. Effects of Environmental Pollution on Aquatic Vertebrates and Inventories of Haleji and Keenjhar Lakes: Ramsar Sites. Canadian Journal of Pure and Applied Sciences. 6(1):1759-1783.

Khan, MZ., Begum, A., Ghalib, SA., Khan, AR., Yasmeen, R., Siddiqui, TF., Zehra, A., Abbas, D., Tabassum, F., Siddiqui, S., Jabeen, T. and Hussain, B. 2012[c]. Effects of Environmental Pollutants on Aquatic Vertebrate Biodiversity and Inventory of Hub Dam: Ramsar Site. Canadian Journal of Pure and Applied Sciences. 6(2):1913-1935.

Khan, MZ., Tabbassum, F., Ghalib, SA., Zehra, A., Hussain, B., Siddiqui, S., Yasmeen, G., Gabol, K., Mahmood, N., Khan, IS., Khan, AB., Abbas, D., Jabeen, T., Samreen, N. and Iqbal, MA. 2014. Distribution, Population Status and Conservation of the Birds in Karachi, Sindh, Pakistan. CJPAS. 8(1):2697-2713.

Nasir, N., Mumtaz, M. and Baig, MMH. 1987. Contamination of Paddy Ecosystem with aerially sprayed DDT formulation. Proc. World Environment Day Department of Zoology, University of Karachi June 6, 1987. Zoologica.

Roberts, TJ. 1991-1992. The Birds of Pakistan. Oxford University Press, Karachi.

Roberts, TJ. 1997. The Mammals of Pakistan. (Revised edi.), Oxford University Press Karachi, Pakistan.

Roberts, TJ. 2005[a]. Field Guide to the Small Mammals of Pakistan. Oxford University Press Karachi. pp280.

Roberts, TJ. 2005[b]. Field Guide to the Large and Medium Sized Mammals of Pakistan. Oxford University Press Karachi. pp260.

Saqib, TA., Naqvi, SNH., Siddiqui, PA. and Azmi, MA. 2005. Detection of Pesticide Residues in muscles, fat and liver of three species of *Labeo* found in Karli and Haleji Lakes. J. Environ. Biol. 26:4333-438.

Siddiqui, PA. 1998. Bioecology of Wetlands of Lower Sindh with reference to Avifauna and Organophosphate Pollution. Ph.D. Thesis, Department of Zoology, University of Karachi. (unpublished).

Tiel, NV. 1972. Pesticides in Environment and Food. Environmental Quality and Safety. Academic Press Inc. New York, USA. 1:180-189.

Welch, SP. 1952. Limnology. New York, USA.

WHO. 1982. Examination of Water for Pollution Control. World Health Organization. Regional Office for Europe. 203-204.

WHO. 1993. Guideline for Drinking Water Quality. World Health Organization. Geneva, Switzerland.

Yahya, M. 2007. The Lost Paradise (Manchar Lake). Proceedings of Taal: The 12th World Lake Conference. 1397-1407.

Received: Oct 12, 2013; Revised: Jan 16, 2014;
Accepted: Jan 25, 2014

SENRA Academic Publishers, British Columbia
Vol. 8, No. 2, pp. 2901-2904, June 2014
Online ISSN: 1920-3853; Print ISSN: 1715-9997

Canadian Journal of pure & applied sciences

Short Communication

THIDIAZURON-INDUCED ANATOMICAL CHANGES AND DIRECT SHOOT MORPHOGENESIS IN *DENDROCALAMUS STRICTUS* NEES

*Madhulika Singh[1,3], VS Jaiswal[1] and Uma Jaiswal[2]
[1]Department of Botany, Banaras Hindu University, Varanasi-221 005, UP
[2]Department of Botany, Mahila Maha Vidyalaya, Banaras Hindu University, Varanasi-221 005, UP., India

ABSTRACT

Thidiazuron (TDZ) has potential for *de novo* multiple shoot induction without any callusing at any stage in *Dendrocalamus strictus* Nees. Longitudinal section through basal node region of the explants cultured in half strength Murashige and Skoog (MS) medium with 2.3µM TDZ showed shoot bud initials within a day of culture initiation while those cultured in TDZ free half strength MS medium did not show any evidence for the presence of shoot bud. The organization of shoot bud initial was tunica corpus type and in 3-4 days a short cylinder of provascular tissue is differentiated as the initial stage of vascular differentiation. After about 8 days of culture the newly differentiated bud began to elongate and new shoot bud initials were originated successively from actively dividing cells at the base of elongating shoots. The above process of regeneration continued even after transfer of explants into medium without TDZ.

Keywords: Thidiazuron, shoot bud, peripheral zone, vascular tissue, safranin.

INTRODUCTION

Thidiazuron (TDZ) has been known for stimulating strong shoot proliferating activity in several plant species (Dhavala and Rathore, 2010; Hutteman and Preece, 1993; Singh *et al*., 2001). It is a substituted phenylurea (N-phenyl-N′-1,2,3-thidiazol-5-ylurea) and has been found more active than other phenylurea compounds in tissue culture systems. Although, structurally it is different from both the auxins and the purine-based cytokinins, but exhibits the unique property of mimicking both auxin and cytokinin effects on growth and differentiation of cultured explants (Murthy *et al*., 1986). Responses of TDZ induced *in vitro* shoot multiplication varies from species to species, thus needs a thorough study in case of each and every plant species. It can stimulate shoot multiplication either alone in some plant species (Lata *et al*., 2009; Kumaria *et al*., 2012) or in combination with other growth regulators (Haddadi *et al*., 2013; Thomas and Philip, 2005). Despite the extensive literature on shoot multiplication in dicotyledonous plants (Dhavala and Rathore, 2010; Hussain *et al*., 2007), little attention has been paid on monocotyledonous plants (Singh *et al*., 2001). Further investigations are needed to confirm the initial cell division pattern and shoot bud morphogenesis which is so far has not been demonstrated under the influence of TDZ in any *in vitro* regeneration system. Moreover, the anatomical details could also be evidence for direct shoot regeneration and the shoots regenerated directly from the cultured explants could be exploited as true clone. In a previous study, we demonstrated that TDZ could induce multiple shoots from different seedling explants in a bamboo (*D. strictus*). The *D. strictus* has a long history of widely used resource (Singh *et al*., 2001) and thus, in order to confirm the mode of direct clonal propagation under the influence of TDZ, the present study was under taken to trace the initial anatomical changes of shoot initiation from the basal node explants of seedlings of *D. strictus*.

MATERIALS AND METHODS

The dehusked seeds were surface sterilized by agitating in 1.0% (v/v) sodium hypochlorite solution for 10 min, followed by 10-12 min washing under running tap water. The seeds were sterilized again with 0.05% (w/v) mercuric chloride solution for 4 to 5min and finally washed 3 times with autoclaved double distilled water. The surface sterilized seeds were aseptically germinated on half strength Murashige and Skoog (1962, MS) medium containing 2% (w/v) sucrose and gelled with 0.8% (w/v) agar. The pH of the medium was adjusted 5.8 ± 0.02 before autoclaving at 1.06 kg cm^{-2} for 15 min. After 10 to 15 days of seed inoculation 2 to 4cm long shoots having 2 or 3 nodes were excised from the seedlings and cultured in half-strength MS liquid medium containing 2% (w/v) sucrose, supplemented with 2.3µM TDZ for 21 days and subsequently transferred into half strength MS basal liquid medium devoid of TDZ. The cultures were incubated at 25 ± 2ºC and under 16h photo

* Corresponding author email: msinghup@gmail.com
[3*]Present Address: Department of Biotechnology, Chhatrapati Shahu Ji Maharaj University, Kanpur-208 024, UP., India

period with intensity 20-30 µmoles m^{-2} s^{-1} provided with cool white fluorescent tube-lights.

To prepare permanent histological slides, at different intervals after the explants inoculation, a small portion of the proliferating region (basal node) of explants were excised and fixed in formalin-acetic acid-alcohol (formalin, glacial acetic acid and 50% ethyl alcohol in a ratio of 5:5:90 by volume) for 24h. The fixed materials were dehydrated using different ratios of absolute alcohol and chloroform (Sass, 1958). For cutting the serial sections dehydrated tissues were infiltrated and embedded in paraffin wax (melting point 58-60ºC). Ten to fifteen micron thick serial sections were cut with the help of rotary microtome and the ribbons of the sections were fixed on the surface of the glass slides using haupt's adhesive. The section were deparaffinised in xylol and hydrated following the reverse way of dehydration schedule used before embedding. The dehydrated sections were stained with 1.0% (w/v) alcoholic safranin solution prepared in 70% alcohol for 4-5h. The safranin stained sections were dehydrated and counterstained with fast green for about 30 seconds and then dehydrated through alcohol and xylol series and mounted with DPX mounted. Observations were carried out under light and inverted microscope.

RESULTS AND DISCUSSION

The present histological investigation revealed that TDZ has high potential for inducing *de novo* shoot multiplication without any callusing at any stage from the seedling explants of *D. strictus.* No any histological abnormalities were noticed during shoot bud differentiation. The shoot bud initiation observed from the basal node of the shoot explants on the second day of culture initiation and initiation of new buds was continued even after transfer of regenerating explants from TDZ containing medium to medium free of TDZ. The permanent histological slides prepared in order to trace the early differentiation showed that the anatomical differentiation begins within a day of culture initiation on the medium having TDZ (Fig. 1B) and no such differentiation was noticed in the explants cultured in medium without TDZ (Fig. 1A), thus, confirming that TDZ could induce and enhance shoot bud formation. The shoot bud initial was hemispherical consisted of few layers of small isodiametric cells. The two outermost darkly stained layers were considered to constitute the tunica in which anticlinal divisions predominated. The tunica corpus organization of shoot bud initials in the process of organogenesis has also been demonstrated in Passionfruit (Da gloria *et al*., 1999) and Black pepper (Sujatha *et al*., 2003). The cells of these two layers were more or less similar in size (Fig. 1C) and in a few cases those of the second layer were slightly larger. The outermost layer was continuous with the protoderm basipetally. In the hemisphere, the cells of the central zone were slightly larger than those of the peripheral zone and were less intensely stained with safranin-fast green (Fig. 1C). McArthur and Steeves (1972) showed that the meristematic cylinder or provascular tissue represented the initial stage of vascular differentiation, which developed under the sole influence of the apical meristem. In the present study also the vascular tissues were found initiated in the form of procambium beneath the peripheral zone, the cells of which assume a rather narrow elongated form may be because of the predominance of longitudinal division (Fig. 1C). This agrees with the description provided by a number of previous workers in various angiosperm species (Esau, 1965; Sujatha *et al*., 2003; Xia and Steeves, 1999). In longitudinal view the provascular tissue was continuous with the peripheral zone of the apex above and with the typical procambium below (Fig. 1C). Similar observation that there was no sharp boundary between provascular tissue and peripheral zone of the apex has been reported in carrot, where the histochemical evidence of the presence of carboxylesterases has been used to distinguish it from the peripheral zone of the apical meristem (Xia and Steeves, 1999). In seed plants it has long been noted that there is a recognizable tissue just under the peripheral region of the apical meristem and in the path of differentiation of procambium to the leaf primordial. Some workers reported that this was a pre or pro vascular tissue because the procambial traces arise from it (Esau, 1965; Xia and Steeves, 1999).

Further growth of the shoot apical meristem was similar to that of the normal shoot apex and the median longitudinal section of an 8 days old culture showed completely differentiated shoot bud (Fig. 1D). Similar pattern of shoot bud differentiation was reported in carrot (Xia and Steeves, 1999), and Eucalyptus (Azmi *et al*., 1997). Once the shoot bud differentiation completed, it began to elongate and grow up into small shoot (1cm long) and considerable increase in shoot length was noticed after the transfer of regenerating shoots from TDZ containing medium to medium devoid of TDZ. Similar observation has been shown in *R. tetraphylla* that MS medium supplemented with TDZ was favourable for induction of maximum number of shoots and that transfer to hormone-free medium was essential for shoot elongation (Faisal *et al*., 2005). The new shoot buds were formed successively from actively dividing cells at the leaf axils of elongating shoots or newly emerging shoots buds. The above process of the regeneration of new shoots was observed even after transfer of cultures to medium without TDZ (Fig. 1F) and thus, confirming the *de novo* initiation of shoot buds in medium devoid of TDZ. This is also in confirmation to earlier reports, where a significant increase in shoot multiplication rate has been reported after the transfer of explants from medium supplemented with TDZ to TDZ-free medium (Singh *et*

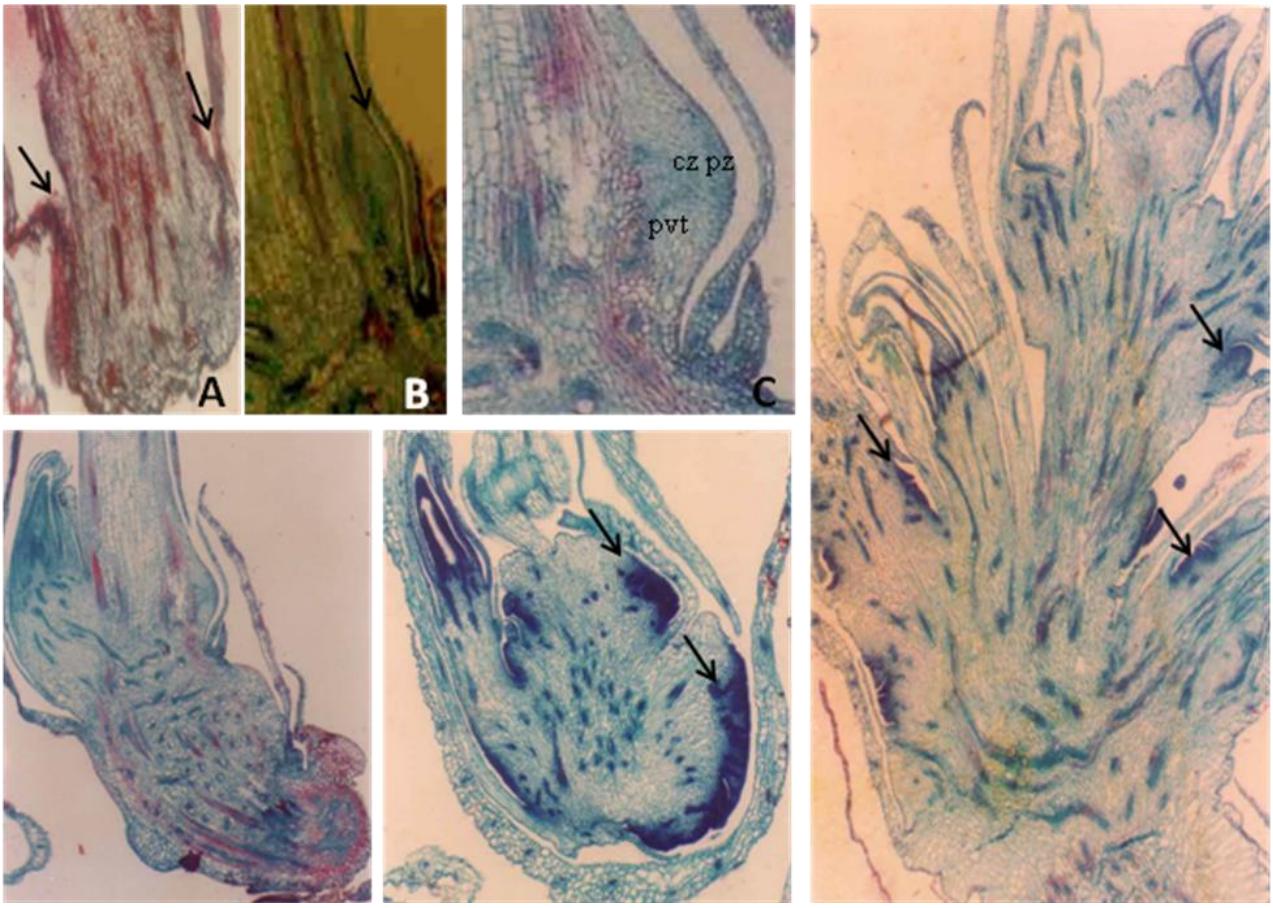

Fig. 1. TDZ induced shoot bud organogenesis from Basal node explants of seedling shoots of *Dendrocalamus strictus*.
A and B: Longitudinal Section of basal node explants after a day of culture initiation. (A) in half-strength MS basal liquid medium (X 87.5). (B) in MS liquid medium with 2.3 µM TDZ (X 87.5).
C: Median Longitudinal Section of shoot bud initials showing distinct zonation pattern. pz-peripheral zone, cz-central zone, pvt-provascular tissue (X 87.5).
D: An 8-day old culture showing completely differentiated shoot bud (X 35).
E: L.S. showing shoot buds differentiation in superficial layer of the cultured explants (X 35).
F: Longitudinal Section a 28-days old culture showing elongation of shoot buds and differentiation of new buds in the leaf axil (X 35).

al., 2001). In the present study, origin of shoot meristem was noticed on superficial layer and in leaf axil only (Fig. 1E). Thus, this histological study is showing that TDZ could be used for clonal multiplication without any callusing at any stage and the development of shoot bud and shoot was similar to that of seed plant. The addition of TDZ into induction medium was necessary for *de novo* shoot bud regeneration.

ACKNOWLEDGEMENT

Madhulika Singh gratefully acknowledges the financial support as JRF/ SRF by University Grants Commission, New Delhi, India.

REFERENCES

Azmi, A., Noin, M., Landre, P., Prouteau, M., Boudet, AM. and Chriqui, D. 1997. High frequency plant regeneration from *Eucalyptus globulus* (Labill.) hypocotyls: Ontogeny and ploidy level of regenerants. Plant Cell Tissue and Organ Culture. 51:9-16.

Da Gloria, B., Vieira, MLC. and Dornelas, MC. 1999. Anatomical studies of *in vitro* organogenesis induced in leaf-derived explants of Passionfruit. Pesq Agropec Bras Brasilia. 34:2007-2013.

Dhavala, A. and Rathore, TS. 2010. Micropropagation of *Embelia ribes* Burm f. through proliferation of adult plant

axillary shoots. In Vitro Cellular and Developmental Biology-Plant. 46:180-191.

Esau, K. 1965. Vascular Differentiation in Plants. Rinehart and Winston, Holt, New York, USA.

Faisal, M., Ahmed. N. and Anis, M. 2005. Shoot multiplication in *Rauvolfia tetraphylla* L. using thidiazuron. Plant Cell Tissue and Organ Culture. 80: 187-190.

Haddadi, F., Aziz, MA., Kamaladini, H. and Ali, S. 2013. Thidiazuron and zeatin-induced high-frequency shoot regeneration from leaf and shoot tip explants of Strawberry. Horticulture Technology. 23:276-281.

Hussain, MK., Anis, M. and Shahzad, A. 2007. In vitro propagation of Indian Kino (*Pterocarpus marsupium* Roxb.) using thidiazuron. In Vitro Cellular and Developmental Biology-Plant. 43:59-64.

Hutteman, CA. and Preece, JE. 1993. Thidiazuron: a potent cytokinin for woody plant tissue culture. Plant Cell Tissue and Organ Culture. 33:105-119.

Kumaria, S., Kehie, M., Das-Bhowmik, SS., Singh, M. and Tandon, P. 2012. *In vitro* regeneration of *Begonia rubrovenia meisneri*, a rare and endemic ornamental plant of Meghalaya, India. Indian Journal of Biotechnology. 11:300-303.

Lata, H., Chandra, S., Khan, I. and Eisohly, MA. 2009. Thidiazuron-induced high-frequency direct shoot organogenesis of *Cannabis sativa* L. In Vitro Cellular and Developmental Biology-Plant. 45:12-19.

McArthur, ICS. and Steeves, TA. 1972. An experimental study of vascular differentiation in *Geum chiloense* Balbs. The Botanical Gazette. 133:276-287.

Murashige, T. and Skoog, F. 1962. A revised medium for rapid growth and bioassays with tobacco tissue cultures. Physiologia Plantarum. 15:473-497.

Murthy, BNS., Murch, SJ. and Praveen, SK. 1986. Review thidiazuron: a potent regulator of *in vitro* plant morphogenesis. Plant Physiology. 82:930-935.

Sass, JE. 1958. Botanical Microtechnique (3rd edi.). The Iowa State University Press, USA.

Singh, M., Jaiswal, U. and Jaiswal, VS. 2001. Thidiazuron-induced shoot multiplication and plant regeneration in bamboo (*Dendrocalamus strictus* Nees.). Journal of Plant Biochemistry and Biotechnology. 10:133-137.

Sujatha, R., Babu, LC. and Nazeem, PA. 2003. Histology of organogenesis from callus cultures of Black pepper (*Piper nigrum* L.). Journal of Tropical Agriculture. 41: 16-19.

Thomas, TD. and Philip, B. 2005. Thidiazuron-induced high frequency shoot organogenesis from leaf derived callus of medicinal climber *Tylophora indica* (Burm. F.) Merrill. In Vitro Cellular and Developmental Biology-Plant. 41:124-128.

Xia, Q. and Steeves, TA. 1999. Initial differentiation of vascular tissue in the shoot apex of carrot (*Daucus carota* L.). Annals of Botany. 83:157-166.

Received: Dec 10, 2013; Accepted: Jan 3, 2014

SENRA Academic Publishers, British Columbia
Vol. 8, No. 2, pp. 2905-2912, June 2014
Online ISSN: 1920-3853; Print ISSN: 1715-9997

Canadian Journal of pure&applied sciences

NEW MEASURES OF INFORMATION AND THEIR APPLICATIONS IN CODING THEORY

*Om Parkash and Priyanka Kakkar
[1]Department of Mathematics, Guru Nanak Dev University, Amritsar- 143005, India

ABSTRACT

New measures of information including entropy, directed divergence and inaccuracy along with their generalizations have been introduced and their essential and desirable properties are studied. The relations between newly developed measures of directed divergence and the well-known standard measure of divergence existing in the literature of distance measures usually known as Kullback-Leibler's measure have been established. Applications of these measures are provided to the field of coding theory for the study of source coding theorems.

Keywords: Entropy, directed divergence, inaccuracy, mean codeword length, uniquely decipherable code.

INTRODUCTION

Shannon (1948) founded the subject of information theory which is closely related to thermodynamics and physics through the similarity of Shannon's uncertainty measure to the entropy function. It was then realized that entropy is a property of any stochastic system and the concept is now used widely in different disciplines. The tendency of the systems to become more disordered over time is described by the second law of thermodynamics, which states that the entropy of the system cannot spontaneously decrease. Today, information theory is still principally concerned with communications systems, but there are widespread applications in statistics, information processing and computing. Shannon (1948) entropy, also known as measure of uncertainty for a probability distribution $P = (p_1, p_2, ..., p_n)$ is given by

$$H(P) = -\sum_{i=1}^{n} p_i \log p_i \qquad (1.1)$$

with the convention that $0 \log 0 := 0$. It is to be noted that the base of logarithm is assumed to be 2, unless until specified.

Besides entropy, another basic and fundamental concept usually applied in information theory is that of divergence. The most important and desirable measure of divergence associated with the probability distributions $P = (p_1, p_2, ..., p_n)$ and $Q = (q_1, q_2, ..., q_n)$ is due to Kullback and Leibler (1951) and is given by

$$K(P:Q) = \sum_{i=1}^{n} p_i \log \frac{p_i}{q_i} \qquad (1.2)$$

Another basic concept in information theory which connects the above two measures mathematically, that is, entropy and divergence, is that of inaccuracy. This concept is basically associated with two probability distributions $P = (p_1, p_2, ..., p_n), Q = (q_1, q_2, ..., q_n)$ where Q is predicted and P is true probability distribution. This fundamental concept was proposed by Kerridge (1961) and is given by

$$H(P:Q) = \sum_{i=1}^{n} p_i \log q_i \qquad (1.3)$$

The above mentioned information measures find their applications in a variety of disciplines such as genetics, finance, economics, political science, biology, analysis of contingency of tables, statistics, signal processing and pattern recognition. It is to emphasis here that the above mentioned non-parametric measures are not sufficient towards their applications in variety of disciplines. For instance, Shannon's measure of entropy always leads to exponential families of distributions but in actual practice, there are many families and distributions which are not exponential in nature. So, restricting to Shannon's entropy means restricting to exponential family only and thus leaving the system to be least flexible. An alternative to this is to use generalized parametric measures of information where the term 'generalized' does not mean superior or more useful but it simply means to be more flexible.

Csiszar (1977) critically investigated Shannon's measure and summarized the significance of this measure and its generalizations along with their scope of applications in the field of coding theory. Some other parametric generalizations of Shannon's entropy have been investigated and studied by Renyi (1961), Havrda and Charvat (1967), Tsallis (1988) etc. Different types of information measures and their mutual relationships have been studied by Garrido (2011). Dahl and Osteras (2010) applied Shannon entropy as a measure of information content in survey data and defined information efficiency as the empirical entropy divided by the maximum attainable entropy. Mathai and Haubold (2007) introduced

*Corresponding author email: omparkash777@yahoo.co.in

generalized entropies, studied some of their properties and examined situations where generalized entropy of order α finds its applications in a variety of mathematical models.

Jain and Mathur (2011) proposed a new symmetric divergence measure and studied its properties and obtained its bounds in terms of some well known divergence measures. Furuichi and Mitroi (2012) introduced some parametric divergence measures combining existing measures of information leading to new inequalities. Taneja (2005) studied some interesting inequalities among symmetric divergence measures whereas some other pioneers who worked towards the deep study of information measures are Csiszar (2008) and Chen *et al*. (2012).

The objective of the present paper is to introduce new measures of information and to extend their applications in the field of coding theory. The organization of this paper is as follows: In section 2 and 3, we have proposed new measures of entropy and studied their essential and desirable properties whereas section 4 and 5 deal with the proposal of new measures of directed divergence and inaccuracy respectively and the study of their properties for validation. In section 6, we have provided the applications of proposed measures to the discipline of coding theory.

2 New non-parametric measure of entropy

In this section, we propose a new measure of entropy to be called M entropy for a probability distribution $P=\left\{(p_1,p_2,...,p_n),\ p_i\geq 0,\sum_{i=1}^{n}p_i=1\right\}$ and study its essential and desirable properties. This new entropy measure is given by the following mathematical expression:

$$M(P)=\prod_{i=1}^{n}\left(\frac{1}{p_i}\right)^{p_i}-1 \qquad (2.1)$$

Here, we take the convention that $0^0:=1$.

To prove that the measure (2.1) is a valid measure of entropy, we study its essential properties as follows:

1. Obviously, $M(P)$ is non-negative.
2. $M(P)$ is permutationally symmetric as it does not change if $p_1,p_2,...,p_n$ are reordered among themselves.
3. $M(P)$ is a continuous function of p_i for all p_i's.
4. **Concavity**: $M(P)$ is a concave function of p_i for all p_i's

To prove concavity property, we proceed as follows:

We have

$$\frac{\partial^2 M(P)}{\partial p_1^{\,2}}=\left((1+\log p_1)^2-\frac{1}{p_1}\right)\prod_{i=1}^{n}\left(\frac{1}{p_i}\right)^{p_i} \qquad (2.2)$$

Now, we know that for all $i=1,2,...,n$, we have $0\leq p_i\leq 1$,

that is, $(1+\log p_i)^2-\frac{1}{p_i}\leq 0$. (2.3)

Thus, using (2.3), we have $\frac{\partial^2 M(P)}{\partial p_1^{\,2}}\leq 0$.

So, $M(P)$ is a concave function of p_1. Similarly, it can be proved that $M(P)$ is a concave function of all p_i's.

Under the above conditions, the function $M(P)$ is a correct measure of entropy. Next, we study most desirable properties of $M(P)$.

1. **Expansibility:** We have $M(p_1,p_2,...,p_n,0)=M(p_1,p_2,...,p_n)$. That is, the entropy does not change by the inclusion of an impossible event.
2. For n degenerate distributions, we have $M(P)=0$. This indicates that for certain outcomes, the uncertainty should be zero.
3. **Maximization of entropy**: We use Lagrange's method to maximize the entropy measure (2.1) subject to the natural constraint $\sum_{i=1}^{n}p_i=1$. In this case, the corresponding Lagrangian is

$$L=\prod_{i=1}^{n}\left(\frac{1}{p_i}\right)^{p_i}-1-\lambda\left(\sum_{i=1}^{n}p_i-1\right) \qquad (2.4)$$

Differentiating equation (2.4) with respect to $p_1,p_2,...,p_n$ and equating the derivatives to zero, we get $p_1=p_2=...=p_n$. This further gives $p_i=\frac{1}{n}\ \forall i$. Thus, we observe that the maximum value of $M(P)$ arises for the uniform distribution and this result is most desirable.
4. **Maximum value:** The maximum value of the entropy is given by $M\left(\frac{1}{n},\frac{1}{n},...,\frac{1}{n}\right)=n-1$.

Again, $M'\left(\frac{1}{n},\frac{1}{n},...,\frac{1}{n}\right)=1>0$. Thus, $M\left(\frac{1}{n},\frac{1}{n},...,\frac{1}{n}\right)$ is an increasing function of n, which is again a desirable result as the maximum value of entropy should always increase.
5. **Non-additivity:** Let $P=(p_1,p_2,...,p_n)$ and $Q=(q_1,q_2,...,q_m)$ be two independent probability distributions of two random variables X and Y, so that

$P(X=x_i)=p_i$, $P(Y=y_j)=q_j$ and

$P(X=x_i, Y=y_j)=P(X=x_i)\,P(Y=y_j)=p_iq_j$.

For the joint distributions of X and Y, there are nm possible outcomes with probabilities p_iq_j; $i=1,2,...,n$ and $j=1,2,...,m$ so that the entropy of the joint probability distribution, denoted by $M(P*Q)$, is given by

$$M(P*Q)=\prod_{i=1}^{n}\prod_{j=1}^{m}\left(p_iq_j\right)^{-p_iq_j}-1$$

$$=\left(\begin{matrix}p_1^{-p_1(q_1+q_2+...+q_m)}p_2^{-p_2(q_1+q_2+...+q_m)}..p_n^{-p_n(q_1+q_2+...+q_m)}\\ q_1^{-q_1(p_1+p_2+...+p_n)}q_2^{-q_2(p_1+p_2+...+p_n)}..q_m^{-q_m(p_1+p_2+...+p_n)}\end{matrix}-1\right)$$

$$=\prod_{i=1}^{n}p_i^{-p_i}\prod_{j=1}^{m}q_j^{-q_j}-1 \qquad (2.5)$$

Also, we have $M(P)+M(Q)+M(P)M(Q)$

$$=\prod_{i=1}^{n}p_i^{-p_i}\prod_{j=1}^{m}q_j^{-q_j}-1 \qquad (2.6)$$

From equation (2.5) and (2.6), we have $M(P*Q)=M(P)+M(Q)+M(P)M(Q)$

Thus, we claim that the new measure of entropy $M(P)$ introduced in (2.1) satisfies all the essential as well as desirable properties of being an entropy measure, it is a valid measure of entropy.

3 Generalized parametric measure of entropy

In this section, we propose a new generalized measure of entropy to be called parametric M-entropy for a probability distribution

$P=\left\{(p_1,p_2,...,p_n),\ p_i\geq 0, \sum_{i=1}^{n}p_i=1\right\}$, given by the following mathematical expression:

$$M_\alpha(P)=\frac{1}{1-\alpha}\left(\prod_{i=1}^{n}\left(\frac{1}{p_i}\right)^{p_i(1-\alpha)}-1\right),\ \alpha>0,\ \alpha\neq 1 \qquad (3.1)$$

with the convention that $0^0:=1$.

We observe that for $\alpha\to 1$, measure (3.1) reduces to Shannon's (1948) entropy as shown below:

$$\lim_{\alpha\to 1}M_\alpha(P)=\lim_{\alpha\to 1}\frac{1}{1-\alpha}\left(\prod_{i=1}^{n}\left(\frac{1}{p_i}\right)^{p_i(1-\alpha)}-1\right)$$

$$=-\sum_{i=1}^{n}p_i\log p_i$$

Hence, this measure is a generalization of Shannon's measure and in particular reduces to measure (2.1) for $\alpha=0$.

Next, we study some essential properties of the generalized measure.

1. $M_\alpha(P)$ is non-negative, that is, $M_\alpha(P)\geq 0$.

Proof: Case-I: When $0<\alpha<1$

$$\frac{1}{1-\alpha}\left(\prod_{i=1}^{n}\left(\frac{1}{p_i}\right)^{p_i(1-\alpha)}-1\right)\geq 0$$

that is, iff $\log\left(\prod_{i=1}^{n}\left(\frac{1}{p_i}\right)^{p_i(1-\alpha)}\right)\geq 0$

that is, iff $-\sum_{i=1}^{n}p_i\log p_i\geq 0$ which is true.

Case-II: When $\alpha>1$, we have

$$\frac{1}{1-\alpha}\left(\prod_{i=1}^{n}\left(\frac{1}{p_i}\right)^{p_i(1-\alpha)}-1\right)\geq 0$$

that is, iff $\log\left(\prod_{i=1}^{n}\left(\frac{1}{p_i}\right)^{p_i(1-\alpha)}\right)\leq 0$

that is, iff $-\sum_{i=1}^{n}p_i\log p_i\geq 0$ which is true.

2. $M_\alpha(P)$ is permutationally symmetric as it does not change if $p_1,p_2,...,p_n$ are re-ordered among themselves.

3. $M_\alpha(P)$ is a continuous function of p_i for all p_i's.

4. **Concavity:** $M_\alpha(P)$ is a concave function of p_i for all p_i's.

To prove concavity property, we proceed as follows: We have

$$\frac{\partial^2 M_\alpha(P)}{\partial p_1^{\,2}}=\left(\left(1+\log p_1\right)^2(1-\alpha)-\frac{1}{p_1}\right)\prod_{i=1}^{n}\left(\frac{1}{p_i}\right)^{p_i(1-\alpha)} \qquad (3.2)$$

Now, using (2.3) and for $\alpha>0$, we have

$$\left(1+\log p_i\right)^2(1-\alpha)-\frac{1}{p_i}\leq 0,\quad i=1,2,....n. \qquad (3.3)$$

that is $\frac{\partial^2 M_\alpha(P)}{\partial p_1^{\,2}}\leq 0$.

So, $M_\alpha(P)$ is a concave function of p_1. Similarly, it can be proved that $M_\alpha(P)$ is a concave function of all p_i's. Hence, under the above conditions, the function $M_\alpha(P)$ is a correct measure of entropy. Next, we study the most desirable properties of $M_\alpha(P)$.

1. **Expansibility**: We have

$M_\alpha(p_1,p_2,...,p_n,0)=M_\alpha(p_1,p_2,...,p_n)$.

2. For n degenerate distributions, we have $M_\alpha(P) = 0$.

3. **Maximization of entropy:** Using Lagrange's method, we observe that the maximum value of $M_\alpha(P)$ arises for the uniform distribution.

4. **Maximum value:** The maximum value of the entropy is given by $M_\alpha\left(\frac{1}{n},\frac{1}{n},...,\frac{1}{n}\right) = \frac{n^{1-\alpha}-1}{1-\alpha}$ which is an increasing function of n, and is again a desirable result as the maximum value of entropy should always increase.

5. **Non-additivity:**

The entropy of the joint probability distribution, denoted by $M_\alpha(P*Q)$, is given by

$$M_\alpha(P*Q) = \frac{1}{1-\alpha}\left(\prod_{i=1}^{n}\prod_{j=1}^{m}\left(p_i q_j\right)^{-p_i q_j(1-\alpha)} - 1\right)$$

$$= \frac{1}{1-\alpha}\left(\begin{array}{l} p_1^{-p_1(1-\alpha)} p_2^{-p_2(1-\alpha)} ... p_n^{-p_n(1-\alpha)} q_1^{-q_1(1-\alpha)} \\ q_2^{-q_2(1-\alpha)} ... q_m^{-q_m(1-\alpha)} - 1 \end{array}\right)$$

$$= \frac{1}{1-\alpha}\left(\prod_{i=1}^{n} p_i^{-p_i(1-\alpha)} \prod_{j=1}^{m} q_j^{-q_j(1-\alpha)} - 1\right) \quad (3.4)$$

Also, we have

$$M_\alpha(P) + M_\alpha(Q) + (1-\alpha) M_\alpha(P) M_\alpha(Q)$$

$$= \frac{1}{1-\alpha}\left(\prod_{i=1}^{n} p_i^{-p_i(1-\alpha)} \prod_{j=1}^{m} q_j^{-q_j(1-\alpha)} - 1\right) \quad (3.5)$$

From equation (3.4) and (3.5), we have

$$M_\alpha(P*Q) = M_\alpha(P) + M_\alpha(Q) + (1-\alpha) M_\alpha(P) M_\alpha(Q)$$

Thus, we claim that the new measure of entropy $M_\alpha(P)$ introduced in (3.1) satisfies all the essential as well as desirable properties of being an entropy measure, it is a valid measure of entropy.

4 Some new measures of directed divergence

First measure of directed divergence

We propose a new non-parametric measure of divergence of probability distribution $P = (p_1, p_2, ..., p_n)$ from another probability distribution $Q = (q_1, q_2, ..., q_n)$ given by

$$D(P:Q) = \prod_{i=1}^{n} q_i^{-p_i} - \prod_{i=1}^{n} p_i^{-p_i} \quad (4.1)$$

Measure (4.1) is a correct measure of directed divergence since it satisfies the following properties

1. $D(P:Q) \geq 0$

Proof: We have

$$\prod_{i=1}^{n} q_i^{-p_i} - \prod_{i=1}^{n} p_i^{-p_i} \geq 0$$

iff $-\sum_{i=1}^{n} p_i \log q_i \geq -\sum_{i=1}^{n} p_i \log p_i$ which is true.

2. $D(P:Q) = 0$ iff $P = Q$.

3. $D(P:Q)$ is a convex function of P and Q.

Proof: We have

$$\frac{\partial^2 D(P:Q)}{\partial p_1^2} =$$

$$(\log q_1)^2 \prod_{i=1}^{n} q_i^{-p_i} + \left(\frac{1}{p_1} - (1+\log p_1)^2\right)\prod_{i=1}^{n} p_i^{-p_i} > 0 \quad (4.2)$$

$$\frac{\partial^2 D(P:Q)}{\partial q_1^2} = \frac{p_1(p_1+1)\prod_{i=1}^{n} q_i^{-p_i}}{q_1^2} > 0 \quad (4.3)$$

From (4.2) and (4.3), it can be seen that $D(P:Q)$ is a convex function of p_1 and q_1. Similarly, it can be proved that $D(P:Q)$ is convex for each p_i and q_i for $i = 1, 2, ..., n$.

Second measure of directed divergence

We propose a new generalized parametric measure of directed divergence of probability distribution $P = (p_1, p_2, ..., p_n)$ from another probability distribution $Q = (q_1, q_2, ..., q_n)$, given by

$$D_\alpha(P:Q) = \frac{1}{\alpha - 1}\left(\prod_{i=1}^{n}\left(\frac{p_i}{q_i}\right)^{-p_i(1-\alpha)} - 1\right),\ \alpha > 1,\ \alpha \neq 1 \quad (4.4)$$

It is observed that for $\alpha \to 1$ in (4.4), we get Kullback-Leibler's (1951) measure of directed divergence.

Thus, we claim that the measure (4.4) is a correct measure of directed divergence as it satisfies all the requisite properties.

Third measure of directed divergence

We introduce another parametric measure of directed divergence corresponding to measure of entropy (3.1), given by

$$D^\alpha(P:Q) = \frac{1}{1-\alpha}\left(\prod_{i=1}^{n} q_i^{-p_i(1-\alpha)} - \prod_{i=1}^{n} p_i^{-p_i(1-\alpha)}\right)$$

for $0 \leq \alpha < 1,\ \alpha \neq 1.$ (4.5)

Measure (4.5) is a correct measure of directed divergence as it also satisfies the requisite properties of a measure of directed divergence and reduces to Kullback -Leibler

(1951) measure as $\alpha \to 1$ and hence is a generalized measure. In particular, for $\alpha = 0$, it becomes measure (4.1).

Relation between Kullback-Leibler measure $K(P:Q)$ and the measure $D(P:Q)$

The following relationship can be established between $K(P:Q)$ and $D(P:Q)$.

Theorem 4.1. The divergence measure $K(P:Q)$ is no greater than divergence measure $D(P:Q)$, that is,

$$K(P:Q) \le D(P:Q) \qquad (4.6)$$

Proof. We know that

$$K(P:Q) = \sum_{i=1}^{n} p_i \log \frac{p_i}{q_i}$$

$$\le \frac{\prod_{i=1}^{n} q_i^{-p_i} - \prod_{i=1}^{n} p_i^{-p_i}}{\prod_{i=1}^{n} p_i^{-p_i}}$$

$$\le \prod_{i=1}^{n} q_i^{-p_i} - \prod_{i=1}^{n} p_i^{-p_i} = D(P:Q)$$

The above relationship can also be shown with the help of figure 1 in which we assume $P = (x, 1-x)$ and $Q = (1-x, x)$, $0 \le x \le 1$. It is to be noted that natural log is taken for calculating the numerical values for the plot of figure 1

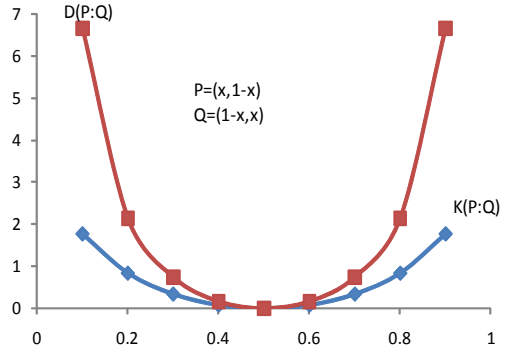

Fig.1. Comparison of the $K(P:Q)$ and $D(P:Q)$ divergence measures for $n = 2$.

Relation between Kullback Leibler measure $K(P:Q)$ and the measure $D_\alpha(P:Q)$:

Theorem 4.2. The divergence measure $K(P:Q)$ is no greater than divergence measure $D_\alpha(P:Q)$, that is,

$$K(P:Q) \le D_\alpha(P:Q), \quad \alpha > 1 \qquad (4.7)$$

Proof. We know that

$$K(P:Q) = \sum_{i=1}^{n} p_i \log \frac{p_i}{q_i}$$

$$= \frac{1}{\alpha - 1} \log \left(\frac{\prod_{i=1}^{n} q_i^{-p_i(1-\alpha)}}{\prod_{i=1}^{n} p_i^{-p_i(1-\alpha)}} \right)$$

$$\le \frac{1}{\alpha - 1} \left(\prod_{i=1}^{n} \left(\frac{p_i}{q_i} \right)^{-p_i(1-\alpha)} - 1 \right) = D_\alpha(P:Q) \qquad (4.8)$$

Relation between Kullback Leibler measure $K(P:Q)$ and the measure $D^\alpha(P:Q)$

Theorem 4.3. The divergence measure $K(P:Q)$ is no greater than divergence measure $D^\alpha(P:Q)$, that is,

$$K(P:Q) \le D^\alpha(P:Q), \quad 0 \le \alpha < 1 \qquad (4.8)$$

Proof. We know that

$$K(P:Q) = \sum_{i=1}^{n} p_i \log \frac{p_i}{q_i}$$

$$\le \frac{1}{1-\alpha} \left(\frac{\prod_{i=1}^{n} q_i^{-p_i(1-\alpha)} - \prod_{i=1}^{n} p_i^{-p_i(1-\alpha)}}{\prod_{i=1}^{n} p_i^{-p_i(1-\alpha)}} \right)$$

$$\le \frac{1}{1-\alpha} \left(\prod_{i=1}^{n} q_i^{-p_i(1-\alpha)} - \prod_{i=1}^{n} p_i^{-p_i(1-\alpha)} \right) = D^\alpha(P:Q)$$

5 New measures of Inaccuracy

First Measure of Inaccuracy

I. We first propose the new non-parametric measure of inaccuracy given by the following mathematical expression:

$$I(P:Q) = \prod_{i=1}^{n} \left(\frac{1}{q_i} \right)^{p_i} - 1 \qquad (5.1)$$

The measure (5.1) represents sum of two uncertainties: (i) Uncertainty due to our not knowing $P = (p_1, p_2, ..., p_n)$, but knowing only $Q = (q_1, q_2, ..., q_n)$.

(ii) Uncertainty of P even when P is known.

The result (i) can be measured by measure of directed divergence, given by $D(P:Q) = \prod_{i=1}^{n} q_i^{-p_i} - \prod_{i=1}^{n} p_i^{-p_i}$ as defined in (4.1).

The result (ii) is measured by measure of entropy, given by $M(P) = \prod_{i=1}^{n} \left(\frac{1}{p_i} \right)^{p_i} - 1$ as defined in (2.1).

Thus, we have

$$I(P:Q) = D(P:Q) + M(P) \qquad (5.2)$$

Also,

$$I(P:P) = D(P:P) + M(P) = M(P) \quad (5.3)$$

and

$$I(P:Q) \geq M(P)$$

and equality sign holds if and only if $Q = P$.

So, measure (5.1) is an appropriate measure of inaccuracy as it satisfies the following properties:

(i) $I(P:Q) \geq 0$

(ii) $I(P:P)$ is an appropriate measure of entropy.

(iii) $I(P:Q) \geq I(P:P)$ and $I(P:Q)$ reduces to $I(P:P)$ only when $Q = P$.

Second Measure of Inaccuracy

II. We now propose another new parametric measure of inaccuracy given by

$$I_\alpha(P:Q) = \frac{1}{1-\alpha} \frac{\left(\prod_{i=1}^{n} p_i^{-p_i(1-\alpha)} \left(\prod_{i=1}^{n} q_i^{-p_i(1-\alpha)} - 1 \right) \right)}{\prod_{i=1}^{n} q_i^{-p_i(1-\alpha)}}, \ \alpha > 1 \quad (5.4)$$

For $\alpha \to 1$, $I_\alpha(P:Q)$ reduces to Kerridge's (1961) measure of inaccuracy and satisfies all the requisite properties of inaccuracy measure.

Third Measure of Inaccuracy

III. Next, we investigate and propose another parametric measure of inaccuracy, given by the following mathematical expression:

$$I^\alpha(P:Q) = \frac{1}{1-\alpha} \left(\prod_{i=1}^{n} \left(\frac{1}{q_i} \right)^{p_i(1-\alpha)} - 1 \right), \ 0 \leq \alpha < 1, \ \alpha \neq 1 \quad (5.5)$$

Again, for $\alpha \to 1$, we have

$$\lim_{\alpha \to 1} I^\alpha(P:Q) = -\sum_{i=1}^{n} p_i \log q_i$$

which is Kerridge's measure of inaccuracy and we claim that measure (5.5) is an appropriate as it satisfies the requisite properties of inaccuracy measure.

In the next section, we provide the applications of the measures of information developed in the above sections.

6 Some new source coding theorems

6.1 Source coding with generalized measure of entropy

Source coding aims to encode the source that produces symbols x_i from X with probabilities p_i where $\sum_{i=1}^{n} p_i = 1$ using an alphabet of size D , that is, to map each symbol x_i to a codeword c_i of length l_i expressed using the D letters of the alphabet. If the set of lengths l_i satisfies the *Kraft's (1949) inequality

$$\sum_{i=1}^{n} D^{-l_i} \leq 1 \quad (6.1)$$

then there exists a uniquely decodable code with these lengths, which means that any sequence $c_{i1}c_{i2}...c_{in}$ can be decoded unambiguously into a sequence of symbols $x_{i1}x_{i2}...x_{in}$ Furthermore, any uniquely decodable code satisfies the Kraft's inequality (6.1). The Kraft's inequality is a basic result in information theory which gives a necessary condition for a code to be uniquely decipherable. Nagaraj (2009) provided a new proof of this inequality and its converse for prefix-free codes by a dynamical systems approach. Parkash and Priyanka (2011) developed some new results which are closely related with the Kraft's inequality.

The Shannon's (1948) source coding theorem indicates that the mean codeword length

$$L = \sum_{i=1}^{n} p_i l_i \quad (6.2)$$

is bounded below by the entropy of the source, that is, Shannon's entropy $H(P)$ and that the best uniquely decodable code satisfies

$$H(P) \leq L < H(P) + 1 \quad (6.3)$$

where the logarithm in the definition of the Shannon entropy is taken in base D . This result indicates that the Shannon entropy $H(P)$ is the fundamental limit on the minimum average length for any code constructed for the source. The lengths of the individual codewords, are given by

$$l_i = -\log_D p_i \quad (6.4)$$

Later, Campbell (1965) introduced the generalized mean codeword length, defined as

$$L_\alpha = \frac{\alpha}{1-\alpha} \log_D \left(\sum_{i=1}^{n} p_i D^{\frac{l_i(1-\alpha)}{\alpha}} \right) \quad (6.5)$$

and proved that Renyi's entropy $H_\alpha(P)$ forms a lower bound to it subject to Kraft's inequality. Sharma and Raina (1980) proved coding theorems for partially received information. Parkash and Kakkar (2012) proposed two new mean codeword lengths, investigated that these lengths satisfy desirable properties as a measure of typical codeword lengths and proved new noiseless coding theorems subject to Kraft's inequality.

Also, we have the following relation between the Shannon's entropy and the generalized entropy (3.1)

$$M_\alpha(P) = \log_\alpha \left(D^{H(P)} \right) \quad (6.6)$$

where $\log_\alpha(.)$ is the $\alpha-$ deformed logarithm defined as $\log_\alpha x = \frac{x^{1-\alpha} - 1}{1-\alpha}$.

Now, we consider the following two cases:

Case-I When $0 < \alpha < 1$, we have

$$L \geq H(P)$$

$$\Rightarrow \frac{D^{L(1-\alpha)}-1}{1-\alpha} \geq \frac{D^{H(P)(1-\alpha)}-1}{1-\alpha}$$

$$\Rightarrow K_\alpha = \log_\alpha \left(D^L\right) \geq \log_\alpha \left(D^{H(P)}\right) = M_\alpha(P) \tag{6.7}$$

Case-II When $\alpha > 1$, we have

$L \geq H(P)$

$$\Rightarrow K_\alpha = \log_\alpha \left(D^L\right) \geq \log_\alpha \left(D^{H(P)}\right) = M_\alpha(P) \tag{6.8}$$

Here comes out the new generalized length K_α from (6.7) and (6.8) to which the generalized entropy $M_\alpha(P)$ forms a lower bound. It is a monotonic increasing function of mean codeword length L and it reduces to L when $\alpha \to 1$. The optimal codeword lengths are given by $l_i = -\log_D p_i$ which is similar to equation (6.4) as in case of Shannon's source coding theorem. K_α is not an average of the type $\phi^{-1}\left(\sum_{i=1}^{n} p_i \phi(l_i)\right)$ as introduced by Kolmogorov (1930) and Nagumo (1930) but is a simple expression of the $\alpha-$ deformed logarithm.

Note: When $l_1 = l_2 = ... = l_n = l$, then $K_\alpha \neq l$. Instead, it reduces to $\frac{D^{l(1-\alpha)}-1}{1-\alpha}$ which further reduces to l when $\alpha \to 1$.The above results (6.7) and (6.8) can also be stated in the form of following theorem:

Theorem 6.1. If $l_1, l_2, ..., l_n$ denote the lengths of the uniquely decipherable code for the random variable X, then $K_\alpha \geq M_\alpha(P)$ with equality if and only if $l_i = -\log_D p_i$.

Proof. We have to minimize the following codeword length:

$$K_\alpha = \frac{D^{(1-\alpha)\sum_{i=1}^{n} p_i l_i}-1}{1-\alpha} \tag{6.9}$$

subject to the Kraft's (1949) inequality

$$\sum_{i=1}^{n} D^{-l_i} \leq 1$$

The corresponding Lagrangian is given by

$$J = \frac{D^{(1-\alpha)\sum_{i=1}^{n} p_i l_i}-1}{1-\alpha} + \lambda\left(\sum_{i=1}^{n} D^{-l_i} - 1\right) \tag{6.10}$$

Differentiating (6.10) with respect to $l_i; i = 1,2,...,n$ and equating to zero, we get

$$p_i = \lambda D^{-l_i} \tag{6.11}$$

Using $\sum_{i=1}^{n} D^{-l_i} = 1$ and $\sum_{i=1}^{n} p_i = 1$, equation (6.11) gives $\lambda = 1$ and hence $p_i = D^{-l_i}$, that is, $l_i = -\log_D p_i$

Substituting l_i in (6.9), we get the minimum value of K_α as

$$[K_\alpha]_{\min} = \frac{1}{1-\alpha}\left(\prod_{i=1}^{n}\left(\frac{1}{p_i}\right)^{p_i(1-\alpha)} - 1\right) = M_\alpha(P)$$

6.2 Shannon's source coding via new measures of directed divergence

We know that the measure of directed divergence $D_\alpha(P:Q)$ as given by (4.4) is non-negative, that is,

$$D_\alpha(P:Q) = \frac{1}{\alpha-1}\left(\prod_{i=1}^{n}\left(\frac{p_i}{q_i}\right)^{-p_i(1-\alpha)} - 1\right) \geq 0,\ \alpha > 1 \tag{6.12}$$

Substituting $q_i = \frac{D^{-l_i}}{\sum_{i=1}^{n} D^{-l_i}}$, $i = 1,2,...,n$ in (6.12), we get

$$\Rightarrow \prod_{i=1}^{n}\left(\frac{p_i}{D^{-l_i}}\sum_{i=1}^{n} D^{-l_i}\right)^{-p_i(1-\alpha)} \geq 1 \tag{6.13}$$

$$\Rightarrow -\sum_{i=1}^{n} p_i \log_D p_i - \log_D \sum_{i=1}^{n} D^{-l_i} \leq \sum_{i=1}^{n} p_i l_i = L$$

Now, since $\sum_{i=1}^{n} D^{-l_i}$ lies between D^{-1} and 1, therefore the lower bound for L lies between $H(P)$ and $H(P)+1$. Hence, we obtain the following result

$H(P) \leq L < H(P)+1$

which is the Shannon's source coding theorem for uniquely decipherable codes.

Note: On substituting $q_i = \frac{1}{n}$, $i = 1,2,...,n$ in (6.12) and then taking logarithms both sides, we get

$$H(P) \leq \log_D n \tag{6.14}$$

which is a known result in information theory that shows that maximum value of Shannon's entropy can never be greater than $\log_D n$.

Similarly, if we take the non-negativity of the measure of directed divergence given in equation (4.1) and substitute $q_i = \frac{D^{-l_i}}{\sum_{i=1}^{n} D^{-l_i}}$, $i = 1,2,...,n$ in it, we get

$$\prod_{i=1}^{n}\left(\frac{D^{-l_i}}{\sum_{i=1}^{n} D^{-l_i}}\right)^{-p_i} \geq \prod_{i=1}^{n} p_l^{-p_i} \tag{6.15}$$

Taking logarithms on both sides of (6.14) and simplifying, we again arrive at inequality (6.3).

Proceeding on similar lines and using the non-negativity of the measure of directed divergence given by (4.5), we again get the Shannon's source coding theorem.

Concluding Remarks: The measures of entropy find tremendous applications in a variety of disciplines viz, biological, economical, physical sciences. Similarly, the measures of divergence have proved to be very useful in a various disciplines of engineering sciences. Since a single measure of information cannot be adequate for each discipline, we need a variety of generalized information measure to extend the scope of their applications. Further, these generalized measures induce flexibility into the system and hence preferred towards optimization problems. Keeping this idea in mind, we have generated various information measures for the discrete probability distribution and provided their applications in field of coding theory. With similar arguments, a variety of information theoretic measures can be developed for continuous probability distributions.

ACKNOWLEDGEMENT

The authors are thankful to Council of Scientific and Industrial Research, New Delhi for providing the financial assistance for the preparation of the manuscript.

REFERENCES

Campbell, LL. 1965. A Coding theorem and Renyi's entropy. Information and control. 8:423-429.

Chen, X., Kar, S. and Ralescu, DA. 2012. Cross-entropy measure of uncertain variables. Information Sciences. 201:53-60.

Csiszar. I. 1977. Information measures: a critical survey. In: Transactions of the 7th Conference on Information Theory, Statistical Decision Functions, Random Processes. Eds. Kozesnik, J. Academia, Prague. B:73-86.

Csiszar, I. 2008. Axiomatic characterizations of information measures. Entropy. 10: 261-273.

Dahl, FA. and Osteras, N. 2010. Quantifying information content in survey data by entropy. Entropy. 12:161-163.

Furuichi, S. and Mitroi, FC. 2012. Mathematical inequalities for some divergences. Physica A. 391:388-400.

Garrido, A. 2011. Classifying entropy measures. Symmetry. 3: 487-502.

Havrda, J. and Charvat, F. 1967. Quantification method of classification processes: concept of structural α – entropy. Kybernetika. 3:30-35.

Jain, KC. and Mathur, R. 2011. A symmetric divergence measure and its bounds. Tamkang Journal of Mathematics .42(4):493-503.

Kerridge, DF. 1961. Inaccuracy and inference. J. R. Statist. Soc. B 23:184-194.

Kolmogorov, A. 1930. Sur la notion de la moyenne. Atti Accad. Naz. Lincei. 12:388-391.

Kullback, S. and Leibler, RA. 1951. On information and sufficiency. Ann. Math. Statistics. 22:79-86.

Mathai, AM. and Haubold, HJ. 2007. On generalized entropy measures and pathways. Physica A. 385:493-500.

Nagaraj, N. 2009. A dynamical systems proof of Kraft–McMillan inequality and its converse for prefix-free codes. Chaos .19(1): 013136 -013140.

Nagumo, M. 1930. Uber eine Klasse der Mittelwerte. Japan. J. Math. 7:71-79.

Parkash, O. and Kakkar, P. 2012. Development of two new mean codeword lengths. Information Sciences. 207:90-97.

Parkash, O. and Priyanka. 2011. Contribution of Kraft's inequality to coding theory. Pacific-Asian Journal of Mathematics. 5(1):45-53.

Renyi, A. 1961. On measures of entropy and information. In: Proc. Fourth Berkeley Symp. Math. Statist. Prob. 1:547-561.

Shannon, CE. 1948. A mathematical theory of communication. Bell System Tech. J. 27:379-423.

Sharma, BD. and Raina, N. 1980. Coding theorem for partial received information. Information Sciences. 20: 181-189.

Taneja, IJ. 2005. Refinement inequalities among symmetric divergence measures. The Australian Journal of Mathematical Analysis and Applications. 2(1):1-23.

Tsallis, C. 1988. Possible generalization of Boltzmann Gibbs statistics. J. Stat. Phys. 52:479-487.

Received: Aug 17, 2013; Revised: Nov 22, 2013; Accepted: Jan 2, 2014

SENRA Academic Publishers, British Columbia
Vol. 8, No. 2, pp. 2913-2923, June 2014
Online ISSN: 1920-3853; Print ISSN: 1715-9997

Canadian Journal of pure & applied sciences

SIMULATION OF AN AMMONIA SYNTHESIS CONVERTER

*Akpa Jackson Gunorubon[1] and Raphael Nwokoma Raphael[2]
Department of Chemical/Petrochemical Engineering
Rivers State University of Science and Technology, Port-Harcourt, Rivers State, Nigeria

ABSTRACT

Steady state one dimensional pseudo-homogeneous models of an axial flow industrial catalytic packed bed ammonia converter have been developed. The converter is a vertical four catalytic bed reactor with varying volumes of catalysts. Effects of temperature changes on the catalyst surface and in its interior were incorporated in the model by an effectiveness factor. The models were used to predict conversions, concentrations of reactant/product mixtures and temperature profiles along the catalyst beds. The developed models consisted of ordinary differential equations which were solved numerically using the 4th order Runge-Kutta algorithm implemented with MatLab ode45 solver. The accuracy of the models was ascertained with industrial plant data from Notore Chemical Industry, Onne, Rivers State. The results obtained from solutions to the models compared favorably with output plant data of the ammonia converter with a maximum deviation between models predictions and actual plant data of 6.7%. Consequently, simulation studies of the converter was performed varying operating parameters such as feed flow rates, inlet temperatures and pressures to determine their effects on the performance of the converter.

Keywords: Modeling, ammonia converter, effect of feed flow rate and inlet temperature.

INTRODUCTION

Ammonia is a widely used raw material for the production of nitrogen compounds of vital importance, such as urea, nitric acid, fertilizer, explosive materials, pharmaceuticals, polymers and coolants; thus its synthesis is an important industrial process. It is produced following the Haber-Bosch process by the reaction between gaseous nitrogen (from air) and hydrogen (from natural gas). The diversification policy of the Nigerian Government aimed at increasing awareness and improvement in mechanized agriculture has resulted in increased agricultural activities across the country and increasing the demand for fertilizers a key requirement/ingredient for agricultural productivity. A sustained availability of fertilizer will be achieved through the efficient operation of exiting fertilizer plants and the construction of new plants of which the converter used for ammonia synthesis a precursor for the manufacture of nitrogenous fertilizers is very vital. The development of suitable models that can be used for simulation studies of the converter is vital in achieving this policy as the simulation would provide a wide range of operating conditions and design possibilities of the converter for prospective investors.

A typical ammonia production process consists of (a) production of the synthesis gas, (b) compression of the gas to the required pressure and (c) synthesis loop in which its conversion to ammonia takes place. This work is focused on the converter of the synthesis loop.

*Corresponding author email: jacksonakpa@yahoo.com

MODEL DEVELOPMENT

Process description

The hydrogen for the synthesis process is obtained from steam reforming of natural gas (chiefly methane) thereafter a shift conversion takes place to produce more hydrogen from reaction of carbon monoxide with water. Carbon dioxide is removed by absorbing in a potassium carbonate solution before passing the process gas to a methanation section where carbon monoxide and carbon dioxide are converted back to methane. The nitrogen input is obtained from the atmosphere through air liquefaction. After passing these stages the process gas is compressed (make-up gas) and sent to the ammonia converter where a portion of the synthesis gas is converted to ammonia in a catalytic reaction. Iron catalyst is used promoted with potassium oxides. The single-pass conversion is not more than 25%. A portion of the effluent emerging from the reactor exit is purged to remove inert contents while the other portion is sent to ammonia separation section where ammonia is condensed out at about -23^{o}C. After separation, the gas is recycled and mixed with fresh makeup gas. A typical four bed ammonia converter in Notore Chemical Industry Limited operating at Onne in Rivers State is depicted in figure 1.

Kinetic Model

Various kinetic models for ammonia synthesis have been proposed over the years. These models were based either on mechanistic considerations or on empirical evaluations and include the works of ICI, 1970; Temkin, 1979; Nielsen, 1981; Boudart, 1981; Ull-mann's, 1985; Appl,

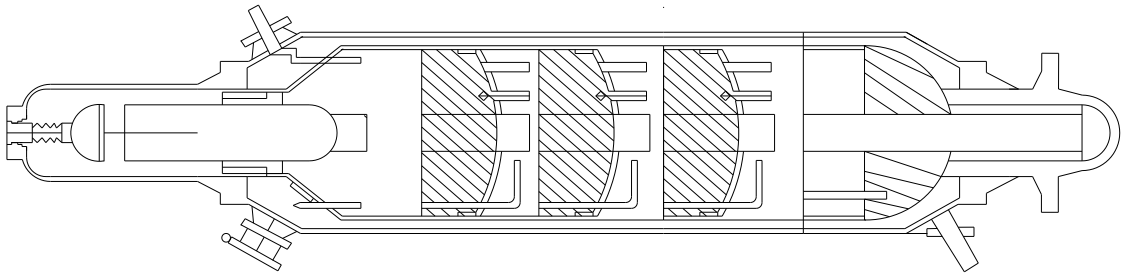

Fig. 1. Typical four Bed Ammonia Converter.

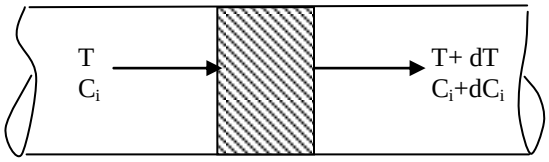

Fig. 2. Elemental portion of the packed bed reactor.

1992, 1997; Aparicho and Dumesic, 1994. The kinetics of ammonia synthesis over various catalyst has also been reported; over Ni-doped CeO2 and Ru/CeO2 catalyst respectively (Izumi*et al*., 1996); over a ruthenium catalyst supported on active carbon (Zbigniew *et al*., 1996) with barium-promoted iron-cobalt alloys (Hagen *et al*., 2003) and over a bimetallic catalyst Fe and Mo supported HZSM-5 catalyst at atmospheric pressure and high temperature (Unde and Gaikwad, 2007). These studies produced reaction rates expressions for the synthesis reaction with varying complexities and operating conditions. However, the rate expression of Temkin – Pyzhez (1940), (Temkin, 1990) is believed and widely accepted to accurately represent the ammonia synthesis reaction over wide and varying conditions; the modified form of the Temkin- Pyzhez equation expressed in activities as developed by Dyson and Simon (1986) will therefore be used in this work. The reaction rate expression is represented as:

$$R_{NH_3} = 2k\left(K_a^2 a_{N_2}\left[\frac{a_{H_2}^3}{a_{NH_3}^2}\right]^{\alpha} - \left[\frac{a_{NH_3}^2}{a_{H_2}^3}\right]^{1-\alpha}\right) \quad (1)$$

Where k is the rate constant for the reverse reaction, K_a is the equilibrium constant, a_i is the activity of component i and α is a constant which takes a value from 0.5 to 0.75 (Dashti*et al*., 2006).

The reaction rate equations for the reactants were determined using the stoichiometry of the reaction: $N_2 + 3H_2 \leftrightarrow 2NH_3$ to relate the individual rates of reactions as follows:

$$-R_{N_2} = -\frac{1}{3}R_{H_2} = \frac{1}{2}R_{NH_3} \quad (2)$$

Reactor Model

To predict the performance of the converter, a mathematical model was developed. The conventional classification of reactor models contains two main categories (Reddy and Husairi, 1982): the pseudo-homogeneous and heterogeneous models. Pseudo-homogeneous models that do not account explicitly for the presence of catalyst can be used by modifying the intrinsic rate of reaction by multiplying it by an effectiveness factor. The empirical relation (Dyson and Simon, 1986) which relates the effectiveness factor at any point along the length of the catalyst bed to the temperature and conversion at that specific point is therefore incorporated in the model to be developed.

Model Assumptions

The following conditions are imposed on the synthesis converter in the development of its mathematical model:
The converter operates at steady state, the flow through it is assumed to be plug flow which means concentration varies along the length (bed) of the reactor. One-dimensional Cartesian coordinate was considered along the bulk flow. (Radial effects were not considered), density of the gas is constant and the effects of

penetration resistance in catalyst, temperature gradient and catalyst inside concentration have been incorporated in the rate equation by a coefficient. Based on these assumptions a pseudo-homogeneous one-dimensional model was developed for the reacting species by applying the principle of conservation of mass and energy on an elemental section (differential section) of the converter as shown in figure 2.

Mass Balance (Molar)

$$u\frac{dC_i}{dL} = \eta R_i \quad (3)$$

This equation can be written for the limiting reactant (nitrogen) as:

$$u\frac{dC_{N_2}}{dL} = \eta R_{N_2} \quad (4)$$

Where u = velocity of gas (m/s)
A = cross-sectional area of the bed (m^2)
C_{NH3} = Exit concentration of ammonia (NH_3) (moles/m^3)
L = Length of bed (reactor) (m)
R_{NH_3} = Rate of depletion of nitrogen (N_2)
η = Effectiveness factor

Expressing equation (4) in terms of nitrogen conversion (X) and initial flow rate $F_{N2,0}$ (mole/hr) as follows:

$$\frac{dX}{dL} = -\eta\frac{(R_{N_2})A}{F_{N_{20}}} \quad (5)$$

Equation (5) can be expressed in terms of rate for ammonia production using the relationship in equation (2) to give:

$$\frac{dX}{dL} = \eta\frac{(R_{NH_3})A}{2F_{N_{20}}} \quad (6)$$

Energy Balance

$$\frac{dT}{dL} = \eta\frac{(-\Delta H_R)R_{NH_3}A}{mCp_{mix}} \quad (7)$$

Where:
m = total mass flow rate of (kg/hour)
$(-\Delta H_R)$ = Heat of reaction (KJ/kmol)
T = Temperature variable in the reactor (K)
Cp_{mix}= Specific heat capacity of the gas mixture (kJ/kmol)

MATERIALS AND METHODS

The component activities in the reaction rate equation were expressed in terms fugacity as:

$$a_i = \frac{f_i}{f_i^0} \quad (8)$$

Where:
f_i^0 = reference fugacity. Taken to be 1 atm
The fugacity of component i (fi) can be determined from the expression of the dimensionless fugacity coefficient: $\emptyset_i = \frac{f_i}{P_i}$ as:

$$f_i = \emptyset_i P_i \quad (9)$$

The component partial pressures were converted to molar concentrations using the expression:

$$P_i = Y_i P_T = \left(\frac{N_i}{\sum N_i}\right)P_T \quad (10)$$

Substituting these, the component activities can be expressed as:

$$a_i = \emptyset_i Y_i P_T \quad (11)$$

The molar concentrations of each component (Y_i) were expressed in terms of fractional conversion of the limiting reactant nitrogen (X) using the expressions in Appendix 1 developed by performing a mole balance on the converter; thus expressing the component activities in terms of fraction conversion of the limiting reactant nitrogen. The respective component activities were substituted into the rate expression to yield the reaction rate expression in terms of fractional conversion of the limiting reagent (nitrogen).

$$R_{NH_3} = 2k\left(K_a^2\emptyset_{N_2}\frac{Y_{N_{2,o}}(1-X)}{1-2XY_{2o}}P\left[\frac{\left(\emptyset_{H_2}\frac{(Y_{H_{2,o}}-3XY_{N2o})}{1-2XY_{2o}}P\right)^3}{\left(\emptyset_{NH_3}\frac{(Y_{NH_{3,o}}+2XY_{N2o})}{1-2XY_{2o}}P\right)^2}\right]^{\infty} - \left[\frac{\left(\emptyset_{NH_3}\frac{(Y_{NH_{3,o}}+2XY_{N2o})}{1-2XY_{2o}}P\right)^2}{\left(\emptyset_{H_2}\frac{(Y_{H_{2,o}}-3XY_{N2o})}{1-2XY_{2o}}P\right)^3}\right]^{1-\infty}\right) \quad (12)$$

Further simplification yields:

$$R_{NH_3} = 2k\left(K_a^2\emptyset_{N_2}\frac{Y_{N_{2,o}}(1-X)}{1-2XY_{2o}}P\left[\frac{P(\emptyset_{H_2}(Y_{H_{2,o}}-3XY_{N2o}))^3}{(1-2XY_{2o})(\emptyset_{NH_3}(Y_{NH_{3,o}}+2XY_{N2o}))^2}\right]^{\infty} - \left[\frac{(1-2XY_{2o})(\emptyset_{NH_3}(Y_{NH_{3,o}}+2XY_{N2o}))^2}{P(\emptyset_{H_2}(Y_{H_{2,o}}-3XY_{N2o}))^3}\right]^{1-\infty}\right) \quad (13)$$

Substituting the reaction rate expression (eqn. 13) into the model equations (eqn. 6 and 7) gives the model equations in terms of fractional conversion of the limiting reactant nitrogen.

The MatLab 7.5 ODE45 solver from Mathworks for non stiff ordinary differential equations which uses the 4th order Runge Kutta algorithm was employed in solving the resulting ordinary differential equations of the model equations using data given in Table 1from the industrial ammonia converter of Notore Chemical Industry Limited operating at Onne in Rivers State, Nigeria. The industrial ammonia converter operates on a 4 catalyst beds system.

The outputs (results) from each catalyst bed were used as inputs into the successive bed and the process re-initiated. This was done for all four (4) catalyst beds until the final fractional conversion, concentrations (of reactants and product) and outlet bed temperature were determined at the end of the last bed (catalyst bed #4). To replicate the industrial converter accurately where the products from catalyst beds 1 and 2 were quenched (cooled) while the products from bed 3 were heated before entering the successive beds respectively, the industrial bed entry temperatures were used for beds 2, 3 and 4.

The results of the model equations gave the fractional conversions of the limiting reactant and temperature progression along each catalyst bed. The exit concentrations (mole %) of the reactants and product at each catalyst bed were obtained using the expressions in Appendix 1.

DETERMINATION OF PARAMETERS

To solve the model equations developed requires the determination of certain constants and parameters. These were determined as follows:

Component Fugacity Coefficient

The fugacity coefficients for Hydrogen (H_2), Nitrogen (N_2) and Ammonia (NH_3) were determined using the expressions given by Dyson and Simon (1986) as:

$$\emptyset_{H_2} = \left(exp\left(\begin{matrix} \exp(-3.802T^{0.125} + 0.541)\,P - exp(-0.1263T^{0.5} - 15.98)P^2 \\ + \left(300\left(\exp(-0.011901T - 5.941)\left(\exp\frac{P}{300}\right)\right)\right) \end{matrix} \right) \right) \quad (14)$$

$$\emptyset_{N_2} = \begin{pmatrix} 0.93431737 + 0.2028538x10^{-3}T + 0.295896x10^{-3}P \\ -0.270727x10^{-6}T^2 + 0.4775207x10^{-6}P^2 \end{pmatrix} \quad (15)$$

$$\emptyset_{NH_3} = \begin{pmatrix} 0.1438996 + 0.2028538x10^{-2}T - 0.4487672x10^{-3}P \\ -0.1142945x10^{-5}T^2 + 0.2761216x10^{-6}P^2 \end{pmatrix} \quad (16)$$

Reaction Rate Constant

The rate constant for the reverse reaction was obtained using the Arrhenius relation with values for the synthesis reaction given by (Dashti*et al*., 2006):

$$K = k_0 \exp\left(-\frac{E}{RT}\right) \quad (17)$$

Where:
K_0 = Arrhenius coefficient; (8.849 x1014)
E= Activation energy with temperature its mean value is 40765 Kcal/kmol
R=Universal Gas constant R (8.314 kJ/kmol.K)

Equilibrium Constant K_a

The equilibrium constant was obtained using the expression in Dashti *et al*. (2006):

$$log K_a = \begin{pmatrix} -2.691122logT - 5051925x10^{-5}T + \\ 1.848863x10^{-7}T^2 + \frac{2001.6}{T} + 2.689 \end{pmatrix} \quad (18)$$

Effectiveness Factor (η)

The effect of temperature, conversion on the length of catalyst bed was accounted for by the expression given by (Babu and Reddy, 2012):

$$\eta = b_0 + b_1T + b_2X + b_3T^2 + b_4X^2 + b_5T^3 + b_6X^3 \quad (19)$$

The coefficients for this equation are given by Babu and Reddy (2012).

Specific Heat Capacity

The specific heat capacity of the reactant gas mixture was obtained using the equation:

$$C_{P_{mix}} = \sum_{i=1}^{n} Y_i C_{P_i} \quad (20)$$

Where: yi = mole fraction of component i,
Cp_i = specific heat capacity of component i

The heat capacities of the components of the reactant gases were obtained with the expression by Elverse *et al.* (1993):

$$C_{p_i} = 4.1884(a_i + b_iT + c_iT^2 + d_iT^3) \quad (21)$$

Where a_i b_i c_i and d_i are constants with values given in table 1.
The heat capacity of the product (ammonia) was obtained with the equation in Elverse *et al.* (1993)

$$C_{P_{NH_3}} = \begin{pmatrix} 6.5846 - 0.61251x10^{-2}T + 0.23663x10^{-5}T^2 - 1.5981x10^{-9}T^3 + 96.1678 \\ -0.067571P + (0.2225 + 1.6847x10^{-4}P)T + (1.289x10^{-4} - 1.0095x10^{-7}P)T^2 \end{pmatrix} \quad (22)$$

Heat of Reaction

The equation developed by Mahfouz *et al*. (1987) was used to calculate the exothermic heat of reaction.

$$\Delta H_R = 4.184\left(-\left(0.54426 + \frac{846.609}{T} + \frac{459.734x10^6}{T^3}\right)P - 5.34685T \right) \quad (23)$$
$$-0.2525x10^{-3}T^2 + 1069197x10^{-6}T^3 - 9157.09$$

Determination of Feed Properties and Operating Conditions

Feed composition and converter bed properties from an industrial ammonia converter (Notore Chemical Industry) at Onne in Rivers State, Nigeria are given in tables 2 and 3.

Table 1. Coefficients of C_p polynomial for feed components.

	Component			
	H_2	N_2	CH_4	Ar
A	6.952	6.903	4.75	4.9675
b x 10^2	-0.04567	-0.03753	1.2	-
C x 10^5	0.095663	0.193	0.303	-
d x 10^5	-0.2079	-0.6861	-2.63	-

Table 2. Feed Composition.

FEED COMPOSITION **(%mole)**						FLOW RATE	
H_2	N_2	CH_4	NH_3	Ar	H_2/N_2	FEED (Kg/Hr)	N_2 (Kmole/hr)
63.32	21.01	10.48	2.08	3.11	2.78	289661	5828

Table 3. Ammonia converter Bed Properties.

	BED #1	BED #2	BED #3	BED #4
INLET TEMPERATURE	439 ^oC	448 ^oC	412 ^oC	453 ^oC
VOLUME (M3)	9.2	11.9	17.8	25
Reactor Diameter	9'8" (2949mm)			
Reactor Pressure	122.44 Bar (120.84 atm)			

RESULTS AND DISCUSSION

The results obtained from the solution of the model equations are presented as follows:

Fractional Conversions along the Reactor Beds
The fractional conversion of the limiting reactant (N_2) along the catalyst beds is shown in figure 3.

Figure 3 shows that the conversion of the limiting reactant (Nitrogen) increases along the length of the reactor from catalyst BED 1 to BED 4as a result of the reaction of the reactants (N_2 and H_2) to form the product (NH_3).

Reactants/Product Concentrations
The concentrations of the reactants and product across each catalyst bed are shown in figure 4.

Figure 4 shows that the concentrations of the reactants (N_2 and H_2) decreases steadily as they are being converted into the product (NH_3), while the concentration of the product (NH_3) increases from its initial value as it is being formed as the reaction proceeds along the length of the reactor beds.

Temperature Profile
The temperature progression along the four catalyst beds using industrial inlet temperatures of each bed and model prediction of effluent concentrations of preceding bed is shown in figure 5. The temperature along each bed increases due to the exothermic reaction of ammonia synthesis leading to the release of heat.

Model Validation
The comparison of model predictions of ammonia converter outputs (exit concentrations of ammonia, nitrogen, hydrogen and temperature of bed 4) and industrial plant outputs are shown in Table 4.

Table 4 shows that the maximum deviation between model prediction and industrial plant outputs is 6.7%. Hence the models developed matched the industrial converter accurately and can be used for simulation studies of the ammonia converter.

The model prediction of the outlet bed temperature was very close to the industrial plant value with a deviation of 1.5% as the temperature was re-initialized at the entrance of the second and third beds using actual industrial data hence the error from the previous bed was not propagated across subsequent beds. However the model prediction of the concentration of reactants and product had a maximum deviation of 6.7% as the exit concentration of the preceeding bed was the entry to the next bed resilting in the propagation of the error across the beds.

PROCESS SIMULATION

The 1st catalyst bed was selected for simulation studies because the products from catalyst beds 1 and 2 were quenched (cooled) while the products from bed 3 were heated before entering the successive beds respectively.

Effect of Feed Flow Rate
The influence of feed flow rate on the converter performance is presented in figures 6 and 7. When the

Table 4. Comparison of plant data with model results.

S/N	PARAMETER	PLANT DATA	MODEL RESULT	%DEVIATION
1	NH_3(Mole %)	11.50	11.81	2.7%
2	N_2(Mole %)	18.19	19.46	6.7%
3	H2 (Mole %)	54.90	53.17	3.2%
4	Outlet Temperature (K)	754	754.87	1.5%

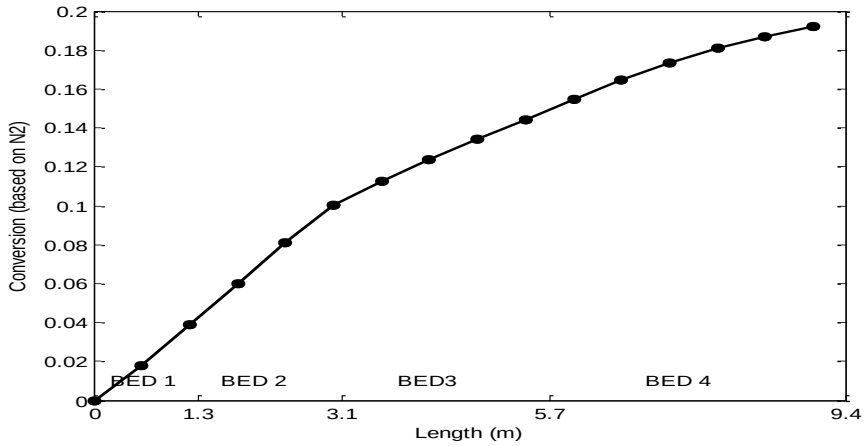

Fig. 3. Fractional Conversion of N_2along the catalyst bed length.

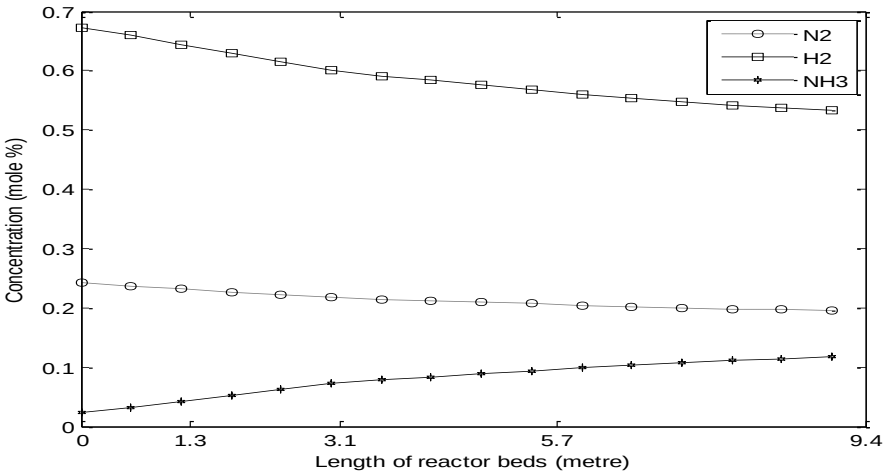

Fig. 4. Concentration (mole percent) of reactants and product along catalyst beds.

feed flow rate is increased, its velocity increases (reactants move faster) and the contact time of the reactants with the catalyst is reduced, resulting in a decrease in conversion and more reactants leaving the bed un-reacted. These trends the model predicts as shown in figure 6 where the reactants concentration increased slightly, the product (ammonia) concentration and conversion decreased with increase in feed flow rate. The decrease in conversion results in a decrease in exothermic heat released as reaction proceeds and subsequent reduction in bed temperatures. This trend model predicts as shown in figure 7.

Effect of Feed Temperature

The effects of feed input temperature into BED 1 on the performance of the converter are shown in figure 8.

For an exothermic equilibrium reaction such as ammonia synthesis, Le Chetalier's principle predicts that when there is a reduction in feed temperature, the system will

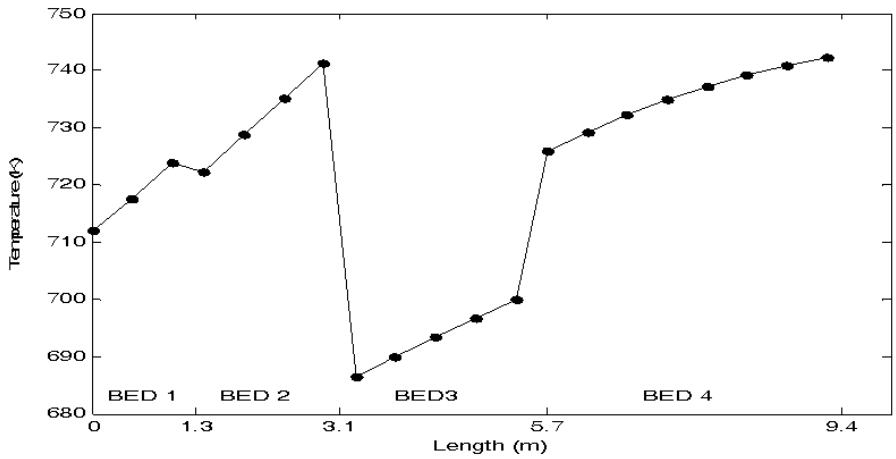

Fig. 5. Temperature profiles along catalyst beds.

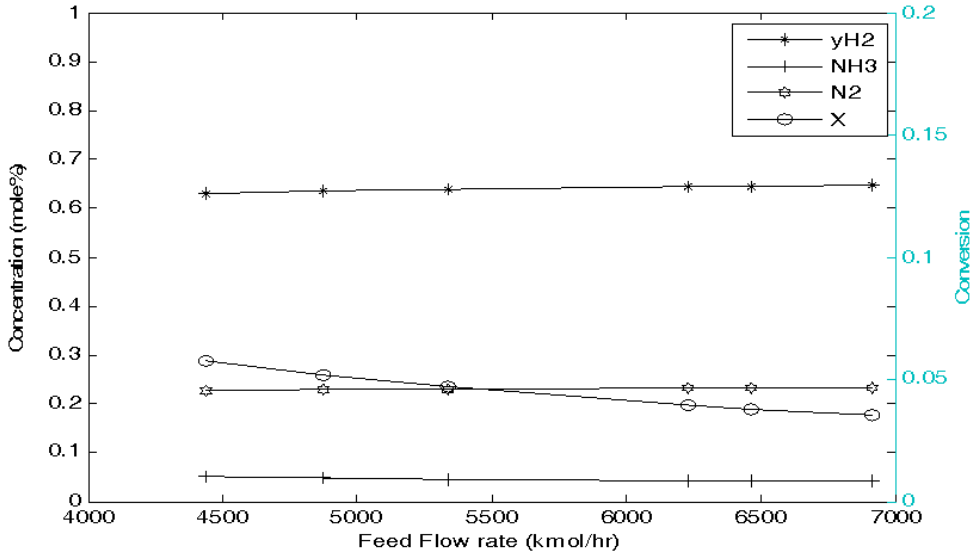

Fig. 6. Effect of Feed Flow rate on concentration and conversion.

adjust to annul the effect of this change, which is towards the production of more heat hence the equilibrium shifts to the right leading to the production of more ammonia. Similarly, when feed temperature is increased, the reaction rate is increased, but equilibrium shifts to the left resulting in decreased conversion of reactants and lower yield of ammonia. These trends the model accurately predicts as shown in figure 8.

The rates of reaction at low temperatures are extremely slow and catalyst deactivation leading to loss of iron surface area and activity is reported (Ye*et al*., 2001) to occur by thermal sintering at high temperature. Therefore, in practice a temperature range of 400-500^{o}C is a compromise designed to achieve an acceptable yield of ammonia within an acceptable time period (Nikola*et al*., 2010).

Effect of Input Pressure

Figure 9 shows the effect of input pressure of the feed on conversion and the reactant and product concentration.

The Ammonia synthesis reaction proceeds with a reduction in gas molecules (volume). According to Le Chetalier's Principle if the pressure of the converter is increased, the system adjusts to reduce the effect of this increase, that is, to reduce the pressure by having fewer gas molecules. Hence equilibrium shifts to the right resulting in higher conversion of reactants (decrease in concentration) and higher yield of ammonia. Higher yield

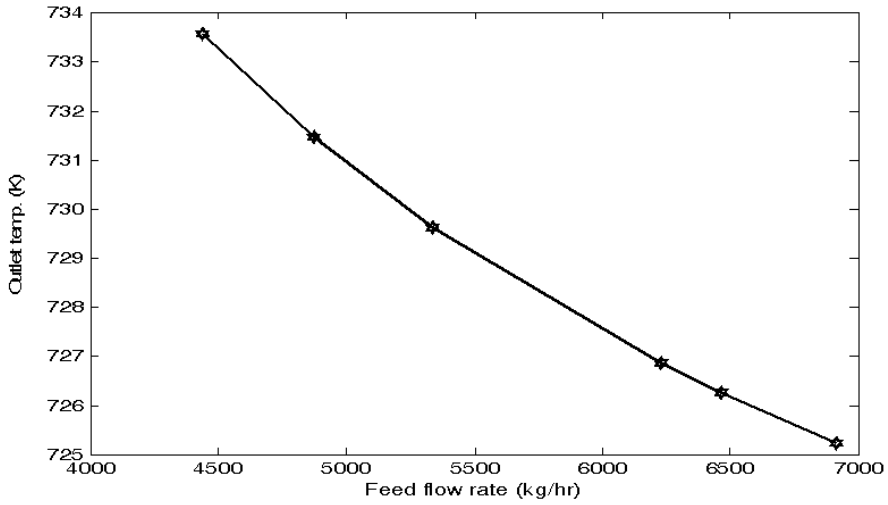

Fig.7. Effect of Feed Flow Rate on Outlet Temperatures.

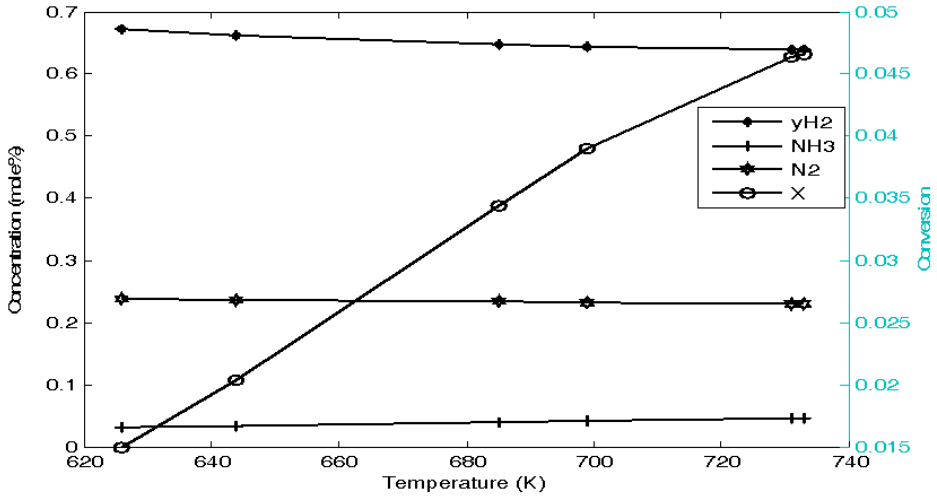

Fig. 8. Effect of Input Temperature on conversion and reactants concentration.

of ammonia means an increase in exothermic reaction leading to the release of more heat and resulting in an increase in outlet temperatures. Similarly, a decrease in pressure causes the equilibrium to shift to the left resulting in lower conversion of reactants and lower yield of ammonia; that is, a decrease in exothermic reaction resulting in a decrease in outlet temperatures. These trends the model accurately predicts as shown in figures 9 and 10 respectively. Although high pressure favors higher conversion, containing larger amounts of materials at high pressures are extremely difficult (Ye*et al*., 2001), therefore relatively low pressures are used industrially.

CONCLUSION

Model equations were developed from first principles by performing material and energy balances on the converter to obtain one dimensional model equations that were used to predict the conversion and temperature variations within the catalyst bed of an ammonia converter. The developed models consisted of two coupled ordinary differential equations with a host of other algebraic/polynomial equations for determining various parameters in the models. The model equations were solved numerically using the 4th order Runge-Kutta algorithm implemented with MatLab ode45 solver. Data from an industrial ammonia converter at Notore - a chemical industry that produces urea and other nitrogenous fertilizer from ammonia, located at Onne in Rivers state, Nigeria were obtained and used in solving the model equations. The results obtained from solutions to the models were compared with output plant data of the ammonia converter and a maximum deviation between outputs from solved models and actual plant data

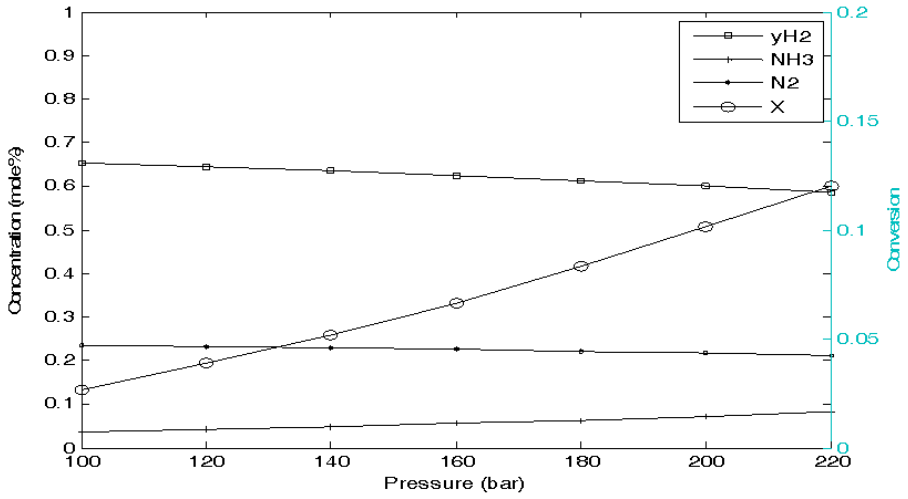

Fig. 9. Effect of Input Pressures on different parameters.

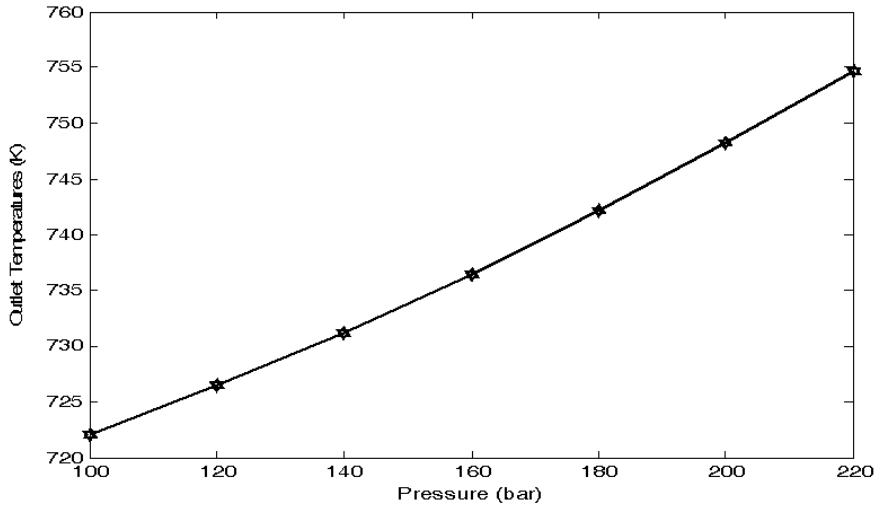

Fig.10. Effect of feed input pressure on the outlet temperatures.

of 6.7% was obtained. Having validated the models, the models were used to simulate the ammonia converter. Parameters such asfeed flow rates, input/quench stream temperatures, and pressures into the first catalyst bed (BED #1) were simulate to investigate their effect the performance of the converter. Consequently, the effect of these variations on conversions, outlet temperature progression and reactants/product mixture concentrations along the reactor beds were determined.

NOMENCLATURE

A	Cross sectional area
a_i	activity of component i
C_i	Concentration of component i
C_{p_i}	Specific heat capacity of component i
Cp_{mix}	Specific heat capacity of gas mixture (KJ/Kml)
E	Activation Energy
Fi_o	Initial flow rate of component i
f_i	Fugacity of component i
f_i^0	Reference fugacity
K	rate constant for the reverse reaction
K_a	Equilibrium constant
K_o	Arrhenius coefficient
L	Length of converter bed (m)
M	Total mass flow rate
N_i	mole of component i
N_T	Total moles of reactants and product
P	Operating Pressure
P_i	Partial pressure of component i
P_T	Total Pressure
R	Universal gas constant
R_i	rate of reaction with respect to component i

T Temperature
U velocity reactant gases (m/s)
X Fractional conversion of Nitrogen
Y_i mole fraction of component i
ΔH_R Heat of reaction
η Effectiveness factor
$\emptyset_i$ Dimensionless fugacity coefficient of component i

REFERENCES

Aparicio, LM. and Dumesic, JA.1994. Ammonia Synthesis Kinetics: Surface Chemistry, Rate Expression and Kinetic Analysis. Top Catal, 1, 233.

Appl, M. 1992.Ammonia Technology: Where have we got to, Where are we going? Nitrogen. 199:46.

Appl , M. 1997. Ammonia, Methanol, Hydrogen, Carbon Monoxide, Modern Production Technologies. Nitrogen, Publ.

Babu, SA. and Reddy, GV. 2012.Mathematical Modeling of Ammonia Converter, International Conference on Chemical, Civil and Environment engineering (ICCEE), Dubai.

Boudart, M. 1981. Kinetics and Mechanism of Ammonia Synthesis, Catal. Rev. Sci. Eng. 23:1.

Dashti, A., Khorsand, K., Marvast, MA. and Kakavand, M. 2006. Modeling and Simulation of Ammonia Synthesis Reactor. Journal of Petroleum & Coal. 48(2):15-23.

Dyson, DC. and Simon, JM. 1986. A Kinetic Expression with Diffusion Correction for Ammonia Synthesis on Industrial Catalyst, Ind. Eng. Chem. Fundamental. 7(4):605.

Elverse, B., Hawkins, S.,Russey, G. and Schulz, G. 1993. Ullman's Encyclopedia of Industrial Chemistry(5^{th} edi.). 85-98

Hagen, S., Barfod, R., Fehrmann, R., Jacobsen, CJH., Teunissen, HT. and Chorkendorff, IB. 2003. Ammonia synthesis with barium-promoted iron-cobalt al-loys supported on carbon. J. Catal. 214:327-335.

ICI. 1970. Catalyst Handbook with special Reference to Unit Processes in Ammonia and Hydrogen Manufacture. Wolfe Scientific Books, London.

Izumi, Y., Iwata, T. and Aika, K. 1996. Catalysis on Ruthenium clusters supported on CeO_2; Adsorption Behavior of H_2 and Ammonia Synthesis, J. Phys. Chem. 100:9421-9428.

Mahfouz, AT., Elshishini, SS. and Elnshaie, SSEH. 1987. Steady State Modeling and Simulation of an Industrial Ammonia Synthesis Reactor, ASME press. 10(3):1.

Nielson, A. 1981. Ammonia Synthesis: Exploratory and Applied Research. Catal. Rev. Sci. Eng. 23, 17.

Nikola, N., Mina, J. and Manka, P. 2010. Enhance Ammonia synthesis in Multifunctionalreactor with in situ Adsorption, Chemical Engineering Research and Design, Faculty of Technology and Metallurgy, University of Belgrade, Serbia.

Reddy, KV. and Husairi, A. 1982. Modeling and Simulation of an ammonia synthesis loop, Ind. Eng. Chem. Process Des. Dev. 21(3):359-367.

Temkin, M. and Pyzhev, V. 1940. Kinetics of the Synthesis of Ammonia on Promoted Iron Catalysts.Journal of Physical Chemistry. 13:851-867.

Temkin, MI. 1979. The Kinetics of some Industrial Heterogeneous Catalytic Reactions, Adv, Catal. 28, 173.

Temkin, MI. 1990. On Kinetics and Mechanism of Ammonia Synthesis, Chim. Prom. 292.

Ullman's, 1985. Encyclopedia of Industrial Chemistry, Ammonia, VCH Verlagsgesiischaft mbH. A2, 143

Unde, RB. and Gaikwad, AG. 2007. Kinetic Studies of Ammonia Formation over Fe and Mo containing HZSM-5 Catalysts, Chem. Biochem Eng, Q. 21. (2):139-144.

Ye, Q., Ying, W. and Fang, D. 2001. Simulation and Design Optimization of Ammonia Synthesis Converter. Chinese Journal of Chemical Engineering. 99(4):441-446.

Zbigniew, K., Slawomir, J. and Jan, S. 1996. Studies on Kinetics of Ammonia Synthesis Over Ruthenium Catalyst Supported on Active Carbon, Applied Catalysis A: General. 138:83-91.

Received: Feb 19, 2014; Accepted: April 3, 2014

APPENDIX1. Mole Model (Stoichiometric) Table.

COMPONENT (symbol)	INITIAL MOLAR CONC. (MOLE/Hr)	AMOUNT OF REACTANT USED /PRODUCT PRODUCED	EXIT MOLAR CONC.	MOLE FRACTION (y_i)
(N_2)	$FY_{N2,0}$	$-FXY_{N2,0}$	$F(Y_{N2,0}-XY_{N2,0})$	$\frac{Y_{N2,0}(1-X)}{1-2XY_{N2,0}}$
(H_2)	$FY_{H2,0}$	$-3FXY_{N2,0}$	$F(Y_{H2,0}-3XY_{N2,0})$	$\frac{Y_{H2,0}-3X\,Y_{N2,0}}{1-2YN_{2,0}}$
(CH4)	$FY_{CH4,0}$	0	$FY_{CH4,0}$	$\frac{Y_{CH4,0}}{1-2XY_{N2,0}}$
(Ar)	$FY_{Ar,0}$	0	$FY_{Ar,0}$	$\frac{Y_{Ar,0}}{1-2XY_{N2,0}}$
(NH_3)	$FY_{NH3,0}$	$2FX\,Y_{N2,0}$	$F(Y_{NH3,0}+2XY_{N2,0})$	$\frac{Y_{NH3,0}+2YX_{N2,0}}{1-2XY_{N2,0}}$
Total	$(\sum_{i=1}^{5} Y_i) = F(1-2XY_{N2,0})$			

SENRA Academic Publishers, British Columbia
Vol. 8, No. 2, pp. 2925-2931, June 2014
Online ISSN: 1920-3853; Print ISSN: 1715-9997

Canadian Journal of pure&applied sciences

A STUDY OF KINETICS OF METAL LEACHING FROM POLYPROPYLENE MATRIX USING A HYPHENATED MASS SPECTROMETRIC TECHNIQUE

*S Stephen[1], T Shah[2], AE Pillay[1] and E Siores[2,3]
[1]Department of Chemistry, The Petroleum Institute, Abu Dhabi, UAE
[2]Institute of Materials Science and Innovation, Bolton University, UK
[3]TEI – Athens, Greece

ABSTRACT

In this study polypropylene samples doped with varying levels of Mg, Ti and Zn were subjected to leaching under different pH conditions for a period of six months. Laser ablation and SEM techniques were used to investigate the samples in order to verify the presence of metals in the matrix. The leachates were subsequently analyzed by ICP-MS and the data were processed to compute the reaction kinetics. It was found that for all three metals of interest the leaching process was governed by first-order kinetics. The rate constant for the leaching reaction was noticeably low denoting that metal migration from polypropylene is protracted and does not particularly constitute a potential hazard. Significant differences between the leaching behavior of Ti and Mg/Zn from the polypropylene matrix were observed. The mechanism of the leaching process was considered to be analogous to aqueous degradation of polymorphic crystal structures of the embedded dopants.

Keywords: ICP-MS, SEM, polymers, metal leaching, laser ablation.

INTRODUCTION

Polymeric materials (e.g. polypropylene) are commonly used for packaging fluids such as edible oil, water, fruit juices, medical implants and oral pharmaceutical solutions. These polymers often contain metal residues, which could migrate into the encapsulated product and affect its performance or increase its level of toxicity. Migration studies of this nature are known; however, the rates of such migration and evaluation of kinetic factors, such as reaction order, have not been previously explored in depth. Leaching of metals from polymeric materials has always been a subject of interest. It is known that metals leach out of polymers under various conditions (Cheng *et al.*, 2010). Sharp thermal changes and other physical and chemical factors are known to influence leaching of metals from polymers. Studies have been conducted on assessing leaching of individual metals, often those that are toxic (Keresztes *et al.*, 2009). Nakashima et al, have studied the extent of toxic metal leaching from macro plastic litter on the Ookushi beach in southwestern Japan (Nakashima *et al.*, 2012). Antimony is known to be used widely as a catalyst for poly-condensation reactions in the production of polyethylene terephthalate used to make PET bottles. A significant amount of antimony is known to leach into beverages stored in PET bottles, which is a genuine health concern (Doremus, 1895). Polymers are also finding wider applications in packaging industries, replacing most or all of the metal containers. Various metals, mostly of the toxic nature are added to polymers as plasticizers, catalysts, stabilizing agents, processing aids and pigments (Takahashi *et al.*, 2008; Teuten *et al.*, 2009). Coe and Rogers (1997) investigated the effects of marine debris and leaching of toxic materials on marine life, which eventually led to toxins entering the food chain. A more recent study by Derraik (2002) has highlighted the fact that marine life is polluted by plastic waste which is seen widely dispersed in the oceans. A recent study was conducted by Nakashima *et al*. (2011) on heavy metals percolated from plastic litter washed on the shores. The study proved to be significant in revealing appreciable concentrations of Pb leaching out of pigments used in marine equipment widely employed in fishing vessels. Several biomedical applications employ polymeric metal complexes as implants and as aids for invasive techniques (Fraser and Fiore, 2008). Modified polymers also find their way into tissue engineering applications (He *et al.*, 2008).

Several heavy metals enter the human food chain after leaching from polymeric materials. Some of them have the potential to accumulate in specific target organs such as kidney and spleen and end up as the root cause of various diseases (Stemmer, 1976). Studies have also revealed that entire regions have been affected by heavy metal contaminations and large parts of the population in these areas have fallen victim to such environmental hazards (Chen *et al.*, 1994 ; Buschmann *et al.*, 2008).

Development of certain kinetic factors associated with percolation (leaching) of metal components from polymeric material is relatively unexplored. Studies on

*Corresponding author email: sstephen@pi.ac.ae

kinetics of leaching will provide a comprehensive insight into the effect of some variables, such as dopant level and pH of the fluid medium, on the rate of migration of metal species from polymeric materials. Significant parameters, such as the reaction order and rate constant, could be obtained to provide useful information in assaying any potential hazard that could be linked to such leaching processes. Much of the available literature documents trace metal levels in selected fluid samples arising from polymer material under ambient conditions without any valid consideration of kinetics. No serious record exists of kinetics of leaching as a function of pH and dopant level and a simulated study of this nature would be of considerable practical interest.

Our work entails a simulated study to determine kinetics of heavy metal leaching from a polymeric matrix. The primary objective of this research reported here is to use an inductively coupled plasma mass spectrometer to indirectly determine specific kinetic parameters, such as the rate constant and reaction order, for heavy-metal percolation of polypropylene as a function of dopant level and pH of aqueous medium.

MATERIALS AND METHODS

Preparation of polymer samples

The samples for this study were prepared using a base homopolymer (HE445FB), obtained from Borealis, Linz (Austria), with standard characteristics of melt flow rate 9.2 (g/10min) and molecular weight 42.08 (g/mol). In preparing the compounded materials, the melt flow rate was measured using a Zwick B4106 melt flow rate machine employing the ISO1133 method (Pillay *et al.*, 2010). A Prism TSE 24 twin screw extrusion machine was employed to prepare the compounded material, maintaining the extrusion conditions of 230°C; the material was further dried and pelletized (Pillay *et al.*, 2010). Three different mineral fillers (dopants) were used individually in samples (titanium oxide; zinc oxide; and magnesium oxide). These metal dopants were selected because they are common components in catalysts and reagents linked to polymer synthesis (Williams *et al.*, 2003; Manzi-Nshuti *et al.*, 2009). For our study we used samples loaded with 3 and 10% zinc (II) oxide, titanium (IV) oxide and magnesium (II) oxide. Finally, tiles of 60x60x2mm of the different compounded materials were prepared using a Ferromatic Milacon FM60 injection molding machine. Each tile was cut into four thin slices measuring 60x14x2 mm, approximately, prior to submerging in the leaching medium. The tiles were also washed thoroughly and rinsed in de-ionized water to get rid of surface contaminants, prior to the leaching process.

Leaching Study

Aqueous media of pH 3, 7 and 10 were prepared using Type 1 de-ionized water (Siemens Ultraclear). 50mL polypropylene tubes with screw caps (VWR Scientific) served as sample jars to hold doped polypropylene samples immersed in the relevant medium. Jars were pre-washed using 6M HNO_3 and further rinsed with de-ionized water to purge them of any possible metal contamination. Each sample was kept individually in the leaching solvent of pH 3, 7 and 10 for 24 weeks. Samples were handled using non-metallic forceps to avoid metal contamination. The solvent media were maintained at room temperature (between 20 and 24°C) and the tubes were shaken for a period of two hours in a flask shaker, once every two days. At the end of each designated time span, the polymer samples were removed from the leaching solvent. Leachates were stored under refrigerated conditions prior to analysis.

Instrumentation

An ICP-MS (Perkin Elmer SCIEX DRC-e) with an integrated reaction cell (Fig. 1) was used to analyze the polymer samples and to quantify the leached metals. A New Wave UP-213 laser ablation system operating at a wavelength of 213nm was used as the front end of the ICP-MS for the surface characterization of the polymer. While analyzing the leachates, an aqueous sample introduction system fitted with a Scot spray chamber was employed as the front end of the mass spectrometer. The polymer plaques were cut to fit into a special sample holder with dimensions 5cm x 5cm. No serious pre-treatment was necessary prior to irradiation. Samples were subjected to 213-nm laser irradiation along a 16-point grid, each point separated by a distance of 1.0mm. The level of the beam energy was 30%, with a fluence of approximately 3 J/cm^2. The laser was programmed to scan the grid 5 times, recording measurements after each ablation. The analytical performance of the instrument was satisfactory producing relative standard deviations (RSD) <5% for repeated measurements on a certified standard (Table 1). Surface characterization of the polymer samples was carried out using a scanning electron microscope (FEI Quanta 200 fitted with Inca x-sight SEM detector from Oxford Instruments, UK) to confirm surface profiles of metals.

RESULTS AND DISCUSSION

Surface characterization / Laser ablation / SEM

Characterizing polymer surfaces in terms of metal distribution could be used to evaluate homogeneity (Pillay *et al.*, 2010) and also to establish where the embedded metals are located in the polymer itself. They may be concentrated on the surface or are they ingrained within the polymer matrix? In some cases high surface purity is necessary to obviate the possibility of extraneous ingrained metals migrating into the environment associated with the polymer – especially if it is used to encapsulate solutions, such as jet-oil and body fluids. In this respect the metal impurity (dopant) could itself play an intricate role in its distribution. As the polymer

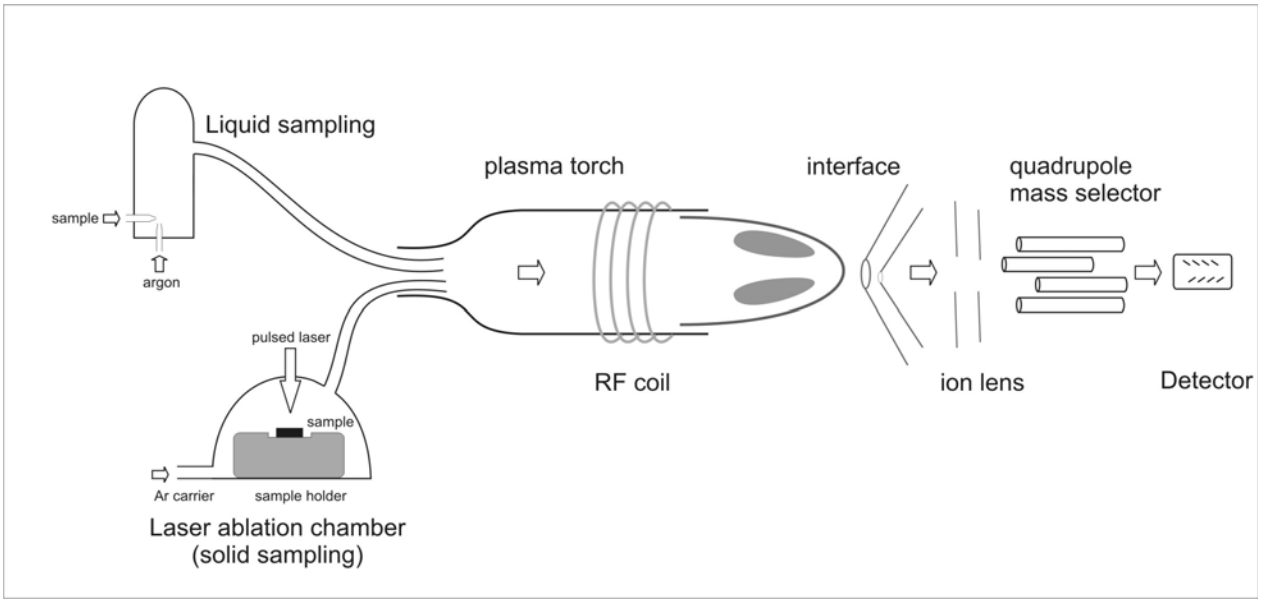

Fig. 1. Schematic of the ICP-MS depicting the laser ablator.

Table 1. Instrumental precision (µg/L) using a multi-elemental quality control sample (20ppb) [Fluka 70007].

Measurement	Be	V	Cr	Mn	Ag	Cd	Ba	Tl	Pb	U
1	20.04	20	18.63	20.01	20.76	19.77	21.11	20.91	20.06	20.23
2	20.78	21.4	20.08	20.35	19.92	20.18	21.5	20.6	19.99	20.87
3	21.75	19.82	18.82	18.78	19.92	18.6	20.46	20.44	20.76	21.01
Mean ± RSD	20.9 ± 4.1%	20.4 ± 4.2%	19.2 ± 4.1%	19.7 ± 4.2%	20.2 ± 2.4%	19.5 ± 4.2%	21.0 ± 2.5%	20.7 ± 1.2%	20.3 ± 2.1%	20.7 ± 2.0%

solidifies, some metals with greater mobility and affinity for the matrix could find themselves bound within the matrix. Others with fewer predilections to remain ingrained could migrate to the surface. The location of metal particles, therefore, depends not only on mixing but the potential of some metals with the capacity to remain ingrained. Laser technology has the unique capability of scanning micro-surfaces in polymer material to locate impurities. The laser technique had been successfully employed by the authors in an earlier study (Pillay *et al.*, 2010). It is not possible for the matrix to be completely devoid of metal impurities, therefore, the laser could be useful for developing surface profiles.

In this work, the SEM and laser ablation studies were conducted in order to establish the random existence and distribution of metals on the surface. When dopant is mixed in the polymer, the mixing itself could be imperfect and may lead to depleted surface levels, or no metals on the surface - which is unlikely. This study is an attempt to establish this premise scientifically using SEM /laser ablation techniques. Figure 2 portrays the spectral trends in metal distribution (for Ti, Mg and Zn) across the polymer surface. Strong and weak lines in figure 2 delineate corresponding elevated and diminished metal levels on the surface, underscoring the point that these dopants are arbitrarily dispersed. Paper-thin slivers (10µm) of the three samples were subsequently examined using a scanning electron microscope (SEM), to re-confirm the irregular distribution of the selected metals (Fig. 3). Analysis of the results presented in figures 2 and 3 shows that the SEM images support the laser ablation study. The uneven heights of the peaks in the ablation spectra (Fig. 2) and the speckled SEM frames in figure 3 clearly establish the random distribution of metals on the surfaces of the samples of interest.

Kinetics of leaching

Tables 2a and 2b present the metal concentrations of the samples subjected to progressive leaching activity over the designated period of 24 weeks. These values (obtained by ICP-MS) show sharp differences – by more than a factor of 5 in some cases - for Mg and Zn compared individually at the 3 and 10% dopant level. This indicates that the rate of leaching rose markedly with increased dopant level. Such pronounced differences were not observed with Ti, with leaching levels remaining about the same for both the 3 and 10% samples. This anomaly may be attributed to polymorphism as discussed below; or possibly due to cluster formations that coalesced Ti and

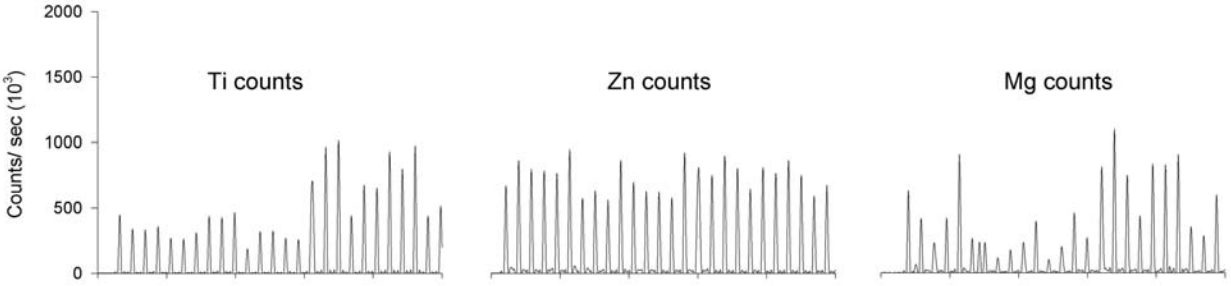

Fig. 2. Spectra of metal distribution at points on the polymer surface (using laser ablation).

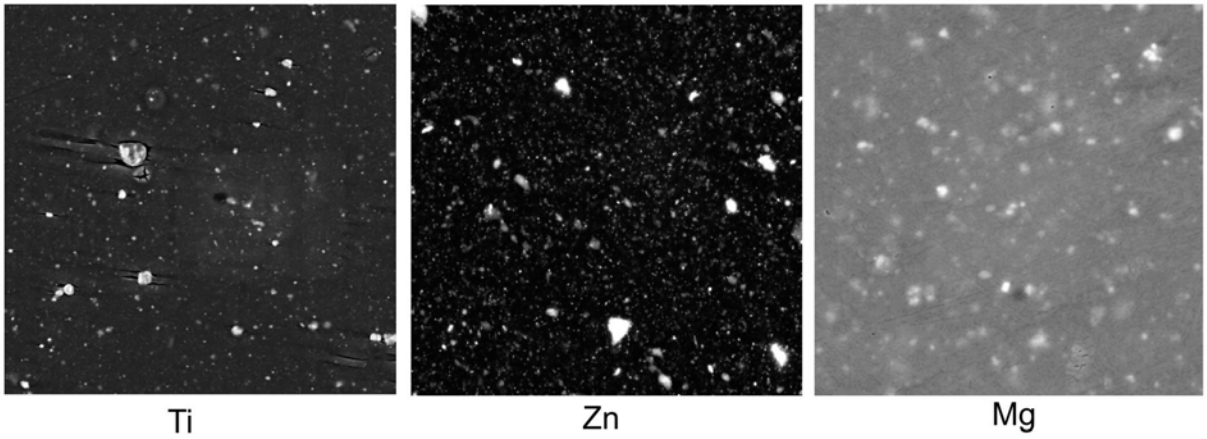

Fig. 3. SEM images of metal distribution on polymer surface.

Table 2a. Metal concentration in the leachate during a span of 24 weeks (3% doping).

Weeks	Ti (ppb)			Zn (ppb)			Mg (ppb)		
	pH 3	pH 7	pH 10	pH 3	pH 7	pH 10	pH 3	pH 7	pH 10
4	3.28±0.07	2.66±0.10	3.19±0.13	651±15.5	207±2.45	18.6±0.44	616±21.0	269±10.8	426±17.6
8	4.31±0.13	2.84±0.08	3.23±0.13	767±25.2	316±13.6	18.2±0.59	637±26.5	353±11.6	563±24.2
12	4.69±0.19	3.08±0.09	4.09±0.13	823±33.1	313±9.75	22.5±0.96	711±23.7	370±8.3	673±23.4
16	4.92±0.14	3.96±0.17	4.36±0.10	910±34.1	498±14.2	37.9±1.56	777±39.0	441±15.2	704±19.9
20	4.87±0.17	4.33±0.10	4.68±0.19	968±37.0	560±7.90	182.8±7.72	820±30.5	452±5.52	739±17.2
24	4.77±0.11	4.62±0.17	4.82±0.11	895±28.7	599±16.3	233.1±9.49	876±24.3	477±15.1	752±18.6

Table 2b. Metal concentration in the leachate during a span of 24 weeks (10% doping).

Weeks	Ti (ppb)			Zn (ppb)			Mg (ppb)		
	pH 3	pH 7	pH 10	pH 3	pH 7	pH 10	pH 3	pH 7	pH 10
4	3.7±0.12	2.28±0.05	2.60±0.08	2671±107.6	745±24.8	20.03±0.56	2447±85.2	2094±84.2	823±35.2
8	4.31±0.17	2.95±0.10	3.48±0.15	3404±112.0	1333±55.4	28.99±0.84	2578±110.6	2250±70.2	937±30.2
12	4.53±0.10	3.38±0.11	3.69±0.10	3641±116.8	1585±43.9	79.78±2.97	2947±72.9	2495±55.1	1202±49.0
16	4.66±0.10	3.39±0.12	4.13±0.12	4083±152.8	2213±110.9	534±22.8	3110±88.3	2607±72.0	1303±53.7
20	4.97±0.21	3.86±0.05	3.93±0.06	4129±157.8	2599±96.7	1300±29.1	2883±67.2	2745±94.7	1393±58.8
24	5.01±0.21	4.13±0.17	4.27±0.05	4098±97.2	2666±90.9	1655±61.6	3527±145.2	2955±65.0	1544±36.6

the polymer chain, thus hindered leaching. The general trends associated with leaching of the metals of interest are illustrated in figures 4-6. It is clear that in each case the process is more pronounced with progressive decreases in pH values. As mentioned earlier, the data show evidence of a higher percolation rate with increased dopant level. Among the selected metals, plots for Mg and Zn (10%) displayed the most prominent rates of leaching (Figs. 5 & 6) suggesting that magnesium and zinc bearing catalysts and reagents should be used sparingly for preparation of polymers. The plots for Ti were interesting and reflected percolation levels about an order of magnitude lower than those recorded for Mg and Zn. This unexpected outcome for Ti suggested complex

crystal structures that hindered degradation; or the possibility that the metal itself could be tightly entrenched within the polymer matrix (Smolensky *et al.*, 2005; Ulrich, 2001) which played a role in inhibiting the leaching process. Titanium resembles the electron configuration of carbon ([Ar] $3d^2$ $4s^2$) and this feature could have contributed to "melding" the metal within the matrix leading to inorganic-organic hybrid cluster formations. Earlier studies also point to the possibility of this metal-melding phenomenon (Smolensky *et al.*, 2005 ;Ulrich. 2001). However more extensive studies are required to establish this particular hypothesis.

The mechanism of the leaching process was considered to be analogous to the degradation of crystal structures in aqueous media (Koutsoukos *et al.*, 2007). The dopants used in this study were in the form of metal oxides, which contain the very reactive O^{2-} ion that is highly attracted to the metal ions in crystal lattice structures. Magnesium oxide, for example, consists of a structural arrangement of Mg^{2+} ions and O^{2-} ions held together by ionic bonding in an octahedral geometry (Zhu *et al.*, 2013). Zinc oxide exists in dual polymorphic structures: hexagonal and cubic symmetries (Fierro, 2006). Titanium oxide exists in multiple polymorphic structures: hexagonal,

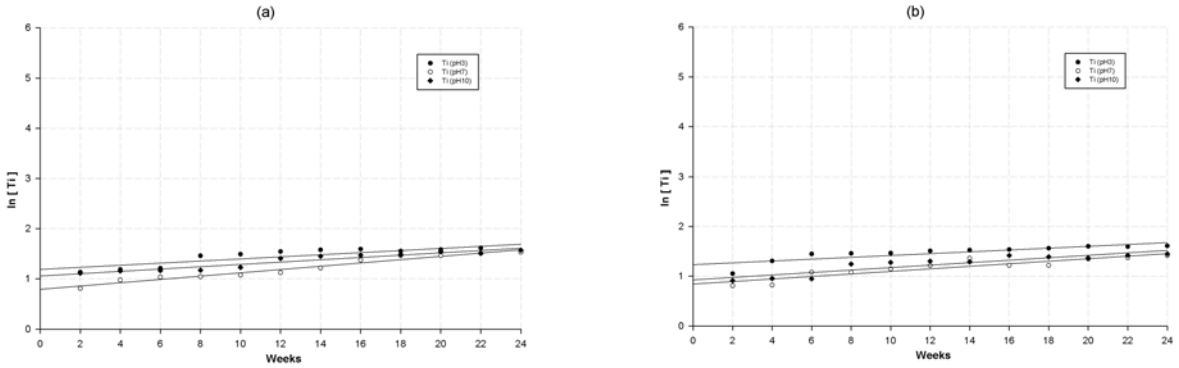

Fig. 4

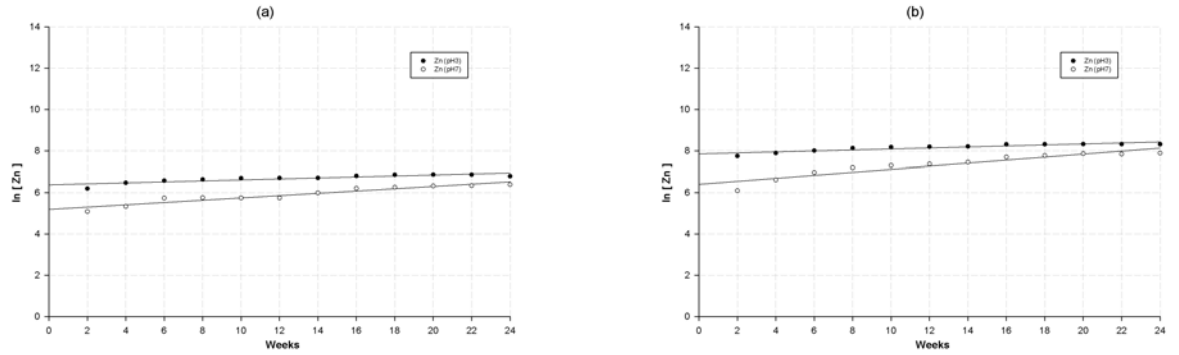

Fig. 5

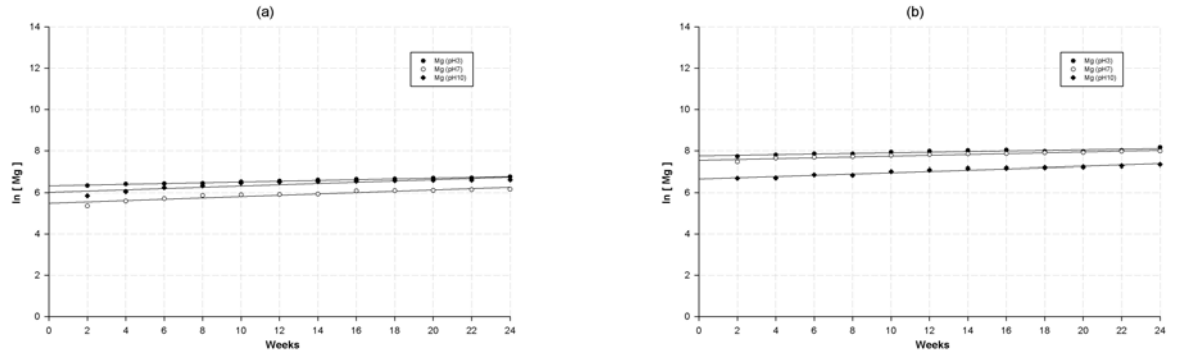

Fig. 6

Figs. 4-6. Concentration-time plots of metal levels in leachates conforming to first-order kinetics.
(a), (b) = 3%, 10% dopants, respectively.

orthorhombic and monoclinic arrangements (Marchand *et al.*, 1980; Latroche *et al.*, 1989; Akimoto *et al.*, 1994). Degradation (or leaching) of crystals in acidic media is related to the complexity of the structure and its polymorphic forms (Fierro, 2006). Leaching levels tend to be lower in the presence of more complex polymorphic structures (Fierro, 2006). This phenomenon agrees with our data in figures 4-6 where Mg levels in leachates were highest, and Ti lowest, reflecting the trend in polymorphism. This also accounted for the differences in the recorded data between Ti and the other metals. Clearly, in acidic media affinity of O^{2-} for H^{+} will increase with decreasing pH of the medium, resulting in elevated leachate levels, as reflected in the plots in Figs 4-6. Hence the mechanism is pH-dependent, leading to enriched leachates as a function of pH.

For metals complexed within the solid matrix (Smolensky *et al.*, 2005; Ulrich, 2001) an interesting mechanism advanced by Abbu *et al*. (2000) proposes displacement of the metal ion by H^{+}, leading to augmented leachate levels with decreasing pH as depicted in figures 4-6. Again, according to this proposed mechanism, the leaching process is pH dependent. And, for highly charged metal ions tightly coalesced within the solid matrix (e.g. Ti^{4+}), displacement will be harder, thus leading to corresponding diminished leachate levels, as is the case for Ti (Fig. 4) which is significantly different from Mg/Zn data.

Within experimental limits the plots in figures 4-6 are linear, thus fulfilling first-order kinetics (Chang, 2010). The rate constants were determined from the corresponding slopes, and are roughly 0.01 wk^{-1} for all samples. This rate constant is particularly low indicating that the process is distinctly protracted for polypropylene, the polymeric material investigated in this study. It is important to point out that the dopant levels used in this study had to be high and distinct enough to determine the order of the leaching reaction. Therefore these levels were deliberately kept high, with appreciable differences in concentrations, so that significant data could be generated to establish the order of the metal leaching process. If the dopant levels were in the ppm range (for example) the effect would not have been sufficiently pronounced and perhaps not even observable. This is why kinetic studies of this nature remain underexplored.

CONCLUSION

Our study has established that metal leaching from polymeric material is pH dependent and of the first order. This has implications for liquids and food products encapsulated in polymer containers. Lower pH values tend to induce accelerated rates of percolation. The observed leaching trends for Mg/Zn impregnated samples were similar and could be representative of most heavy metals. However, Ti doped samples did not leach easily suggesting that either its multiple polymorphic structures inhibited the leaching process; or Ti could be intrinsically bound to the polymer chain. This latter phenomenon was considered anomalous and could form an interesting subject for future study, especially if titanium as a dopant forms inorganic-organic hybrid clusters. This suggests that the use of additives and catalysts based on Mg and Zn should be avoided for the production of this type of polymers, especially if such materials are intended for use in critical applications such as liquid food packaging and medical applications.

ACKNOWLEDGEMENTS

The authors gratefully appreciate the financial assistance provided by The Petroleum Institute, Abu Dhabi.

REFERENCES

Abbu, R., Moodley, KG. and Pillay, AE. 2000. A study of ICP-AES of sorption phenomena in aqueous solutions containing medium-weight and heavy trace metals. J Trace and Microprobe Techniques. 18:15-21.

Akimoto, J., Gotoch, Y., Oosawa, Y., Nonose, N., Kumagai, T., Aoki, K. and Takei, H. 1994. Topotactic Oxidation of Ramsdellite-Type $Li_{0.5}TiO_2$, a New Polymorph of Titanium Dioxide: TiO_2(R). Journal of Solid State Chemistry. 113:27-36.

Buschmann, J., Berg, M., Stengel, C., Winkel, L., Sampson, ML., Trang, PTK. and Viet, PH. 2008. Contamination of drinking water resources in the Mekong delta floodplains: Arsenic and other trace metals pose serious health risks to population. Environment International. 34:756-764.

Chang, R. 2010. Chemistry. Mcgraw-Hill. pp570.

Chen, SL., Dzeng, SR. and Yang, MH. 1994. Arsenic Species in Groundwaters of the Blackfoot Disease Area, Taiwan. Environmental Science & Technology. 28:877-881.

Cheng, XL, Shi, HL, Adams, CD. and Ma, YF. 2010. Assessment of metal contaminations leaching out from recycling plastic bottles upon treatments. Environmental Science & Pollution Research. 17:1323-1330.

Coe, JM. and Rogers, DB. 1997. Marine Debris: Sources, Impacts and Solutions. Springer-Verlag, New York, USA.

Derraik, JGB. 2002. The pollution of the marine environment by plastic debris: a review. Mar. Pollut. Bull. 44:842-852.

Doremus, CA. 1895. The Chemical History of a case of Combined Antimony and Aresenic Poisoning. Journal of the American Chemical Society. 17:667-682.

Fierro, JLG. 2006. Metal Oxides: Chemistry & Applications. CRC, Taylor Francis.

Fraser, CL. and Fiore, GL. 2008. Polymers for Biomedical Applications. American Chemical Society. 95-115:

He, W., Feng, Y., Ma, Z. and Ramakrishna, S. 2008. Polymers for Biomedical Applications. American Chemical Society. 310-335.

Keresztes, Szilvia., Tatár, E., Mihucz, GV., Virág, István, Majdik., Cornelia, Z. and Gyula. 2009. Leaching of antimony from polyethylene terephthalate (PET) bottles into mineral water. Science of The Total Environment. 407:4731-4735.

Koutsoukos, PG., Kofina, AN. and Kanellopoulou, DG. 2007. Solubility of salts in water: Key issue for crystal growth and dissolution processes. Pure Appl. Chem. 79:825-850.

Latroche, M., Brohan, L., Marchand, R. and Tournoux, R. 1989. New hollandite oxides: $TiO_2(H)$ and $K_{0.06}TiO_2$. Journal of Solid State Chemistry. 81:78-82.

Manzi-Nshuti, C., Songtipya, P., Manias, E., Jimenez-Gasco, MM., Hossenlopp, JM. and Wilkie, CA. 2009. Polymer nanocomposites using zinc aluminum and magnesium aluminum oleate layered double hydroxides: Effects of LDH divalent metals on dispersion, thermal, mechanical and fire performance in various polymers. Polymer. 50:3564-3574.

Marchand, R., Brohan, L. and Tournoux, M. 1980. A new form of Titanium dioxide and the potassium octatitanate $K_2Ti_8O_{17}$. Materials Research Bulletin. 15:1129-1133.

Nakashima, E., Isobe, A., Kako, SI., Itai, T. and Takahashi, S. 2011. Toxic Metals Derived from Plastic Litter on a Beach. Inter Disciplinary Studies on Environmental Chemistry-Environmental Pollution and Ecotoxicology. 2012. pp321-328.

Nakashima, E., Isobe, A., Kako, SI., Itai, T. and Takahashi, S. 2012. Quantification of Toxic Metals Derived from Macroplastic Litter on Ookushi Beach, Japan. Environmental Science & Technology. 46:10099-10105.

Pillay, AE., Vukusic, S., Stephen, S. and Abd-Elhameed, A. 2010. Rapid Ablative Laser Technique (ICP-MS) for Monitoring Material Homogeneity in Polypropylene. Chemical Sciences Journal. 2010:1-9.

Smolensky, E., Kapon, M., Woollins, JD. and Eisen, MS. 2005. Formation of Elastomeric Polypropylene Promoted by a Dynamic Octahedral Titanium Complex. Organometallics. 24:3255-3265.

Stemmer, KL. 1976. Pharmacology and toxicology of heavy metals: antimony. Pharmacol. Therapeut A. 1:157-160.

Takahashi, Y., Sakuma, K., Itai, T., Zheng, G. and Mitsunobu, S. 2008. Speciation of Antimony in PET Bottles Produced in Japan and China by X-ray Absorption Fine Structure Spectroscopy. Environmental Science & Technology. 42:9045-9050.

Teuten, EL., Saquing, JM., Knappe, DRU., Barlaz, MA., Jonsson, S., Bjorn, A., Rowland, SJ., Thompson, RC., Galloway, TS., Yamashita, R., Ochi, D., Watanuki, Y., Moore, C., Viet, PH., Tana, TS. and Predent, M. 2009. Transport and release of chemicals from plastics to the environment and to wildlife. Phil. Trans. Roy. Soc. Biol. Sci. 364:2027-2045.

Ulrich, S. 2001. Polymers Reinforced by Covalently Bonded Inorganic Clusters. Chemistry of Materials. 13:3487-3494.

Williams, CK., Breyfogle, LE., Choi, SK., Nam, W., Young, J., Victor. G., Hillmyer, MA. and Tolman, WB. 2003. A Highly Active Zinc Catalyst for the Controlled Polymerization of Lactide. J. Am. Chem. Soc. 125:11350-11359.

Zhu, Q., Oganov, AR. and Lyakhov, AO. 2013. Novel stable compounds in the Mg-O system under high pressure. Phys. Chem. Chem. Phys. 15:7696-7700.

Received: Feb 12, 2014; Accepted: April 8, 2014

SENRA Academic Publishers, British Columbia
Vol. 8, No. 2, pp. 2933-2942, June 2014
Online ISSN: 1920-3853; Print ISSN: 1715-9997

Canadian Journal of pure&applied sciences

MODELING OF THINLIQUID FALLINGFILM IN H_2O-LiBr AND H_2O-LiCl ABSORPTION REFRIGERATION SYSTEMS

*KM Odunfa[1], RO Fagbenle[2], O O Oluwole[1] and OS Ohunakin[3]
[1]Mechanical Engineering Department, University of Ibadan, Ibadan, Oyo State
[2]Mechanical Engineering Department, Obafemi Awolowo University, Ile-Ife, Osun State
[3]Mechanical Engineering Department, Covenant University, Ota, Ogun State, Nigeria

ABSTRACT

Experimental modeling has over the past three decades been used in analyzing simultaneous heat and mass transfer in thin-liquid falling-film absorption processes. However, numerical modeling applications in this area have been minimal due to complications arising from the presence of waves. An approach in numerical modeling is to consider waves as a second order effect, thereby making it a smooth falling-film. The objective of this paper was to develop a numerical model for the absorption process on a thin-liquid smooth falling-film using lithium bromide (LiBr) and lithium chloride (LiCl) solutions. The absorption process of a thin-liquid smooth falling-film was considered as a two-dimensional steady laminar flow within the film thickness to the absorber wall. The conservation equations were used to determine temperature and concentration distribution within the film-thickness using the finite difference technique. Existing data on LiBr and LiCl solutions in the literature were used to validate the developed model. Standard values of absorber wall length, film thickness, solution mass flow-rate, absorbent inlet concentration, inlet temperature, absorber wall temperature, conventional film Reynolds number and absorption design effectiveness were used for both LiBr and LiCl solutions. Data were analyzed using descriptive statistics and student's t-test ($p<0.05$). The physical properties distribution for both LiBr and LiClsolutions were not significantly different from published results available in the literature($p<0.05$). The nodal temperature distribution obtained within the film thickness both in the bulk and interface between the liquid and vapour regions were between 44.4 and 35.0^oC while concentration was between 60.0 and 54.5% for LiBr-H_2O. Similarly for LiCl-H_2O, the model temperature distribution was between 35.0 and 30.0^oC while the concentration was between 45.0 and 35.8%.A numerical model on a thin-liquid smooth falling film using LiBr and LiCl solutions was developed. Lithium bromide was also observed to have higher concentration values than lithium chloride thus suggesting a better working fluid combination especially in the absorption air-conditioning system.

Keywords: Absorption refrigeration, lithium bromide, lithium chloride, air-conditioning.

INTRODUCTION

Energy conservation and environmental safety in recent years, have become a thing of global concern due to the increasing energy prices and the consequent environmental impact. The current imbalance of energy demand and supply coupled with the environmental degradation in many developing countries has further increased the urgent need for highly efficient and sustainable energy technologies. The worldwide demand for this phenomenon has prompted the emergence of new technologies in many areas of the global economy, such as in the cooling system development sector. Basically, cooling system may be divided into two categories:vapour compression and sorption systems. The vapour compression system involves the use of a compressor for the compression process. Sorption system can be sub-divided into absorption and adsorption systems; an absorption system is simply the replacement of the traditional compression with a thermo-chemical fluid lifting process. In other words, it is the mixture of a gas in a liquid, the two fluids present a strong affinity to form a solution, while adsorption is a process that occurs when a gas or liquid solute accumulates on the surface of a solid or more rarely, a liquid (adsorbent) forming a molecular or atomic film (adsorbate). However, in the manufacturing of the cooling machine/system, the global demand for efficient use of energy at minimum environmental cost has necessitated the increased demand for absorption refrigeration systems driven by waste heat or solar thermal energy instead of conventional systems driven by electrical energy. In the absorption process, heat and mass transfer usually take place within a thin-liquid falling-film. Heat and mass transfer in thin-liquid falling film absorption process has received the attention of many researchers over the years especially in the last two decades. This is as a result of its wider application in many modern devices such as absorption air-conditioners, absorption chillers, absorption heat pumps etc (Yang and Wood, 1992).

*Corresponding author email: m.odunfa@mail.ui.edu.ng

Many researchers such as Andberg (1983), Grossman (1983) and Andberg and Vliet (1983) have approached the study of this area using various modeling techniques which may be categorized either into (i) numerical or (ii) experimental.Numerical methods (including finite element, finite difference, boundary element, Monte Carlo technique and vortex methods etc.) have been developed over many decades and are still being developed to effectively tackle many engineering problems. These methods may be categorized into two: deterministic approach and probabilistic approach. Probabilistic methods such as Monte Carlo and vortex element techniques make constant recourse to random numbers while finite element, finite difference and boundary element techniques are deterministic in nature.

Several works have been carried out on modeling with experimental data of heat and mass transfer in thin-liquid falling film absorption while there are relatively few studies on numerical modeling of the problem. For instance, the technical feasibility of driving a lithium chloride-water solution absorption-cooling unit by a low-temperature heat source (such as solar energy using a simple flat-plate collector) for air-conditioning applications was thoroughly investigated by Ali and El-Ghalban, 2002. The operating characteristics of the unit were extensively investigated and the Coefficient of Performance (COP) of the unit was found to be 19% as against the expected designed value of 21%. Safarik *et al.* (2004), also carried out an experimental modeling on a solar power absorption chiller with low capacity using lithium bromide-water solution as the working fluid. The field test carried out at three sites in the summer of 2003 after the prototype test in this experimental modeling showed that the absorption chiller works reliably and flexibly over a wide range of external conditions. Abdelmessih *et al*. (2004) experimentally investigated the use of non-traditional absorbent/refrigerant pairs such as ethylene glycol-water in an absorption refrigeration cycle. The investigation was successful in replacing the traditional hazardous absorbent/refrigerant pairs with a safe working fluid (ethylene glycol-water pair). Yaxiu *et al*. (2008) also experimented a compact solar pump-free lithium bromide absorption refrigeration system equipped with a second generator, a falling-film absorber, a falling-film evaporator and an efficient luminate thermosiphon elevation tube. The experiment confirmed a 48.5% increase in the COP.The numerical modeling is complicated by the presence of the waves in the falling liquid-film; an approach in numerical modeling is therefore to consider waves as a second order effect, thereby, making it a smooth falling-film. This smooth falling film absorption approximation has been more popularly investigated,the earliest of such being the work of Grossman (1983). The work was even considered complicated in formulation due to the restriction of the model to the case with the inlet absorbent temperature being equal to that of the wall. Andberg and Vliet (1983) also investigated the smooth falling-film absorption under laminar flow using a different model from the work of Grossman (1983), it was also considered most sophisticated and somewhat too complicated in formulation.

In Yang and Wood (1992), the finite difference approach was adopted to develop a simple, smooth-film absorption model using LiCl-H_2O and LiBr-H_2O systems with Reynolds number of 2.7, 27 and 100. The model handles various initial/boundary conditions and gives solutions similar to the earlier work of Grossman (1983) and also with experimental data. Ghaddar *et al*. (1996) modeled solar lithium bromide absorption system performance in Beirut using a simulated computer program; the result shows that for each ton of refrigeration, it is required to have a minimum collector area of 23.3m^2 with an optimal water storage tank capacity ranging from 1000 to 1500 liters for the system to operate solely on solar energy for about seven hours a day. The energy use in cooling was also found to be of function of solar collector area and storage tank capacity. Based on the economic assessment performed on the current cost of the conventional cooling system, it was also found that the solar cooling system is marginally competitive only when combined with domestic water heating Ghaddar *et al*. (1996). An overview of the performance assessment of a developed prototype low capacity (10kw) solar assisted lithium bromide absorption heat pump (AHP) coupled with a sub-floor system with the use of a commercial simulator known as TRNSYS was carried out by Argiriou *et al*. (2005). The assessment was done for two building types (high and low thermal mass) in three climatic conditions with different types of solar collectors, hot water storage tank sizes and different control systems for the operation of the installation. The results indicated that the estimated energy savings against a conventional cooling system using a compression type heat pump was in the range of 20-27%. In Bruno *et al*. (2004), Ammonia-water-sodium hydroxide mixtures absorption refrigeration plant was modeled using a commercial process simulator "Aspen Plus 2003". It was found that the system performance is notably increased (lower driving temperature and higher COP).

However, Fernandez *et al*. (2005) solved the simultaneous heat and mass transfer equations in Ammonia-water absorption system using finite difference approach. The results established the expected typical range of values $x_{vb} < z < \infty$ or $-\infty < z < x_{Lb}$ and $x_{Lb} < z < x_{vi}$ for mass transfer against temperature variations in different components of the plant such as absorber and evaporator; where x, z, b, L, i *and* v are defined as ammonia molar concentration, ammonia to net molar flux transferred ratio, bulk conditions, liquid, liquid-vapour interface and vapour respectively. In Staicovici and Isvoranu (2005)

water-lithium bromide absorption/generation processes in a Marangoni Convection Cell (applied practical method by the thermal absorption technology in the past decades to significantly improve the absorption process) using the Two-Point Theory (TPT) of mass and heat transfer was modelled. The model established the capability of TPT approach in the Marangoni convection assisted water-lithium bromide absorption process following the successful modeling of the ammonia-water absorption process. It also confirms Marangoni convection basic mechanism explanation in the case of the water-lithium bromide medium. Zohar *et al*. (2007) investigated the influence of diffusion in the ammonia-water Diffusion Absorption Refrigeration (DAR) cycle configuration on the system performance using a computer simulator known as Engineering Equation Solver (EES). The result reveals that DAR cycle without condensate sub-cooling shows higher COP of 14-20% compared with the DAR cycle with the condensate sub-cooling, but it occurs at a higher evaporator temperature of about 15^{o}C.

Niu *et al*. (2007) performed a numerical analysis of falling film ammonia-water absorption in a magnetic field using a computer program referred to as TDMA due to the tri-diagonal matrix formation of the equations after discretization. It was found that when the magnetic induction intensity at the solution's inlet was 3Tesla, the increment in concentration of ammonia-water solution at outlet was 1.3%, the absorbability increased by 5.9%, COP of the absorption refrigeration system increased by 4.7% and the decrement in circulation ratio was 8.3%. This establishes a positive effect on the ammonia-water falling film absorption to some degree. Kyung *et al*. (2007) further developed a water-lithium bromide absorption process model over a horizontal tube using finite difference approach. The model predicted a significant absorption in the drop formation regime with a considerable variation of temperature and mass fraction. Simulation of aqueous lithium bromide (H_2O-LiBr) advanced energy storage system using finite difference method was carried out by Xu *et al*. (2007a, b). The result predicted the dynamic characteristics and performance of the system, including the temperature and concentration of the working fluid, the mass and energy in the storage tanks, the compressor intake mass or volume flow rate, discharge pressure, compression ratio, power and consumption work, the heat loads of heat exchanger devices in the system and so on. The result also indicated that the Integrated Coefficient of Performance (COP_{int}) of the system was as high as 3.26 as against the expected value of 3.0 under the two storage strategies, while the isentropic efficiency of water vapour compressor was set as 60%. These results were found to be very helpful in understanding and evaluating the system as well as for system design, operation and control. Gustavo *et al*. (2008), studied a two-stage water-LiBr absorption chiller driven at two temperature levels using thermodynamic modeling technique. The study established that the machine can operate in summer as a double-stage chiller driven by heat at 170^{o}C from natural gas, as a single-stage chiller driven by heat at 90^{o}C from solar energy, or simultaneously in combined mode at both temperatures. It also established the capability of operating in winter in "double-lift" mode for heating with a driving heat at 170^{o}C from natural gas. In Balghouthi *et al*. (2008), model work on both experimental and numerical modeling of solar water-lithium bromide absorption air conditioning in Tunisian climatic conditions (36^{o} latitude and 10^{o} longitude, 400cal/cm^{2}day average solar irradiation, and 3700h/year of the total insolation period) were conducted using the TRNSYS and EES programs. The model established that the absorption solar air-conditioning system was suitable for Tunisia. Although, the system has a high initial cost, but with its advantage of near zero maintenance cost, the system could help to minimize fossil fuel-based energy use, reduce electricity demand on the national grid (especially at peak demand periods in summer), and eliminate the use of CFCs.

The finite difference method has been applied much more than any other methods in the analysis of absorption/adsorption systems. Probabilistic or deterministic methods could also be used depending on the degree of accuracy required of the solution in comparison with the solutions obtained experimentally or analytically. This paper thus employs the finite difference method for establishing temperature and concentration distributions during the absorption process on a thin-liquid falling-film in a cooling system using (H_2O-LiBr) and (H_2O-LiCl) refrigerants/absorbents combinations. Such an investigation would reveal sections of the absorber that need to be redesigned for optimal efficiency of refrigerant absorption by the absorbent.

MATHEMATICAL MODEL

Assumptions

In formulating the model equations, the following assumptions are made.

1. The flow is a fully developed smooth laminar flow in a steady state as shown in figure1.
2. The fluid properties are constant and not varying with temperature and concentration.
3. The mass rate of vapour absorbed is very small compared to the solution flow rate such that the film thickness and flow velocities can be treated as constant.
4. Heat transfer in the vapor phase is negligible.
5. Vapor pressure equilibrium exists between the vapour and liquid at the interface.
6. The Peclet numbers are large enough such that the diffusion in the flow direction can be neglected.
7. Diffusion thermal effects are negligible.

Table 1. Data for LiBr-H_2O and LiCl-H_2O solutions as obtained in literatures.

Working fluid parameters	symbols	LiBr-H_2O	LiCl-H_2O
film dynamic viscosity	μ	4×10^{-4}kgm^{-1}s^{-1}	4×10^{-4}kgm^{-1}s^{-1}
mean velocity	ν_o	3.15×10^{-4}ms^{-1}	3.15×10^{-4}ms^{-1}
Thermal diffusivity	α	0.155m^{2}s^{-1}	0.155m^{2}s^{-1}
Liquid density	ρ	127kgm^{-3}	1000kgm^{-3}
Thermal conductivity	K	176Wm^{-1}k^{-1}	176Wm^{-1}k^{-1}
Species diffusivity	D	1×10^{-10} m^{2}s^{-1}	2.0×10^{-9} m^{2}s^{-1}
Wall Temperature	T_w	35^{o}C	30^{o}C
Inlet Temperature	T_{in}	44.44^{o}C	35^{o}C
Initial absorbent Conc.	C_{in}	60%	45%
Equilibrium absorb. Con	C_{eq}	60%	35.8%
Gravity	g	9.8ms^{-2}	9.8ms^{-2}
Mean film thickness	h_o	1.74×10^{-3}m	1.74×10^{-3}m
Heat of absorption	H_a	3466kj/kg	3466kj/kg
Absorbent Vapour Pressure	Pv	7.02mmHg	9.2mmHg
Film Reynolds number	R_{ef}	100	100
Film mass flowrate	I	0.01kgm^{-1}s^{-1}	0.01kgm^{-1}s^{-1}

Data source: Yang and Wood (1992)

8. The shear stress at the liquid – vapor interface is negligible.

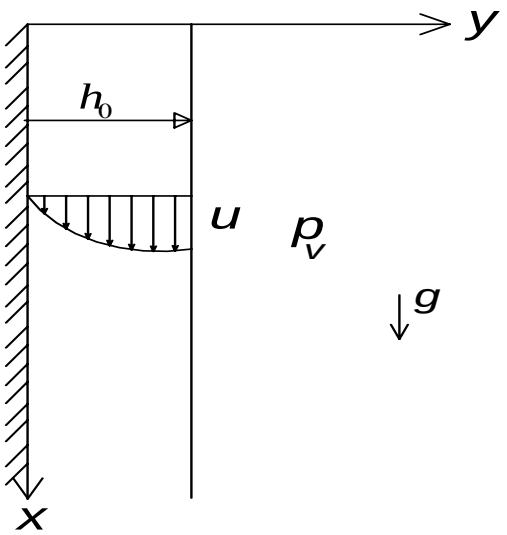

Fig. 1. 2-D representation of a thin-liquid falling-film.

Governing equations

The general governing heat and mass transfer equations for the falling film medium areas follows:

$$U\frac{\partial T}{\partial x}+v\frac{\partial T}{\partial y}=\alpha\frac{\partial^2 T}{\partial y^2} \quad (1)$$

$$U\frac{\partial C}{\partial x}+v\frac{\partial C}{\partial y}=D_{ab}\frac{\partial^2 C}{\partial y^2} \quad (2)$$

From the preceeding assumptions (mathematical model), the heat and mass transfer equations in thin-liquid falling-film (corresponding to the coordinate system) shown in figure 1 and expressed in Equations 1 and 2 will become Equations 3 and 4:

$$U\frac{\partial T}{\partial x}-\alpha\frac{\partial^2 T}{\partial y^2}=0 \quad (3)$$

$$U\frac{\partial C}{\partial x}-D\frac{\partial^2 C}{\partial y^2}=0 \quad (4)$$

$$U=\frac{3}{2}V_0\left[2\frac{y}{h_0}-\left(\frac{y}{h_0}\right)^2\right] \quad (5)$$

where, T is temperature, C is concentration (absorbent), α is thermal diffusivity and D or D_{ab} is species diffusivity

$$V_0=\frac{\rho g h_0^2}{3\mu}, \qquad h_0=\left(\frac{3\mu V_0}{\rho g}\right)^{\frac{1}{2}}$$

Boundary conditions

At x = 0; T = T_{in} and $C=C_{in}$ (6)

At y = 0 (non-permeable wall); $T=T_w$, $\frac{\partial C}{\partial y}0$ (7)

At $y=h_0$;

$$-K\frac{\partial T}{\partial y}=\rho D\frac{\partial C}{\partial y}H_a, C=C_{equil}\left(T,P_v\right) \quad (8)$$

Table 2. LiBr-H_2O solution.

X (m)	a) Temperature Distribution					
	Bulk			Interface		
	Literature result	Present result	Percentage deviation	Literature result	Present result	Percentage deviation
0 or 10^{-6}	44.44	44.44	0.00	44.44	44.44	0.00
$10^{-5.5}$	44.40	43.65	-1.69	44.44	44.35	-0.20
10^{-5}	43.50	42.87	-1.45	44.44	43.50	-2.18
$10^{-4.5}$	43.20	42.08	-2.59	44.44	42.65	-4.03
10^{-4}	43.00	41.29	-3.98	44.44	41.80	-5.94
$10^{-3.5}$	41.50	40.51	-2.39	44.44	40.95	-7.85
10^{-3}	39.50	39.72	+0.56	44.00	40.10	-8.86
$10^{-2.5}$	38.00	38.93	+2.45	42.00	39.25	-6.55
10^{-2}	36.60	38.15	+4.23	39.50	38.40	-2.78
$10^{-1.5}$	36.40	37.36	+2.64	38.00	37.55	-1.18
10^{-1}	36.00	36.57	+1.58	37.00	36.70	-0.81
$10^{-0.5}$	35.50	35.79	+0.82	36.00	35.85	-0.42
10^{0}	35.00	35.00	0.00	35.00	35.00	0.00

X (m)	b) Concentration Distribution					
	Bulk			Interface		
	Literature result	Present result	Percentage deviation	Literature result	Present result	Percentage deviation
0 or 10^{-6}	0.600	0.600	0.00	0.599	0.592	-1.17
$10^{-5.5}$	0.600	0.59545	-0.76	0.599	0.583	-2.67
10^{-5}	0.600	0.59090	-1.52	0.599	0.580	-3.17
$10^{-4.5}$	0.600	0.58635	-2.28	0.599	0.576	-3.84
10^{-4}	0.600	0.58180	-3.03	0.599	0.573	-4.34
$10^{-3.5}$	0.600	0.57724	-3.79	0.599	0.569	-5.01
10^{-3}	0.600	0.57267	-4.56	0.591	0.566	-4.23
$10^{-2.5}$	0.599	0.56810	-5.16	0.580	0.562	-3.10
10^{-2}	0.590	0.56352	-4.49	0.570	0.559	-1.93
$10^{-1.5}$	0.575	0.55892	-2.80	0.560	0.555	-0.89
10^{-1}	0.567	0.55432	-0.01	0.550	0.552	+0.36
$10^{-0.5}$	0.559	0.54970	0.07	0.548	0.549	+0.18
10^{0}	0.545	0.54500	0.00	0.545	0.545	0.00

where H_a = heat of absorption, T_w = wall temperature, P_v = vapour pressure and $C_{equil}(T, P_v)$ = equilibrium concentration at the interface temperature and ambient vapour pressure.

At the boundary, usually the parameters such as temperature and concentration are known (Dirichlet conditions) or the boundary is considered to be perfectly insulated (Newmann or Adiabatic conditions). Insulated boundaries are handled by developing boundary element/nodal equations. Hence, Newmann or Adiabatic boundary condition was used along the absorber wall in this model.

Solution of the model equations

The Gaussian elimination method is adopted in this work towards the development of a computer program written in FORTRAN 90 language. The main program with the flow chart shown in figure 2 solves equations (3) and (4) using modified Gaussian elimination scheme. This program utilizes two different subroutines (1 and 2) having their flowchart shown in figure 3. These subroutines are developed to execute various steps involved in applying the finite difference scheme and function after the implementation of the boundary conditions in the global domain. Solution1 generates the temperature profile of the domain, while solution 2 produces a concentration profile within the domain. The problem data are introduced into the program in the "data

Table 3. LiCl-H_2O solution.

X (m)	a) Temperature Distribution					
	Bulk			Interface		
	Literature result	Present result	Percentage deviation	Literature result	Present result	Percentage deviation
0 or 10^{-6}	35.00	35.00	0.00	36.00	36.62	+1.72
$10^{-5.5}$	35.00	34.58	-1.20	36.25	38.25	+5.52
10^{-5}	35.00	34.17	-2.37	37.00	37.50	+1.35
$10^{-4.5}$	35.00	33.75	-3.57	37.60	36.75	-2.26
10^{-4}	35.00	33.33	-4.86	38.00	36.00	-5.26
$10^{-3.5}$	35.00	32.92	-6.00	38.20	35.25	-7.72
10^{-3}	35.00	32.50	-7.14	38.20	34.50	-9.68
$10^{-2.5}$	34.80	32.08	-7.82	37.00	33.75	-8.78
10^{-2}	33.90	31.67	-6.52	36.00	33.00	-8.33
$10^{-1.5}$	32.10	31.25	-2.65	34.50	32.25	-6.52
10^{-1}	32.00	30.83	-3.66	33.00	31.50	-4.55
$10^{-0.5}$	31.50	30.42	-3.43	31.90	30.75	-3.61
10^{0}	30.00	30.00	0.00	30.00	30.0	0.00

X (m)	b) Concentration Distribution					
	Bulk			Interface		
	Literature result	Present result	Percentage deviation	Literature result	Present result	Percentage deviation
0 or 10^{-6}	0.450	0.450	0.00	0.400	0.426	+6.50
$10^{-5.5}$	0.450	0.450	0.00	0.402	0.402	0.00
10^{-5}	0.450	0.4406	-2.08	0.405	0.398	-1.73
$10^{-4.5}$	0.450	0.4360	-3.12	0.410	0.394	-4.00
10^{-4}	0.450	0.4313	-4.15	0.414	0.390	-5.80
$10^{-3.5}$	0.450	0.4267	-5.18	0.414	0.386	-6.76
10^{-3}	0.448	0.4221	-5.79	0.414	0.382	-7.73
$10^{-2.5}$	0.440	0.4174	-5.13	0.400	0.378	-5.50
10^{-2}	0.440	0.4128	-6.18	0.390	0.374	-4.10
$10^{-1.5}$	0.430	0.4082	-5.07	0.380	0.370	-2.63
10^{-1}	0.420	0.4036	-3.91	0.370	0.366	-1.08
$10^{-0.5}$	0.390	0.3990	2.30	0.365	0.362	-0.82
10^{0}	0.358	0.3580	0.00	0.358	0.358	0.00

block", where the input parameters can easily be modified to suit any case study. The input data utilized were obtained from literature in the work of Andberg (1983) and Yang and Wood (1992), as used for the available experimental and numerical modelingin order to obtain high quality output of temperature and concentration profiles in the domain. The data utilized from the literature are as shown in table 1 (LiBr–H_2O and LiCl–H_2O).

RESULTS AND DISCUSSION

Results in the direction of falling film (X)

The model run has been executed using the two working fluid pairs (lithium bromide-water and lithium chloride-water). The respective temperature and concentration distributions obtained from the models as compared with that found in literatures (previous work by Andberg (1983) and Yang and Wood (1992) are presented in table 2 for lithium bromide-water and table 3 for lithium chloride-water.Temperature and concentration profiles of smooth film absorption were further plotted as shown in figures 4 (a, b) and 5 (a, b) respectively to compare previous work with the developed model for thelithium bromide-water solution and lithium chloride-water solution. It was observed that downstream the wall, the absorbent solution approaches the equilibrium condition corresponding to the given wall temperature and the absorber pressure. The results agree quite well with previous work in literatures within 9% for interface temperature, but much better at approximately 5% for bulk temperature. Concentration results are much closer for both interface and bulk calculations, being generally less than 1% and also confirm the stated assumptions (3) and (7) of the mathematical model.

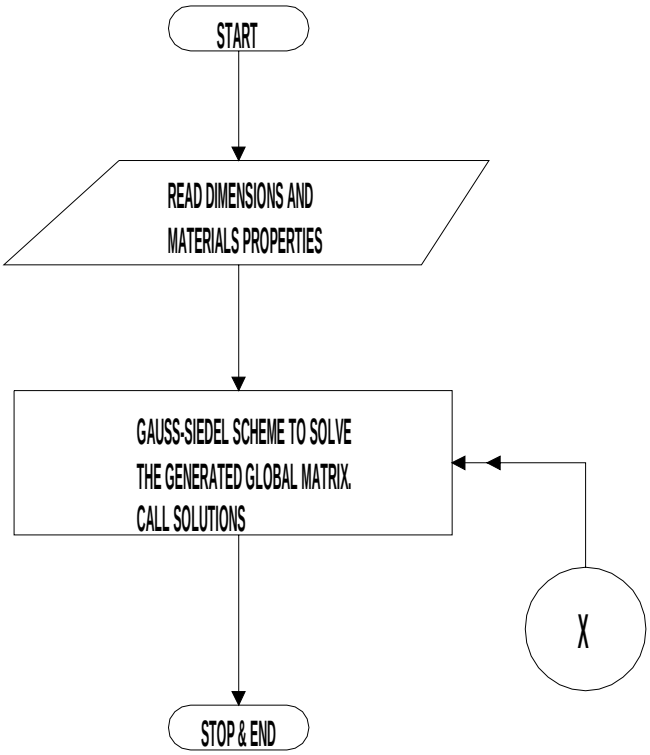

Fig. 2. Main program flow chart.

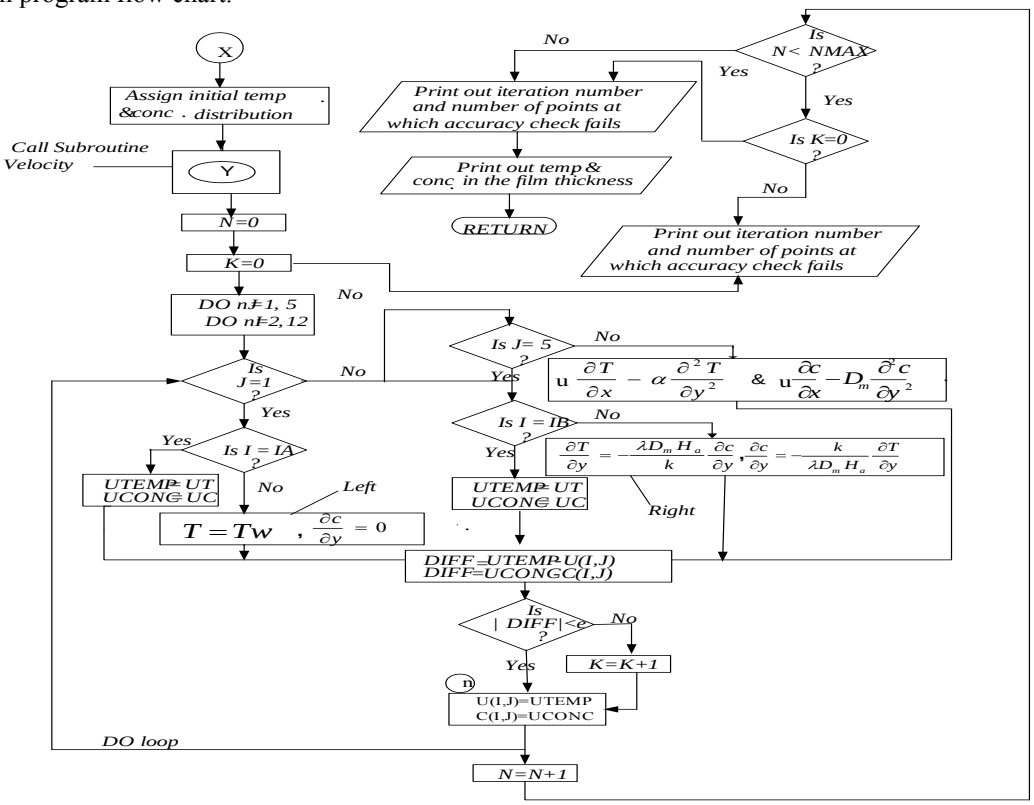

Fig. 3. Model subroutine solution flow chart.

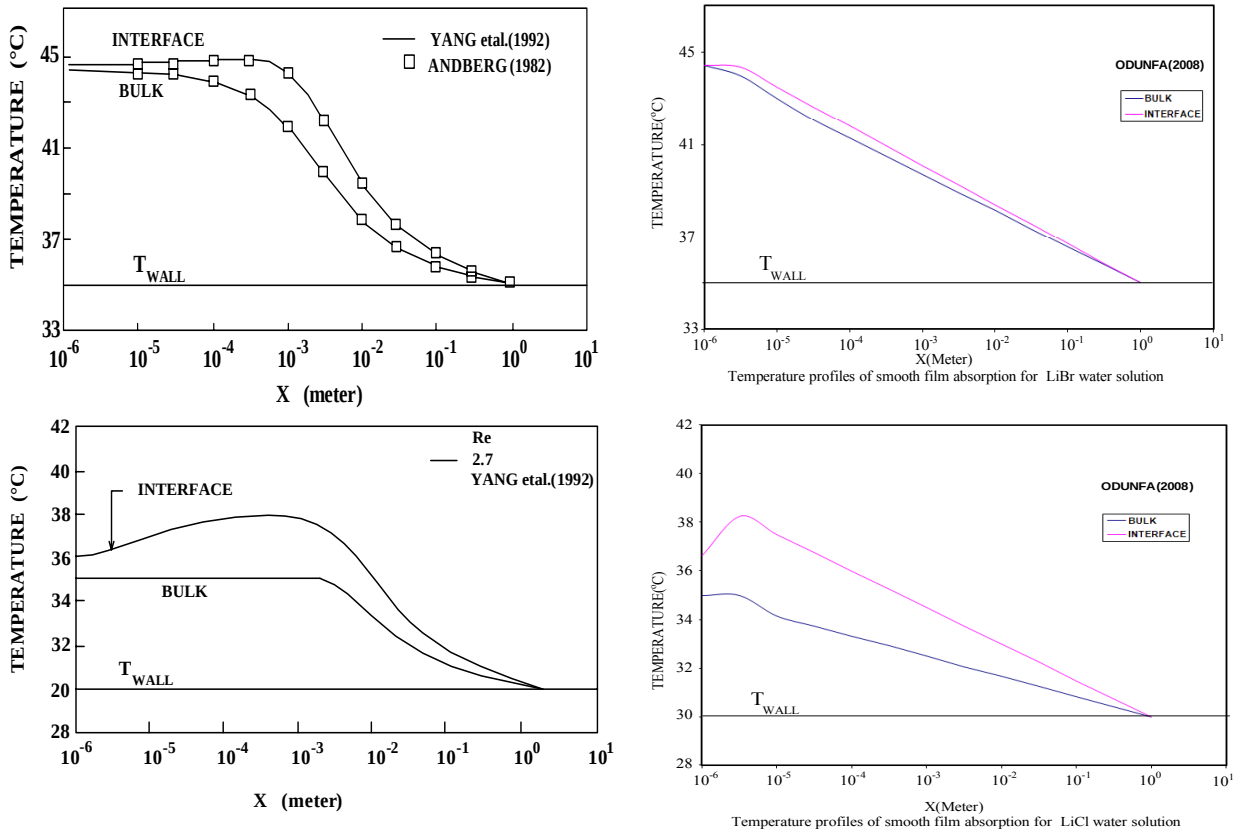

Fig. 4. Temperature profiles of smooth film absorption for (a) LiBr-Water Solution and (b) LiCl-water solution.

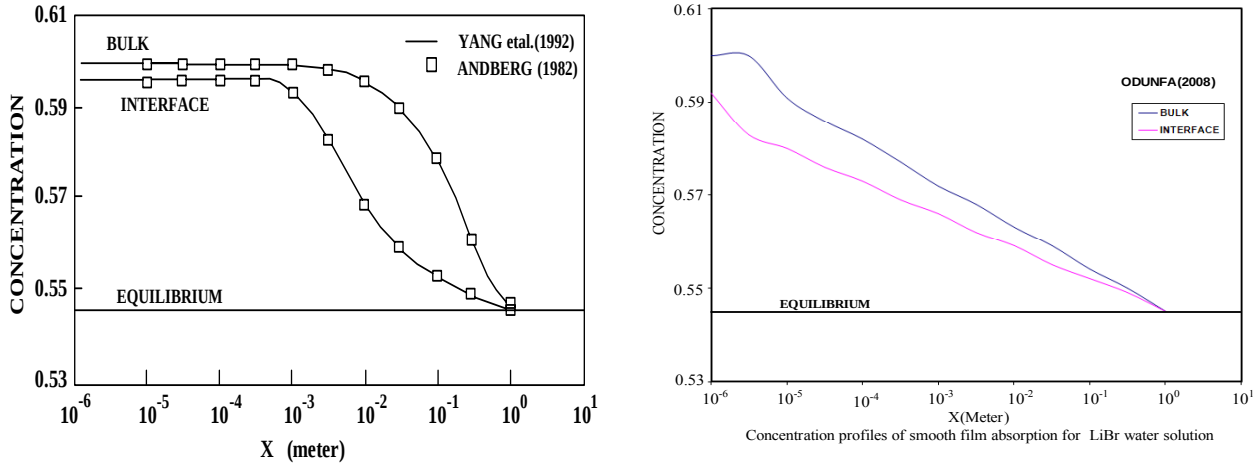

Fig. 5. Concentration profiles of smooth film absorption for (a) LiBr-Water Solution.

CONCLUSION

The use of finite difference method for simulation of an absorption process of a liquid falling-film in a cooling system using lithium bromide-water and lithium chloride-water working fluids was investigated in this work.

- It was observed that the simple finite difference solution method is quite adequate for first order analysis of the smooth falling-film absorption problem, especially where accuracy of less than 10% in interface temperature is acceptable.
- Bulk temperatures and concentration profiles are however very well predicted by the method,

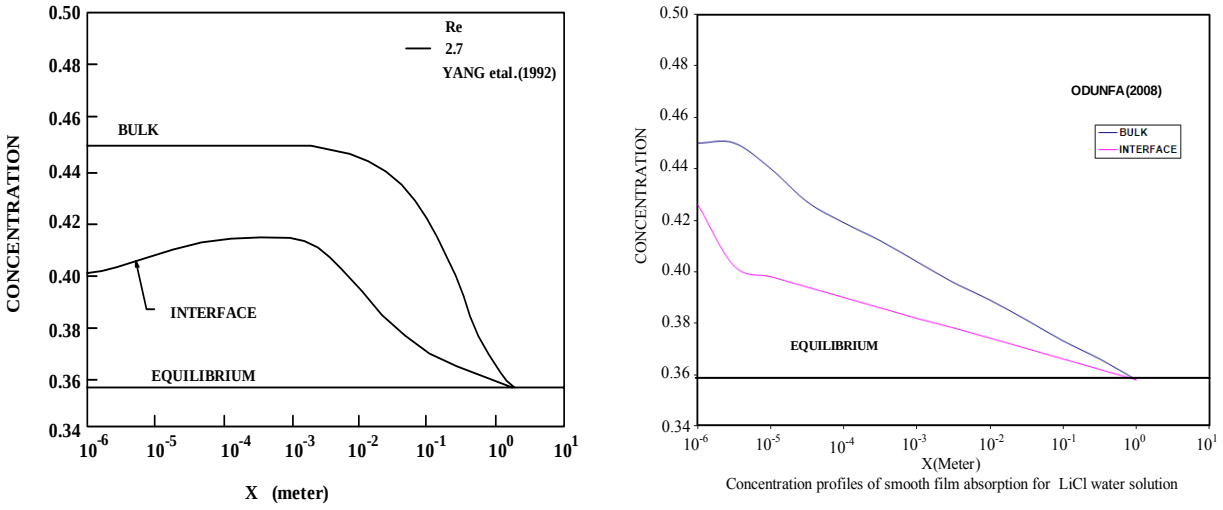

Fig. 5. Concentration profiles of smooth film absorption for (b) LiCl-water solution.

generally within 1% for both bulk and interface concentration values;these results are normally expected even from the more sophisticated methods available with proprietary software. The developed model was also found to be promising, precise and can provide results that are in good agreement with those of complicated formulation found in the literature as well as with experimental data.

- The viability of the finite difference method, on a thin-liquid smooth falling-film in a cooling system was established. The Lithium-bromide solution was also confirmed to be of excellent performing working fluid pairs when it comes to an absorption air conditioning system.

REFERENCES

Abdelmessih, AN., Mohammad, A., Abdulwahab, A. and Jay, M. 2005. An Experimental Absorption Refrigeration Cycle. 4th International Conference on Heat Transfer, Fluid Mechanics and Thermodynamics (HEFAT), Egypt.

Ali, R. and El-Ghalban, D. 2002. Operational results of an intermittent absorption cooling unit. International Journal of Energy Research. 26:825-835.

Andberg, GW. 1983. Non-Isothermal absorption of gases into falling liquid film. M.Sc Thesis. University of Texas at Austin, Austin TX, USA.

Andberg, JW., Vliet, GC. 1983. Design guildlines for water Libr absorbers.ASHRAE Transactions.89:220.

Argiriou, AA., Balaras, CA., Kontoyiannidis, S. and Michel, E. 2005. Numerical Simulation and performance assessment of a low capacity solar assisted absorption heat pump coupled with a sub-floor system. Solar Energy. 79: 290-301.

Balghouthi, M., Chahbani, MH. and Guizani, A. 2008. Feasibility of Solar absorption air-conditioning in Tunisia. International Journal of Building and Environment. 43: 1459-1470.

Bruno, JC., Vidal, A., San-Roman, MF., Ortiz, I. and Coronas, A. 2004. Modeling of absorption refrigeration plants using ammonia-water-sodium hydroxide mixtures. 3rd International Conference on Heat and Powered Cycles (HPC), Cyprus.

Fernandez-Seara, J., Siere, J., Uhia, FJ. and Vazquez, M. 2005. Solution of the Simultaneous heat and mass transfer Equations in Ammonia-water absorption system processes. 4th International Conference on Heat Transfer, Fluid Mechanics and Thermodynamics (HEFAT), Egypt.

Ghaddar, NK., Shihab, M. and Bdeir, F. 1996. Modeling and Simulation of Solar Absorption System Performance in Beirut. Renewable Energy.10(4):539-558.

Grossman, G. 1983. Simultaneous heat and mass transfer in film absorption under laminar flow. International Journal of Heat and Mass Transfer. 26:357.

Gustavo, RF., Mahmoud, B. and Alberto, C 2008. Thermodynamic modeling of a two-stage absorption chiller driven at two-temperature levels.Applied Thermal Engineering. 28 (2/3):211-217.

Kyung, I., Keith, EH. and Tae-Kang, Y. 2007. Model for absorption of water vapor into aqueous LiBr flowing over a horizontal smooth tube. International Journal of Refrigeration.30:591-600.

Niu, X., Du, K. and Du, S. 2007. Numerical analysis of falling film absorption with ammonia–water in magnetic field.Applied Thermal Engineering. 27:2059-2065.

Safarik, M., Richter, L. and Otto, M. 2004. Solar Powered H_2O/LiBr-Absorption chiller with low capacity. 3rd International Conference on Heat and powered Cycles (HPC), Cyprus.

Staicovici, MD. and Isvoranu, D. 2005. Model of the water/Lithium Bromide Absorption/Generation Processes in a Marangoni Convection Cell, Using the Two-Point Theory (TPT) of Mass and Heat Transfer. 4th International Conference on Heat Transfer, Fluid Mechanics and Thermodynamics (HEFAT), Egypt.

Xu, SM., Zhang, L., Xu, CH., Liang, J. and Du, R. 2007[a]. Numerical simulation of an advanced energy storage system using H_2O-LiBr as working fluid, Part 1: System design and modeling. International Journal of Refrigeration. 30:364-376.

Xu, SM., Zhang, L., Xu, CH., Liang, J. and Du, R. 2007[b]. Numerical simulation of an advanced energy storage system using H2O-LiBr as working fluid, Part 2: System simulation and analysis. International Journal of Refrigeration. 30:354-363.

Yang, R. and Wood, BD. 1992. A numerical modeling of an absorption process on a liquid falling film. Solar Energy. 48 (3):195-198.

Yaxiu, G., Yuyuan, W. and Xin, K. 2008. Experimental research on a new solar pump-free lithium bromide absorption refrigeration system with a second generator.Solar Energy. 82:33-42.

Zohar, A., Jelinek, M., Levy, A. and Borde, I. 2007. The influence of diffusion absorption refrigeration cycle configuration on the performance.Applied Thermal Engineering. 27:2213-2219.

Received: Dec 2, 2013; Accepted: Jan 25, 2014

SENRA Academic Publishers, British Columbia
Vol. 8, No. 2, pp. 2943-2954, June 2014
Online ISSN: 1920-3853; Print ISSN: 1715-9997

Canadian Journal of pure & applied sciences

TAIL TOLERANCE OF WEB SERVICES SOLUTION BUILT ON REPLICATION ORIENTED ARCHITECTURE (ROA)

*Godspower O Ekuobase[1] and Ifeanyichukwu E Anyaorah[2]
[1]Department of Computer Science, University of Benin, Benin City, Edo State
[2]Department of Computer Science, Auchi Polytechnic, Auchi, Edo State, Nigeria

ABSTRACT

Guaranteed responsiveness of Web Services solutions may not be possible on a large scale, if the solutions are not tail tolerant i.e. able to consistently keep latency within reasonable limit. Software techniques that tolerate latency variability and in particular, tail latency are vital to building responsive large-scale Web services solutions. Replication Oriented Architecture (ROA) though proposed to help application programmers build scalable Web Services solutions appears capable of mitigating latency variability and tail latency. Consequently, we investigated ROA for tail tolerance. To do this, we built two ATM Web Services solution using Java technology – the first was not built on ROA (conventional solution) but the other was built on ROA (ROA solution). These Web Services solutions were subjected to load performance test using Apache JMeter. The results showed that the tail tolerance of Web Services solution built on ROA is significantly better than its equivalent conventional solution. Specifically, we established that ROA is capable of improving the tail tolerance of Web Services solution by about 4.60% with 96% confidence. The results also affirm the scalability capability of ROA.

Keywords: ROA, latency variability, tail tolerance, java EE and web services.

INTRODUCTION

Scalability of Web Services is vital to its large scale deployment (Ekuobase and Onibere, 2011). However, guaranteed responsiveness of web services solutions may not be possible on a large scale, if the solutions are not tail tolerant (Dean and Barroso, 2013). Tail tolerant systems are systems that tolerate or mitigate latency variability including high tail-latency i.e. rare outrageous response times (Dean and Barroso, 2013). High tail-latency is therefore a serious threat to a responsive large scale Web Services solution.

Several techniques basically centered on replication have been proposed to curb high tail-latency in online service systems/applications (Dean and Barroso, 2013). These systems/applications are seriously prone to the problem of latency variability and tail latency. However, none of these techniques appears to target building responsive large scale Web Services solution (service applications built on the middle ware architecture called web services). Web Services solution has a unique nature of stateful/conversational asynchronous distributed orientation and use of TCP based technology such as SOAP (Baldoni *et al*., 2002; Ekuobase and Onibere, 2011, 2013; Ekuobase and Ebietomere, 2012). This drew our attention to the server-side software architecture – Replication Oriented Architecture (ROA) proposed by Ekuobase and Onibere (2011) which is aimed at helping application programmers build scalable Web Services solution. However, a critical examination of ROA in our domain of interest – latency variability and tail tolerance, exposed the need to also authenticate ROA's capability to mitigate latency variability including high tail-latency. The following observations encouraged this decision:

- The originators of ROA (Ekuobase and Onibere, 2011) only saw latency variability (guaranteed responsiveness) as an inherent scalability attribute (Ekuobase and Ebietomere, 2012) but never investigated it specifically for latency variability much less high tail-latency (Ekuobase and Onibere, 2013); thus creating an impression that scalable (web services) applications also guarantee responsiveness.
- Round the clock guaranteed responsiveness is a critical attribute of tail-tolerant systems but they could only give a 90% guarantee of 32% scalability assurance.

Consequently, we investigated whether or not ROA accommodates tail tolerance and if it does, by how much? This is the essence of this project, to determine the tail-tolerance capability of ROA.

The data collected, manipulated and interpreted were basically response times i.e. the time needed to process a query which is the time from sending a request until receiving the response (Yang *et al*., 2006; Repp *et al*., 2007). It is an important attribute of Web Services' Performance (Yang *et al*., 2006; Repp *et al*., 2007). According to the World Wide Web consortium (W3C), performance is defined in terms of throughput, response

*Corresponding author email: godspower.ekuobase@uniben.edu

time, latency, execution time, and transaction time (www.w3.org). However, execution time and latency are sub-concepts of the W3Cs definition of response time (Repp *et al*., 2007).

A service's response time for a request, R, can be represented as shown below:

Response time(R) = Execution time(R) + Waiting time(R) (1)

The execution time is the duration of performing service functionality. The waiting time is the amount of time for all possible mediate events including message transmissions between service consumers and providers (Yang *et al*., 2006). From the service consumer perspective, we can see response time as the duration starting from the issue of a request to the end of the receipt of a service's response. On the other hand, service providers see response time as not being different from the execution time of a service, so it does not include all possible mediate events, which are seen as incontrollable variables during service execution (Yang *et al*., 2006).

Latency, which is an attribute of response time, is defined as the delay between the start of a message transmission from one process and the beginning of its receipt by another. It can be measured as the time required in transferring an empty message (Coulouris *et al*., 2012). In its general sense, it covers; (1) the time taken for the first bit of a string of bits transmitted in a distributed system to reach its destination. (2) The delay in accessing resources, which increases significantly when the system is heavily loaded, and (3) The time taken by the system's communication services at both the sending and the receiving processes, which varies according to the current load on the system (Coulouris *et al*., 2012).

The data transfer rate (speed at which data can be transferred between the two resources in distributed systems once transmission or message passing has begun, usually quoted in bits per second) is also a contributing factor to performance. It is determined primarily by physical characteristics, whereas latency is determined primarily by software overheads, routing delays and a load-dependent statistical element arising from conflicting demands for access to transmission channels. Considering that many of the messages transferred between processes in distributed systems are small in size; latency is therefore often of equal or greater significance than the transfer rate in determining performance (Coulouris *et al*., 2012). Thus, Web Services solution's architecture like ROA should be able to mitigate latency variability and present to the service consumers a consistent response time that is within an acceptable standard.

Keeping latency consistent within reasonable limit, thereby keeping the tail of latency distribution short, is a challenge to Web Services solutions as the size and complexity of the system scales up or as overall use increases (Dean and Barroso, 2013). Latency variability results from occasional high-latency episodes that tends to overshadow the overall service performances of large scale systems/applications. Software techniques that tolerate latency variability are vital to building responsive large-scale Web services (Dean and Barroso, 2013). Factors that may encourage variability in latency include (Dean and Barroso, 2013):

- Sharing of systems resources such as CPU cores, processor caches, memory bandwidth etc. between and within applications.
- Usage of systems resources by background daemons.
- Global resource sharing by applications running on machines.
- Periodic maintenance activities.
- Multiple layers of queuing in intermediate resource such as servers and network switches.
- Garbage collection
- Energy management due to switching between inactive power saving modes and active modes

Dean and Barroso (2013) established that it is not feasible to eliminate latency variability completely and hence introduced two tail-tolerant techniques that mask or work around temporary latency deviations. The techniques are of two classes: the Within-Request Short-Term Adaptations and the Cross-Request Long-Term Adaptations.

Within-Request Short-Term Adaptations (WRSTA)

This class of techniques basically deploys multiple replicas of data items to provide additional throughput capacity and maintain availability in the presence of failures. One challenge posed by WRSTA is that it is basically suited for read-only and loosely consistent datasets, and is effective only when the phenomena that causes variability does not tend to simultaneously affect multiple request replicas. The techniques under this class include Hedged and Tied requests:

Hedged requests: Here a user send the same request to multiple replicas (e.g. servers) and use the results from whichever replica that responds first. The client first send the request to the replica believed to be the most appropriate but then falls back on sending a secondary request after a brief delay. Once a response is received, other requests are cancelled.

Tied requests: Here a request is simultaneously queued in multiple replicas. The replicas communicate with one another concerning the status of the resultant responses. An executing server sends a cancellation message to the other servers. Delay interval can be introduced to avoid sending the request at the same time.

Observe that these techniques will likely congest transmission channels further and result in wastage of computational resources. Besides, they defy a necessary property of replication - transparency (Coulouris *et al*., 2012; Ekuobase and Onibere, 2011).

Cross-Request Long-Term Adaptations (CRLTA)
These techniques are suited for reducing latency variability caused by coarse-grained phenomena such as service-time variations and load balancing. They include:

Micro-Partitions: The systems generate many more partitions than there are machines in the service, then do dynamic assignment and load balancing of these partitions to particular machines.

Selective Replication: This is an enhancement of the micro-partitioning scheme, it detects items that are likely to cause load imbalance and create additional replicas of these items. Load balancing systems can then use the additional replicas to spread the load of these hot micro-partitions across multiple machines without having to actually move the micro partitions.

Latency-Induced Probation: Here machines with high latency are placed on probation and reincorporated when its latency has improved.

Though CRLTA addresses the problem of transparency, resource wastage and congestion of transmission media, it is however difficult to implement. Besides, they are more oriented towards handling latency at the systems level and not at the application level. A situation we choose to refer to as macro and micro latency respectively. ROA appears to be more oriented towards handling micro latency.

MATERIALS AND METHODS

The following sub-section describes the hardware and software tools as well as the process used in this research.

Hardware Tools
A notebook computer (HP Pavilion dv6 Notebook PC, Intel® Core(TM) i3 CPU @ 2.13 GHz 2.13 GHz, 4.0GB of RAM and 300GB of Hard Disk) was used not only in development and testing of the Web Services solution but also to carry out performance test to check for latency variability and tail tolerance. It also served as host to the software used and developed in this research. A lower configuration may not conveniently cope with the huge size and nature of our development platform as well as the high computational resource requirements for executing our applications and testing them for tail tolerance.

Software Tools
We shall discuss software tools under Operating System, Development Platform, Language, Integrated Development Environment (IDE) and Packages.

❖ **Operating System:** We settled for Microsoft Windows 7 Home Premium edition which worked seamlessly with the other tools used in the research. The Operating System enabled our applications and other software tools to interact with the machine and tap its computational and peripheral resources.

❖ **Development Platform**: The choice of Java EE (Jendrock *et al*., 2006) as our development platform for building the Web Services solution in preference to the .NET platform is because Java EE is non-proprietary and it rivals with .NET platform as the dominant application developer's platform for enterprise applications in general and Web Services solution in particular (Vawter and Roman, 2001; Williams, 2003; Birman, 2005). Also our prior comfortable programming experience in Java boosted our choice of Java EE.

❖ **Language:** Language here covers programming language, modeling language and Database Management System (DBMS). Java 7.0 was the preferred programming language of choice since the application was built on Java EE platform which has support for only Java. Java Persistence Query Language (JPQL), a version of the Structured Query Language (SQL) was adopted because of its rich Application Programming Interfaces (APIs) for interacting with databases. Our choice of Objectdb as our DBMS for building and managing the databases was based on its very good performance and seamless compatibility with Java and Netbeans – our Integrated Development Environment of choice.

❖ **Integrated Development Environment (IDE):** We have several IDEs that support Java and these include JBuilder, JCreator, Eclipse, and Netbeans. We chose Netbeans (Netbeans 7.0) on the ground of familiarity though it is not in any way less powerful than the others. IDE makes application development easy, nimble and interesting.

❖ **Packages:** Argo UML (Ramirez *et al*., 2006; Tolke and Klink, 2006) was used for the UML design. Though there are many testing packages which include Apache JMeter, JUnit, Grinder, Siege, JProfiler, selenium, Tsung, and Load Runner; for request generation, load testing of Web Services application and capturing of response time which is vital to this research. We used Apache JMeter (http://jakarta.apache.org/) because it is open source, Java based and has rich and easy to use User Interface (UI). Besides, it is the testing tool also used by the originators of ROA (Ekuobase and Onibere, 2013). JMeter was added as plug-in to Netbeans to ease its use with IDE. Microsoft Excel was used for result computation. The Alentum

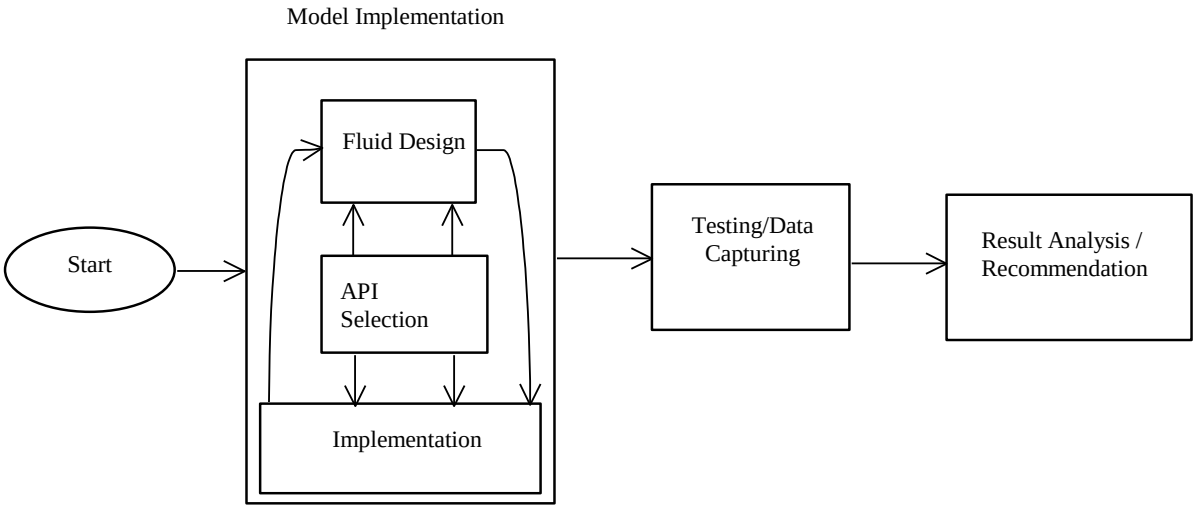

Fig.1. The Research Process.

Software Advanced Grapher was used for the graphical reporting of results.

Process

Figure 1 depicts a tailored systems analysis and design (SAD) research process used in this work.

We relied on the agile software development methodology established by Ekuobase and Onibere (2012, 2013) as the most appropriate for the project. Our test software development project of choice is the Automated Teller Machine (ATM) Fund Transfer System. This choice is predicate on the fears raised by Ekuobase and Onibere (2011) and the features of the ATM system also exposed by Ekuobase and Onibere (2012, 2013). The design of the ATM system as modelled by Ekuobase and Onibere (2012, 2013) was adopted. A Web Services solution was built using appropriate APIs of the Java platform using Netbeans 7.0 IDE. The solution consists of five endpoint replica built on ROA. We chose to implement only the five endpoint replica of ROA since it gave the optimum scalability result for our test problem – the ATM Fund Transfer Service (Ekuobase and Onibere, 2013). Besides, the five endpoint replica solution's computational strength data appears more regular (Ekuobase and Onibere, 2013). We also built a similar web services solution using the conventional approach void of ROA.

We, however used a different set of Java APIs for the implementation of the prototype ATM Fund Transfer system on ROA. The new set of implementation API's were Enterprise Java Bean (EJB), Java API for XML Web Services (JAX-WS), Java Message Service (JMS), Message Driven Bean (MDB) and Java Persistent API (JPA). These APIs were selected to design the implementation equivalence of ROA depicted in figure 2. The choice of these APIs is predicate on the drive not only to refine the implementation of ROA but also to demonstrate that ROA can be realised in several ways using diferrent technology and platforms. In particular, JPA a relatively new Java API handles how relational data is mapped to persistent entity objects, how these objects are stored in a relational database, and how an entity's state is persisted. In this realization, the JAX-WS receives a SOAP request, implicitly deserializes the request and, using the round robin mechanism, enqueues the resultant data in a JMS queue for some queues defined by the number of replicas; each replica has its own queue. A replica, implemented as MDB, listens and fetches the data in its JMS queue that it is statically bound to, using the MDB onMessage method. The replica then invokes the EJB that performs the business logic and with help of the JPA persist in memory (database) the computational state of the operation performed.

For the conventional implementation of the system i.e. implementation not based on ROA, we made use of JAX-WS, EJB and JPA as depicted in figure3. The EJB and JPA allow the web services to seamlessly communicate with the database. Observe that the selected APIs for the ROA implementation have JMS and MDB, in addition, that were used to realize the replicas in ROA. The use of JAX-WS for the ROA implementation as with the conventional implementation is particularly soothing because of the criticism that the ROA implementation equivalent used by Ekuobase and Onibere (2012, 2013) does not realize a Web Services solution but just a service solution. Besides, this ROA implementation is more coarsely grained than that of Ekuobase and Onibere (2012, 2013).

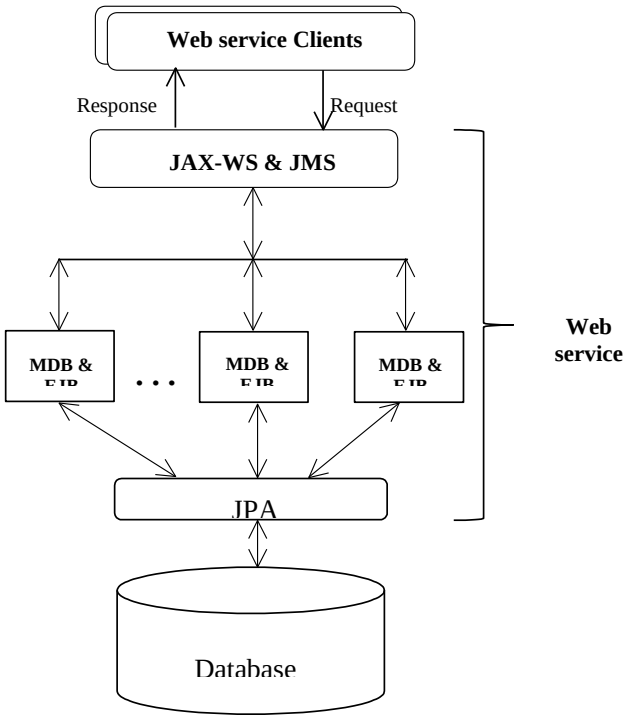

Fig. 2. A ROA Implementation Equivalence using Java Technology.

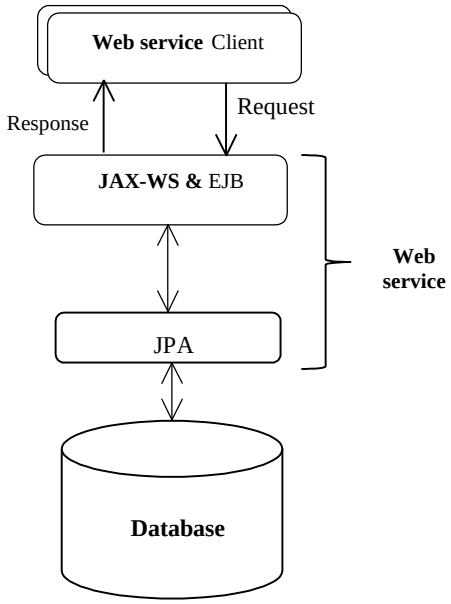

Fig. 3. A Conventional Implementation of Web Services using Java Technology.

We also made us of a small sized database built using ObjectDB an open source Object Database Management System (ODBMS) for about 30 account holders with a varying fictitious amounts in the accounts. The software development and deployment environment was Netbeans 7.0 with GlassFish 3.1 as the server.

Codes for the Conventional and ROA implementations will be supplied on request.

These systems are all server side applications and we therefore need a client to consume them. Apache JMeter played this role. Apache JMeter (Halili, 2008) is not only a load generator but a load and performance testing tool.

Table 1. Data Capture for Conventional Web Services Solution.

DATA CAPTURE FROM IMPLEMENTATION WITHOUT ROA					
NO OF SAMPLES	AVERAGE	MEDIAN	90TH PERCENTILE	MINIMUM	MAXIMUM
5	4	4	6	4	6
10	3	3	4	2	6
20	4	4	7	3	7
30	3	3	4	3	10
40	4	4	4	3	17
50	4	3	4	2	35
100	3	3	4	2	15
200	3	3	3	2	154
300	5	3	4	2	208
400	5	3	4	2	209
500	8	3	6	2	317
1000	27	4	16	2	2386
2000	42	14	92	2	2478
3000	291	321	514	2	4411
4000	563	569	944	3	5428
5000	791	790	1420	3	6299
10000	1930	1753	4230	3	10884

Table 2. Data Capture for the ROA Web Services Solution.

DATA CAPTURE FROM ROA IMPLEMENTATION					
NO OF SAMPLES	AVERAGE	MEDIAN	90TH PERCENTILE	MINIMUM	MAXIMUM
5	3	3	3	3	6
10	5	4	8	3	9
20	4	4	7	2	10
30	6	6	6	4	16
40	3	3	4	2	5
50	3	3	5	2	22
100	3	3	4	2	5
200	2	3	3	2	11
300	3	3	4	2	18
400	3	3	4	2	23
500	3	3	3	2	22
1000	3	3	4	2	68
2000	6	3	9	1	227
3000	8	4	19	1	163
4000	18	7	41	1	423
5000	30	9	80	1	577
10000	25	10	51	1	1045

It can handle variety of request from HTTP request to SOAP request depending on how its test plan is prepared.

We subjected the web services solutions to performance test under varying loads ranging from five to 10000 requests per 5 seconds using Apache JMeter. The resultant data samples' median, maximum, minimum, average and 90th percentile response times for each of the solutions were collected. We then entered this data into Alentum Grapher for appropriate graphical presentation. The maximum response times value were further

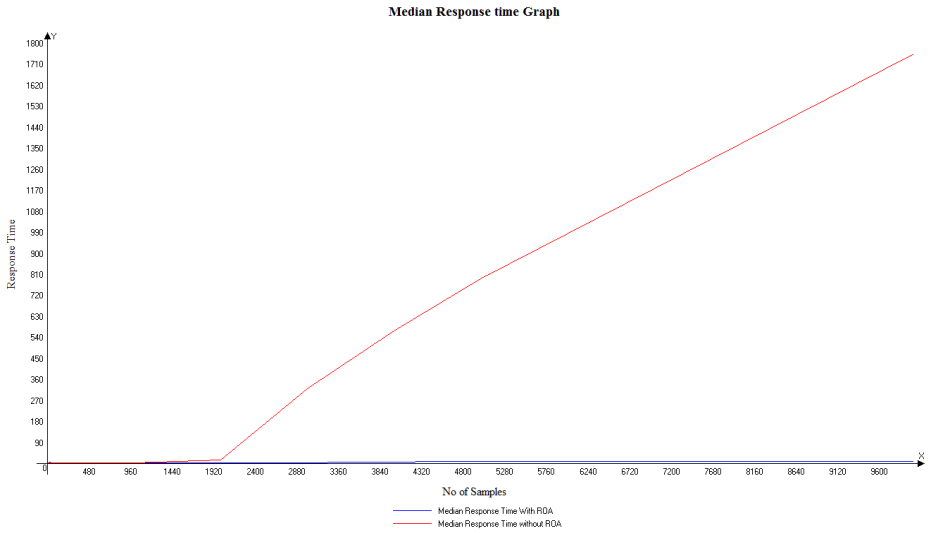

Fig. 4. The Mid-response Time of Conventional vs. ROA Web Services Solutions.

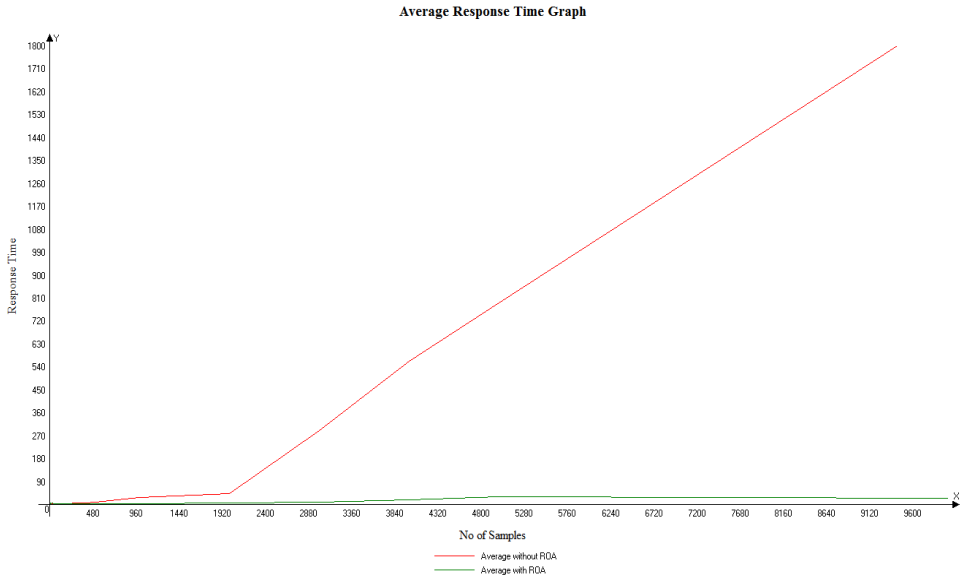

Fig. 5. The Average-response Time of Conventional vs. ROA Web Services Solutions.

subjected to statistical analysis and interpretation; since maximum response times best captures the highest tail latency of applications.

In particular, we ascertained the tail tolerance significance of the Web Services solution built on ROA over that built using the conventional approach. Since the two classes of Web Services solution were built on the same problem and platforms but with different development approaches, the student t-distribution for difference of two means was found most appropriate and adopted. The samples x and y are the maximum response times for the conventional and ROA solutions respectively. Let x and y be normally distributed with means μ_x and μ_y, and variance σ_x and σ_y respectively. The problem is to decide whether or not the use of ROA will mitigate the tail latency of Web Services solution.

Consequently, we tested the hypothesis H_0: $\mu_x = \mu_y$ (no tail tolerant significance between conventional and ROA systems), H_1: $\mu_x > \mu_y$ (ROA systems are significantly tail tolerant) and H2: $\mu_x < \mu_y$ (conventional system are significantly tail tolerant).

RESULTS AND DISCUSSION

After configuration the JMeter, we executed the package for varying number of threads (sample size) for each of

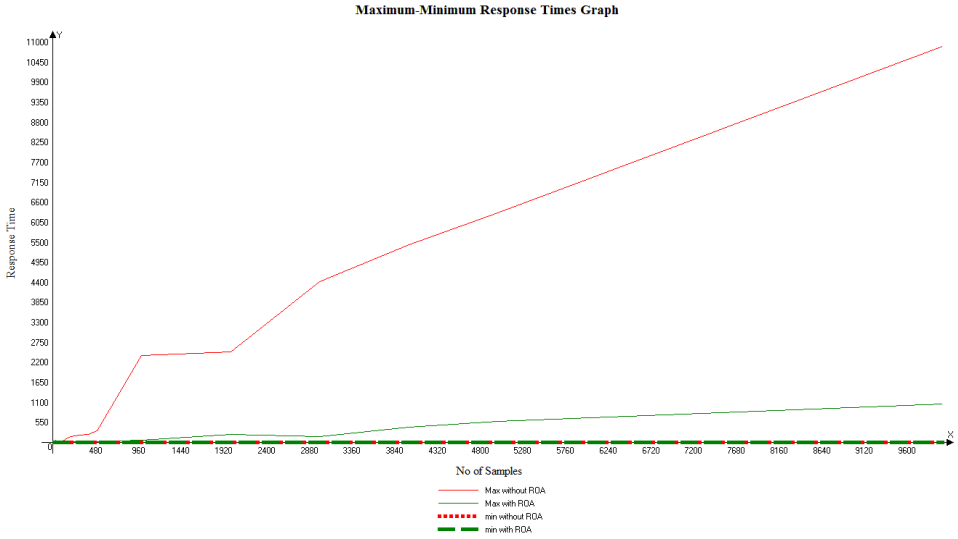

Fig. 6. The Maximum and Minimum Response Time of Conventional vs. ROA Web Services Solutions.

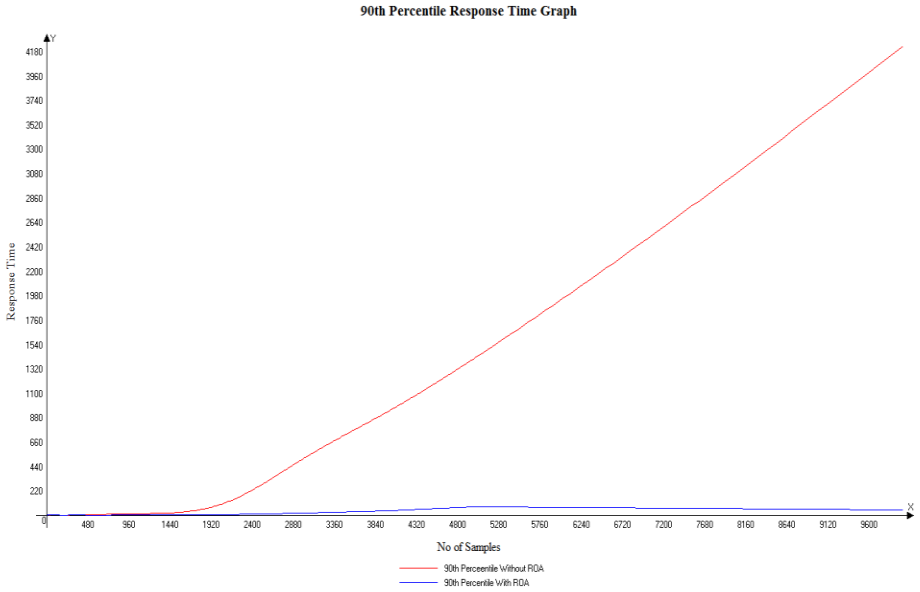

Fig. 7. The 90th Percentile Response Time of Conventional vs. ROA Web Services Solutions.

the two system implementations and the valuable data: average, median (mid), 90th percentile line, minimum and maximum response times; all in milliseconds were collected. Tables 1 and 2 contain these data for the conventional and ROA web services solution respectively.

For ease of appreciation, figures 4 to 8 depict graphically the relative behaviour of both applications with increasing number of request per unit time as explained underneath each of the figures.

Figure 4 captures the mid response times of both the conventional web services solution and those of the web services solution built on ROA with increasing number of request per unit time. Observe the near constant response time of the ROA solution even with increasing request per unit time as against that of the conventional solution which assumed a near exponential increase of response time with increasing request per unit time. The implication of this is that web services solutions built on ROA is far more stable and hence more scalable than its conventional counterparts. This affirms Ekuobase and Onibere (2013) scalability authentication of ROA. Also their maximum sample size was 2000 requests per 5 seconds against ours with a maximum sample size of 10000 requests per 5 seconds. Note that the behaviour of the conventional solution against the ROA solution

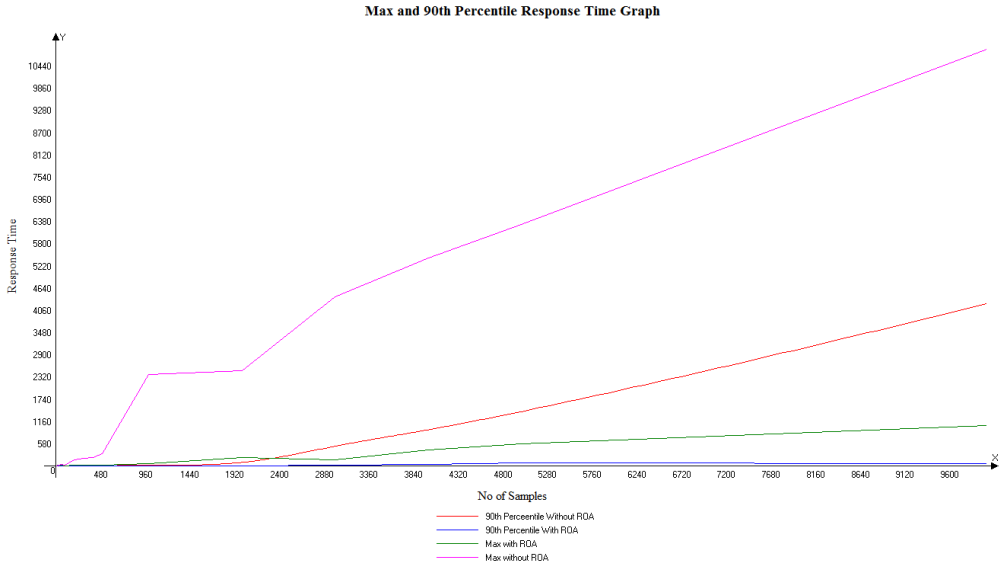

Fig. 8. The 90th Percentile and Maximum Response Time of Conventional vs. ROA Web Services Solutions

Table 3. Showing the computation of ns^2 for each web services solution.

S/n	Conventional Tail Latency (x)	$(x-\bar{x})^2$	ROA Tail Latency (y)	$(y-\bar{y})^2$
1	6	3715369.633	6	22464.71972
2	6	3715369.633	9	21574.42561
3	7	3711515.574	10	21281.6609
4	10	3699965.398	16	19567.07266
5	17	3673084.986	5	22765.48443
6	35	3604413.927	22	17924.48443
7	15	3680755.104	5	22765.48443
8	154	3166724.927	11	20990.89619
9	208	2977451.751	18	19011.54325
10	209	2974001.692	23	17657.71972
11	317	2613167.339	22	17924.48443
12	2386	204729.6332	68	7723.307958
13	2478	296448.2215	227	5057.719723
14	4411	6137860.516	163	50.66089965
15	5428	12211324.69	423	71351.83737
16	6299	19057333.46	577	177340.0727
17	10884	80110923.75	1045	790530.1903
	$\bar{x}$ =1933.529412	$n_x s_x^2$ =155550440.2	$\bar{y}$ =155.8823529	$n_y s_y^2$=1275981.765

skyrocketed particularly after the 2000 mark. An indication that the 32% scalability performance of web services solution built on ROA over the conventional solution is the least it could be. Mid response time is however not a useful indicator of latency variability or tail latency.

Figure 5 captures the average response time of the conventional and ROA web services solutions with increasing number of requests per unit time. It appears not to be different from the graph in figure 4 and therefore same analysis holds for both.

Figure 6 captures the maximum and minimum response time with increasing number of requests per unit time for both the conventional and ROA web services solutions. Note that the difference between the maximum and minimum for the conventional web services solution is far wider than that of the web services solution built on ROA. In particular, the response time for the ROA solution hardly exceeded 0.5seconds. This shows that web services solution built on ROA has tighter latency variability or guaranteed responsiveness against their conventional counterparts.

Figure 7 captures the 90th percentile response time of conventional vs. ROA web services solutions with increasing number of request per unit time. It appears not to be different from the graph in figures 4 and 5 and therefore same analysis holds here too. Besides, the graph also shows that web services solution built on ROA has tighter latency variability or guaranteed responsiveness against their conventional counterparts.

Figure 8 captures the 90th percentile and maximum response times of conventional vs. ROA web services solutions with increasing number of request per unit time. It obviously indicates that both applications are bedeviled with the problem of tail latency with the ROA solution however more tail tolerant. Whether this tail tolerant advantage of ROA web services solution over its conventional counterpart is significant and if it is, by what degree is however not obvious?

Statistical Analysis and Interpretation

It will be noted that the two sets of Web Services solutions were built on the same platform, using the same technology except that the ROA's solution was built on unique development architecture – ROA. It is also important to note that the performance load test and request generator was handled by the same package – Apache JMeter, and configured the same way.

The samples x and y are the maximum response time (tail latency) at varying but increasing request rates for the conventional and ROA solutions respectively. Let x and y be normally distributed with means μ_x and μ_y and variance σ_x and σ_y respectively. The problem is to decide whether or not the use of ROA will improve the tail tolerance of Web Services solution. Consequently, we tested the hypothesis H_0: $\mu_x = \mu_y$ (no tail tolerant significance between conventional and ROA systems), H_1: $\mu_x > \mu_y$ (ROA systems are significantly tail tolerant) and H2: $\mu_x < \mu_y$ (conventional system are significantly tail tolerant); since tail tolerance is about mitigating tail latency with increasing request per unit time.

It is safe to assume that $\sigma_x = \sigma_y$, and then apply the formula below (Hoel, 1966):

$$t = \frac{(\bar{x}-\bar{y})-(\mu_x-\mu_y)}{\sqrt{n_x s_x^2+n_y s_y^2}} \sqrt{\frac{n_x n_y (n_x+n_y-2)}{n_x+n_y}} \quad (2)$$

Where, t is the student's t distribution for difference of two means and every other elements of equation (2) assume the conventional statistical use.

In our case, sample sizes are equal and equal to 17 i.e. $n_x = n_y = 17$; therefore equation (2) can be rewritten as:

$$t = \frac{(\bar{x}-\bar{y})-(\mu_x-\mu_y)}{\sqrt{n_x s_x^2+n_y s_y^2}} \sqrt{272} \quad (3)$$

Adopting the null hypothesis H_0, we can rewrite equation (3) as equation (4) below:

$$t = \frac{(\bar{x}-\bar{y})}{\sqrt{n_x s_x^2+n_y s_y^2}} \sqrt{272} \quad (4)$$

but, $ns^2 = \sum_{i=1}^{n}(x-\bar{x})^2$ (5)

Table 3 shows the computation of ns^2 for each solution: conventional solution followed by solutions built on ROA while table 4 shows the calculation details of t, for each Web Services solution.

From the student's t table (Hoel, 1966) the 0.02 critical value of t is 2.224. Observe that the calculated t value (2.3411022) is greater than 2.224, therefore, the hypothesis H_1: $\mu_x > \mu_y$ is valid and hereby accepted. Thus, tail tolerance of Web Services solution built on ROA is significantly better than its equivalent conventional solution.

Table 4. Showing the Computed t Value and Confidence Limit for Conventional vs. ROA's Solution.

Computed Value	ROA web services solution
$\bar{x}-\bar{y}$	1777.6471
$n_x s_x^2 + n_y s_y^2$	156826422
$\sqrt{n_x s_x^2 + n_y s_y^2}$	12523.036
$(\bar{x}-\bar{y})/\sqrt{n_x s_x^2 + n_y s_y^2}$	0.1419502
t	**2.3411022**
k = $(\sqrt{n_x s_x^2 + n_y s_y^2})/\sqrt{272}$	759.3206
2.224 * k	1688.729
α	88.91811
β	3466.376
$(\alpha/\bar{x}) * 100$	**4.5987**

It is also important we calculate the confidence limit for μ_x - μ_y as ROA's solution show significantly better tail tolerance performance over its equivalent conventional solution. Here equation (3) comes handy and in our case 96 percent confidence limits is given by:

$|t| < 2.224$ (6)

Substituting (3) in (6), reduces (6) to:

$$\alpha < \mu_x - \mu_y < \beta \quad (7)$$

Where α and β are the lower and upper limits respectively and are given by:

$$\alpha = (\bar{x} - \bar{y}) - 2.224\left(\frac{\sqrt{n_x s_x^2 + n_y s_y^2}}{\sqrt{272}}\right) \quad (8)$$

$$\beta = (\bar{x} - \bar{y}) + 2.224\left(\frac{\sqrt{n_x s_x^2 + n_y s_y^2}}{\sqrt{272}}\right) \quad (9)$$

Table 4 also show these calculated value for the ROA's solution.

Consequently, we can only guarantee α unit of increase i.e. $\alpha/\bar{x}$ percent in tail tolerance performance, if ROA is used to build Web Services solution. These results show that ROA can improve tail tolerance of Web Services solution by 4.60% with 96% confidence. This is the maximum degree of significance that can be guaranteed.

CONCLUSION

Guaranteed responsiveness of Web Services solutions may not be possible on a large scale, if the solutions are not tail tolerant i.e. able to consistently keep latency within reasonable limit. Software techniques that tolerate latency variability and in particular, tail latency are vital to building responsive large-scale Web services (Dean and Barroso, 2013). However, such efforts directed at making network applications tail tolerant are basically oriented towards handling latency at the systems or deployment level and not at the application or development level. ROA though proposed to help application programmers build scalable Web Services solutions (Ekuobase and Onibere, 2011), appears capable of mitigating latency variability and tail latency at the application or development level. Consequently, we investigated ROA for tail tolerance.

We realized a new ROA implementation equivalence also using Java technology but with a different set of Java APIs from that of Ekuobase and Onibere (2012, 2013). This implementation equivalence appears more of a Web Service implementation than theirs. We built two ATM Web Services solution using Java technology – the first was not built on ROA (conventional solution) but the other was built on ROA (ROA solution). The choice of the ATM system as the test problem was to investigate ROA in its worst case scenario (Ekuobase and Onibere, 2011, 2012, 2013).

The graphical and statistical analysis of the resultant data on subjecting the Web Services solution built on ROA to load performance test using Apache JMeter compared to the conventional solution showed that the tail tolerance of Web Services solution built on ROA is significantly better than its equivalent conventional solution. Besides, the statistical analysis of the results shows that ROA is capable of improving the tail tolerance of Web Services solution by about 4.60% with 96% confidence. The results also affirm the scalability capability of ROA (Ekuobase and Onibere, 2013).

REFERENCES

Baldoni, R., Marchetti, C. and Termini, A. 2002. Active Software Replication through a Three-tier Approach. Proceedings of the 21st IEEE Symposium on Reliable Distributed Systems (SRDS). IEEE Computer. pp10.

Birman, K. 2005. Can Web Services Scale Up? IEEE Computer. 38(10): 107-110.

Coulouris, G., Dollimore, J., Kindberg, T. and Blair, G. 2012. Distributed System: Concepts and Design. Addison-Wesley, USA. pp1047.

Dean, J. and Barroso, LA. 2013. The Tail at Scale. Communications of the ACM. 56(2):74-80.

Ekuobase, GO. and Ebietomere, EP. 2012. The Making of Replication Oriented Architecture. Journal of Computer Science. 23(2):71-78.

Ekuobase, G. and Onibere, E. 2011. Architecture For Scalable Web Services Solution. Canadian Journal of Pure and Applied Sciences. 5(1):1449-1453.

Ekuobase, GO. and Onibere, EA. 2012. Web Services Solution on Replication Oriented Architecture (ROA). Journal of the Ghana Science Association. 14(2):25-34.

Ekuobase, GO. and Onibere, EA. 2013. Scalability of Web Services Solution Built on ROA. Canadian Journal of Pure and Applied Sciences. 7(1):2251-2270.

Halili, E. 2008. Apache JMeter: a practical beginner's guide automated testing and performance measurement for your websites. Packt Publishing, United Kingdom. pp129.

Hoel, PG. 1966. Introduction to Mathematical Statistics, (3rd edi.). John Willey & Sons, USA. pp427.

Jendrock, E., Ball, J., Carson, D., Evans, I., Fordin, S. and Haase, K. 2006. The Java EE 5 Tutorial (3rd edi.). Sun Microsystems, USA. pp1304.

Ramirez, A., Vanpeperstraete, P., Rueckert, A., Odutola, K., Bennett, J., Tolke, L. and van der Wulp, M. 2006. Argo UML User Manual: A Tutorial and Reference Description. Open Content, USA. Also available online at http://www.opencontent.org/openpub/. pp386.

Repp, N., Berbner, R., Heckmann, O. and Steinmetz, R. 2007. A cross-Layer Approach to Performance

Monitoring of Web Services. Emerging Web Services Technology. Birkhauser Verlag, Switzerland. Whitestern Series:21-32.

Tolke, L. and Klink, M. 2006. Cook book for Developers of ArgoUML: An Introduction to Developing ArgoUML. University of California, USA. pp157.

Vawter, C. and Roman, E. 2001. J2EE vs. Microsoft.NET: A Comparison of Building XML-based Web Services. Sun Microsystems, USA. pp28.

Williams, J. 2003. The Web Services Debate: J2EE vs. NET. Communication of the ACM. 46(6):59-63.

Yang, S. J., Zhang, J. and lan, BC. 2006. Service Level Agreement-Based QoS Analysis for Web Services Discovery and Composition. International Journal of Internet and Enterprise Management. Inderscience. 1251-1271.

Received: Feb 15, 2014; Accepted: April 3, 2014

SENRA Academic Publishers, British Columbia
Vol. 8, No. 2, pp. 2955-2961, June 2014
Online ISSN: 1920-3853; Print ISSN: 1715-9997

Canadian Journal of pure&applied sciences

A NEW APPROACH FOR THE LOGARITHMS OF REAL NEGATIVE NUMBERS

*Ashwani K Thukral[1] and Om Parkash[2]
[1]Department of Botanical and Environmental Sciences, Guru Nanak Dev University, Amritsar -143005
[2]Department of Mathematics, Guru Nanak Dev University, Amritsar -143005, India

ABSTRACT

Logarithms were defined for real positive numbers with a real positive base, but were later extended to real negative numbers with a real positive base. Logarithms of real negative numbers to a real positive base were defined as complex numbers. The Neparian logarithms take into consideration the hyperbola transcribed by the function $f(x) = 1/x$, $x>0$ for real positive axis. On a parallel analogy, we extend this concept to the real negative axis for the hyperbola transcribed by $1/x$ for $x<0$. This paper examines the concept of logarithms from its basics to prove that the logarithms of real negative numbers to real negative base are real numbers. The concept of logarithms as applicable to both real positive and real negative numbers has been generalized.

Keywords: Logarithms; real negative numbers; exponential function, computational sciences.

INTRODUCTION

It is a known fact that in the field of mathematics, logarithms have introduced new transcendent sizes and have widened the field of comprehension of numericals. The origin of the concept of logarithms goes back to John Napier (1950-1617) who used arithmetic and geometric progressions as a basis of his work. Neparian logarithms as given by Napier are shifted by $10^7 \ln 10^7$ with respect to the logarithms used presently (Lexa, 2013). Napier designed an ingenious mathematical tool at a time when the concepts of modern mathematics were not laid. The Napier's concept evolved into the present day logarithmic function which became indispensable to the development of science and technology.

1 Development of the concept

Napier, initially described logarithms through geometry and not as the inverse of the exponential function. Today, the natural logarithmic function is usually defined as the inverse of the natural exponential function or through the integral equation

$$\ln(x) = \int_1^x (1/t)dt, x > 0 \qquad (1.1)$$

Logarithms were initially defined for all real positive numbers, and it was Euler who discovered ways to describe logarithms in terms of power series, and also successfully defined logarithms of complex and negative numbers, which expanded the field of logarithms. Earlier to Euler, logarithms of real negative numbers were defined as equal to logarithms of real positive numbers of the same magnitude (Wikipedia, 2013) as given by

$$\log_b(x) = \log_b(-x)$$

This fact emanates from the additivity property of logarithms, given by

$$2\log_b(-x) = \log_b(-x)^2 = \log_b(x)^2 = 2\log_b(x) \qquad (1.2)$$

Later Euler gave a formula known as Euler's identity, given by

$$e^{i\pi} + 1 = 0, \qquad (1.3)$$

where '*e' is Euler's constant and* $i = \sqrt{-1}$. This defined the logarithm of (-1):

$$\log_e(-1) = i\pi .$$

This paved a way for the field of logarithms of complex numbers.

Logarithmic functions play a significant role in solving complicated mathematical expressions and thus are important in the field of mathematics. Shannon (1948) whose discovery of entropy made a remarkable impact for measuring uncertainty contained in probabilistic experiments, had to develop his mathematical model involving logarithmic function for measuring information content. Many other researchers extended Shannon's (1948) entropy in terms of logarithmic functions under diverse situations. Recently, Parkash and Thukral (2010) investigated and developed certain logarithmic models for measuring diversity in biological systems.

*Corresponding author email: akthukral.gndu@gmail.com

Logarithms are extensively used in various disciplines like population dynamics Vandermeer (2010), social sciences (2013) and other fields. Developments in the field of logarithms may be attributed to several authors, notably Joost Burgi, Johannes Kepler, Gregoire de Saint-Vincent, Leonard Euler and others (Lexa, 2013; Wikipedia, 2013). Euler first defined the exponential function and related it to the natural logarithm. The present day terminology of the logarithms is attributed to Leibnitz and Newton (Lefort, 2013).

The present paper provides a new approach to define the logarithms of negative real numbers using a multiplicative constant (-1) as a coefficient to the logarithm base. The necessity for the present work arises to fulfill the gaps in the derivation of the logarithmic functions for the negative real numbers defined over the negative real axis. The software used in this paper are http://rechneronline.de/function-graphs/, http://wims.unice.fr and MS-Excel software.

As is seen from figure 1, $y = \frac{1}{x}$ transcribes hyperbolas in the first and the third quadrants. The curve in the first quadrant defines the logarithmic function for positive real numbers whereas the curve in the third quadrant has never been considered for defining any such function. The curve for $y = \ln(x)$ for positive real x-axis is given in figure 2. We stress here that a similar curve can be constructed for the real negative axis using the graphical presentation provided in the third quadrant of figure 2.

2 Logarithms of real negative numbers

In the literature, the logarithms of real positive numbers are defined as the inverse function of exponential function, given by

$$b^y = x \tag{2.1}$$

such that logarithm of x to the base b is defined as,

$$\log_b x = y \tag{2.2}$$

where x is a real positive number, y is a real number, and b is a real positive number base of the logarithm (generally 10, or 2 or e). Multiply equation (2.1) with a constant $c = \pm 1$, referred to herein as the coefficient,

$$c(b^y) = cx. \tag{2.3}$$

Keeping in view the equation (2.3), we now define the logarithmic function as

$$\log_{c,b}(cx) = y \tag{2.4}$$

where c represents the coefficient ($\pm$ 1) to the base b>1 and x>0.

For c = +1, the logarithmic equation (2.2) for real positive numbers is obtained. For, c = -1 we get, the logarithms of real negative numbers as

$-(b^y) = -x$, b>1 and x>0, i.e.,

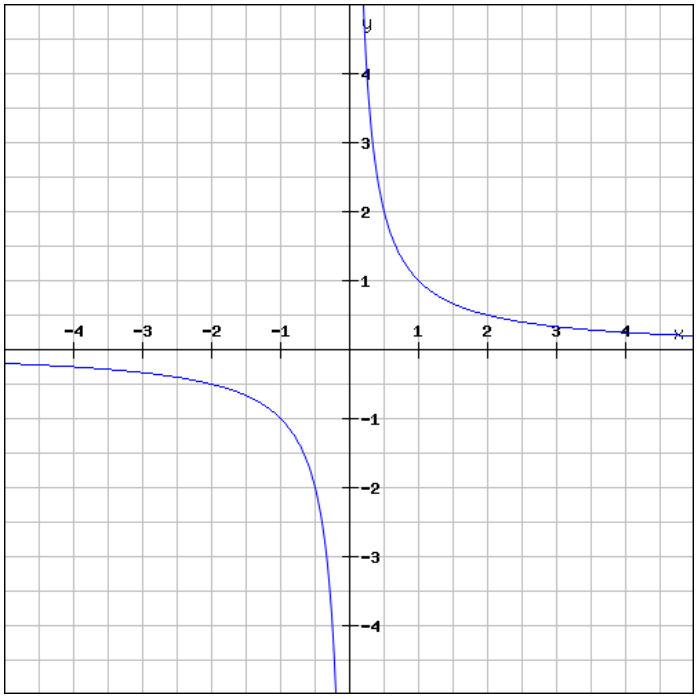

Fig. 1. Graph between x and 1/x.

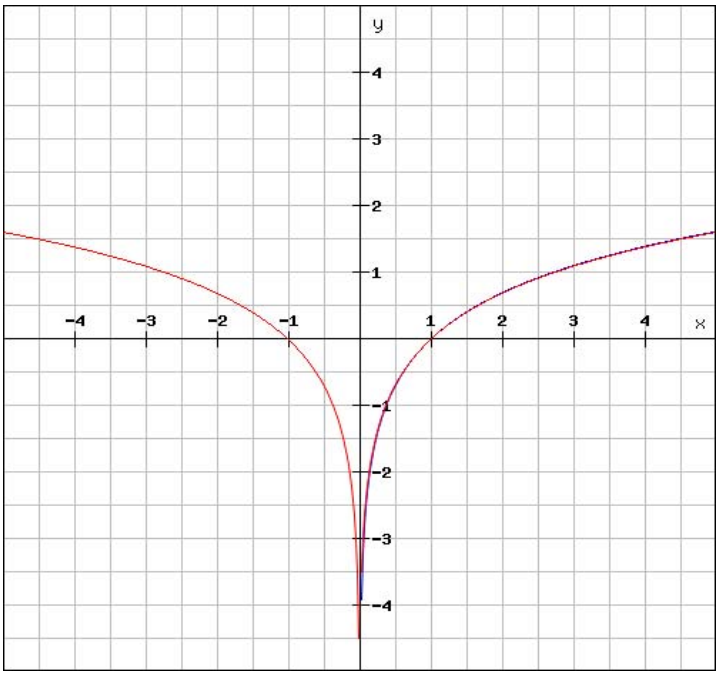

Fig. 2. Graph between x and lnn(x) (left), and ln(x) (right)

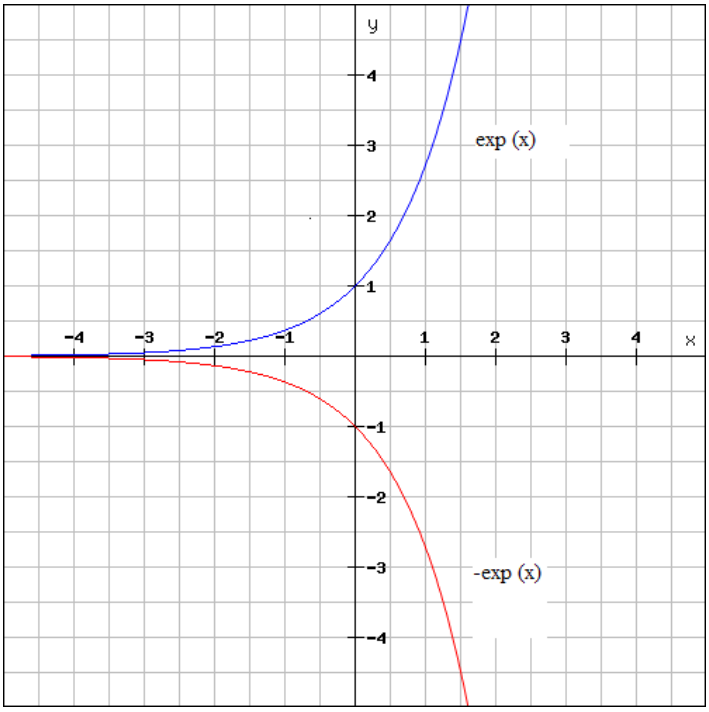

Fig. 3. Graph between x and exp(x) (upper curve), and -exp(x) (lower curve)

$$\log_{-1,b}(-x) = y \qquad (2.5)$$

For example,

$\log_{-1,10}(-100) = 2$, since, $-(10^2) = -100$.

In this case, the coefficient (-1) is not raised to the power 'y' and is a multiplicative constant only. In the terminology of the present context, the base of a logarithm is cb, where b>1, and c = 1 for logarithms on the positive real axis 'x', and c = -1 for the negative real axis 'x'.

3. Necessity for the present concept

Under the notion held till now, the logarithm of a real negative number say, x = -100, to the base 'b', say, b=10, is $\log_{10}(-100) = y$, such that,

$$b^y = -x. \quad (3.1)$$

That is, the logarithm of (– 100) will be the value of y that satisfies the equation,

$$(10)^y = -100. \quad (3.2)$$

Equation (3.2) contradicts equation (2.5) since the coefficient, c = -1 multiplies only on one side of the equation (2.1). Another alternative to evaluate this logarithm would be

$$(-b)^y = -x. \quad (3.3)$$

That is, the logarithm of - 100 will be the value of y which satisfies the equation

$$(-10)^y = -100. \quad (3.4)$$

Equation (3.4) contradicts equation (2.5) since the coefficient (-1) on the left hand side is not to be raised to the power y. The logarithms of real positive or real negative numbers should therefore be defined as per the equations (2.3, 2.4).

Thus, to obtain the logarithm of (-100), we apply equation (2.5) as follows:

$$\log_{-1,10}(-100) = 2, \quad (3.5)$$

Since

$$-(10)^2 = -100 \quad (3.6)$$

which justifies the proposed method to find the logarithm of negative real numbers. If the base of the function is Euler's constant e, then

$$-(e^y) = -x, \quad (3.7)$$

that is,

$$\log_{-1,e}(-x) = y. \quad (3.8)$$

It is self evident that logarithm of a real positive number with a coefficient of c = 1, is equal to the logarithm of real negative number with a coefficient of c = -1. The logarithm of -1 to the base $-e$ will be,

$\log_{-1,e}(-1) = 0$, Since,

$$-(e^0) = -1. \quad (3.9)$$

The inverse of the natural negative logarithmic function is, $-(e^x)$. The present paper also proves the existence of negative exponential function. A graph for positive and negative exponential functions is given in figure 3.

For convenience, log to the base (-e) may be called lnn(x) (log natural negative). In its integral form lnn (x) may be defined as

$$\log_{-1,e}(-x) = \int_{-1}^{-x} \frac{1}{t} dt = -\int_{-x}^{-1} \frac{1}{t} dt, \text{ for } x>0. \quad (3.10)$$

The properties of logarithms of negative real numbers to a negative base are given in table 1.

Table 1. Properties of logarithms of real negative and real positive numbers as per the proposed concept.

Property	Coefficient	Explanation
General definition of logarithm	c = +1, or c = -1	$\log_{c,b}(cx) = y$ Such that $c(b^y) = cx,\ x > 0, b > 1$
	c = 1	$\log_{+1,b}(x) = y$, or $\log_b(x) = y$ Such that $b^y = x,\quad x > 0, b > 1$
	c = -1	$\log_{-1,b}(-x) = y$ Such that $-(b^y) = -x \quad x > 0, b > 1$

Table 1 continue..

Property	Coefficient	Explanation
Earlier definition of logarithms of negative real numbers with a positive real base	$c_1 = +1$, $c_2 = -1$	$\log_{c_1,b}(c_2 x) = y$ Such that $c_1(b^y) = c_2 x$, $x > 0, b > 1$ Or, $\log_{+1,b}(-x) = y$ Such that $(b^y) = -x$, $x > 0, b > 1$, y is a complex number.
Equivalence		$\log_{-1,b}(-x) = \log_{+1,b}(+x)$, $x > 0, b > 1$
Product	c_1 and c_2 are same or different real number coefficients $(c_1, c_2 = \pm 1)$.	$\log_{c_1,b}(c_1 x_1) + \log_{c_2,b}(c_2 x_2) = \log_{c_1 c_2,b}(c_1 c_2 x_1 x_2)$, $x_1, x_2 > 0, b > 1$
	c_1 , $c_2 = +1$	$\log_{+1,b}(+x_1) + \log_{+1,b}(+x_2) = \log_{+1,b}(x_1 x_2)$, $x_1, x_2 > 0, b > 1$
	c_1 , $c_2 = -1$	$\log_{-1,b}(-x_1) + \log_{-1,b}(-x_2) = \log_{+1,b}(x_1 x_2)$, $x_1, x_2 > 0, b > 1$
	$c_1 = -1$, $c_2 = +1$ (or *vice versa*)	$\log_{-1,b}(-x_1) + \log_{+1,b}(x_2) = \log_{-1,b}(-x_1 x_2)$, $x_1, x_2 > 0, b > 1$
Quotient	When c_1 , c_2 are the same or different real number coefficients c_1 , $c_2 = \pm 1$.	$\log_{c_1,b}(c_1 x_1) - \log_{c_2,b}(c_2 x_2) = \log_{(c_1/c_2),b}(c_1 x_1 / c_2 x_2)$, $x_1, x_2 > 0, b > 1$
	When the coefficients of both real numbers x_1 and x_2 are negative (c_1 , $c_2 = -1$).	$\log_{-1,b}(-x_1) - \log_{-1,b}(-x_2) = \log_{+1,b}(x_1 / x_2)$, $x_1, x_2 > 0, b > 1$
	When the coefficient of real number x_1 is negative -1 and x_2 is positive +1.	$\log_{-1,b}(-x_1) - \log_{+1,b}(x_2) = \log_{-1,b}(-x_1 / x_2)$, $x_1, x_2 > 0, b > 1$
Power, $c(x^n)$	$c = +1$, or $c = -1$	$\log_{c,b} c(x^n) = n(\log_{c,b} cx)$, $x > 0, b > 1$
	$c = +1$	$\log_{+1,b}[+(x^n)] = n[\log_{+1,b}(x)]$, $x > 0, b > 1$, The log will be a real number.
	$c = -1$	$\log_{-1,b}[-(x^n)] = n[\log_{-1,b}(-x)]$, $x > 0, b > 1$, The log will be a real number.
Power, $(-x)^n$		$\log_b(-x)^n = n[\log_b(-x)]$, $x > 0, b > 1$ The value of log will be a complex number.
Base switch	$c = +1$, or c = -1	$\log_{c,b}(cx) = \dfrac{1}{\log_{c,x}(cb)}$, $x > 0, b > 1$
	$c = +1$	$\log_{+1,b}(+x) = \dfrac{1}{\log_{+1,x}(+b)}$, $x > 0, b > 1$

continue…

Table 1 continue..

Property	Coefficient	Explanation
Base switch		
	c = -1	$\log_{-1,b}(-x) = \dfrac{1}{\log_{-1,x}(-b)},\ x>0, b>1$
Base change	c = +1, or c = -1	$\log_{c,b}(cx) = \dfrac{\log_{c,e}(cx)}{\log_{c,e}(cb)},\ x>0, b>1$
	c = +1	$\log_{+1,b}(+x) = \dfrac{\log_{+1,e}(+x)}{\log_{+1,e}(+b)}, x>0, b>1$
	c = -1	$\log_{-1,b}(-x) = \dfrac{\log_{-1,e}(-x)}{\log_{-1,e}(-b)},\ x>0, b>1$
Antilog of log	c = +1, or c = -1	If $\log_{c,b}(cx) = y$, then $x = b^y,\ x>0, b>1$
	c = +1	If $\log_{+1,b}(+x) = y$, then $x = b^y$
	c = -1	If $\log_{-1,b}(-x) = y$, then $-x = -b^y$
Inverse functions of log natural and log natural negative	c = +1, or c = -1	$ce^x,\ x>0$
	c = +1	$e^x,\ x>0$
	c = -1	$-e^x,\ x>0$
Log natural of coefficient, c	c = +1, or c = -1	$\log_{c,e} c = 0$
	c = +1	$\log_{+1,e}(+1) = 0$
	c = -1	$\log_{-1,e}(-1) = 0$
Integral form	c = +1, or c = -1	$\log_{c,e}(cx) = \int_c^{cx} (1/t)dt$, $x>0$
	c = +1	$\log_{+1,e}(+x) = \int_1^{x} (1/t)dt$, $x>0$.
	c = -1	$\log_{-1,e}(-x) = \int_{-1}^{-x} (1/t)dt = -\int_{-x}^{-1} (1/t)dt$, $x>0$.

CONCLUSION

The present concept uses hyperbola in quadrant III of the graph for 1/x, and proves that the logarithms of real negative numbers on a real negative base are real numbers. The concept will have wide applications in basic and computational sciences.

ACKNOWLEDGEMENTS

Thanks are due to the University Grants Commission, New Delhi, India for financial assistance.

REFERENCES

Lefort, X. 2013. History of the logarithms. An example of the development of a concept in mathematics. www.gobiernodecanarias.org. 1-9.

Lexa, MA. 2013. Remembering John Napier and his logarithms. www.see.ed.ac.uk/~mlexa/supportingdoc/mlexa_napier_revised.pdf. 1-13.

Parkash, O. and Thukral, AK. 2010. Statistical measures as measures of diversity. Int. J. Biomath. 3:173-185.

Shannon, CE. 1948. A mathematical theory of communication. Bell System Technical Journal. 27:379-423, 623-659.

Vandermeer, J. 2010. How populations grow: The exponential and logistic equations," Nature Education Knowledge. 3-10 (15):1-7.

Wikipedia. 2013. Logarithm. http://en.wikipedia.org/wiki/Logarithm. 1-20.

Wikipedia. 2013. Contributions of Leonhard Euler to mathematics. http://en.wikipedia.org/wiki/Contributions_of_Leonhard_Euler_to_mathematics. 1-6.

Received: Feb 8, 2014; Accepted: April 1, 2014

SENRA Academic Publishers, British Columbia
Vol. 8, No. 2, pp. 2963-2967, June 2014
Online ISSN: 1920-3853; Print ISSN: 1715-9997

Canadian Journal of pure & applied sciences

PORTFOLIO OPTIMIZATION USING MEASURES OF CROSS ENTROPY

*Om Parkash and Mukesh
[1]Department of Mathematics, Guru Nanak Dev University, Amritsar- 143005, India

ABSTRACT

It is a well-known fact that in the literature of information theory, a variety of divergence (distance or cross entropy) measures is available, each with its own merits and limitations. These measures are applicable to various disciplines of Mathematical Sciences. One such discipline pertaining to Operations Research is portfolio analysis. In the present communication, we have developed two new parametric measures of cross entropy and consequently provided the applications of these measures for the study of optimization principles for the development of measures of risk in portfolio analysis. We have observed that minimizing these measures implies the minimization of the expected utility of the risk-prone person and maximization of the expected utility of a risk-averse person.

Keywords: Portfolio selection theory, cross entropy, mean-variance efficient frontier, uncertainty.

INTRODUCTION

Markowitz (1952) introduced the modern portfolio selection theory, which deals with the relevant beliefs about future performances and ends with the choice of portfolio. We consider a fundamental rule that the investor should consider expected return a desirable thing and variance of return an undesirable thing. Markowitz (1952) illustrated geometrically relations between beliefs and choice of portfolio according to the "expected returns-variance of returns" rule. It is worth mentioning that some of the investments made by the investor may yield low returns, but these may be compensated by considerations of relative safety because of a proven record of non-volatility in price fluctuations. On the other hand, there might be some better investments which would be promising and achieve high expected returns, but these may be prone to a great deal of risk. However, investor's major problem is to find a satisfactory measure of risk. The earliest measure proposed for the return on all investments was variance and its proposal was based upon the fundamental argument that risk increases with variance. Accordingly, Markowitz (1952) introduced the concept of mean-variance efficient frontier, which enabled him to find all the possible efficient portfolios that simultaneously maximize the expected returns and minimize the variance.

Jianshe (2005) developed a new theory of portfolio and risk based on incremental entropy and Markowitz's (1952) theory. He developed this theory by replacing arithmetic mean return adopted by Markowitz (1952), with geometric mean return as a criterion for assessing a portfolio. The new theory emphasizes that there is an objectively optimal portfolio for given probability of returns. Some portfolio optimization methodology has been discussed by Bugár and Uzsoki (2011) whereas other work related with diversification of investments has been provided by Markowitz (1959). Bera and Park (2008) remarked that Markowitz's (1952) mean-variance efficient portfolio selection is the one of the most widely used approaches in solving portfolio diversification problem. However, contrary to the notion of diversification, mean-variance approach often leads to portfolios highly concentrated on a few assets. In their paper, Bera and Park (2008) have proposed to use cross entropy measure as the objective function with side conditions coming from the mean and variance-covariance matrix of the resampled asset returns and illustrated their procedure with an application to the international equity indexes. Now since risk is associated with the concept of uncertainty, we should be able to develop measures of risk based on the concepts of divergence or cross entropy. We can develop such measures of divergence and then show how we can develop efficient frontiers for maximizing expected returns and simultaneously minimize measures of risk.

In the literature, there exist many well-known measures of divergence which find their applications to a variety of fields. One such measure is due to Kullback-Leibler (1951), which is an important measure of distance and is very useful in many real life situations. This measure is given by

$$D_{KL}(P;Q)=\sum_{i=1}^{n} p_i \log\frac{p_i}{q_i}. \qquad (1.1)$$

Recently, Parkash and Mukesh (2011) have introduced a new measure of cross entropy (divergence), given by

$$D(P;Q)=\sum_{i=1}^{n}\left(\frac{p_i^2}{q_i}+\frac{q_i^2}{p_i}-2p_i\right), \qquad (1.2)$$

and based on this divergence measure (1.2), Parkash and

*Corresponding author email: omparkash777@yahoo.co.in

Mukesh (2012a) have developed an optimization principle for the measurement of risk in portfolio analysis.

It has been observed that generalized measures of cross entropy should be introduced because upon optimization, these measures lead to useful probability distributions and mathematical models in various disciplines. These generalized measures introduce flexibility in the system. Some parametric measures of directed divergence are:

$$D_R(P;Q)=\frac{1}{\alpha-1}\log\left(\sum_{i=1}^{n}p_i^{\alpha}q_i^{1-\alpha}\right),\ \alpha\neq 1,\alpha>0, \qquad (1.3)$$

which is Renyi's (1961) probabilistic measure of directed divergence.

$$D_{HC}(P;Q)=\frac{1}{\alpha-1}\left(\sum_{i=1}^{n}p_i^{\alpha}q_i^{1-\alpha}-1\right),\ \alpha\neq 1,\alpha>0, \qquad (1.4)$$

which is Havrada and Charvat's (1967) probabilistic measure of divergence. Some other interesting findings related with the literature of cross entropy have been provided by Taneja and Kumar (2004), Pardo (2003), Parkash and Mukesh (2012b) etc.

In the present communication, we introduce two new parametric measures of cross entropy and make their use for the measurement of risk in portfolio analysis. Before developing these measures, we need a brief introduction to the concept of mean-variance efficient frontier due to Markowitz (1952). This introduction has been provided by Kapur and Kesavan (1992) as explained below:

1.1 Markowitz (1952) mean-variance efficient frontier

Let π_j be the probability of the jth outcome for $j=1,2,\ldots,m$ and r_{ij} be the return on the ith security for $i=1,2,\ldots,n$ when the jth outcome occurs. Then the expected return on the ith security is given by

$$\bar{r}_i=\sum_{j=1}^{m}\pi_j r_{ij},\quad i=1,2,\ldots,n. \qquad (1.5)$$

Also, variances and covariances of returns are given by

$$\sigma_i^2=\sum_{j=1}^{m}\pi_j\left(r_{ij}-\bar{r}_i\right)^2,\ i=1,2,\ldots,n, \qquad (1.6)$$

and

$$\rho_{ik}\sigma_i\sigma_k=\sum_{j=1}^{m}\pi_j\left(r_{ij}-\bar{r}_i\right)\left(r_{kj}-\bar{r}_k\right),\ i,k=1,2,\ldots,n;\ i\neq k. \qquad (1.7)$$

Let a person decide to invest proportions $x_1,x_2,\ldots,x_n$ of his capital in n securities. Assume that $x_i\geq 0$ for all i, and that

$$\sum_{i=1}^{n}x_i=1. \qquad (1.8)$$

Then, the expected return and variance of the return are given by

$$E=\sum_{i=1}^{n}x_i\bar{r}_i, \qquad (1.9)$$

And

$$V=\sum_{i=1}^{n}x_i^2\sigma_i^2+2\sum_{k=1}^{n}\sum_{i<k}x_i x_k\rho_{ik}\sigma_i\sigma_k\ . \qquad (1.10)$$

Markowitz (1952) suggested that $x_1,x_2,\ldots,x_n$ be chosen to maximize E and to minimize V or alternatively, to minimize V when E is kept at a fixed value. Now

$$V=\sum_{j=1}^{m}\pi_j\left(x_1r_{1j}+x_2r_{2j}+\cdots+x_nr_{nj}-x_1\bar{r}_1-x_2\bar{r}_2-\cdots-x_n\bar{r}_n\right)^2$$
$$=\sum_{j=1}^{m}\pi_j\left(R_j-\bar{R}\right)^2, \qquad (1.11)$$

where

$$R_j=\sum_{i=1}^{n}x_i r_{ij}\quad\text{and}\quad\bar{R}=\sum_{i=1}^{n}x_i\bar{r}_i. \qquad (1.12)$$

that is, R_j is the return on investment when the jth outcome arises and $\bar{R}$ is the mean return on investment.

Next, we discuss an optimizational principle developed by Parkash and Mukesh (2012a) by using divergence measure (1.4).

1.2 Optimization Principle developed by Using Measure (1.2)

Markowitz's (1952) criterion for a choice from $x_1,x_2,\ldots,x_n$ was to minimize the variance, that is, to make $R_1,R_2,\ldots R_m$ as equal as possible among themselves. Any departure of $R_1,R_2,\ldots R_m$ from equality was considered a measure of risk. The same purpose can be accomplished if we choose $x_1,x_2,\ldots,x_n$ so as to minimize the directed divergence measure given by (1.2) of the distribution $P=\left(\frac{\pi_1R_1}{\sum_{j=1}^{m}\pi_jR_j},\frac{\pi_2R_2}{\sum_{j=1}^{m}\pi_jR_j},\cdots,\frac{\pi_mR_m}{\sum_{j=1}^{m}\pi_jR_j}\right)$ from $\pi=(\pi_1,\pi_2,\ldots,\pi_m)$, that is, we choose $x_1,x_2,\ldots,x_n$ so as to minimize the following measure:

$$D(P;\pi)=\sum_{j=1}^{m}\left(\frac{P_j^2}{\pi_j}+\frac{\pi_j^2}{P_j}-2P_j\right)$$
$$=\sum_{j=1}^{m}\left(\frac{\pi_j^2R_j^2}{\bar{R}^2\pi_j}+\frac{\pi_j^2\bar{R}}{\pi_jR_j}-\frac{2\pi_jR_j}{\bar{R}}\right)$$
$$=\frac{1}{\bar{R}^2}\sum_{j=1}^{m}\pi_jR_j^2+\bar{R}\sum_{j=1}^{m}\frac{\pi_j}{R_j}-2, \qquad (1.13)$$

where $\sum_{j=1}^{m}\pi_jR_j=\sum_{j=1}^{m}\pi_j\sum_{i=1}^{n}x_ir_{ij}=\sum_{i=1}^{n}x_i\bar{r}_i=\bar{R}.$ (1.14)

Thus, we can formulate an optimization principle as follows:

Choose $x_1,x_2,\ldots,x_n$ so as to minimize

$$\sum_{j=1}^{m}\pi_j\left(x_1r_{1j}+x_2r_{2j}+\cdots+x_nr_{nj}\right)^2+\sum_{j=1}^{m}\frac{\pi_j}{\left(x_1r_{1j}+x_2r_{2j}+\cdots+x_nr_{nj}\right)}, \qquad (1.15)$$

subject to

$$\sum_{j=1}^{m}\pi_j\left(x_1r_{1j}+x_2r_{2j}+\cdots+x_nr_{nj}\right)=\text{Constant}, \quad (1.16)$$

$$x_1+x_2+\cdots x_n=1, \quad (1.17)$$

and $x_1\geq 0, x_2\geq 0,\ldots,x_n\geq 0$.

Next, we propose two new parametric measures of cross entropy and study some of their essential properties.

2 New parametric measures of cross entropy

In this section, we consider the following set of all complete finite discrete probability distributions:

$$\Omega_n=\left\{P=(p_1,p_2,\ldots,p_n):\ p_i>0,\sum_{i=1}^{n}p_i=1\right\},\ n\geq 2, \quad (2.1)$$

and introduce the following parametric measure of cross entropy.

2.1 One parametric measure of cross entropy

For $P,Q\in\Omega_n$, we propose a new parametric measure of cross entropy given by the following expression:

$$D_\alpha(P;Q)=\frac{\sum_{i=1}^{n}p_i\left(\alpha+\frac{1}{2}\right)^{\log\frac{p_i}{q_i}}-1}{\alpha-\frac{1}{2}},\ \alpha>0,\ \alpha\neq\frac{1}{2}. \quad (2.2)$$

where α is a real parameter.

Note: We have

$$\lim_{\alpha\to\frac{1}{2}}D_\alpha(P;Q)=\lim_{\alpha\to\frac{1}{2}}\left[\frac{\sum_{i=1}^{n}p_i\left(\alpha+\frac{1}{2}\right)^{\log\frac{p_i}{q_i}}-1}{\alpha-\frac{1}{2}}\right]=\sum_{i=1}^{n}p_i\log\frac{p_i}{q_i},$$

which is Kullback-Leibler's (1951) measure of cross entropy. Thus, $D_\alpha(P;Q)$ is a generalized measure of cross entropy.

Some of the important properties of this cross entropy are:

1. $D_\alpha(P;Q)$ is a continuous function of $p_1,p_2,\ldots,p_n$ and $q_1,q_2,\ldots,q_n$.
2. $D_\alpha(P;Q)\geq 0$ and vanishes if and only if $P=Q$.
3. We can deduce from condition (2) that the minimum value of $D_\alpha(P;Q)$ is zero.
4. We shall now prove that $D_\alpha(P;Q)$ is a convex function of both P and Q. This result is important in establishing the property of global minimum.

Let

$$D_\alpha(P;Q)=f(p_1,p_2,\ldots,p_n;q_1,q_2,\ldots,q_n)$$

$$=\frac{\sum_{i=1}^{n}p_i\left(\alpha+\frac{1}{2}\right)^{\log\frac{p_i}{q_i}}-1}{\alpha-\frac{1}{2}}.$$

Thus $\frac{\partial f}{\partial p_i}=\frac{\left[1+\log\left(\alpha+\frac{1}{2}\right)\right]\left(\alpha+\frac{1}{2}\right)^{\log\frac{p_i}{q_i}}}{\alpha-\frac{1}{2}}$,

$$\frac{\partial^2 f}{\partial p_i^2}=\frac{\log\left(\alpha+\frac{1}{2}\right)\left[1+\log\left(\alpha+\frac{1}{2}\right)\right]\left(\alpha+\frac{1}{2}\right)^{\log\frac{p_i}{q_i}}}{\left(\alpha-\frac{1}{2}\right)p_i}\ \forall\ i=1,2,\ldots,n,$$

and $\frac{\partial^2 f}{\partial p_i\partial p_j}=0\ \forall\ i,j=1,2,\ldots,n;\ i\neq j$.

Hence, the Hessian matrix of the second order partial derivatives of f with respect to $p_1,p_2,\ldots,p_n$ is given by $H_1=a_{ij}$, where

$$a_{ij}=\begin{cases}\dfrac{\log\left(\alpha+\frac{1}{2}\right)\left[1+\log\left(\alpha+\frac{1}{2}\right)\right]\left(\alpha+\frac{1}{2}\right)^{\log\frac{p_i}{q_i}}}{\left(\alpha-\frac{1}{2}\right)p_i}, & i=j\\ 0, & i\neq j\end{cases},$$

which is positive definite. Similarly one can prove that the Hessian matrix of second order partial derivatives of f with respect to $q_1,q_2,\ldots,q_n$ is positive definite. Thus, we conclude that $D_\alpha(P;Q)$ is a convex function of both $p_1,p_2,\ldots,p_n$ and $q_1,q_2,\ldots,q_n$. Moreover, with the help of numerical data shown in the following table 1, we have presented $D_\alpha(P;Q)$ as shown in the following figure 1.

Table 1. $D_\alpha(P;Q)$ against p for $n=2,\alpha=10$.

p	q	$D_\alpha(P;Q)$
0.1	0.5	0.5906
0.2	0.5	0.3104
0.3	0.5	0.1310
0.4	0.5	0.0317
0.5	0.5	0.0000
0.6	0.5	0.0317
0.7	0.5	0.1310
0.8	0.5	0.3104
0.9	0.5	0.5906

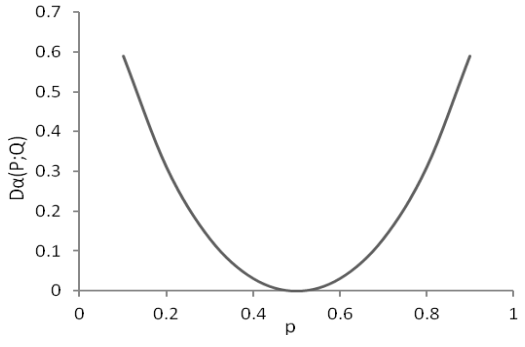

Fig. 1. Convexity of $D_\alpha(P;Q)$ with respect to P.

Under the above conditions, the function $D_{\alpha}(P;Q)$ is a valid parametric measure of cross entropy.

Next, we propose a two parametric measure of cross entropy.

2.2 Two parametric measure of cross entropy

For any $P,Q \in \Omega_n$, we propose a new parametric measure of cross entropy given by

$$D_{\alpha,\beta}(P;Q)=\frac{\sum_{i=1}^{n} p_i\left(\frac{\alpha}{2\beta}+\frac{1}{2}\right)^{\log\frac{p_i}{q_i}}-1}{\alpha-\beta},\ \alpha>0,\beta>0,\ \alpha\neq\beta. \quad (2.3)$$

Where α,β are real parameters representing some environmental factors, and the presence of these parameters gives a great deal of flexibility towards applications and also take into account the factors which might not have been possible otherwise.

Note: We have

$$\lim_{\substack{\alpha\to\frac{1}{2}\\ \beta\to\frac{1}{2}}} D_{\alpha,\beta}(P;Q)=\lim_{\substack{\alpha\to\frac{1}{2}\\ \beta\to\frac{1}{2}}}\left[\frac{\sum_{i=1}^{n} p_i\left(\frac{\alpha}{2\beta}+\frac{1}{2}\right)^{\log\frac{p_i}{q_i}}-1}{\alpha-\beta}\right]=\sum_{i=1}^{n} p_i\log\frac{p_i}{q_i}.$$

Thus, $D_{\alpha,\beta}(P;Q)$ is a generalization of Kullback-Leibler's (1951) measure of cross entropy.

Some of the important properties of this cross entropy are:

1. $D_{\alpha,\beta}(P;Q)$ is a continuous function of $p_1,p_2,\ldots,p_n$ and $q_1,q_2,\ldots,q_n$.
2. $D_{\alpha,\beta}(P;Q)\geq 0$ and vanishes if and only if $P=Q$.
3. We can deduce from condition (2) that the minimum value of $D_{\alpha,\beta}(P;Q)$ is zero.
4. We shall now prove that $D_{\alpha,\beta}(P;Q)$ is a convex function of both P and Q.

Let $D_{\alpha,\beta}(P;Q)=g(p_1,p_2,\ldots,p_n;q_1,q_2,\ldots,q_n)$

The Hessian matrix of the second order partial derivatives of g with respect to $p_1,p_2,\ldots,p_n$ is given by $H_2=b_{ij}$, where

$$b_{ij}=\begin{cases}\dfrac{\log\left(\frac{\alpha}{2\beta}+\frac{1}{2}\right)\left[1+\log\left(\frac{\alpha}{2\beta}+\frac{1}{2}\right)\right]\left(\frac{\alpha}{2\beta}+\frac{1}{2}\right)^{\log\frac{p_i}{q_i}}}{(\alpha-\beta)p_i}, & i=j,\\ 0, & i\neq j\end{cases}$$

which is positive definite. A similar result is also true when we consider the partial derivatives of g with respect to $q_1,q_2,\ldots,q_n$. Thus, we conclude that $D_{\alpha,\beta}(P;Q)$ is a convex function of both $p_1,p_2,\ldots,p_n$ and $q_1,q_2,\ldots,q_n$. Moreover, we have presented $D_{\alpha,\beta}(P;Q)$ against p for $n=2,\alpha=10,\beta=15$ as shown in the following figure 2.

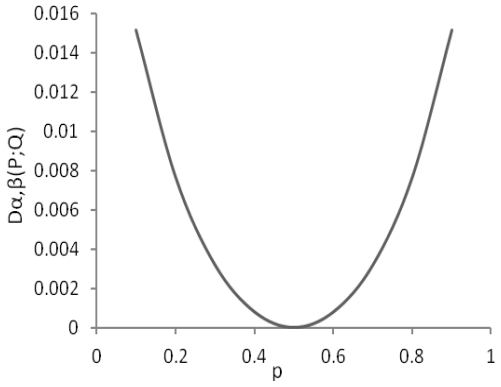

Fig. 2. Convexity of $D_{\alpha,\beta}(P;Q)$ with respect to P.

Under the above conditions, the function $D_{\alpha,\beta}(P;Q)$ is a valid parametric measure of cross entropy.

3 Measuring risk in portfolio analysis using parametric measures of cross entropy

In this section, we consider the following two cases for measuring risk in portfolio analysis by using two different parametric measures of cross entropy:

3.1 Measure of risk by using cross entropy (2.2)

Recently, Parkash and Mukesh (2012a) provided an optimization principle involving non-parametric measure of cross entropy (1.2) for the development of measures of risk when a person decides to invest proportions of his capitals in different securities. If we use one parametric measure of divergence developed in (2.2), we get a measure of risk in accordance with the optimization principle discussed in subsection 1.2. This measure is developed as follows:

$$R_1=\frac{\sum_{j=1}^{m} P_j\left(\alpha+\frac{1}{2}\right)^{\log\frac{P_j}{\pi_j}}-1}{\alpha-\frac{1}{2}}=\frac{\sum_{j=1}^{m}\frac{\pi_j R_j}{\bar{R}}\left(\alpha+\frac{1}{2}\right)^{\log\frac{\pi_j R_j}{\bar{R}\pi_j}}-1}{\alpha-\frac{1}{2}}$$

$$=\frac{\frac{1}{\bar{R}}\sum_{j=1}^{m}\pi_j\left[R_j\left(\alpha+\frac{1}{2}\right)^{\log\frac{R_j}{\bar{R}}}\right]-1}{\alpha-\frac{1}{2}}$$

$$=\frac{1}{\alpha-\frac{1}{2}}\left[\frac{1}{\bar{R}}E\left(R\left(\alpha+\frac{1}{2}\right)^{\log\frac{R}{\bar{R}}}\right)-1\right]. \quad (3.1)$$

If $\alpha<\frac{1}{2}$, minimizing the measure (3.1), we mean the maximization of expected utility of a person whose utility function is given by $u_1(x)=x\left(\alpha+\frac{1}{2}\right)^{\log\frac{x}{\bar{R}}}$. In this case the

person is risk-averse. If $\alpha > \frac{1}{2}$, minimizing the measure (3.1), we mean minimization of the expected utility of a person whose utility function is given by $u_1(x) = x\left(\alpha + \frac{1}{2}\right)^{\log\frac{x}{\bar{R}}}$. In this case the person is risk-prone.

Thus, minimizing this measure implies the minimization of the expected utility of the risk-prone person and maximization of the expected utility of a risk-averse person.

3.2 Measure of risk by using cross entropy (2.3)

If we use the two parametric measure of cross entropy developed in (2.3), we can get another measure of risk discussed below:

$$R_2 = \frac{\sum_{j=1}^{m} P_j\left(\frac{\alpha}{2\beta}+\frac{1}{2}\right)^{\log\frac{P_j}{\pi_j}} - 1}{\alpha-\beta} = \frac{\sum_{j=1}^{m} \frac{\pi_j R_j}{\bar{R}}\left(\frac{\alpha}{2\beta}+\frac{1}{2}\right)^{\log\frac{\pi_j R_j}{\bar{R}\pi_j}} - 1}{\alpha-\beta}$$

$$= \frac{\frac{1}{\bar{R}}\sum_{j=1}^{m}\pi_j\left[R_j\left(\frac{\alpha}{2\beta}+\frac{1}{2}\right)^{\log\frac{R_j}{\bar{R}}}\right] - 1}{\alpha-\beta}$$

$$= \frac{1}{\alpha-\beta}\left[\frac{1}{\bar{R}}E\left(R\left(\frac{\alpha}{2\beta}+\frac{1}{2}\right)^{\log\frac{R}{\bar{R}}}\right) - 1\right]. \qquad (3.2)$$

If $\alpha < \beta$, minimizing the measure (3.2), we mean the maximization of expected utility of a person whose utility function is given by $u_2(x) = x\left(\frac{\alpha}{2\beta}+\frac{1}{2}\right)^{\log\frac{x}{\bar{R}}}$. In this case the person is risk-averse. If $\alpha > \beta$, minimizing the measure (3.2), we mean minimization of the expected utility of a person whose utility function is given by $u_2(x) = x\left(\frac{\alpha}{2\beta}+\frac{1}{2}\right)^{\log\frac{x}{\bar{R}}}$. In this case the person is risk-prone.

Thus, minimizing this measure implies the minimization of the expected utility of the risk-prone person and maximization of the expected utility of a risk-averse person.

Concluding Remarks

Our study reveals that by using parametric measures of cross entropy, we can talk of maximizing the expected utility of risk-averse persons and of minimizing the expected utility of risk-prone persons. Such a study can be made available by the use of some other measures of cross entropy.

ACKNOWLEDGEMENTS

The authors are thankful to the University Grants Commission, New Delhi, for providing financial assistance for the preparation of the manuscript.

REFERENCES

Bera, AK. and Park, SY. 2008. Optimal portfolio diversification using maximum entropy principle. Econometric Reviews. 27:484-512.

Bugár, G. and Uzsoki, M. 2011. Portfolio optimization strategies: Performance evaluation with respect to different objectives. Journal of Transnational Management. 16:135-148.

Havrada, JH. and Charvat, F. 1967. Quantification methods of classification process: Concept of structural α-entropy. Kybernetika. 3:30-35.

Jianshe, O. 2005. Theory of portfolio and risk based on incremental entropy. Journal of Risk Finance. 6(1):31-39.

Kapur, JN. and Kesavan, HK. 1992. Entropy Optimization Principles with Applications. Academic Press, Inc.

Kullback, S. and Leibler, RA. 1951. On information and sufficiency. Annals of Mathematical Statistics. 22:79-86.

Markowitz, HM. 1952. Portfolio selection. The Journal of Finance. 7(1):77-91.

Markowitz, HM. 1959. Portfolio Selection: Efficient Diversification of Investments. John Wiley and Sons.

Pardo, MC. 2003. On asymptotic properties of information-theoretic divergences. IEEE Transactions on Information Theory. 49(7):1860-1867.

Parkash, O. and Mukesh. 2011. Two new symmetric divergence measures and information inequalities. International Journal of Mathematics and Applications. 4:165-179.

Parkash, O. and Mukesh. 2012[a]. Development of optimizational principle for minimizing risk in portfolio analysis. Global and Stochastic Analysis: An International Journal. 2:21-26.

Parkash, O. and Mukesh. 2012[b]. New generalized parametric measures of entropy and cross entropy. American Journal of Mathematics and Sciences. 1:91-96.

Renyi, A. 1961. On measures of entropy and information. Proceedings 4th Berkeley Symposium on Mathematical Statistics and Probability. 1:547-561.

Taneja, IJ. and Kumar, P. 2004. Relative information of type s, Csiszár's *f*-divergence and information inequalities. Information Sciences. 166:105-125.

Received: Jan 5, 2014; Accepted: Feb 14, 2014

SENRA Academic Publishers, British Columbia
Vol. 8, No. 2, pp. 2969-2978, June 2014
Online ISSN: 1920-3853; Print ISSN: 1715-9997

Canadian Journal of pure&applied sciences

Scientific Communication

ROBUST MULTI-OBJECTIVE STATIC OUTPUT FEEDBACK CONTROL BASED ON $H_2/H_\infty/\mu$ COMBINATION

*Javad Mashayekhi Fard[1], Mohammad Ali Nekoui[2] and Roya Amajdifard[3]
[1]Department of Electrical Engineering, Science and Research Branch, Islamic Azad University, Tehran
[2] Department of Electrical Engineering, K. N Toosi University of Technology, Tehran
[3] Department of Computer engineering, Kharazmi University, Tehran, Iran

ABSTRACT

This paper presents an overview on an output feedback controller with a combination of $H_2/H_\infty/\mu$. The design objective is a mixture of robust stability, nominal/robust performance, strict limitations on control signal and minimization of disturbance effects. In a physical system, the several targets contribute in a system control. Each one of the nominal and robust performance targets has their own strengths and weaknesses. A new approach in the presented paper is a combination of the two output feedback controllers of μ and H_2/H_∞. When all objectives are formulated in terms of a bounded real lemma, controller design results in a solution for a system of LMI. The purpose of the presented paper is to make balance between the nominal and the robust performance of output feedback. First, we use mixed H_2 and H_∞ norm for a nominal performance target while the other use μ synthesis for the robust performance. By combining these two controllers, the procedure of weights achievement will be formulated. Finally, modeling of an unmanned aircraft is applied to show the effectiveness and benefits of this method.

Keywords: $H_2/H_\infty/\mu$ controller, LMI, multi-objective output feedback, uncertain dynamic systems, single person aircraft.

INTRODUCTION

Unmodeled dynamics, non linearity of systems and the availability of disturbance are among some of the reasons explaining why the linear control systems theory has never reached to the ideal solution. For this reasons, several targets have been employed in a system control (Mashayekhi *et al*., 2013). Robust Stability means that the system will be stable with uncertainty, while the nominal performance which implies considering the system operation without uncertainty, has decisive effect on the operation of a system. By robust performance, we mean considering the system operation with uncertainty. It is obvious that whenever the singular values of controller are higher, the performance of systems will be more desirable, but at the same time, it provides higher chances of saturation occurrence. In order to consider the robust performance, we used μ analysis. Operating limitation on controlling signal increase of controlling signal leads to saturation of the actuators. H_2 norm essence can be responsible for such targets. Minimizing disturbance effect distortion can result in undesirable effect of transient response, therefore, reduction of the effect of disturbance, is one of the controlling targets. Mixed norm of H_2 and H_∞ can be a useful strategy to reach the mentioned controlling targets. To date, several studies have been performed on the mixed norm and the multi-objective control. This paper tends to reduce controlling signal, robust performance and stability and design weight functions. One of the new approaches of this paper is the combination of two controllers of μ and H_2/H_∞ based on output feedback. The controller for robust stability status, nominal performance, robust performance and noise reduction are continuously designed. First, the controller of H_2/H_∞ will be designed for nominal performance targets, robust stability and noise reduction, and then μ controller will be designed for robust performance. Now, add up these two controllers and achieve their weights with LMI. Controller will be achieved from solving the optimization problem. At first, a controlling problem will be changed to LFT standard form, considering uncertainty, then, the status equations will be written and by use of the constraint's weight function the robust controlling targets will be reached. The static output-feedback problem is one of the problems in systems and control theory that has been researched a lot. The use of output feedback provides the flexibility and simplicity of implementation. Moreover, in practical applications, full state measurements are not usually possible. Therefore, the restricted-measurement static output-feedback problem is of the issues with extreme importance in practical controller design

*Corresponding author email: mashayekhijavad@yahoo.com

applications such as flight control. The first formulation of the H_∞ control problem was performed in 1981 by Zames. Next to Zames (1981) and Doyle *et al*. (1989, 1991) were the pioneers of robust control. To date, large numbers of researches have been performed to study of the robust control, the H_2 control and H_∞ control. (Doyle *et al*., 1989) analyzed the state space with H_∞ and H_2 standard form and its solving. The conditions of solving problem and its solution using Hamiltonian matrix introduction could be mentioned as the highlights of this paper. Also Doyle *et al*. (1991) presented a tutorial overview on the linear fractional transformations (LFTs) and the roles of the structured singular value, μ, and linear matrix inequalities (LMIs) in solution of LFT problems. Lescher *et al*. (2006) designed a multivariable, multi-objective controller to set the wind turbine. Controlling problem of this paper was the minimization of H_2/H_∞. This problem was solved by LMI. His controller resulted in reduction of costs and mechanical depreciation. Also, it increased the lifelong of the system. Rotea *et al*. (1991) combined H_2/H_∞, in this way, two important approaches were presented, 1) H_2 optimized control with H_∞ bound (in fact a bounded optimization), and 2) Simultaneous H_2/H_∞ optimized control. In each step, the problem formulation and the controller were implimented. Scherer *et al*. (1997) presented an overview on the approach of linear matrix inequality (LMI) for the multi-objective synthesis of the linear output-feedback controllers. The design objectives could be a mixture of H_∞ performance, H_2 performance, passivity, asymptotic disturbance rejection, time-domain constraints, and constraints on the closed-loop pole location. In addition, these objectives could be specified on different channels of the closed-loop system. In the work of Echchatbi *et al*. (2009) the robust static output feedback stabilization of an induction machine was addressed. The machine was described by a non homogenous bilinear model with structural uncertainties, and the feedback gain was computed via an iterative LMI (ILMI) algorithm. Pereira *et al*. (2004) addressed the mixed H_2/H_∞ robust control problem. An algorithm based on GAs and LMIs was proposed in order to find a fixed structure output feedback robust controller**.** H_∞ design has been considered for the static output feedback, Holl *et al*. (2004) addressed the applicability of the matrix-valued sum-of-squares (SOS) techniques for the computations of LMI lower bounds. In a study conducted by Gadewadikar *et al*. (2009) the problem of stabilization of an autonomous rotorcraft platform in a hover configuration exposed to external disturbances was discussed. Necessary and sufficient conditions were presented for the static output-feedback control of linear time invariant systems using the H_∞ approach. Prempain *et al*. (2001) claimed that the existence of a static output feedback control law is given in terms of the solvability of two coupled Lyapunov inequalities which results in a non-linear optimization problem. However, by the use of state-coordinate and congruence transformations and by imposing a block-diagonal structure on the Lyapunov matrix to find the solution of a system of Linear Matrix Inequalities, they saw a reduction in the determination of a static output feedback gain, for a specific class of plants. Kanev (2004) expressed the reason of why the output feedback problem in the presence of uncertainty is a bilinear matrix inequality (BMI) problem, and BMI problems are not convex. Actually, such problems have been shown to be NP-hard which means that they cannot be expected to have polynomial time complexity. Raissi Dehkordi *et al*. (2009) dealt with the robust performance problem in a linear time-invariant control system in the presence of the robust controller uncertainty. Assuming that the plant uncertainty is modeled as an additive perturbation; a geometrical approach was followed in order to find a necessary and sufficient condition for the robust performance in the form of a bound on the magnitude of controller uncertainty. This method is performable for the SISO systems. Authors know that this method is more efficient than the approach of structured singular value. Another study, Mashayekhi *et al*. (2013) presented a state feedback control of linear time invariant systems using the $H_2/H_\infty/\mu$ approach. The rest of this paper is organized as follows: Section I establishes the problem which will be addressed and the H_2/H_∞, μ and $H_2/H_\infty/\mu$ combination control will be demonstrated. Section II presents the example design of Single Person Aircraft (X-29). In Section III, the approach will be illustrated and the results of the simulations will be discussed.

Problem Statement

A. H_2/H_∞ Controller

The existence of uncertainty is due to an uncertain and erratic input (for example noise and disturbance) and the Unmodeled dynamic is caused when we cannot completely and precisely describe a true system by a mathematical model at all. On the other hand, the important issues of a true system are the following objects: robust stability, robust and nominal performance, settling time, and maximum over shoot and so on, which try to gain these objectives about the controlling problem (Akbar *et al*., 2009; Lescher *et al*., 2006; Rotea *et al*., 1991). The type of uncertainty is an important problem in analysis. Zhou *et al*. (1994) and Liu (2002) researched on the optimization approach of mixed H_2 and H_∞ norm.

According to small gain Theorem, a system shown in figure 1 is well-posed and internally stable for all $\Delta(s) \in RH_\infty$ with $\|\Delta\|_\infty < \gamma^{-1}$ *if and only if* $\|M\|_\infty < \gamma$.

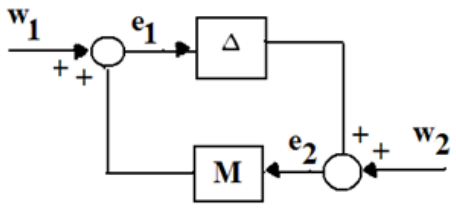

Fig. 1. M – Δ MODEL.

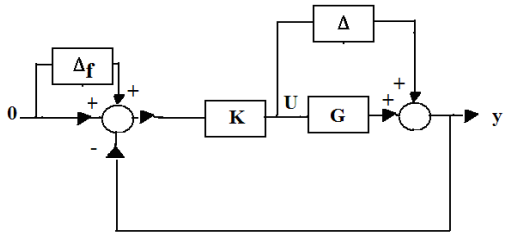

Fig. 2. Additive uncertainty.

Additive uncertainty shown in fig. 2 robust stability task is: $q=(I+KG)^{-1}KP \Rightarrow \left\|(I+KG)^{-1}K\right\|_{H_\infty} < \gamma^{-1}$ (1).

The objective for the inner loop control is to design an output feedback law such that the close loop system satisfies the following performance specifications:

Objective 1: if $\Delta = 0$ then $\|FS\|_\infty < 1$ (nominal performance). $S=(I+GK)^{-1}$ (S is sensitivity function and F(s) is weighting function).

Objective 2: if $\Delta \neq 0$ then system has been robust stability. $M=(I+KG)^{-1}K$, if $\bar{\sigma}(\Delta(j\omega)) \leq \gamma(j\omega) \Rightarrow \|\gamma(S)M\|_\infty < 1$

Objective 3: n is white noise with one PSD (power spectral density). H_2 Norm, cause decreasing of controlling signal. $\left\|T_{nU_1}\right\|_{H_2} < 1$ (To minimize U_1 variance with noise input). (Mashayekhi *et al*., 2013)

Then we have three tasks for controller design ($\|FS\|_\infty < 1$, $\|\gamma(S)M\|_\infty < 1$ $\left\|T_{nU_1}\right\|_\infty < 1$), such that, $\left\|\begin{bmatrix} FS(K,G) \\ \gamma M(K,G) \\ RT((K,G) \end{bmatrix}\right\|_\infty < 1$ (2). Problem (2) shown in figure 4. Rotea and Doyle offer two methods to solve this problem (Rotea *et al*., 1991; Zhou *et al*., 1994). Mashayekhi *et al*. (2013) shows similar method for solution of the simultaneous multivariable controller. A large class of systems with uncertainty can be treated as LFT (Linear fractional Transformation). LFT model is shown in figure 3 (Zhou *et al*., 1998).

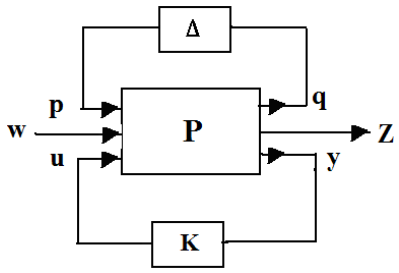

Fig. 3. LFT Model.

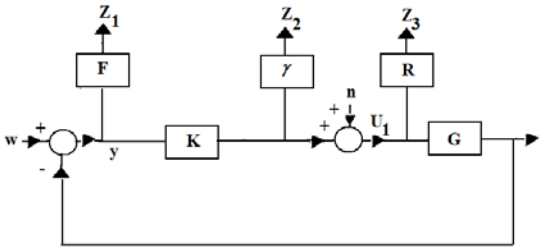

Fig. 4. Graphical model of problem (2).

W: the disturbance signals to the system which will not be a function of states of the system, Z: the variable that will be controlled, P: the nominal open loop system, Y: the system measurable output. To transform the changed diagram of figure 4 to the LFT model, we will be written the problem to standard form, and we will be dissolving using of riccati equation (Scherer, 1990). The (2) LFT model is practicable in form (4) and it can be used to design a controller by theorem 2. The state space of figure 4 is written in (4).

Determining 3 weight matrices, specified in figure 4, contain special importance. Using robust optimal output feedback method for (4) equations, and this is a new approach.

$$\begin{aligned} \dot{x} &= Ax + B_1 W + B_2 u \\ z &= C_1 x + D_{11} W + D_{12} u \\ y &= C_2 x + D_{21} W + D_{22} u \end{aligned} \quad , \quad Z = \begin{bmatrix} Z_1 \\ Z_2 \\ Z_3 \end{bmatrix} = \begin{bmatrix} FS \\ \gamma M \\ RT \end{bmatrix} r \tag{3}$$

$$\begin{bmatrix} \dot{x} \\ \dot{x}_f \\ \dot{x}_\gamma \\ \dot{x}_R \end{bmatrix} = \underbrace{\begin{bmatrix} A & 0 & 0 & 0 \\ -B_f C & A_f & 0 & 0 \\ 0 & 0 & A_\gamma & 0 \\ 0 & 0 & 0 & A_R \end{bmatrix}}_{A_{CL}} \begin{bmatrix} x \\ x_f \\ x_\gamma \\ x_R \end{bmatrix} + \underbrace{\begin{bmatrix} 0 & B & B \\ B_f & -B_f D & -B_f D \\ 0 & 0 & B_\gamma \\ 0 & B_R & B_R \end{bmatrix}}_{[B_1 \ B_2]} \begin{bmatrix} \underbrace{r \ n}_{W} \\ u \end{bmatrix}$$

$$\begin{bmatrix} z_1 \\ z_2 \\ z_3 \\ y \end{bmatrix} = \underbrace{\begin{bmatrix} -D_f C & C_f & 0 & 0 \\ 0 & 0 & C_\gamma & 0 \\ 0 & 0 & 0 & C_R \\ -C & 0 & 0 & 0 \end{bmatrix}}_{\begin{bmatrix} C_1 \\ C_2 \end{bmatrix}} \begin{bmatrix} x \\ x_f \\ x_\gamma \\ x_R \end{bmatrix} + \underbrace{\begin{bmatrix} D_f & -D_f D & -D_f D \\ 0 & 0 & D_\gamma \\ 0 & D_R & D_R \\ 1 & -D & -D \end{bmatrix}}_{D_{CL}} [r \ n \ u] \tag{4}$$

B. μ Controller

Here we try to assess robust performance of this closed-loop system using μ-analysis associated. Robust performance condition is equivalent to the following structured singular value μ test (Doyle *et al*., 1991).

$$\|T_{wz}(M,\Delta)\|_\infty < \gamma^{-1}, \forall \|\Delta\|_\infty < \gamma \Leftrightarrow \mu_{\Delta P}(M) < \gamma, \forall W \quad (5)$$

The complex structured singular value $\mu_{\Delta(M)}$ is defined as $\mu_{\Delta(M)} = \frac{1}{\min\{\bar{\sigma}(\Delta)|\det(I - M\Delta) = 0\}}$. Lower and Upper bond of μ can be shown to $P(UM) \le \mu_\Delta(M) < \min \bar{\sigma}(DMD^{-1})$ (Packard *et al*., 1993).

1) D-K iteration

Unfortunately, it is not known how to obtain a controller achieving the structured singular value test directly but, we can obtain the lower and upper bounds of μ**.** Our approach taken here is the so-called *D-K* iteration procedure (Doyle *et al*., 1992). First, for D = I fixed, the controller K is synthesized using the well-known state-space H_∞, optimization method. LFT form of figure 2 is written in equation 6.

$$\dot{x} = Ax + [0 \quad 0 \quad B]\begin{bmatrix} P \\ W \\ U \end{bmatrix}$$
$$\begin{bmatrix} q \\ z \\ y \end{bmatrix} = \begin{bmatrix} 0 \\ -C \\ -C \end{bmatrix} x + \begin{bmatrix} 0 & 0 & I \\ -I & I & -D \\ -I & I & -D \end{bmatrix}\begin{bmatrix} P \\ W \\ U \end{bmatrix} \quad (6)$$

C. New approach: H_2/H_∞, μ combination

Now, we tend to synthesize two controllers according to figure 5. As mentioned before, Nominal performance means considering system operation without uncertainty has decisive effect on the operation of a system. Robust performance means considering operation with uncertainty. It is obvious that whenever the singular values of controller are higher, systems performance is more desirable, but also it provides higher chances of saturation occurrences. So, we tend to balance between robust and nominal performances. W_1 and W_2 are weight functions as matrices in multivariable systems. Of course, it is important that robust performance contains nominal performance, so, controller coefficient of μ should be smaller than H_2/H_∞ controller coefficient (Mashayekhi *et al*., 2013). In a more explicit description, controller includes two parts, the first one using mixed H_2 and H_∞ norm and the other using μ synthesis. These two parts, include weights each of which have Important roles in systems control, because robust and nominal performance targets, has its own definiteness which their combination can create a new solution.

Problem A: Determine W_1 and W_2, in a way that an additive uncertainty system contains robust stability.

$$M = (W_1K_1G + W_2K_2G + I)^{-1}(W_1K_1 + W_2K_2)$$
$$\|M\|_\infty < 1 \quad (7)$$

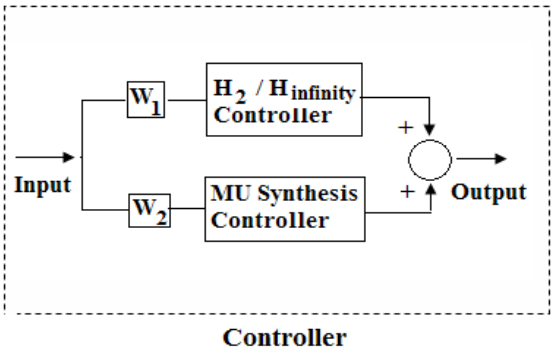

Fig. 5. Controller $H_2/H_\infty/\mu$.

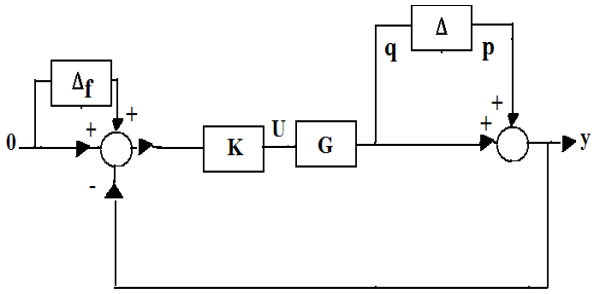

Fig. 6 Multiplication uncertainty.

Problem B: Determine W_1 and W_2, in a way that a system having Multiplication uncertainty contains robust stability.

$$M = (GW_1K_1 + GW_2K_2 + I)^{-1}(GW_1K_1 + GW_2K_2)$$
$$\|M\|_\infty < 1 \quad (8)$$

According to figures 2 and 6 we use state space to solve the problem A and B.

1) Robust optimal static output feedback

In this section we intended to follow the analysis of the conditioning of the pole placement problem with the multi-input case which is called the generalized output feedback. The Static Output-feedback (SOF) synthesis problem deals with a given class of systems, to derive theoretical conditions for the existence of a static control law and associate them with the numerical methods. The class of continuous-time, Linear Time-Invariant (LTI) systems is addressed. The systems are given as multi-input/multi-output state-space models. In addition to the control input vector and the measure output vector that define the control loop, the models may include some other input/output signals. They are introduced for input/output performance specifications defined by H_2 and H_∞ norms and μ synthesis. In this paper, we assume that the state of the generalized plant G is available for

the feedback. To be more precise, let a state-space description of P (Fig. 3) be given by (LFT Model):

$$\begin{aligned}&\dot{\mathbf{x}} = A_{cl}\mathbf{x} + B_{cl}\mathbf{w}\\ &\mathbf{y} = C_{cl}\mathbf{x} + D_{cl}\mathbf{w}\\ &A_{cl} = A + BKC \quad , \quad B_{cl} = B_w + BKD_w\\ &C_{cl} = C \ , \ D_{cl} = D_w\end{aligned} \tag{9}$$

The signal W refers to disturbance. The signals U and Y represent the control input and the measured output, respectively. After gaining K_1 by H_2/H_∞ and K_2 by μ analysis, we tend to determine the weight functions, by the use of linear matrix inequality.

Lemma1: (bounded-real lemma) given a constant $\gamma > 0$, for system, M(s) = (A, B, C) the following two statements are equivalent, 1) this system is stable $\| M(s) \|_\infty < \gamma$, 2) A symmetric positive definite matrix Q exists such that: (Boyd *et al*., 1994)

$$\begin{bmatrix} A^T Q + QA & QB_p & C_q^T \\ B_p{}^T Q & -\gamma^{-1} I & D_q^T \\ C_q & D_q & -\gamma^{-1} I \end{bmatrix} < 0 \tag{10}$$
$$Q > 0$$

Lemma 2: Consider the feedback system of Figure.3, where G is given by (8). Then, a given controller K is admissible and closed loop system is robust stability and desired performance if and only if there exists W_1 *and* W_2 solving the following LMI problem:

LMI of system (9), considering BRL theorem will be (11). ($\beta = \gamma^{-1}$)

$$\begin{bmatrix} A\Omega + BY_1C + BY_2C + C^T Y_1^T B + C^T Y_2^T B + \Omega A^T & B_W + BKD_w & \Omega C^T \\ (B_W + BKD_w)^T & -\beta I & D_w^T \\ C\Omega & D_w & -\beta I \end{bmatrix} < 0 \tag{11}$$
$$\Omega > 0 \quad , \quad Y_1 > 0 \quad , \quad Y_2 > 0$$

Where, $Y_1C = W_1K_1C\Omega, Y_2C = W_2K_2C\Omega, \Omega = Q^{-1}, Q > 0 \Rightarrow \Omega > 0$

Proof: LMI of system (9), considering BRL theorem will be (12). ($\beta = \gamma^{-1}$)

$$\begin{bmatrix} (A + BW_1K_1C + BW_2K_2C)^T Q + Q(A + BW_1K_1C + BW_2K_2C) & Q(B_W + BKD_W) & C^T \\ (B_W + BKD_W)^T Q & -\beta I & D_w{}^T \\ C & D_w & -\beta I \end{bmatrix} < 0$$
$$Q > 0 \quad , \quad W_1 > 0 \quad , \quad W_2 > 0 \tag{12}$$

$$\begin{bmatrix} Q^{-1}(A + BW_1K_1C + BW_2K_2C)^T + (A + BW_1K_1C + BW_2K_2C)Q^{-1} & B_W + BKD_w & C^T \\ (B_w + BKD_w)^T Q & -\beta I & D_w^T \\ CQ^{-1} & D_W & -\beta I \end{bmatrix} < 0$$
$$Q > 0 \quad , \quad W_1 > 0 \quad , \quad W_2 > 0$$

We multiply the $\begin{bmatrix} Q^{-1} & 0 & 0 \\ 0 & I & 0 \\ 0 & 0 & I \end{bmatrix}$ on the left and the right of the matrix, define

$$Y_1C = W_1K_1C\Omega, Y_2C = W_2K_2C\Omega, \Omega = Q^{-1}, Q > 0 \Rightarrow \Omega > 0$$

Substituting into (12) yields:

$$\begin{bmatrix} A\Omega + BY_1C + BY_2C + C^T Y_1^T B + C^T Y_2^T B + \Omega A^T & B_W + BKD_W & \Omega C^T \\ (B_W + BKD_w)^T & -\beta I & D_w^T \\ C\Omega & D_w & -\beta I \end{bmatrix} < 0$$
$$\Omega > 0 \quad , \quad Y_1 > 0 \quad , \quad Y_2 > 0$$

In this method must be m=1. m, number of inputs and n, number of outputs.

2) METHODOLOGY

a. To design the H_2 /H_∞ output controller for the process with uncertainty. (it helps to select the weighting function properly).

b. For H_2/H_∞ design we can use Rotea and Doyle method. (Rotea *et al*., 1991; Zhou *et al*., 1994; Doyle *et al*., 1994) or use $\left\| \begin{bmatrix} FS(K,G) \\ \gamma M(K,G) \\ RT((K,G) \end{bmatrix} \right\|_\infty < 1$ and obtained K_1.

c. For F, γ *and* R, we use weighting functions to limit the magnitude of the sensitivity and complementary sensitivity functions.

d. To design the μ output controller for the process with uncertainty (if the process is unstable, at the beginning, it must be stabilized). D-K iteration method can be used to improve the performance of the controller design for the system. Peak value of the μ (D-K iteration) bound should be less than one, and obtained K_2.

e. Order reduction method can be used to reduce the order of the I+GK, and transfer to state space equation and given A_c.

f. $K_1 = B^{-1} \times (A_{c1} - A) C^{-1}$, $K_2 = B^{-1} \times (A_{c2} - A) C^{-1}$. A, B are in P-K system (LFT Model).

g. W_1, W_2 are given with LMI (11) then the robust stability of the system has to be established.

h. H infinity norm of W_2 must be smaller than W_1.

i. $K = W_1K_1 + W_2K_2$. This controller (K) has robust stability and desired performance.

I. Example Design

A. Single Person Aircraft(X-29)

In an airplane five main sections could be listed they are: motor, body section, landing system and wheels, wing and tail. The pitch angle of an airplane is controlled by adjusting the angle (and as a result, the lift force) of the rear elevator. The aerodynamic forces (lift and drag) as well as the airplane's inertia are taken into account. The X-29 aircraft is a recent example of a control configured vehicle which was designed with a high degree of longitudinal static instability (up to 35 percent at low subsonic speeds). The vehicle is stabilized by a full-authority, fly – by – wire flight control system. Prior to the flight, the linear models were used extensively to determine the close loop stability, controllability, and handling qualities with the various control system modes through the flight envelope. This section describes the commercials aircraft models which are now implemented. In the work of Bosworth (1992) which is a comprehensive report of NASA; the research has been conducted over X-29 state equation and model. Tae (2000) only designed the H_∞ controller over X-29. While Minisci *et al*. (2008) designed the multi-objective robust control for F-16 and F-18 airplanes. The X-29 airplane is a relatively small, single seat, high-performance aircraft powered by a single F404-GE-400 engine (General Electric, Lynn, Massachusetts). Its empty weight is 6350kg and the aircraft dimensions are shown in figure 7 also, the aircraft picture is shown in figure 8 in order to provide a low-drag configuration the vehicle incorporates a forward-swept wing with close-coupled canards. The airplane physical characteristics are listed in table 1.

The aircraft model is obtained by linearization of the nonlinear equations of motion about a 280 ft/sec (307km/h) landing configuration (Bosworth, 1992). The three input three output model which describes the longitudinal dynamics is given as follows (Bosworth, 1992; Tae, 2000):

Table. 1. X-29 physical characteristics.

6350 kg	weight	N.M 8130	Maximum trust force
3.437 m^2	Canard area	α	Angel attack
8.29m	Wing span	17.185 m^2	Wing area
δ_{sf}	Symmetric flap position	δ_{stf}	Strake flap position
θ	Pitch Euler angel	δ_c	Canard position
v	Horizontal speed	$\dot{\theta}$	Pitch rate

$$\dot{x} = Ax + Bu \quad , y \quad = Cx \; , x = \begin{bmatrix} v & - & (ft/sec) \\ \alpha & - & (rad) \\ \dot{\theta} & - & (rad/sec) \\ \theta & - & (rad) \end{bmatrix} \quad (13)$$

$$u = \begin{bmatrix} \delta_c & - & (deg) \\ \delta_{sf} & - & (deg) \\ \delta_{stf} & - & (deg) \end{bmatrix}, \quad y = \begin{bmatrix} \theta & - & (rad) \\ v & - & (ft/sec) \\ \alpha & - & (rad) \end{bmatrix}$$

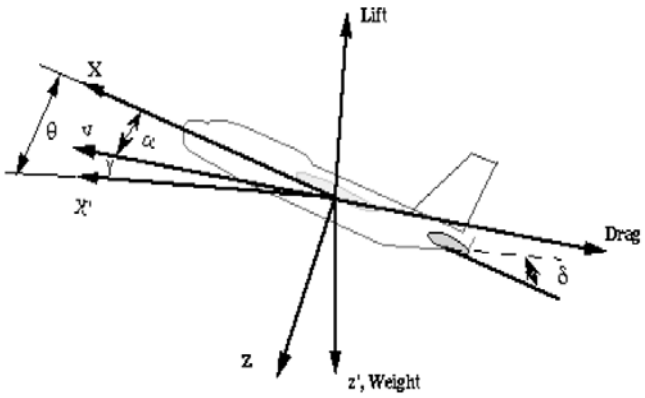

Fig. 7. Axes coordinate in aircraft.

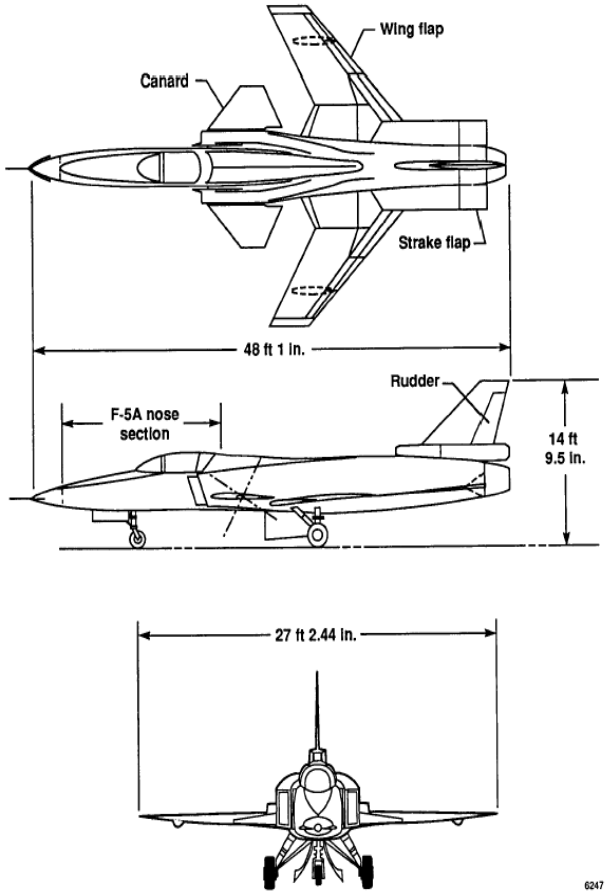

Fig. 8. X-29 airplane.

III. Simulation results

The longitudinal dynamics of an aircraft has one natural mode: the short period mode. For the X-29, the short period mode, however, is composed of the stable mode and an unstable one. At first, we design H_2/H_∞ controller and design μ controller. These controllers designed for P-K system. This system is four input four outputs. Then, for reducing the order of I + GK, a residualization method was implemented. By consideration of the practical experiments and in accordance with equation (2), the weight functions selection with $R = \frac{0.0001(s+0.01)}{s+1}I$, $F = \frac{0.2222s+0.6667}{0.11s+1}I$, $\gamma = \frac{0.0001(0.25s+2)}{1.5s+0.0001}I$ (Lanzon, 2000). K_1 *and* K_2 design with equations 2 and 8. W_1, W_2, are obtained via equation 11. According to figure 5, K is design. At first we designed the weight functions which

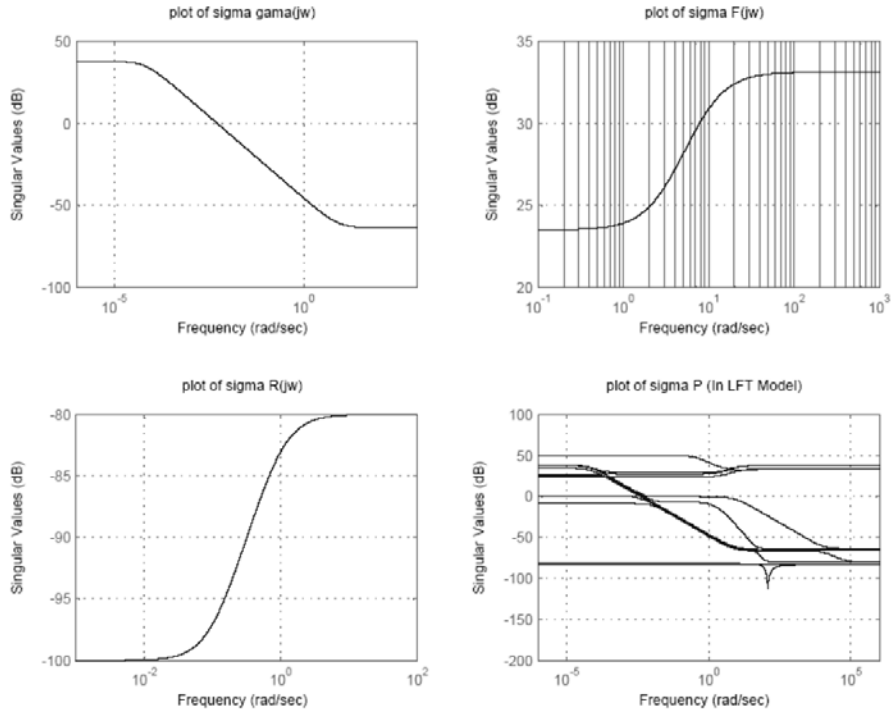

Fig. 9. Singular value for weighting functions and P (LFTModel).

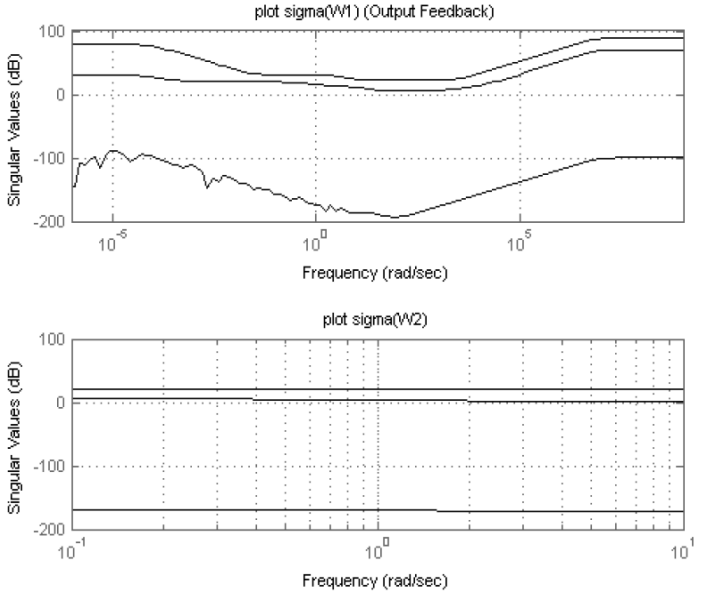

Fig. 10. Singular value for W_1 and W_2 Weighting function of H_2/H_∞, μ combination.

were drawn in figure 9, a, b, c. are selected the weighting functions (Beaven *et al*., 1996; Sararth, 2011) by taking into account the practical experiments, The singular values of LFT model are drawn in figure 9-d. The Singular value for W_1 and W_2 Weighting function of H_2/H_∞, μ combination is shown in figure 10.

While, the Singular value for T complementary sensitivity function is drawn in fig.11. the step response of T function is depicted in fig.12. It must be noted that, as it was mentioned, the system is multi input-output; and the

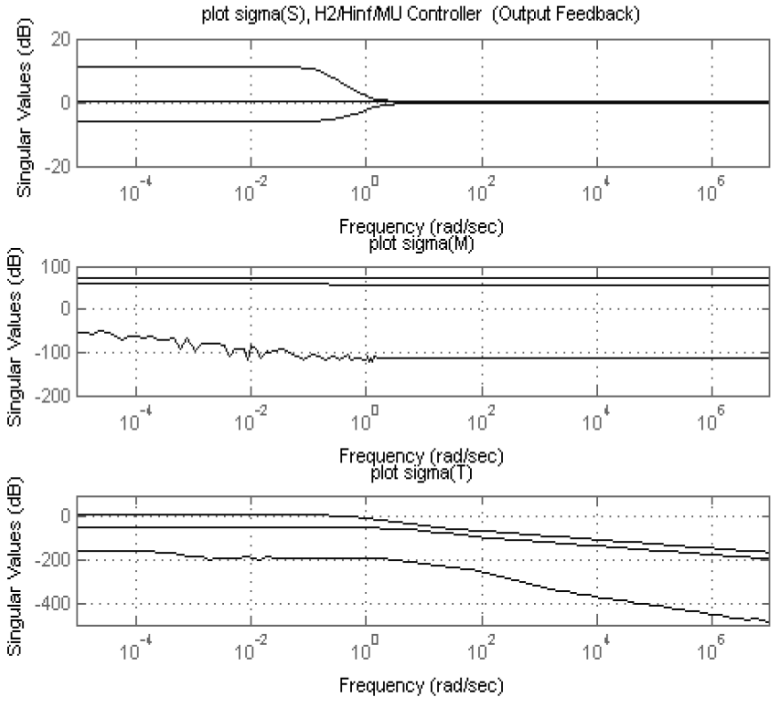

Fig.11. Singular value for T complementary sensitivity function.

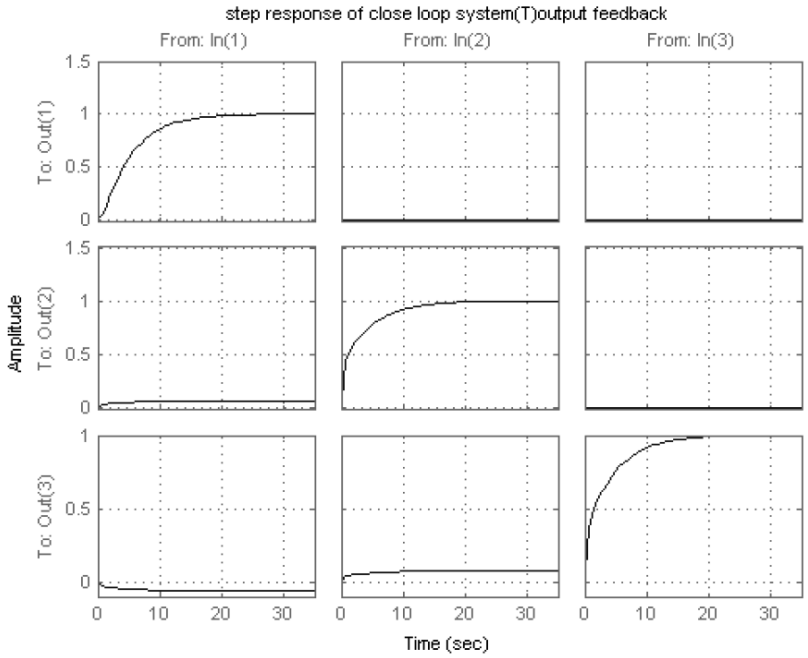

Fig. 12. Step responses for T complementary sensitivity function.

weight and sensitivity functions are the shape of matrix. The sign of success is the combination of nominal and robust performance, together. Accomplishment in reaching to the targets with the minimum controlling signal is of the gains of noted controller. The open-loop system is an unstable one, but the close-loop system showed appropriate results.

CONCLUSION

The paper brings out a global approach for robust static output-feedback design in which the multiple specifications can be simultaneously defined. In this paper, the problem of the mixed $H_2/H_\infty/\mu$ robust control was addressed. An algorithm based on LMIs has been proposed in order to find a reach to a static output feedback robust controller which minimizes the cost of an H_2 performance subjected to H_∞ norm and μ synthesis constraints. Each of the nominal and the robust performances has their own strengths and weaknesses.
The availability of robust performance has lead to the intensive limitations on the controller, which sometimes exhales it from a possible problem (Keel *et al.*, 1997). Also, availability of the nominal performance means considering the system operation without uncertainty, and it is usual that the essence of uncertainty has a decisive effect on the operation of the system. New approach of this paper is a combination of two controllers of μ and H_2/H_∞ based on output feedback. The controllers for robust stability status, nominal performance, robust performance and noise reduction are continuously designed. First, the controller of H_2/H_∞ will be designed for nominal performance targets, robust stability and reduction of noise, and then μ controller will be designed for robust performance. Afterwards, these two controllers are added up and their weights would be obtained through LMI. Also, the controller will be achieved from solution of the optimization problem. This paper attempts to present an implementation approach for the multivariable controlling systems. In operation, we look for minimization of the faults. If the available error function is not desirable, the use of a suitable weight function can lead us to the target. So, design of the weight function is extremely important. By knowing the data of the problem, we will have the information on which of the frequencies has more uncertainty effect. It is obvious that the controller effect of μ should be considered here. Because of multivariable exceptional values system, controller and considered inputs-outputs were shown. Using two low pass filters and one high pass filter for H_2/H_∞ controller, we tended to optimize the solutions. First, the equations of X-29 aircraft state space are written. Then, the robust static output-feedback controller will be designed. The results which are shown in the figures indicate that the unstable system becomes stable in the presence of uncertainty using the proposed controller. The results are also indicative that the proposed approach shows an appropriate and desired performance.

ACKNOWLEDGMENT

The authors wish to thank Prof. A. Khaki-Sedigh for helpful discussions.

REFERENCES

Akbar, SA. , Singh, AK. and Datta, KB. 2009. Study of Response and Robustness Measures of Mixed H_2/H_∞, LQG and H_∞ Controllers for Continuous-Time Singularly Perturbed Systems. Faculty of Electrical Engineering University Technology Malaysia. 11(2):7-15.

Beaven, W., Wright, MT. and Seaward, DR. 1996. Weighting Function selection in the H_∞ design process, control engineering practice. 4(5):625-633.

Bosworth, J. 1992. Linearized aerodynamic and control law models of the X-29 airplane and comparison with flight data, NASA technical memorandum 4356.

Boyd, S., Ghaoui, LE., Feron, E. and Balakrishnan, V. 1994. Linear Matrix Inequalities in System and Control Theory. Society for Industrial and Applied Mathematics, Philadelphia.

Doyle, JC. , Glover, K. and Khargonekar, PP. 1989. State-Space Solution to Standard H_2 and H_∞ Control Problems. IEEE Transactions on Automatic Control. 34(8):831-847.

Doyle, JC. , Packard, A. and Zhou, K. 1991. Review of LFTs, LMIs, and μ, Proc. IEEE Conference on Decision and Control. Brighton, UK. 1227-1232.

Doyle, JC., Francis, B. and Tannenbaum, A. 1992. Feedback Control Theory, Published by Macmillan.

Doyle, JC. , Zhou, K., Glover, K. and Bodenheimer, B. 1994. Mixed H_2 and H_∞ performance objectives. II. Optimal control. IEEE Transactions on Automatic Control. 39(8):1575-1587.

Echchatbi, A., Rizki, A., Haddi, A., Mrani, N. and Elalami, N. 2009. ILMI Approach for Robust Output Feedback Control of Induction Machine, World Academy of Science. Engineering and Technology. pp51.

Gadewadikar, J., Lewis, F., Subbarao, K., Peng, K. and Chen, BM. 2009. H-Infinity Static Output-feedback Control for Rotorcraft. Journal of Intelligent and Robotic Systems. 54:629-626.

Holl, C. and Scherer, C. 2004. Computing optimal fixed order H_∞-synthesis values by matrix sum of squares relaxation. In: 43rd IEEE Conference on Decision and Control. Atlantis, Paradise Island, Bahamas. 3147-3153.

Kanev, S. 2004. Robust Fault-Tolerant Control, Ph.D. Thesis. University of Twente, Netherlands.

Keel, LH. and Bhattacharyya, SP. 1997. Robust, Fragile, or Optimal? IEEE Transactions on Automatic Control. 42(8):1098-1105.

Lanzon, A. 2000. Weight Selection in Robust Control: An Optimization Approach, Wolfson College, Control Group. Ph.D. Thesis. Department of Engineering, University of Cambridge.

Lescher, F., Yun, J. and Martinez, A. 2006. Multiobjective H_2/H_∞ Control of a Pitch Regulated Wind Turbine for Mechanical Load Reduction. European Wind Energy Conference, Athens, Greece.

Liu, G., Yang, JB. and Whidborne, JF. 2002. Multiobjective Optimization and Control. Research Studies Press.

Mashayekhi Fard, J., Nekoui, MA., Sedigh, A. and amjadifard, R. 2013. Robust controller design by multi-objective optimization with H_2 /H_∞/μ combination. International Journal of Computer Science and Technology. 4(1):586-593.

Mashayekhi Fard, J., Nekoui, MA., Sedigh, A. and Amjadifard, R. 2013. Robust multivariable controller design with the simultaneous H_2 /H_∞/μ for a single person aircraft. International Journal of Electrical and Computer Engineering. 3(2):279-286.

Minisci, EA., Avanzini, G., D'Angelo, S. and Dutto, M. 2008. Multi-Objective Design of Robust Flight Control Systems, Mathematical Problems in Engineering. Aerospace and Sciences, Genoa, Italy.

Packard, A. and Doyle, JC. 1993. The Complex Structured Singular Value. Automatica. 29 (1):71-109.

Pereira, GJ. and de Marajo, HX. 2004. Robust Output Feedback Controller Design via Genetic Algorithms and LMIs: The Mixed H2/H∞ Problem, Proceeding of the 2004 American Control Conference Boston, Massachusetts, USA.

Prempain, E. and Postlethwaite, I. 2001. Static Output Feedback Stabilization with H-infinity Performance for a Class of Plants. Systems & Control Letters. 43(3):159-165.

Raissi Dehkordi, V. and Boulet, B. 2009. Frequency-Domain Robust Performance Condition for Controller Uncertainty in SISO LTI Systems: A Geometric Approach. Journal of Control Science and Engineering, Hindawi Publishing Corporation.

Sarath, SN. 2011. Automatic Weight Selection Algorithm for Designing H Infinity controller for Active Magnetic Bearing. International Journal of Engineering Science and Technology. 3(1):122-138.

Scherer, C. 1990. The Riccati Inequality and State-Space H_∞- Optimal Control. Ph.D. Thesis, University of Wurzburg.

Rotea, MA. and Khargonekar, PP. 1991. H_2-optimal Control with an H∞ constraint. The State Feedback Case, Automatica. 27(2):307-316.

Scherer, C., Gahinet, P. and Chilali, M. 1997. Multiobjective Output-Feedback Control via LMI Optimization. IEEE Transactions on Automatic Control. 42(7):896-911.

Tae, YK. 2000. Development of an interactive modeling, simulation, animation and real time control aircraft environment, MS. Thesis. Arizona State University, USA.

Zames, G. 1981. Feedback and optimal sensitivity: model reference transformation, multiplicative semi norms and approximate inverses. IEEE Transactions on Automatic Control. 26(2):301-320.

Zhou, K., Glover, K., Bodenheimer, B. and Doyle, JC. 1994. Mixed H_2 and H_∞ performance objectives I: robust performance analysis, IEEE Transactions on Automatic Control. 39(8):1564-1574.

Zhou, K. and Doyle, JC. 1998. Essential Robust Control. Prentice Hall.

Received: June 19, 2013; Revised: March 17, 2014;
Accepted: April 4, 2014

SENRA Academic Publishers, British Columbia
Vol. 8, No. 2, pp. 2979-2984, June 2014
Online ISSN: 1920-3853; Print ISSN: 1715-9997

Canadian Journal of pure&applied sciences

Short Communication

ONTOLOGY CONSTRUCTION AND REASONING USING OWL: A CASE STUDY FROM SEAFOOD DOMAIN

*Vinu PV[1], Sherimon PC[1] and Reshmy Krishnan[2]
[1]Department of Computer Science, M. S University, India
[2]Department of Computing, Muscat College, Oman

ABSTRACT

Ensuring the quality of any type of food, particularly seafood has increasingly become an important issue nowadays. The environment is polluted in many ways, such that the consumption of seafood by compromising the quality may cause diseases due to infection or intoxication. So the adoption of proper quality control systems is mandatory in any organization that deals with food processing and distribution. In this regard, we have proposed an ontology based system in seafood companies to ensure the quality of seafood. Ontology is a formal specification of the concepts within a domain and their interrelationships. It describes the logical structure of a domain, its concepts and the relations between them. The aim of ontology is to capture knowledge in related fields, provide a shared under standing of conceptual knowledge, define a common vocabulary in this field, and give clear definition to the mutual relationship between these words from different levels of formal models. This paper presents the initial phase of our research viz, design and construction of seafood ontology in Web Ontology Language [OWL]. It is an extension of our work which is published earlier. Protégé is used to implement the ontology.

Keywords: Ontology, seafood, taxonomy, protégé.

INTRODUCTION

Seafood has traditionally been a popular part of the diet in many parts of the world and in some countries constituted the main supply of animal protein (Vinu *et al*., 2012a). The global consumption of fish and seafood has doubled since 1973 and is expected to increase by 25% by 2015 (EIA, 2012). However, ensuring seafood quality has increasingly become an important issue nowadays and is the first step to get attention to countries seafood products. Consumption of seafood may cause diseases due to infection or intoxication (Vinu *et al*., 2012a). The environmental risks of seafood include water pollution, metal pollution and other bacterial pollution (Vinu *et al*., 2012a). The main hazards associated with seafood are bacteria such as E. coli, Salmonella, Vibrio Cholera etc., virus, bio-toxins such as PSP, DSP, NSP etc., histamine poisoning, parasites, chemicals such as cadmium, lead, mercury etc. Food regulations, such as Hazard Analysis Critical Control Point (HACCP), Good Manufacturing Practice (GMP), or Good Hygiene Practice (GHP), aim to guarantee a certain level of quality. To ensure the quality of seafood, we have proposed an ontology based systemin seafood companies and in this paper, we present the initial phase of our research viz, development of seafood ontology. It is an extension of our work published earlier (Vinu *et al*., 2012b).

The Semantic Web is simply a web of data described and linked in ways to establish context or semantics that adhere to defined grammar and language constructs (Hebler *et al*., 2009). The idea of Semantic Web is to make web resources more accessible to automated processes. WWW is formatted for human consumption rather than programs. So by incorporating semantics, if web pages are clearly understood by the machines, then they will be able to integrate information from different sources, automate the processes and reuse the information across various other applications in an automated way. The basis of the Semantic Web is semantic relationships. The relationships include definitions, associations, aggregations, and restrictions (Hebler *et al*., 2009). Semantic Web does not rely on text-based manipulation, but rather on machine processeble metadata. Metadata is data about data and it is able to capture the meaning of the data. Meta data consists of (attribute, value) pairs that helps to categorize web pages. Ontologies play an important role here, by providing a domain vocabulary for metadata using which the semantic description is built. They are well known for many years in the Artificial Intelligence and Knowledge representation communities (Akerkar, 2009). Ontology is a formal specificationof the concepts within a domain and their interrelationships

*Corresponding author email: vinusherimon@yahoo.com

(Sherimon *et al*., 2013a). Ontology defines the basic terms and relations comprising the vocabulary of a domain as well as the rules for combining terms and relations to define extensions to the vocabulary (Neches *et al*., 1991). They define vocabularies and their meanings, with explicit, expressive, and well-defined semantics, that can be easily interpreted by machines. Ontology contains both the asserted knowledge and the inferred knowledge (Sherimon *et al*., 2013c). Asserted Knowledge is the knowledge that is explicitly defined by the ontology developers. When ontologies are reasoned by machines, valid deductions and inferences are generated which iscalled inferred knowledge (Sherimon *et al*., 2013c).

To create ontology, W3C has proposed a number of languages. The first semantic web language as part of metadata standardization from World Wide Web consortium [W3C] is RDF (Hebler *et al*., 2009). The core format for representation of data in semantic web is RDF (Resource Description Framework) which is based on triples subject (resource)-predicate (property)-object (property-value). The fundamental concepts of RDF are resources, properties and statements. A resource can be anything in the world; for example a website, or a real object like 'apple'. Resources are identified using Uniform Resource Identifiers (URI), Uniform Resource Locator (URL) or a global, unique code based on W3C standards. Properties are a special kind of resources. They describe the relations between the resources. It is linked with other resources via URI which uniquely identifies documents. But using RDF, it is not possible to describe neither the relationship between the relationships themselves, nor the relationships between resources and properties. So W3C extended RDF to RDFS (RDF Schema) (Thottupuram *et al*., 2011). Using RDF Schema vocabulary terms and the relations between those terms can be defined. RDFS has still weaknesses; so on top of RDFS, W3C has built OWL. OWL ontologies are web documents referred to by URIs (Arroyo *et al*., 2004). OWL is a stronger language as compared to RDF and has much machine interpretability (Gupta *et al*., 2010).

MATERIALS AND METHODS

Ontology Design and Construction

To design ontology, many design decisions have to be made to ensure that it will suit the stated purpose. There is no single method to design ontology. We cannot say this is the right way or this is the wrong way, but still some of the designs provide clarity in the functionalities than others. The ontologies are derived from the real world conceptualization shared by humans as a knowledge base and implemented in digital through machine readable languages such as OWL, XML (Gupta *et al*., 2010). The first step consists of determining the domain and the scope of the ontology. It will be the first step to answer questions like for what purpose the ontology is being developed. It identifies the range of the users and the type of questions which the ontology should answer. Next is to decide whether to use already existing ontologies, and if so, how to use them. Then all the terms that are needed in the development of ontology is listed. Next, define the hierarchical structure (taxonomy) to organize the domain knowledge. The concepts in the domain are described by the main component of the ontology, which is class. Classes are defined using owl:Class. <owl:Thing> is the base class under which, the fundamental ontology constructs provided by OWL such as other classes, properties and instances are created. Classes may contain subclasses that inherit their characteristics and they also contain instances. Instances may have properties which connect them to values or other instances. Then the properties, facets and instances are defined. OWL supports two types of properties – data type and object. Object Properties relate objects to objects, whereas Data type properties relate objects to data type values.

Implementation of Seafood Ontology

Ontology Tools

Protégé, developed by Stanford University is currently the best known ontology editor. It is a free, open-source platform that provides a growing user community with a suite of tools to construct domain models and knowledge-based applications with ontology (Sherimon *et al*., 2013c). Further, Protégé can be extended by way of a plug-in Architecture and a Java based Application Programming Interface for building knowledge-based tools and applications (Sherimon *et al*., 2011). Protégé supports a number of plug-ins. OWL plug in produces ontologies in OWL language. OWLViz is the plugin used to visually represent the class hierarchies in the ontology. OntoGraf tool is used to represent the relationships in the ontology. SWRL [Semantic Web Rule Language] plugin supports the use of rules.

Classes and Subclasses

The ontology requires the representation of each concept in Seafood domain and its attributes. The Seafood ontology has been defined in OWL, and Protégé is used to model the ontology. Figure 1 represents the implementation of seafood ontology in Protégé. The main domain concepts which are disjoint are *Product, Fish, Test, Test-Specification, and Country*. *owl:Thing* is the most general class, which contains all the above concepts. The class *Product* is further categorized into disjoint subclasses *Chilled_Product, Frozen_Productand Raw_Material*. *Test Specification* is another main class which is further categorized into disjoint subclasses, *External-test* and *Internal-Test*. This is to describe the tests done in the factory (Internal-Test) and in outside governmental agencies (External-test). Each of these subclasses are again subdivided into two subclasses each for representing the test specifications of Seafood and non-food items like Water, Ice, Salt etc. Each of these

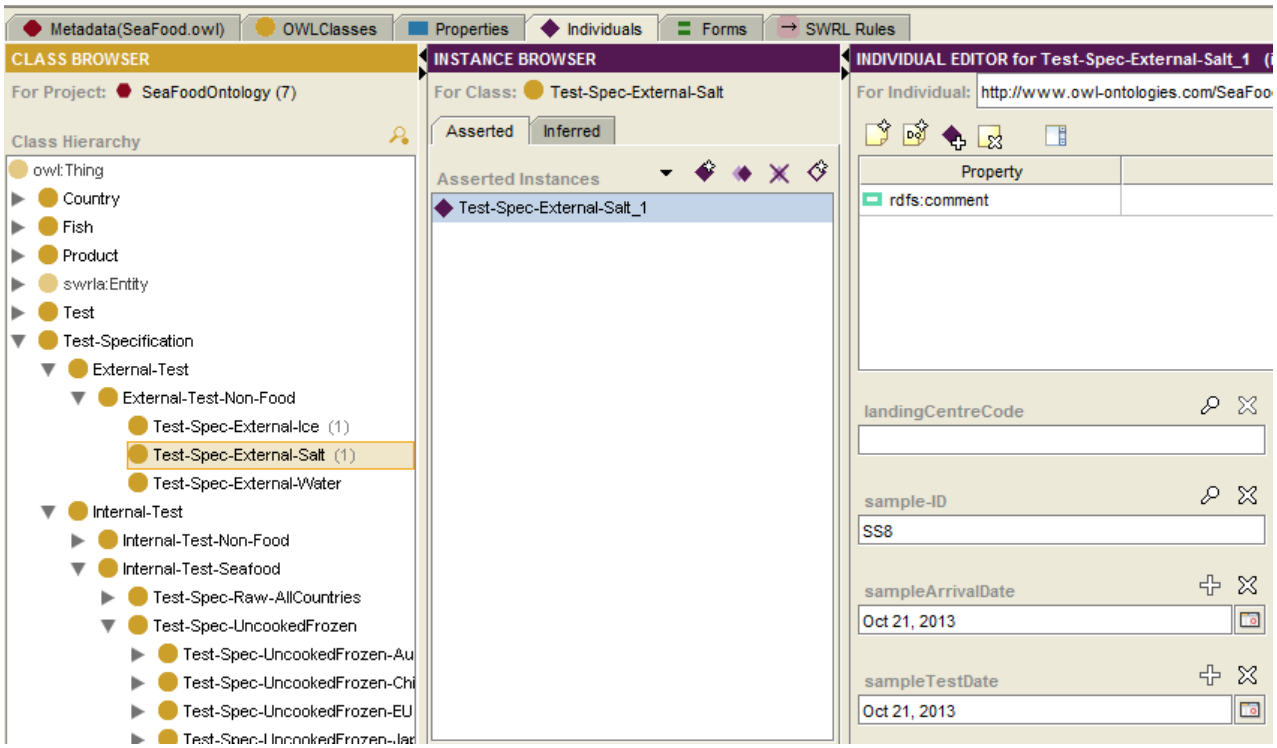

Fig. 1. Seafood Ontology.

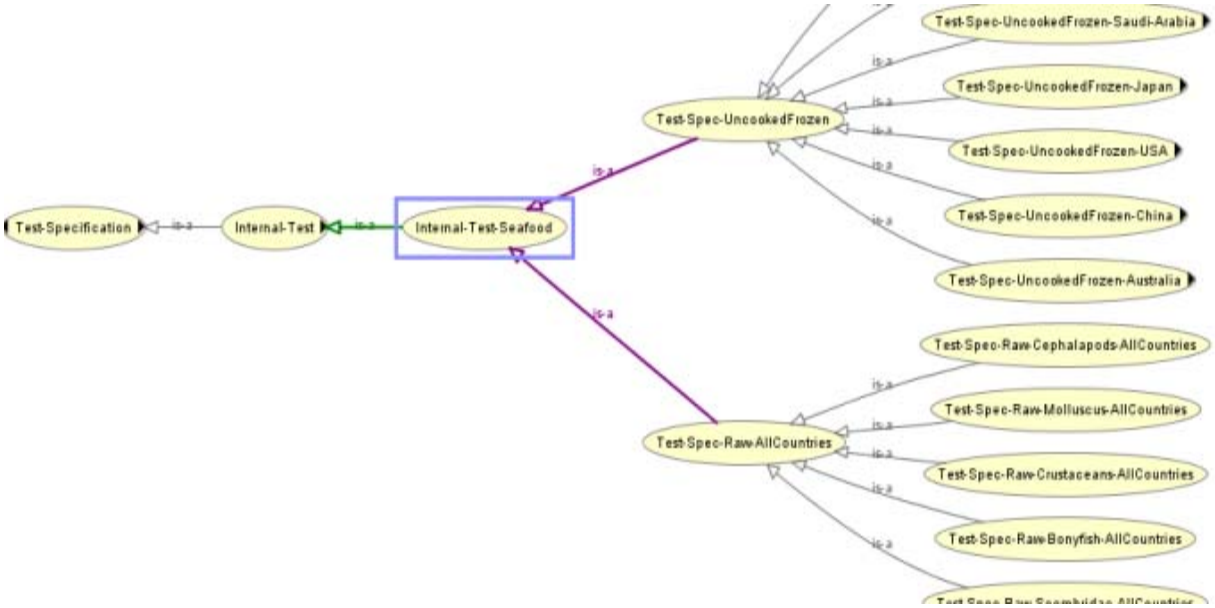

Fig. 2. Taxonomy Representation in OWLViz.

subclasses is further subdivided into many more subclasses which represents specific test item based on country, item type etc. To represent a product sample, an ID, the arrival date of the sample in lab, the date in which the sample is tested, and the country to which it is intended to export needs to be defined by building object and data properties such as *exportTo*, *sampleId*, *sampleArrivalDate*, *sampleTestDate* etc.

The plugin OWLViz enables class hierarchies in ontology to be viewed and incrementally navigated. Figure 2 represents a part of the taxonomy of Seafood ontology.

Fig. 3. Property Restrictions (Necessary Conditions) of Test-Spec-External-Salt class.

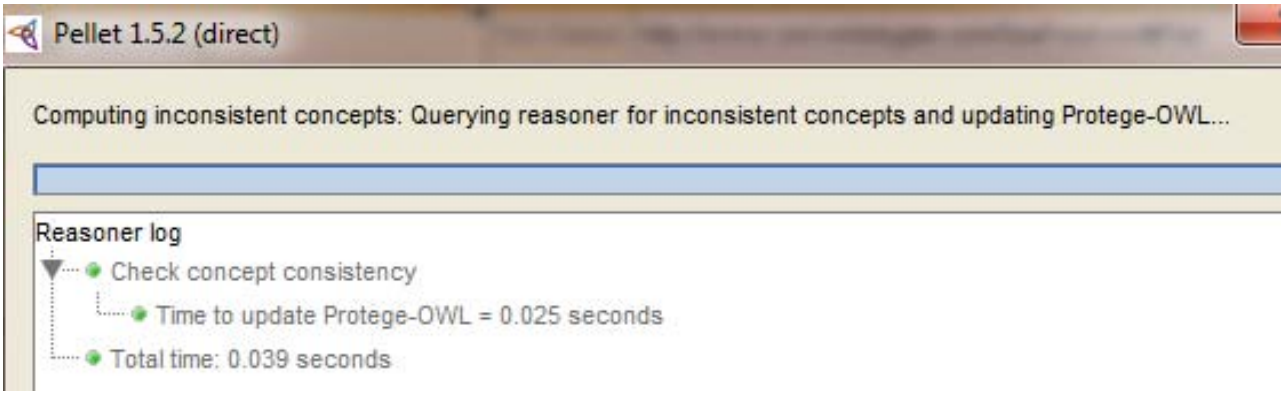

Fig. 4. Checking the Consistency of Ontological Concepts.

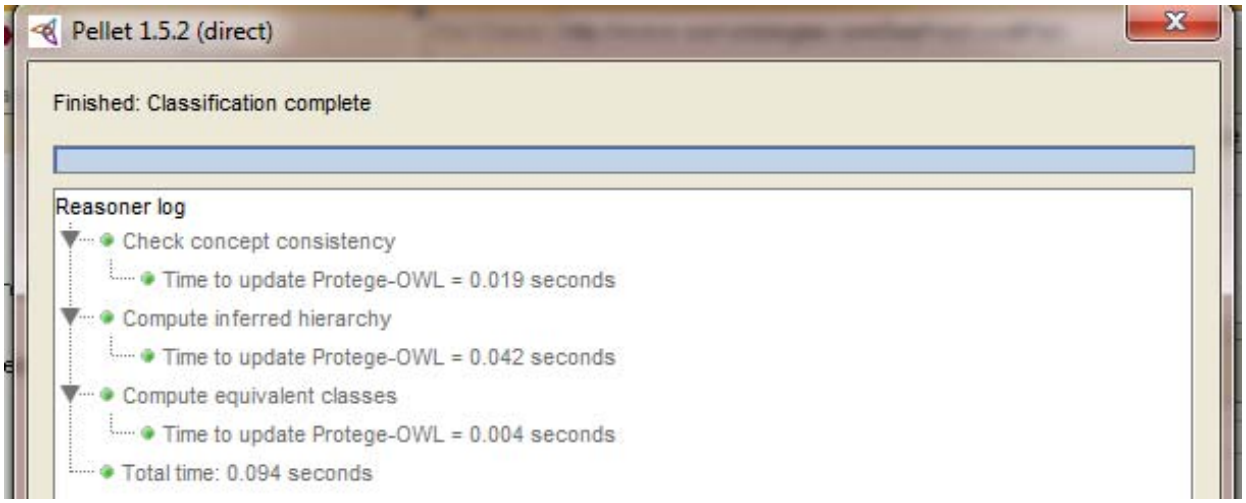

Fig. 5. Taxonomy Classification.

Apart from object and data properties, property restrictions are also specified in the ontology. A property restriction describes the class of individuals that meet the specified property-based conditions. Here necessary conditions are asserted to different classes and some are inherited from the parent class through cardinality restriction and value restriction. For instance, Property Restrictions defined in Test-Spec-External-Salt class are given below:

Test-Spec-External-Salt $\subseteq \forall$ testType only Purity (1)

Test-Spec-External-Salt $\subseteq =$ testType exactly 1 (2)

Test-Spec-External-Salt $\subseteq =$ foodType exactly 1 (3)

The equation (1) represents a value restriction to specify the condition that all instances of External Test Specification of salt contains only purity test. The equation (2) is a cardinality restriction and it specifies that the instances of this class will have exactly one *testType*. This condition is implemented by the universal restriction *allValuesFrom* (only) and the cardinality exactly on the property *testType*. Both the above conditions are necessary conditions. This property specifies that all instances in this class must have values only from the

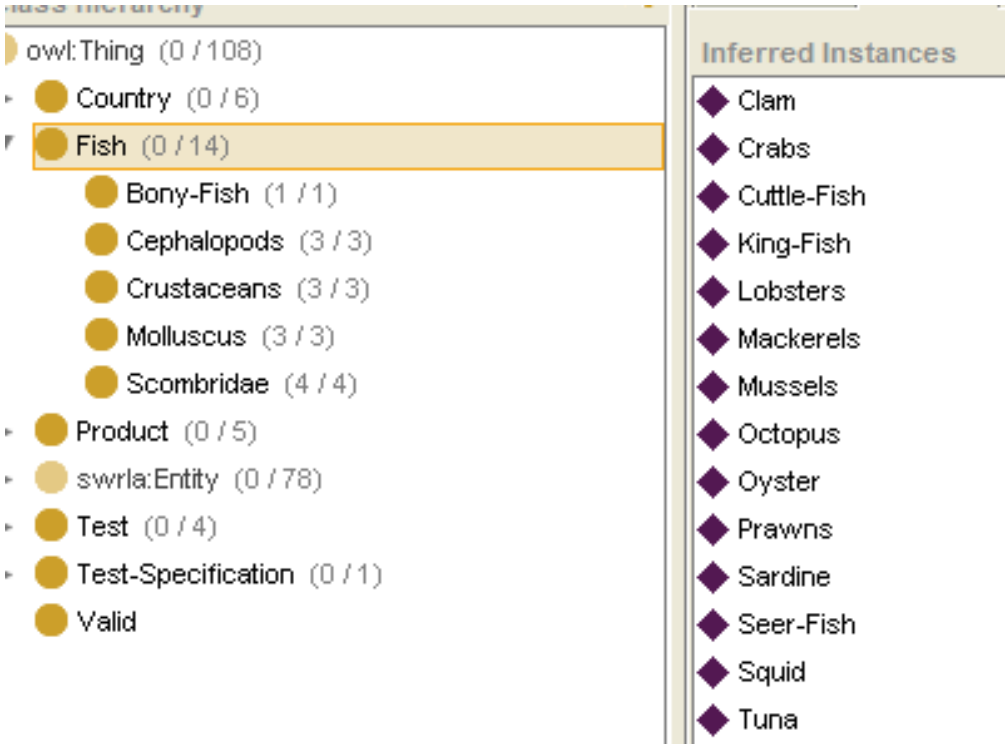

Fig. 6. Inferred Instances.

specified range for the specified property. Also the *Test-Spec-External-Salt* class inherits a value restriction from the parent class Test-Specification (See Fig. 3). Figure 2 represents the property restrictions of Test-Spec-External-Salt class.

RESULTS AND DISCUSSION

Ontology Reasoners are used to check the consistency of the ontology and to automatically compute the ontology class hierarchy (Sherimon *et al.*, 2013b). The reasoner helps to check the consistency, classification, realization, and concept satisfiability. Reasoner checks whether there is any inconsistency in the class hierarchy. The reasonerwill find out any hidden relationship in the ontology (Sherimon *et al.*, 2013d). If a class does not contain any individuals, it would be an inconsistent class. Also based upon the class description, reasoner will find out if there exist any subclasses of a given class. Thus class hierarchy will be inferred by the reasoner. Also all inferred axioms are generated by the reasoner. Ontology based reasoning makes a way to discover new knowledge, which can lead to new directions in research (Sherimon *et al.*, 2014). Protégé does not include a reasoner. So we have to use external reasoners. By default, Protégé doesn't include any reasoning ability. But it supports many third party reasoners such as Fact++, HermiT and Pellet. Here, Pellet Reasoner, a popular open-source reasoner developed by University of Mary Land is used to reason the ontology.

In Seafood Ontology, reasoning is done using Pellet 1.5.2. The consistency is checked, taxonomy is classified and the inferred instances are computed. Figure 4 represents the result obtained when consistency checking is done. It was found that there are no inconsistent classes in the ontology. Figure 5 represents the result of taxonomy classification. Here inferred hierarchy and equivalent classes are computed and the total time to complete the task is generated. Figue 6 represents the inferred instances of the class 'Fish'. Thus the seafood ontology was tested and validated to verify the correctness of data.

CONCLUSION

The OWL based ontology for the Seafood, was constructed with Protégé according to the standard ontology development process. We have extended the seafood ontology that was developed earlier by us, by adding more concepts, properties and property restrictions. Consistency checking of ontology and classification of classes has been done with the support of Pellet reasoner. When ontologies are reasoned by machines, valid deductions and inferences are generated. Ontology provides a shared and common understanding of a domain that can be communicated across people and application systems. Ontologies are able to define relationships, semantics, enhanced clarity, all of which collectively enable information retrieval in a meaningful way. The future scope of this paper is to add rules to the ontology using SWRL [Semantic Web Rule Language]

and to implement the ontology based seafood quality assurance system.

REFERENCES

Executive Instructions for Approval and Monitoring of Fish & Fishery Products for Export. 2012. Export Inspection Council of India. Document No. EIC/F&FP/Ex. Inst/March.

Fr. Rubin Thottupuram, Sumathy Easwaran. 2011. Farm-Agro Ontology formation: A black pepper model, International Journal of Research and Reviews in Software Engineering, Vol. 1. No.1, March, Science Academy Publisher.

Hebler, J. *et al*. 2009. Semantic Web Programming, Wiley Publishing.

Neches, R., Fikes, RE., Finin, T., Gruber, TR. and Swartout, WR. 1991. Enabling Technology for Knowledge Sharing. AI Magazine. 12(3):36-56.

Rajendra Akerkar. 2009. Foundations of the Semantic Web. Narosha Publishing House.

Sherimon, PC., Reshmy, K., Vinu, PV., Youssef, T., Yousuf Al Kaabi. and Yousuf Al Farsi. 2014. Adaptive Questionnaire Ontology in Gathering Patient Medical History in Diabetes Domain. Lecture Notes in Electrical Engineering. 285:453-460.

Sherimon, PC., Vinu, PV., Reshmy, K. and Youssef, T. 2013[a]. Risk Assessment Prediction of Hypertension and its Associated Diseases – An Ontology Driven Model, International Conference on Computer Medical Applications, ICCMA' 2013, January 20-22, Sousse, Tunisia. IEEE Xplore, doi: 10.1109/ICCMA.2013.6506183

Sherimon, PC., Vinu, PV., Reshmy, K. and Youssef, T. 2013[b]. Developing Survey Questionnaire Ontology for the Decision Support System in the Domain of Hypertension, IEEE South East Conference, Florida, USA.

Sherimon, PC., Reshmy, K., Vinu, PV. and Youssef, T. 2013[c]. Ontology Based System Architecture to Predict the Risk of Hypertension in Related Diseases. International Journal of Information Processing and Management. doi:10.4156/ijipm.

Sherimon, PC., Reshmy, K., Vinu, PV. and Youssef, T. 2013[d]. Exhibiting Context Sensitive Behavior in Gathering Patient Medical History in Diabetes Domain using Ontology. International Journal of Advancements in Computing Technology. 5(13):41-47.

Sherimon, PC., Vinu, PV. and Reshmy, K. 2011. Development Phases of Ontology for an Intelligent Search System for Oman National Transport Company. International Journal of Research and Reviews in Artificial Intelligence. 1(4):97-101.

Gupta, S. and Narina, T. 2010. Semantic Query Optimisation with Ontology Simulation, International Journal of Web and Semantic Technology. Vol 1, October.

Sinuhe, A. *et al*. 2004. Semantic Web Languages – Strengths and Weakness, IADIS International Conference, Lisbon, Portugal.

Vinu, PV., Sherimon, PC. and Reshmy, K. 2012[a]. Knowledge - Base Driven Framework for Assuring the Quality of Marine Seafood Export. International Journal of Artificial Intelligence and Knowledge Discovery. 2(3): (in press).

Vinu, PV., Sherimon, PC. and Reshmy, K. 2012[b]. Development of Seafood Ontology for semantically enhanced Information Retrieval International Journal of Computer Engineering and Technology. 3(1):154-162.

Received: Nov 11, 2013; Revised: March 6, 2014;
Accepted: March 7, 2014